Capillary Electrochromatography of Inorganic and Small Organic Anions using Pseudo and Wall-Coated Ion Exchange Phases

by

Michael Charles Breadmore

A thesis submitted in fulfilment of the requirements for the degree

of

Doctor of Philosophy

Chemistry

UNIVERSITY OF TASMANIA

April 2001

DECLARATION

To the best of my knowledge, this thesis contains no copy or paraphrase of material previously published or written by another person, except where due reference is made in the text of the thesis.

Michael Charles Breadmore

6th April 2001

This thesis may be available for loan and limited copying in accordance with the Copyright Act 1968.

Michael Charles Breadmore

6th April 2001

ACKNOWLEDGMENTS

No undertaking of this size can be accomplished without the support and help of numerous people, and I would like to offer my sincere thanks to the following people:

First and foremost, my supervisor, Professor Paul Haddad for his continued support and insightful contributions, and perhaps above all else for his tolerance (particularly during cricket season).

Dr Miroslav Macka who has contributed vast amounts of time to encourage a high quality of science. I also thank him for his many ideas, particularly my initial project concept, although I must say I think it has deviated slightly.

Professor Josef Havel, Dr Mary Boyce, Professor Jim Fritz and Dr Jeremy Glennon for their involvement and numerous contributions to this work.

All the past and present members of the Separation Science Group including, John Madden, Cameron Johns, Helmy Cook, John O'Reilly, Greg Dicinoski, Philip Doble, Narumol Vachirapatama, Baoguo Sun, Takashi Yokoyama, Matt Shaw, Peter Fagan and Andrew Grosse. I especially thank all the occupants of Rm 413, namely Emily Hilder, Kai Ling Ng, Philip Zakaria and of course, the fish, for creating a relaxed and productive working environment.

The staff and students of the School of Chemistry for providing such a friendly workplace.

Dr Nebojsa Avdalovic and Dr Chris Pohl of Dionex Corporation for generously supplying the latex particles used in this work and for answering my many questions. Rod Minett, David Wilkinson and Mike Whitby of Agilent Technologies Australia for technical support. Financial support from the Australian Research Council is also gratefully acknowledged.

To my friends, I thank you for you friendship over the past 3 (or more) years.

I would like to thank my immediate family for their love and support: my parents, Denis and Lorraine, my sister Julie, and my brothers Craig, David, Danny and their significant others Robin, Angela and Robin. Also my nieces and nephews, Melissa, Sarah, Kim, Daniel, Jacqueline, Andrew, Katherine, Patrick, Cassandra, Marcus, Elliott and Oliver.

Finally I am eternally grateful to Anne Palmer for her love and support over the last 4 years.

LIST OF ABBREVIATIONS

CE	Capillary electrophoresis
CEC	Capillary electrochromatography
EKC	Electrokinetic electrochromatography
EOF	Electroosmotic flow
IE	Ion-exchange
IEC	Ion-exchange chromatography
NDS	1,5-Naphthalenedisulfonate
OT	Open tubular
PDDAC	Poly(diallyldimethylammonium chloride)
RP	Reversed-phase
SPE	Solid-phase extraction
Tris	Tris(hydroxymethyl)aminomethane

LIST OF PUBLICATIONS

Type of Publication	Number	Reference
Papers in refereed journals	10	1-10
News/Feature articles	1	11
Posters at international meetings	2	12-13
Oral presentations at international meetings	5	14-18

1. M.C. Breadmore, M.C. Boyce, M. Macka, N. Avdalovic and P. R. Haddad, On-capillary ion-exchange preconcentration of inorganic anions using open-tubular capillaries followed by elution with a transient isotachophoretic gradient, *The Analyst*, 125, (2000) 799-802.
(*Chapter 3*)

2. M.C. Breadmore, M.Macka and P.R. Haddad, Open Tubular Ion Exchange Separation of Inorganic Anions, *The Analyst*, 125(7), (2000), 1235-1241.
(*Chapter 5*)

3. M.C. Breadmore, M. Boyce, M. Macka and P.R. Haddad, Peak shapes in Open Tubular Capillary Electrochromatography of Inorganic Anions, *J. Chromatogr. A*, 892, (2000) 303-313.
(*Chapter 3*)

4. M. C. Boyce, M.C. Breadmore, M. Macka, P. Doble and P.R. Haddad, Indirect spectrophotometric detection of inorganic anions in ion exchange capillary electrochromatography, *Electrophoresis*, 21(15), (2000), 3073-3080.
(Chapter 3)

5. M. C. Breadmore, P.R. Haddad and J.S. Fritz, Modelling and optimisation of the separation of anions in ion chromatography – capillary electrophoresis, *Electrophoresis*, 21(15), (2000), 3181-3190.
(*Chapter 4*)

6. M.C. Breadmore, E.F. Hilder, M. Macka an P.R. Haddad, Modelling the Migration of Inorganic Anions in Ion-Exchange Capillary Electrochromatography,. *Electrophoresis*, in press (2001).
(*Chapter 3*)

7. M. C. Breadmore, M. Macka, P.R. Haddad and N. Avdalovic, On-capillary ion-exchange preconcentration of inorganic anions in open tubular capillary electrochromatography with elution using transient isotachophoretic gradients. II Characterisation of the isotachophoretic gradient, *Anal. Chem*, In press. (2001).
(*Chapter 5*)

8. M. C. Breadmore, P. R. Haddad and J. S. Fritz, Optimisation of the separation of anions in Ion Chromatography – Capillary Electrophoresis using indirect UV detection, Accepted in *J. Chromatogr A*, Nov 2000.
(*Chapter 4*)

9. M. C. Breadmore, A. S. Palmer, M. Curran, M. Macka, P. R. Haddad and N. Avdalovic, Ion-exchange preconcentration of inorganic anions in open tubular capillary electrochromatography with elution using transient isotachophoretic gradients. III Method development and application, *in preparation (Anal. Chem.)*.
(*Chapter 5*)

10. M. C. Breadmore E, F, Hilder, M. Macka and P. R. Haddad, Ion exchange Capillary Electrochromatography of inorganic ions, A Review, *in preparation (TrAC)*.
(*Chapter 1*)

11. Chromatography with tunable selectivity for inorganic anions, *Analytical Chemistry News and Features*, 71, (1999), 593A.

12. M.C. Breadmore, M. Macka and P.R. Haddad, Open-Tubular Ion-Exchange Electrochromatography of Inorganic Ions, Poster, *Australian International Symposium on Analytical Science 1999*, Melbourne, Australia.

13. M.C. Breadmore, M.Macka and P.R. Haddad, Selectivity Manipulation of Alkali Metals and Ammonium using Anionic Particles as a Pseudo-Stationary Phase, Poster, *International Ion Chromatography Symposium 1999*, San Jose.

14. M.C. Breadmore, M.Macka and P.R. Haddad, Introducing Ion Exchange Interactions into CE separations, Oral, *International Ion Chromatography Symposium 1999*, San Jose, USA.

15. J. S. Fritz, W. Ding, J. Li, M. C. Breadmore, Separation of inorganic and small organic ions by Capillary Electrophoresis; Some recent developments, Oral, *Asia Pacific Capillary Electrophoresis (APCE) 2000*, Hong Kong.

16. M. C. Breadmore, E. F. Hilder, M. C. Boyce, M. Macka and P. R. Haddad, On-column ion-exchange preconcentration of inorganic anions for capillary electrophoresis, Oral, *International Ion Chromatography Symposium 2000*, Nice, France.

17. M. C. Breadmore, P. R. Haddad and J. S. Fritz, Ion Chromatography – Capillary Electrophoresis : Optimisation and Detection, Oral, *International Ion Chromatography Symposium 2000*, Nice, France.

18. M. Macka, M. C. Breadmore, E. F. Hilder and P. R. Haddad, CE or CEC? Capillary Electrochromatography disguised as Capillary Electrophoresis or Capillary Electrophoresis disguised as Capillary Electrochromatography?, Oral, *Australian Electrophoresis Society*, 2000, Sydney, Australia.

ABSTRACT

This work presents a systematic study on the use of pseudo-phase and wall-coated ion-exchange (IE) phases for the separation of anions by ion-exchange capillary electrochromatography (IE-CEC).

The viability of using open tubular (OT) columns prepared by adsorbing small cationic particles onto the capillary wall for the selectivity manipulation of inorganic anions by IE-CEC was examined. The introduction of an IE component into the separation mechanism allowed the separation selectivity to be varied by changing the type and concentration of the electrolyte anion. This enabled the migration order of a mixture of ions to be changed from a chromatographic selectivity to an electrophoretic selectivity, via novel intermediate selectivities. When separating UV transparent ions, the IE competing ion also acted as the indirect detection probe, which restricted the range over which the concentration could be varied. Selectivity manipulation in this case was achieved by varying the type of probe rather than its concentration. Using a theoretical model equation derived from IC and CE theory, the manner in which mobilities changed with varying electrolyte composition was modelled, with excellent correlation being obtained between predicted and experimental analyte mobilities ($r^2 > 0.98$). Values for analyte constants determined from non-linear regression allowed a quantitative comparison of the strengths of interaction of different ions with the ion-exchange phase.

The addition of the cationic polymer, poly(diallyldimethylammonium chloride), to the electrolyte as an alternative to OT columns provided superior flexibility due to the ability to vary the IE capacity. The model derived for the migration of anions in the OT system was extended to include the ability to vary the IE capacity and was validated with a test set of 16 UV absorbing inorganic and organic anions. Excellent agreement ($r^2 > 0.98$) was obtained between experimental and predicted mobilities for all ions. The model was used to find the optimum separation conditions, with

the separation of 16 ions being achieved on the basis of only 5 initial experiments. The system was then extended to the analysis of UV transparent ions where the separation of 24 anions was optimised using the derived model equation. The potential of using pseudo-phase IE-CEC for the separation of real samples was demonstrated with the separation of anions in Bayer liquor.

The advantage of having a heterogeneous phase in an OT column was exploited to enable the on-capillary preconcentration of inorganic anions via IE interactions. A new elution method, namely the use of a transient isotachophoretic gradient, was introduced and shown to be a very efficient method for analyte elution from the preconcentration column. A fundamental study of the generation and implementation of the gradient was undertaken and the optimum conditions enabled nearly a 1000-fold increase in sensitivity over conventional CE without the use of electrokinetic injection. The potential of the method was demonstrated by the determination of nitrate in Antarctic ice cores.

TABLE OF CONTENTS

Chapter 1

Introduction and Literature Review

1.1 Introduction

Capillary electrochromatography (CEC) is often considered to be the combination of capillary electrophoresis (CE) and high performance liquid chromatography (HPLC) and involves the application of a high electric field over a capillary packed with chromatographic particles. This definition has predominantly historical origins, as many of the early applications of CEC involved using packed capillary columns. The first potential of CEC was shown in 1974 by Pretorius, Hopkins and Schieke [1] who applied an electric field over a glass column (1000 μm i.d.) packed with micro-particulate silica to demonstrate the superior efficiency of electroosmotic flow (EOF) over pressure-driven flow. This was later extended by Jorgenson and Lukacs in 1981 [2] who used small columns (170 μm i.d.) packed with reversed-phase material to separate 9-methylanthracene and perylene with high efficiency. The use of narrower capillaries provided better heat dissipation and improved the quality of the separation. Since then, this area of CEC has grown immensely to become a popular alternative to more widely used HPLC methods.

Since CEC has developed as a rather diverse technique, a more appropriate definition of CEC today is 'any electroseparation technique that involves both an electrophoretic and a chromatographic component'. Using this broad definition, the manner in which the chromatographic component is introduced is not restricted solely to packed columns, but is extended to include monolithic and open tubular columns in addition to buffer additives (such as micelles, polymers and particles) used as a pseudo-stationary phase. While convention dictates that the use of pseudo-stationary phases (also called pseudo-phases) is termed electrokinetic chromatography (EKC) as named initially by Terabe, Otsuka and Ando [3,4], recent

trends have been towards a more unified approach regarding terminology, classifying pseudo-phases as a form of CEC. Knox [5] suggested that electrophoretic terminology should be used for electrophoretic techniques and likewise for chromatographic terminology. However, when both electrophoretic and chromatographic components are present and variation of the conditions can lead to a change in the dominant mechanism from electrophoretic to chromatographic, implementation of these guidelines becomes difficult.

Irrespective of the manner in which the chromatographic phase is introduced into an electrophoretic separation, CEC offers several advantages over other electrophoretic and chromatographic methods. Firstly, the use of electrodriven flow results in a flat flow profile instead of the parabolic profile produced with hydrodynamic flow. This means that CEC offers separation efficiencies that are considerably higher than those achieved using other chromatographic separation techniques.

Secondly, CEC offers the potential to combine two or more complementary separation mechanisms. For neutral analytes, analyte migration depends solely on the degree of interaction with the stationary phase (a chromatographic mechanism). However, for charged analytes, migration will also be influenced by the analyte's own electrophoretic mobility (an electrophoretic mechanism). Variation of the chromatographic and electrophoretic components therefore enables the relative contribution of each to be changed thus changing the overall migration and potentially also the separation selectivity. This is particularly useful for samples that have disproportionate sample concentrations.

Thirdly, CEC with its combination of electrophoretic and chromatographic mechanisms offers the ability to perform on-line preconcentration methods. The use of a fixed heterogenous phase (as in packed and OT columns) enables large volumes of sample to be injected with analytes being adsorbed onto the front of the column, hereby providing large preconcentration factors without loss of efficiency. While pseudo-phases are not heterogenous, the possibilities for preconcentration are still

quite impressive. This was illustrated by a recent report of nearly a 1 million fold increase in sensitivity using electrokinetic injection in a pseudo-phase system [6].

To date most CEC has focussed on the separation of neutral analytes, however more recently there has been considerable interest in the separation of ionic analytes. As CEC in general has been extensively reviewed over the last few years in all forms [7-15], the focus of this review will be on the separation of inorganic and small organic analytes using all forms of CEC. Particular attention is paid to the use of CEC for selectivity manipulation and also for methods to improve the detection sensitivity in CE.

1.2 Selectivity manipulation

One of the main advantages in separating charged species by CEC is that two different separation mechanisms, namely chromatography and electrophoresis, may be combined to separate the analytes. In the case of inorganic anions and small organic anions the chromatographic method of choice is ion-exchange chromatography (IEC), where the analyte anions may "exchange" with eluent anions present as a counter-ion at the positively charged functional group (usually a quaternary ammonium functional group) bound to the stationary phase. The interaction between both analyte and eluent anions is an equilibrium, the position of which is influenced by both the concentration and type of eluent anion. The use of an eluent anion with a higher affinity for the charged functional group or the use of a higher concentration will decrease analyte interactions with the stationary phase. In this way the chromatographic interaction with the stationary phase can be varied. In contrast, electrophoretic separation is achieved based on the differing migration rates of ions in an electric field, as governed by the size to charge ratio of the analytes. The higher this ratio, the lower the mobility and the slower the analytes will migrate.

As a result of these two completely different separation mechanisms, the separation selectivities of IEC or CE are substantially different and the two techniques are

considered to be complementary rather than competitive [16]. This is perhaps best illustrated by considering the migration of fluoride and sulfate, with sulfate migrating prior to fluoride in CE, but fluoride being eluted earlier in an IEC system. The combination of IEC and CE to give ion-exchange CEC (IE-CEC) can therefore provide a separation selectivity that is different from both IEC and CE and this selectivity can also be manipulated by changing the relative contribution of the two separation mechanisms by changing the composition of the eluent/electrolyte.

While the nature of inorganic anions dictates that IEC is going to be the chromatographic method of choice to influence the migration of ions, it is not the only potential mechanism, with reversed-phase (RP) and inclusion complexation also offering viable alternatives.

1.2.1 Packed columns

Packed capillary columns are one of the more popular methods by which a chromatographic phase can be introduced into an electrophoretic separation since packed capillary columns are directly analogous to larger bore columns such as those used in liquid chromatography. Packed capillary columns are typically prepared by packing the capillary with chromatographic particles retained in the capillary by frits. Whilst the use of packed columns for CEC has demonstrated success, especially with regard to separation efficiency, there are substantial problems related to the practical implementation of such a method. Firstly, it is challenging to pack small particles (typically less than 5 μm in size) into a capillary with a diameter of 50-100 μm. Secondly, the formation of homogenous and reproducible frits is difficult and introduces weak points into the column where the possibility of breakage is increased. Thirdly, the presence of different physical zones in the capillary (open section, frits and column bed) can result in substantial differences in EOF which often results in the formation of bubbles unless pressure (5-12 bar) is applied to both ends of the column during the separation. Lastly, packed capillary columns are

prone to overheating, resulting in the column bed drying out. Therefore, low ionic strength buffers and/or low field strengths are required which place significant constraints on the ability to control the relative contributions of CE and IEC in the IE-CEC separation. Despite these limitations, there is still great potential for the use of packed capillary columns for the separation of inorganic anions, and this has already been demonstrated in the literature, as summarised in Table 1.1.

The first report of the separation of inorganic anions by packed column CEC was by Li *et al.* [17] who compared the separation of iodide, iodate and perrhenate by CE and IE-CEC using a silica-based strong anion-exchanger (SAX). The selectivity obtained in IE-CEC was different from that obtained in CE and was shown to be a combination of IEC and electromigration. Furthermore, IE-CEC separations offered higher efficiencies and lower detection limits by up to a factor of 20 than CE. However, no explanation was offered as to why the lower detection limits were obtained and this is an interesting area for further investigations.

A simple, but effective method for changing the contribution of electromigration in a pressure-assisted IE-CEC system was demonstrated by Kitagawa *et al.* [18] who used small changes in voltage to control the separation selectivity. By varying the voltage from +4 kV to −1kV, significant changes in the separation selectivity for sulfate, sulfite and thiosulfate were obtained. The potential of IE-CEC for the analysis of samples having disproportionate analyte levels was illustrated by using a small change in voltage to enable malonic acid to be separated from a 100x excess of sulfate.

The separation of partially ionised weak acids by IE-CEC using a silica based SAX material was reported by Ye *et al.* [19]. They found the IE-CEC separation to be superior to the corresponding reversed phase-CEC (RP-CEC) separation in terms of separation time, efficiency and selectivity owing to the different chromatographic retention mechanism. The chromatographic interaction could be influenced by

Table 1.1: Separations of inorganic and small organic anions by CEC using packed columns

Analytes	Chromatographic phase	Electrolyte	Column dimensions	Detection	Efficiency (plates/m)	Ref.
Iodide, iodate and perrhenate	5 μm Nucleosil SB SAX	5 mM phosphoric acid, pH 2.6	400 mm x 75 μm i.d. (600 mm total)	Direct UV, 190 nm	2.9×10^5 for iodide	[17]
Sulfite, sulfate and thiosulfate	5 μm TSK-gel IC-anion SW	Methanol/5 mM phthalic acid and 5 mM hexamethylene diamine containing 0.15% HEPES, pH 6.8 (10:90 v/v)	220 mm x 50 μm i.d. (304 mm total)	Indirect UV, 210 nm	NS	[18]
Malonic acid and sulfuric acid	5 μm TSK-gel IC-anion SW	Methanol/5 mM phthalic acid and 5 mM hexamethylene diamine, pH 6.8 (10:90 v/v)	230 mm x 50 μm i.d. (289 mm total)	Indirect UV, 236 nm	NS	
Lithium, sodium, potassium, chloride, nitrite, nitrate, iodide, sulfate and perchlorate	5 μm TSK-gel IC-anion SW	Methanol/5 mM phthalic acid and 5 mM hexamethylene diamine containing 0.15% HEPES, pH 6.8 (10:90 v/v)	220 mm x 50 μm i.d. (304 mm total)	Indirect UV, 210 nm	NS	
Nitrate, iodide, benzoate, salicylate, pyridine, aniline, phenol, 4-methoxyphenol, 4-chlorophenol, toluene and 4-nitrotoluene	3 μm silica based C_6/SAX	5 mM Bis-Tris, pH 6.5 adjusted with hydrochloric acid, 45% acetonitrile, 2.5 mM sodium chloride	265 mm x 75 μm i.d., (360 mm total)	Direct UV, 210 nm	7500 – 197 000	[19]

Table 1.1: Separations of inorganic and small organic anions by CEC using packed columns. (ctd)

Analytes	Chromatographic phase	Electrolyte	Column dimensions	Detection	Efficiency (plates/m)	Ref.
Bromide, bromate, nitrite, nitrate, iodide, thiocyanate, thiosulfate, molybdate and chromate	3 μm silica based SAX	5 mM phosphate, pH 7.20	250 mm x 75 μm i.d. (360 mm total)	Direct UV, 214 nm	NS	[20]
Bromide, bromate, nitrite, nitrate, iodide, thiocyanate, thiosulfate, molybdate and chromate	3 μm silica based SAX	1.25, 2.5 and 5 mM sulfuric acid titrated with Tris to pH 8.05	250 mm x 75 μm i.d. (360 mm total)	Direct UV, 214 nm	NS	
Chloride, bromide, chlorate, cyanate, fluoride, formate, methanesulfonate, perchlorate, carbonate, thiocyanate, thiosulfate, ethanesulfonate, propanesulfonate, butanesulfonate, pentanesulfonate, sulfate and hexanesulfonate	3 μm silica based SAX	2.5 mM nitrate, pH 6.80	250 mm x 75 μm i.d. (360 mm total)	Indirect UV, 214 nm	NS	
3,5-dinitrobenzoic acid, p-nitrobenzoic acid, p-bromobenzoic acid, o-toluic acid, benzoic acid and o-bromobenzoic acid	5 μm Spherisorb SAX	Acetonitrile/20 mM phosphoric acid (50:50 v/v)	100 mm x 50 μm i.d. (310 mm total)	Direct UV, 214 nm	NS	[21]
p-bromobenzoic acid, m-bromobenzoic acid and o-bromobenzoic acid	5 μm Spherisorb ODS1	Acetonitrile/10 mM phosphoric acid (50:50 v/v)	100 mm x 50 μm i.d. (310 mm total)	Direct UV, 214 nm	NS	

Table 1.1: Separations of inorganic and small organic anions by CEC using packed columns. (ctd)

Analytes	Chromatographic phase	Electrolyte	Column dimensions	Detection	Efficiency (plates/m)	Ref.
Iodate, bromate, nitrite, bromide, nitrate, iodide, thiocyanate, and chromate	IonPac AS9-HC (9 μm latex agglomerated alkyl quaternary ammonium)	(a) 5 mM sulfuric acid titrated with Tris to pH 8.05 (b) 2.5 mM carbonate, 2.5 mM bicarbonate, pH 10 (c) 5 mM perchloric acid titrated with Tris to pH 8.05	250 mm x 75 μm i.d. (360 mm total)	Direct UV, 214 nm	NS	[22]
Iodate, bromate, nitrite, bromide, nitrate, iodide, thiocyanate, and chromate	IonPac AS9-HC (9 μm latex agglomerated alkyl quaternary ammonium)	9 mM perchloric acid titrated with Tris to pH 8.05	250 mm x 75 μm i.d. (360 mm total)	Direct UV, 214 nm	NS	
Iodate, bromate, nitrite, bromide, nitrate, iodide, thiocyanate, and chromate	IonPac AS9-HC (9 μm latex agglomerated alkyl quaternary ammonium)	2.5 mM hydrochloric acid titrated with Tris to pH 8.05, -30 kV at 1.3 min	85 mm x 75 μm i.d. (360 mm total)	Direct UV, 214 nm	NS	
Iodate, bromate, nitrite, bromide, nitrate, iodide, thiocyanate, and chromate	IonPac AS9-HC (9 μm latex agglomerated alkyl quaternary ammonium)	2.5 mM sulfuric acid titrated with Tris to pH 8.05	85 mm x 75 μm i.d. (360 mm total)	Direct UV, 214 nm	NS	

NS- not stated; HEPES - 4-(2-hydroxyethyl)-1-piperazineethane sulfonic acid, Tris – tris(hydroxymethyl)amino methane; Bis-Tris - 1,3-bis[tris(hydroxymethyl)methylamino]propane.

changing the composition of the buffer, with increasing the concentration of buffer anion reducing the IE interaction with the stationary phase. The addition of acetonitrile was also found to reduce chromatographic interaction, believed to be by a reduction in hydrophobic interaction with the phase, although it should be noted that this effect may have resulted from changes in ionisation of the acids due to the addition of organic modifier.

Work by Hilder *et al.* [21] on the separation of inorganic anions by IE-CEC using silica based SAX material has shown that the separation selectivity was substantially different from that seen in either IEC or CE. Observed mobilities for most of the anions in the IE-CEC system when a phosphate eluent was used were very low (< 10 x 10^{-9} m^2/Vs). In the case of the strongly retained anions (chromate, thiocyanate and molybdate) the mobilities were positive (i.e. migrating after the EOF peak) indicating substantial interaction with the stationary phase. In order to control the separation selectivity, it was demonstrated that the concentration of competing ion could be increased to decrease the chromatographic component of the separation mechanism allowing co-migrating peaks to be resolved. However, there were problems with this method relating to the long column flushing time due to high back pressure caused by the small particle size and also the restricted operating pH due to the use of a silica-based stationary phase.

The separation of anionic, neutral and cationic analytes by IE-CEC using a mixed-mode C_6/SAX stationary phase has been reported by Klampfl *et al.* [20]. Migration was observed to be composed of a ternary separation mechanism comprising electrophoretic, RP and IE components. The chromatographic component could be influenced by adding organic modifier which changed the ionisation of the analytes as well as reducing the RP interaction, and/or by changing the concentration of anion in the buffer which reduced the IE interaction with the stationary phase. The influence of pH was also examined whereby changing the pH from 6.0 to 7.5 produced significant changes in migration of the fully ionised analytes and this was

attributed to the increased eluotropic strength of the electrolyte due to an increase in the concentration of hydroxide.

Many of the problems encountered using silica based columns have been overcome by Hilder *et al.* [22] who used polymeric based packing material for CEC. The larger particle size allowed the column to be flushed at a faster rate and enabled the system to be used in a pressure-assisted mode (pCEC) where pressure was applied to the column inlet only. This allowed the chromatographic and electrophoretic components to be controlled independently. Varying the eluent anion concentration changed the chromatographic component, while the electrophoretic component was changed by varying the separation voltage. The contribution of these two mechanisms was optimised using an Artificial Neural Network (ANN) resulting in the separation of 8 UV absorbing anions in 2.3 minutes under optimal conditions.

1.2.2 Monolithic columns

Monolithic columns are considered to be an easier alternative to packed columns offering many of the same advantages to packed columns but without many of the problems [23]. They are formed by generation of a continuous polymeric network inside the capillary [9], and can be classified according to construction as (i) moulded porous polymers [24], (ii) moulded porous Sol-Gel [25], (iii) particle-fixed continuous bed [26], and (iv) microfabricated monolithic [27]. While each method has particular advantages, they all have the common advantage that no frits are needed to retain the packing in the columns. As a result, there is often no need to use overpressure to stop bubble formation. However, the development of monolithic columns faces considerable challenges, particularly with regard to column fabrication. There are still major problems regarding stability, reproducibility and heterogeneity of the different types of columns.

While the use of monolithic columns has already been demonstrated to have great potential in CEC (for example, see refs [23] and [9]), the application of such columns to the separation of inorganic and small organic anions has yet to be demonstrated.

1.2.3 Open tubular columns

There has been a recent resurgence in the use of open tubular (OT) columns in CEC because of the difficulties associated with packed capillaries and this has led to a large number of separations of ions by OT-CEC, as illustrated in Table 1.2. As the stationary phase is on the wall of the capillary, there is no packing in the column and the separation efficiency can potentially be higher than that obtained with packed columns due to the elimination of the eddy diffusion term in the van Deemter equation. Also, many OT-CEC columns are easy to prepare, with fabrication involving either simple flushing procedures or chemical modification of the capillary wall. OT columns are also instrumentally simpler to use because there is no need to use high pressure: there are no bubble problems and the lack of packing means that the capillary can be flushed quickly as for a normal CE capillary. While these reasons would imply that OT columns are very desirable for CEC it should be noted that they also have a substantial disadvantage. That is, that in order to achieve highly efficient separations, it is necessary to use narrow capillaries (typically less than 25 μm i.d.) due to the resistance to mass transfer across the capillary. However, the use of narrow capillaries creates serious problems when using on-capillary photometric detection. Another general problem of OT columns is their relatively lower capacity when compared to packed capillaries because of the small stationary-to-mobile phase ratio. This problem can be overcome by using various methods to increase the surface area (e.g. by etching, see Pesek *et al.* [8]) and hence the stationary phase amount.

Table 1.2: Separations of inorganic and small organic anions by CEC using open tubular columns

Analytes	Chromatographic phase	Electrolyte	Column dimensions	Detection	Efficiency (plates/m)	Ref.
4-amino-1-naphthalenesulfonic acid, 2-amino-1-naphthalenesulfonic acid, 5-amino-1-naphthalenesulfonic acid, 8-amino-1-naphthalenesulfonic acid and 1-naphthol-5-sulfonic acid	Covalently bound PS-264 dynamically modified with TBA	10 mM phosphate, pH 7.0, 1.25 mM TBA-hydroxide	400 mm x 10 μm i.d. (500 mm total)	Direct LIF, 325 nm	NS	[28]
4-amino-1-naphthalenesulfonic acid and 5-amino-1-naphthalenesulfonic acid	Covalently bound OV-17v dynamically modified with CTAB	32 mM phthalate, pH 7.0, 400 μM CTAB	400 mm x 10 μm i.d. (500 mm total)	Direct LIF, 325 nm	NS	[29]
Thiosulfate, chloride, sulfate, selenate, perchlorate, tungstate, carbonate and selenite	Covalently bound 1,5,9,13,17,21-hexaazacyclotetraeicosane	5 mM chromate, pH 10.0	100 μm i.d. (500 mm total)	Indirect UV, 254 nm	NS	[30]
Bromide, oxalate, malonate, citrate, tartrate, malonate, succinate, acetate, lactate, butanoate, *p*-hydroxybenzoate, salicylate and octanesulfonate	Covalently bound 1,5,9,13,17,21-hexaazacyclotetraeicosane	10 mM potassium hydrogen phthalate, pH 5.0	100 μm i.d. (500 mm total)	Indirect UV, 254 nm	NS	
Nitrite, nitrate, bromide, iodide and thiocyanate	Fused silica coated with PEI	20 mM Tris pH 8	760 mm x 75 μm i.d. (630 mm total)	Direct UV, 210 nm	NS	[31]
Tartaric, malic, citric, lactic, succinic and acetic	Fused silica coated with PEI	20 mM 2,4-dihydroxybenzoic acid, pH 4.9	455 mm x 75 μm i.d. (630 mm total)	Indirect UV, 249 nm	NS	[32]

Table 1.2: Separations of inorganic and small organic anions by CEC using open tubular columns (ctd)

Analytes	Chromatographic phase	Electrolyte	Column dimensions	Detection	Efficiency (plates/m)	Ref.
4-nitrophenol, 3-nitrophenol, 4-chlorophenol, 3-chlorophenol and 2-chlorophenol	Fused silica coated with PEI	25 mM borate, pH 9.2	580 mm x 75 μm i.d. (730 mm total)	Direct UV, 210 nm	NS	[33]
Ferrocyanide and ferricyanide	Covalently bound 4,8,12,18,22,26-hexaaza-1,15-dioxacyclooctaeicosane	10 mM phosphate pH 10.4	500 mm x 75 μm i.d. (700 mm total)	Direct UV, 220 nm	NS	[34]
Bromide, chloride, sulfate, nitrate, bromate, iodate, molybdate and tungstate	Covalently bound 4,8,12,18,22,26-hexaaza-1,15-dioxacyclooctaeicosane	5 mM chromate, pH 8.1	500 mm x 75 μm i.d. (700 mm total)	Indirect UV, 270 nm	NS	
Arsenate, arsenite, selenate and selenite	Covalently bound 4,8,12,18,22,26-hexaaza-1,15-dioxacyclooctaeicosane	5 mM chromate, pH 8.1	500 mm x 75 μm i.d. (700 mm total)	Indirect UV, 270 nm	NS	
Arsenate, phenylarsonic acid, arsenite and dimethylarsonic acid	Covalently bound 4,8,12,18,22,26-hexaaza-1,15-dioxacyclooctaeicosane	2 mM phthalate, pH 5.6	500 mm x 75 μm i.d. (700 mm total)	Indirect UV, 270 nm	NS	

Table 1.2: Separations of inorganic and small organic anions by CEC using open tubular columns (ctd)

Analytes	Chromatographic phase	Electrolyte	Column dimensions	Detection	Efficiency (plates/m)	Ref.
Chromate, chromium, phenylarsonic acid, arsenite, selenate and selenite	Covalently bound 4,8,12,18,22,26-hexaaza-1,15-dioxacyclooctaeicosane	20 mM phosphate, pH 6.2	160 mm x 75 μm i.d. (160 mm total)	ICP-MS	NS	[35]
Arsenate and chloride	Covalently bound 4,8,12,18,22,26-hexaaza-1,15-dioxacyclooctaeicosane	20 mM phosphate, pH 6.2	160 mm x 75 μm i.d. (160 mm total)	ICP-MS	NS	
Chloride, sulfate, nitrite, nitrate phosphate and carbonate	Copolymerisation of trmiethylammoniumstyrene chloride with vinyl groups covalently bound to the wall	5 mM chromate, pH 7.7	595 mm x 50 μm i.d. (670 mm total)	Indirect UV, 254 nm	NS	[36]
Bromide, iodide, chromate, nitrite, nitrate, thiocyanate and molybdate	Copolymerisation of trmiethylammoniumstyrene chloride with vinyl groups covalently bound to the wall	40 mM borate, pH 9.0	900 mm x 50 μm i.d. (900 mm total)	Direct 210 nm	NS	
Bromide, chloride, sulfate, nitrate, fluoride and phosphate	Reactive polyamide	2.25 pyromellitic acid, 1.6 mM triethanolamine, pH 7.9 adjusted with sodium hydroxide	550 mm x 75 μm i.d. (600 mm total)	Indirect UV, 250 nm	NS	[37]

Table 1.2: Separations of inorganic and small organic anions by CEC using open tubular columns (ctd)

Analytes	Chromatographic phase	Electrolyte	Column dimensions	Detection	Efficiency (plates/m)	Ref.
o-nitrobenzoic acid, citraconic acid, *m*-nitrobenzoic acid, *o*-toluic acid, benzoic acid, *p*-toluic acid, *p*-hydroxybenzoic acid and *p*-aminobenzoic acid	Thermal immobilisation of Poly(vinyl amine) via internal crosslinking	50 mM sodium acetate, pH 4.0	320 mm x 50 μm i.d. (400 mm total)	Direct UV, 254 nm	NS	[38]
o-nitrobenzoic acid, citraconic acid, *m*-nitrobenzoic acid, *o*-toluic acid, benzoic acid, *p*-toluic acid, *p*-hydroxybenzoic acid and *p*-aminobenzoic acid	Immobilised Poly(vinyl amine) derivatised with N,N,N-trimethylaminoacrylamide	50 mM sodium acetate, pH 4.0	320 mm x 50 μm i.d. (400 mm total)	Direct UV, 254 nm	NS	

NS – not stated; TBA – tetrabutylammonium; Tris - tris(hydroxymethyl)amino methane; PEI – poly(ethyleneimine)

The first demonstration of OT columns for IE-CEC was by Pfeffer and Yeung [28] who dynamically coated capillaries with the ion-pair reagent, tetrabutylammonium (TBA). In order to maximise the amount of chromatographic contribution in the separation mechanism, they used narrow (10 μm i.d.) columns and modified the surface to have RP characteristics which increased the amount of adsorbed TBA on the surface. This allowed the separation of 5 substituted naphthalenesulfonic acids which were not resolved by conventional CE to be achieved. The resolution of the separation was found to be dependent on the concentration of TBA in the electrolyte, with higher concentrations increasing the dynamic capacity of the column and resulting in an increase in resolution. In a second report, Garner and Yeung [29] examined the use of cetyltrimethylammonium bromide (CTAB) for dynamic modification of RP-OT columns. They found that migration times decreased as the concentration of phthalate in the electrolyte was increased due to less interaction of the analytes with the stationary phase. The addition of acetonitrile was also examined as a potential method to control both the RP interaction and the amount of dynamic ion-exchanger adsorbed onto the phase.

One solution to overcome the limited capacity encountered in OT columns is to use electrostatically adsorbed IE particles as the stationary phase. This approach to increasing the surface area stationary phase has found popularity in ion chromatography particularly in columns developed by Dionex. This method was adapted to IE-CEC by Gjerde and Yengoyan [39] who used small cationic latex particles to coat bare fused silica capillaries. They showed that the separation selectivity of inorganic anions in these columns was different to that encountered in CE. However, methods to control the contribution of the chromatographic and electrophoretic components were not discussed.

The adsorption of water-soluble cationic polymers to provide IE sites for OT-CEC was first reported Nutku *et al.* [31]. They showed the separation of several UV absorbing inorganic anions in capillaries coated with the cationic polymer

poly(ethylene imine) (PEI). Highly efficient separations were obtained at pH 8, but when the pH was lowered to pH 5 the mobilities were found to decrease substantially, the efficiency decreased and the peaks became significantly asymmetrical. This was attributed to increased IE interactions with the adsorbed PEI which became protonated as the pH was lowered. Since then, PEI coated capillaries have been used for the separation of substituted phenols [33] and organic acids in fruit juices and wine [32].

In an attempt to influence the migration of ions in a manner different to IE, Hsu *et al.* [30] have used OT columns in which the polyaza macrocycle, 1,5,9,13,17,21-hexaazacyclotetraeicosane was covalently bound to the capillary wall. They found that decreasing the pH resulted in a higher reversed EOF due to an increase in the degree of protonation of the macrocycle, while electrophoretic mobilities of inorganic anions increased due to a decrease in complexation with the macrocycle. This is in contrast to expected trends if an IE mechanism was dominant where an increase in protonation would result in a decrease in observed mobilities due to more interaction with the wall.

A similar approach was employed by Liu and Chen [34] who bound the macrocycle 4,8,12,18,22,26-hexaaza-1,15-dioxaxycloоctaeicosane to the capillary wall for CEC. The use of this column enabled the separation of ferricyanide and ferrocyanide with a reversal of the conventional CE migration order. The same bound macrocycle was used for the speciation of arsenic, selenium and chromium using ICP-MS detection, where the OT-CEC format was found to provide superior efficiency and selectivity compared to conventional CE [35].

The distinction between CE and OT-CEC is not always straight forward, as is evidenced by a report by Chiari *et al.* [38] who made OT columns by adsorbing the cationic polymer poly(vinylamide) onto the capillary wall. While the capillary wall had a positive charge, no IE interaction with the wall was observed, with the positive surface charge used solely to provide a reversed EOF and thus avoid the need to use

a cationic surfactant. Similar approaches have been reported by Burt *et al.* [37] and Finkler *et al.* [36] and while not strictly CEC, the potential for IE interactions exists and modification of the electrolyte conditions may be sufficient to show this.

1.2.4 Pseudo-phase 'columns'

Since the introduction of micellar electrokinetic chromatography (MEKC) in 1984 by Terabe, Otsuka and Ando [3,4], the area of pseudo-phase (or pseudo-stationary phase) CEC (also known as electrokinetic chromatography, EKC) has grown to be a major electroseparation technique. Various pseudo-phases have been used, including micelles [13], cyclodextrins [10], dendrimers [15], polymers [15], particles [12] or microemulsions [7]. In all cases, the chromatographic phase is added to the electrolyte making it experimentally one of the simpler ways to introduce a chromatographic component into the separation mechanism. This has many advantages over both packed and open tubular capillary columns such as being able to replace the "column bed" before each separation by flushing with the electrolyte and also being able to change both the type and capacity of the "column" simply by making a new electrolyte. This can be advantageous because the same separation selectivity can be achieved without the use of extreme conditions (such as high/low ionic strength electrolytes) as may often be the case with packed and OT columns. However, this approach can create difficulties as conditions must be selected to avoid precipitation both with the buffer and the sample.

The separation of inorganic and small organic anions by pseudo-phase CEC is dominated by the use of three types of pseudo-phases: surfactants, polymers and macrocyclic compounds.

1.2.4.1 Surfactants

Surfactants were one of the first types of pseudo-phases introduced to CEC, and as such there has been much work into the use of surfactants for selectivity control of

inorganic anions, as illustrated by Table 1.3. This area was pioneered by the work of Jones and Jandik [40] who were the first to examine the effect of adding a cationic EOF modifier on the migration of inorganic anions. They found that increasing the concentration of cationic EOF modifier (Waters OFM anion BT) up to 5.0 mM resulted in a decrease in analyte mobility, particularly for nitrate, sulfate and bromide. They proposed that ion-association between the anions and the long chain quaternary ammonium compound was responsible.

Kaneta *et al.* [41] observed greater changes than those observed by Jandik and Jones when they added high concentrations of the cationic surfactant cetyltrimethylammonium chloride (CTAC) to the electrolyte for the separation of inorganic anions. They found that when CTAC was added below its critical micelle concentration (1.0 mM) the migration order resembled that based on electrophoretic mobilities, with only iodide showing some interaction with the monomer surfactants. However, above the cmc (25 mM) they found considerable interaction of all anions (bromide, iodide, nitrate, bromate and iodate) with the micelle, resulting in a complete reversal of separation selectivity. They observed that the way in which the mobility changed with surfactant concentration depended on whether the surfactant was added above or below the cmc suggesting different association constants with the micelles and monomers.

The effect of varying the chain length of the surfactant and its influence on the separation of ions was examined by Buchberger and Haddad [42]. The addition of dodecyltrimethylammonium bromide (DTAB, C_{12}), tetradecyltrimethylammonium bromide (TTAB, C_{14}) and hexadecyltrimethylammonium bromide (HTAB, C_{16}) all reduced the mobilities of inorganic anions, with a more pronounced effect observed for the longer chain length surfactant. It was noted that the different surfactants influenced the migration of each anion in a different manner. This was later exploited by using combinations of DTAB and CTAB to modulate the separation selectivity of inorganic and small organic anions [43]. The migration order was

Table 1.3: Separations of inorganic and small organic anions by CEC using a surfactant as a pseudo-phase

Analytes	Chromatographic phase	Electrolyte	Column dimensions	Detection	Efficiency (plates/m)	Ref.
Thiosulfate, bromide, chloride, sulfate, nitrite, nitrate, molybdate, azide, tungstate, monofluorophosphate, chlorate, citrate, fluoride, formate, phosphate, phosphite, chlorite, galactartrate, carbonate, acetate, ethanesulfonate, propionate, propanesulfonate, butyrate, butanesulfonate, valerate, benzoate, L-glutamate, pentanesulfonate and D-gluconate	Waters OFM anion BT (0.5 mM)	5 mM sodium chromate	520 mm x 50 μm i.d. (600 mm total)	Indirect UV, 254 nm	NS	[40]
Bromide, nitrate, bromate, iodide and iodate	CTAC (0.2 – 25 mM)	20 mM phosphate – tris buffer, pH 7.0	300 mm x 50 μm i.d. (500 mm total)	Direct UV, 214 nm	NS	[41]
Fluoride, thiocyanate, chlorite, nitrite, nitrate, sulfate, iodide, chloride, bromide and thiosulfate	DTAB, TTAB and HTAB (0.5 mM)	5 mM sodium chromate	520 mm x 75 μm i.d. (600 mm total)	Indirect UV, 254 nm	NS	[42]
Bromide, chloride, sulfate, nitrite, nitrate, fluoride, formate, carbonate, acetate, propionate, butyrate, valerate	Waters OFM anion BT (0.075 mM)	5 mM chromate, 0, 3 or 5% (v/v) 1-butanol	625 mm x 75 μm i.d. (700 mm total)	Indirect UV, 254 nm	NS	[44]
Chromate	TTAB (0-90 mM)	20 mM phosphate, pH 10	330 mm x 50 μm i.d. (530 mm total)	Direct UV, 237 nm	NS	[45]

Table 1.3: Separations of inorganic and small organic anions by CEC using a surfactant as a pseudo-phase (ctd)

Analytes	Chromatographic phase	Electrolyte	Column dimensions	Detection	Efficiency (plates/m)	Ref.
Chloride, nitrite, sulfate, nitrate, fluoride, bromate, phosphate and carbonate	Mixture of DTAB (2.65 mM) and TTAB (2.35 mM)	5 mM sodium chromate adjusted to 8.8 with NaOH	520 mm x 75 μm i.d. (600 mm total)	Indirect UV, 254 nm	NS	[43]
Chloride, sulfate, oxalate, fluoride, formate, malonate, succinate, tartrate, phosphate, carbonate, acetate and citrate	Mixture of DTAB (1 mM) and TTAB (5 mM)	7.5 mM sodium chromate, adjusted to pH 9.1 with NaOH	520 mm x 75 μm i.d. (600 mm total)	Indirect UV, 254 nm	NS	[46]
Iodide, nitrite, nitrate and thiocyanate	DTAB (50 mM)	18 mM borate, 30 mM phosphate, 10% propanol, pH 7.0	530 mm x 50 μm i.d. (760 mm total)	Direct UV, 235 nm	100,000-125-000	[47]
Nitrite, nitrate and bromide	CTAC (1.1 mM)	20 mm tetraborate, pH 8.94	255 mm x 50 μm i.d. (500 mm total)	Direct UV, 200 nm	NS	[48]
Bromide, chloride, sulfate, nitrite, nitrate and phosphate	HMB (0.4 mM) TTAB (0.2 mM) CTAB (0.02 mM) HDMB (2×10^{-4} mM)	5 mM sodium chromate, pH 8.0	500 mm x 50 μm i.d. (720 mm total)	Indirect UV, 254 nm	NS	[49]
Bromide, chloride, nitrite, sulfate, nitrate, chlorate, fluoride and phosphate	HMB (0.1 mM) DMB (0.1 mM) TTAB (0.1 mM) THPB (0.1 mM)	5 mM potassium dichromate, 1.6 mM triethanolamine, pH 8	400 mm x 75 μm i.d. (470 mm total)	Indirect UV, 260 nm	NS	[50]

Table 1.3: Separations of inorganic and small organic anions by CEC using a surfactant as a pseudo-phase (ctd)

Analytes	Chromatographic phase	Electrolyte	Column dimensions	Detection	Efficiency (plates/m)	Ref.
1-naphthalenesulfonic acid, 2-naphthalenesulfonic acid, 1,5-naphthalenedisulfonate acid, 1,6-naphthalenedusiufonate, 2,6-naphthalenedisulfonate, 2,7-naphthalenedisulfonate, 1,4-naphthalenedicarboxylic acid, 2,3-naphthalenedicarboxylic acid, 2,6-naphthalenedicarboxylic acid, phthalate, isophthalate, and terephthalate	1,5-bis(triethylammonium) propane (10 mM) 1,5-bis(triethylammonium) pentane (10 mM) 1,5-bis(trimethylammonium) hepane (10 mM) TMAB(10 mM) TBAB (10 mM)	10 mMphosphate, pH 7	Celect – N coatint (Supelco) 500 mm x 50 μm i.d. (720 mm total)	Direct UV, 230 nm	NS	[51]
AD-1, AD-2, AD-3 and AD-4	25 mM TBAB	10 mM sodium tetraborate, pH 9.2	500 mm x 50 μm i.d. (720 mm total)	Direct vis, 550 nm	NS	[52]
1-naphthalenecarboxylic acid, 2-naphthalenecarboxylic acid, -1-naphthalenesulfonic acid, 2-naphthalenesulfonic acid, 2,3-naphthalenedicarboxylic acid, 2,6-naphthalenedicarboxylic acid, 1,5-naphthalenedisulfonate acid, 2,6-naphthalenedisulfonate, phthalate, isophthalate, and terephthalate	Brij – 35 (30 mM0 Brij – 58 (30 mM) Brij – 78 (30 mM)	10 mM sodium tetraborate	500 mm x 50 μm i.d. (750 mm total)	Direct UV, 230 nm	NS	[53]

NS – not stated; CTAC – cetyltrimethylammonium chloride; CTAB – cetyltrimethylammonium bromide; DTAB – dodecyltrimethylammonium bromide; TTAB – tetradecyltrimethylammonium bromide; HTAB – hexadecyltrimethylammonium bromide; HMB – hexamethonium bromide; HDMB – hexadimethrine bromide; TMAB – tetramethylammonium bromide; TBAB – tetrabutylammmonium bromide; DMB – decamethnoium bromide; THPB – tributylhexadecylphosphonium bromide

found to be dependent on both the total concentration of surfactant and on the ratio of the two surfactants. This approach was used to optimise the separation of anions in Bayer liquor [44].

The effect of using different electrolyte anions on analyte interaction with cationic surfactants was briefly examined by Martínez and Aguilar [45]. They found that the amount of TTAB required to give chromate an observed mobility of 0.0 x 10^{-9} m^2/Vs varied from 90 mM when using a 20 mM phosphate electrolyte (pH 10) to 2.9 mM when using 20 mM carbonate (pH 10). This was attributed to the weaker ion-exchange effect of carbonate in comparison to phosphate.

Optimisation of the surfactant concentration to improve resolution of anions has been undertaken by Bjergegaard *et al.* [47] who used the cationic surfactant DTAB for the analysis of iodide, thiocyanate, nitrate and nitrite in biological samples. The addition of the cationic surfactant was found to improve resolution between each anion and also between the analytes and the organic sample matrix when compared to conventional CE. The method was applied to the determination of ions in milk and plasma.

The use of different EOF modifiers and their effect on the separation of anions was examined by the separate groups of Galceran *et al.* [49] and François *et al.* [50]. Low concentrations in the range 0 - 0.8 mM were sufficient to provide a reversed, stable EOF for all the surfactants studied, but changes in selectivity were only slight due to the low concentration of modifier added. The effect of adding higher concentrations of TTAB was examined by François *et al.* [50] where it was observed that the mobility of the anions became slower and resolution between crucial peak pairs was improved, but only this surfactant was employed at these higher concentrations.

The potential of CEC to separate positional isomers was demonstrated by Takayangi *et al.* [51] who analysed positional isomers of naphthalenesulfonic and naphthalenecarboxylic acids. They found that mono-amine additives, such as

tetrabutylammonium and tetramethylammonium ions, provided better resolution than CE, but not all the anions were resolved. The use of divalent additives (such as 1,5 – bis(triethylammonium) propane) enabled the separation to be achieved due to more interaction with the polymer. Ion-association constants were determined and were found to increase with the number of methylene groups in the divalent amine, which was correlated to inter-atomic distances as estimated using a molecular modelling package. The method was successfully applied to the separation of azo dyes which were insufficiently resolved by CE [52].

The influence of mixtures of the cationic surfactant TTAB and the zwitterionic surfactant coco amidopropylhydroxydimethylsolfobetaine (CAS U) on separations of inorganic anions was examined by Yeung and Lucy [54]. While the addition of CAS U had marked effects on the EOF, changes in mobilities of anions were slight with no changes in selectivity observed. However, the small changes in mobility were sufficient to improve the resolution of the separation.

Positional isomers of naphthalenesulfonic acids have also been separated using the non-ionic surfactants Brij-35, Brij-58 and Brij-78 [53]. These three surfactants were selected on the basis of their different hydrophobicity, but surprisingly all three surfactants provided similar reductions in mobility, which was attributed to interaction of the analytes with the polyethylene moiety within the surfactant (which was the same in all cases).

1.2.4.2 Polymers

The use of polymers as a pseudo-phase offers substantial advantages over surfactants, with the most notable being the fixed structure of the polymer molecule in comparison to the constantly changing micelle due to the monomer-micelle equilibrium occurring for surfactants. This enables organic modifiers to be used at much higher concentrations than is possible when using. As a result, there is

effectively only one type of interaction in contrast to both monomer and micelle interactions with surfactants.

The use of cationic polymers to influence the migration of ions was first introduced by Terabe and Isemura in 1990 [55] and since then, numerous publications have appeared in this field (Table 1.4). In their initial work, the cationic polymer poly(diallyldimethylammonium chloride) (PDDAC) was added to the electrolyte to influence the migration of positional isomers of naphthalenesulfonic acids which were difficult to separate by CE. In a subsequent report [56], the overall migration was changed by varying the concentration of polymer added to the electrolyte, with more interaction being observed at higher concentrations. The name ion-exchange electrokinetic chromatography (IE-EKC) was used to describe the technique.

The first application to the separation of inorganic anions was reported by Stathakis and Cassidy [57] who examined the effect of adding different polymers to the electrolyte. They found that the degree of interaction of the analyte with the polymer depended on the type of polymer, the concentration of polymer, and on the analyte, with analyte interaction correlating with observed retention in IEC separations. In a second report [58], the same authors evaluated the influence of two different counter-ions, chromate and benzoate, on analyte interaction with the polymer. Selectivity changes were more apparent when using benzoate as the polymer counter-ion due to more analyte interaction with the separation phase. The method was applied to the determination of bromide, chloride and sulfate in potash using the interaction of sulfate with the polymer to improve resolution from bromide and chloride.

The separation of inorganic anions and anionic metal complexes using cationic polymers as electrolyte additives has been extensively studied by Krohkin and co-workers. They have examined the separation of metal complexes of 4-(2-pyridylazo)resorcinolate (PAR) [59,60], *trans*-1,2-diaminocyclohexane-N,N,N',N'-tetraacetic acid (CDTA) and ethylenediaminetatreacetic acid (EDTA) [61], ethylenediaminedi(*o*-hydroxyphenylacetic acid) (EDDHA) [62] and more recently,

Table 1.4: Separations of inorganic and small organic anions by CEC using a water-soluble polymer as a pseudo-phase

Analytes	Chromatographic phase	Electrolyte	Column dimensions	Detection	Efficiency (plates/m)	Ref.
1-naphthalenesulfonic acid, 2-naphthalenesulfonic acid, 2,6-naphthalenedisulfonate acid, 2,7-naphthalenedisulfonate, 1,6-naphthalenedisulfonate acid, 1,5 naphthalenedisulfonate acid and 1,7-naphthalenedisulfonate acid	DEAE-dextran (2% w/v) and PDDA-chloride (0.3% w/v)	50 mM phosphate, pH 7.0	500 mm x 50 μm i.d. (750 mm total)	Direct UV, 210 nm	NS	[55]
Benzoate, *o*-, *m*-, and *p*-aminobenzoic acid, 1-napthoic acid, *o*-, *m*-, and *p*-hydroxybenzoic acid, 2-napthoic acid and 1-naphthalenesulfonate	PDDA-chloride (0.3 % w/v)	50 mM phosphate, pH 7	500 mm x 50 μm i.d. (750 mm total)	Direct UV, 210 nm	NS	[56]
Bromide, chloride, fluoride, nitrite, nitrate, phosphate and sulfate	PDDPi-chromate (0.2% w/v) PDDPy-chromate (0.17 % w/v) HDM-chromate (0.30 % w/v) DEAED-chromate (0.55% w/v)	5 mM sodium chromate, pH 8.0	520 mm x 75 μm i.d. (600 mm total)	Indirect UV, 254 nm	NS	[57]

Table 1.4: Separations of inorganic and small organic anions by CEC using a water-soluble polymer as a pseudo-phase (ctd)

Analytes	Chromatographic phase	Electrolyte	Column dimensions	Detection	Efficiency (plates/m)	Ref.
Benzoate, salicylate, 3-methylsalicylate, 3,5-dihydroxybenzoate,	PDDPi-chloride (0.2 % w/v)	5 mM phosphate, pH 6.8	530 mm x 77 μm i.d. (600 mm total)	direct UV, 214 nm	100,000 – 300,000	[58]
Iron (III) EDTA, oxalate, citrate and EDTA	PDDPi-chromate (0.23 % w/v)	5 mM chromate pH 8.4	530 mm x 77 μm i.d. *600 mm total)	Indirect UV, 254 nm	NS	
Chloride, bromide and sulfate	PDDPi-chromate (0.154 % w/v)	5 mM chromate, pH 8.0	530 mm x 77 μm i.d. *600 mm total)	Indirect UV, 254 nm	NS	
Malonate, lactate, acetate, succinate and citrate	PDDPi-chromate (0.154 % w/v)	5 mM chromate, pH 8.0	530 mm x 77 μm i.d. *600 mm total)	Indirect UV, 254 nm	NS	
Bromide, chloride, iodide, nitrite, nitrate, sulfate, perchlorate, fluoride, phosphate, carbonate, acetate, PAR, cobalt(II) PAR, nickel(II) PAR and Iron(II) PAR	Polybrene (0.05% w/v)	5 mM potassium chromate, pH 8.90	460 mm x 50 μm i.d. (600 total)	Indirect UV, 254 nm for first 2 min, direct vis 490 nm after 2 min	Up to 400,000	[59]
Nitrite, bromide, nitrate, iodide and thiocyanate	PEI (0 – 0.1% w/v)	20 mM acetate, pH 5	630 mm x 75 μm i.d. (760 total)	Direct UV, 210 nm	NS	[31]
4-nitrophenol, 3-nitrophenol, 2-chlorophenol, 3-chlorophenol and 4-chlorophenol	PEI (0.5% w/v)	20 mM Tris, pH 8.3	600 mm x 75 μm i.d. (750 mm total)	Direct UV, 210 nm	NS	[64]

Table 1.4: Separations of inorganic and small organic anions by CEC using a water-soluble polymer as a pseudo-phase (ctd)

Analytes	Chromatographic phase	Electrolyte	Column dimensions	Detection	Efficiency (plates/m)	Ref.
Nitrate, iron(III) CDTA, manganese(II) CDTA, cadmium(II) CDTA, palladium(II) CDTA, nickel(II) CDTA, cobalt(II) CDTA, zinc (II) CDTA and coper(II) CDTA	PDDAC (50 mM)	3 mM sodium sulfate, 10 mM sodium acetate, pH 7.0	450 mm x 50 μm i.d. (500 total)	Direct UV, 210 nm	220,000 – 300,000	[61]
Bromide, iodide, nitrite, nitrate, chromate, thiocyanate and molybdate	PDDA-chloride (0.05% w/v)	150 mM lithium sulfate, 20 mM borate, pH 8.5	325 mm x 50 μm i.d. (400 mm total)	Direct 214 nm	NS	[65]
Benzoate, benzoatesulfonate, *p*-toluenesulfonate, *p*-aminobenzoate, *p*-hydroxybenzoate, 2-naphthalenesulfonate, 1-naphthalenesulfonate, 3,5-dihydroxybenzoate and 2,4-dihydroxybenzoate	PDDA-chloride (1.0% w/v)	150 mM lithium sulfate, 20 mM borate, pH 8.5	325 mm x 50 μm i.d. (400 mm total)	Direct 214 nm	NS	
Bromide, nitrite, nitrate, chromate, iodide, molybdate, phthalate, 1,2,3-benzenetricarboxylate, 1,2-benzenedisulfonate, terephthalate, isophthalate, benzoate, *p*-toluenesulfonate, 1,3,5-benzenetricarboxylate, 2-naphthalenesulfonate, 1-naphthalenesulfonate, 3,5-dihydroxybezoate and 2,4-dihydroxybenzoate	PDDA-chloride (0.3% w/v)	120 mM lithium sulfate, 20 mM borate, pH 8.5	325 mm x 50 μm i.d. (400 mm total)	Direct 214 nm	NS	

Table 1.4: Separations of inorganic and small organic anions by CEC using a water-soluble polymer as a pseudo-phase (ctd)

Analytes	Chromatographic phase	Electrolyte	Column dimensions	Detection	Efficiency (plates/m)	Ref.
Cobalt(II) HBED, alminium HBED, manganese(III) HBED, lead(II) HBED, iron(III) HBED, cadmium(II) HBED, copper(II) HBED, zinc(II) HBED, nickel(II) HBED	PDDA-hydroxide (50 mM)	10 mM sodium tetraborate, 0.1 mM HBED adjusted to pH 10 with acetic acid	455 mm x 50 μm i.d. (500 mm total)	Direct UV, 242 nm	NS	[63]
Bismuth(III) HBED, scandium(III) HBED, indium(III) HBED, cobalt(III) HBED, gallium(III) HBED, aluminium(III) HBED, chromium(III) HBED, manganese(III) HBED, lead(II) HBED, iron(III) HBED, cadmium(II) HBED, palladium(II) HBED, cobalt(II) HBED, copper(II) HBED, zinc(II) HBED, nickel(II) HBED, manganese(II) HBED, Vanadate	PDDA-hydroxide (55 mM)	10 mM sodium tetraborate, 0.1 mM HBED adjusted to pH 10 with acetic acid	455 mm x 50 μm i.d. (500 mm total)	Direct UV, 242 nm	NS	[62]
Copper(II) EDDHA	PDDA-chloride (10 mM)	5 mM sodium sulfate, 10 mM tetraborate, pH 9.2	455 mm x 50 μm i.d. (500 mm total)	Direct UV, 242 nm	NS	

NS – not stated; DEAE-dextran – (diethylamino)ethyldextran; PDDA – poly(diallyldimethylammonium); PDDPi– poly(1,1-dimethyl-3,5-dimethylenepiperidinium); PDDPy– poly(1,1-dimethyl-3,5-dimethylenepyrrolidinium), HDM - hexadimethrine, DEAED-chromate – diethylaminodextran; EDTA – ethylenediaminetatreacetic acid, CDTA – *trans*-1,2-diaminocyclohexane-N,N,N',N'-tetraacetic acid; PAR – 4-(2-pyridylazo)resorcinolate; PEI – poly(ethyleneimine); HBED – N.N-bis(hydroxybenzyl)ethylenediamine-N,N-diacetic acid, EDDHA - ethylenediaminedi(*o*-hydroxyphenylacetic acid)

N,N-bis(hydroxybenzyl)ethylenediamine-N,N-diacetic acid (HBED) [62,63]. In all cases they found the addition of cationic polymer improved the separation providing better resolution between many of the complexes. Interestingly, the use of HBED as a ligand gave two peaks for cobalt(III), palladium(II) and vanadium(V) due to different internal complexation with the ligand thereby making its practical use somewhat restricted.

The effect of adding poly(ethyleneimine) (PEI) to the electrolyte on the migration of inorganic anions [31] and phenols [64] has been reported by Erim and co-workers. In both cases, the addition of polymer to the electrolyte improved the resolution of the analytes, and high concentrations could be employed to make the analytes migrate after the EOF. However, in these conditions, the baseline became unstable, peak shapes deteriorated, the analysis time was prolonged, and the resolution was similar to that obtained at lower concentrations.

Recently, Fritz and co-workers [65] demonstrated that varying the salt type and the concentration of the polymer could control the ion-exchange interaction with the pseudo-phase. In contrast to previously reported work, the salt was added in concentrations higher than usually employed in CE (up to 150 mM) with no detrimental effects from Joule heating. Such addition of high concentrations of salt was found to be beneficial as it overrode the effect of the counter-ion added with the polymer, allowing the concentration of salt to be used as an additional variable to control selectivity. This provided excellent separations of mixtures of UV-absorbing inorganic and organic anions.

1.2.4.3 Macrocyclic molecules

Macrocyclic pseudo-phases offer the potential to provide different separation selectivity to IE pseudo-phases, which has led to the examination of various macrocycles for use as a pseudo-phases (Table 1.5). The first use of non-IE type interactions to moderate the selectivity of inorganic anions was by Lamb *et al.* [66]

Table 1.5: Separations of inorganic and small organic anions by CEC using macrocyclic compounds as a pseudo-phase

Analytes	Chromatographic phase	Electrolyte	Column dimensions	Detection	Efficiency (plates/m)	Ref.
Bromide, chloride, iodide, sulfate, nitrite, nitrate and thiocyanate	Cryptand 2.2.2 (2-16 mM)	2 mM potassium tetraborate, 1.8 mM sodium dichromate and 43 mM boric acid	550 mm x 75 μm i.d. (600 mm total)	Indirect UV, 254 nm	NS	[66]
Iodide, nitrate, thiocyanate, bromate, chromate and iodate	Cryptand 22 (10 mM)	pH 7 adjusted with acetic acid	600 mm x 75 μm i.d. (800 mm total)	Direct UV, 214 nm	NS	[67]
p-hydroxybenzoate, *p*-chlorobenzoate, *p*-nitrobenzoate, benzoate and terephthalate	Cryptand 22 (0.5 mM)	pH 7 adjusted with acetic acid	600 mm x 75 μm i.d. (800 mm total)	Direct UV, 254 nm	NS	
Chloride, sulfate, nitrate and nitrite	*p*-sulfonic calix[6]arene (0.05 mM)	4 mM potassium bromide, pH 3.1	570 mm x 75 μm i.d. (NS)	NS	NS	[70]
Nitrate, iodide, bromate, thiocyanate, perchlorate, iodate, ethanesulfonate, butanesulfonate, pentanesulfonate and octanesulfonate	γ-cyclodextrin (12 mM)	5 mM chromate, pH 8	520 mm x 75 μm i.d. (600 mM total)	Indirect UV, 254 nm	NS	[68]
Nitrate, iodide, bromate, thiocyanate and perchlorate	α-cyclodextrin (20 mM)	5 mM chromate, pH 8	520 mm x 75 μm i.d. (600 mM total)	Indirect UV, 254 nm	NS	
Chloride, bromide, iodide, sulfate, nitrate, nitrite, fluoride and phosphate	α-cyclodextrin (25-90 mM)	7 mM succinic acid, 0.5 mM Bis-Tris, 0.2% (w/v) MHEC, pH 3.55	130 mm x 300 μm i.d. (230 mm total) PTFE capillary	Contactless conductivity detection	60,000 – 180,000	[69]

NS – not stated; Bis-Tris – 1,3-bis[tris(hydroxymethyl)methylamino]propane, MHEC - methylhydroxyethylcellulose

who used a crown ether complexed with an alkali metal as a modifier for CE. They observed that increasing the concentration of cryptand 2.2.2 from 2 to 16 mM resulted in an increase in resolution between chloride and iodide due to increased association with the cryptand.

A similar approach was undertaken by Chiou and Shih [67] who used the marcocylic polyether cryptand-22 to influence the migration of UV-absorbing anions. As the concentration was increased up to 5 mM, mobilities for all ions levelled off except for thiocyanate which showed a sharp decrease in mobility at the higher concentrations. No explanation for this effect was given, but the potential use of this type of analyte discrimination is great.

Stathakis and Cassidy [68] used α-, β-, and γ-cyclodextrins as separation phases to change the migration order of inorganic anions. They found that polarisable anions (iodide, thiocyanate and perchlorate) were influenced the most by the addition of cyclodextrin to the electrolyte. Analyte-cyclodextrin association was found to decrease in the order α, β and γ-cyclodextrin, which corresponded to an increase in the cavity size of the macrocycle. Changing the electrolyte anion from chromate to phthalate provided lower mobilities, indicating increased interaction with the chromatographic phase. A subsequent report by Masár *et al.* [69] using α-cyclodextrin showed great potential for selectivity manipulation of high mobility inorganic anions, with the resolution being improved markedly upon the addition of low concentrations (10 mM) of the cyclodextrin. Greatest changes were observed for iodide and this approach was used to analyse iodide in a dietary salt which contained a large excess of chloride.

The use of calixarenes for selectivity manipulation of inorganic anions was examined by Arce *et al.* [70], however no detailed results were presented on the ability of the *p*-sulfonic calix[6]arene to complex inorganic and small organic anions, and the separation provided showed a selectivity similar to that observed in CE.

1.3 Sensitivity improvement

The substantially higher detection limits offered by electrophoretic techniques in comparison to LC methods is considered to be one of the major disadvantages of CE methods. Many ways to improve the sensitivity of CE have been developed and can be divided very generally into three categories: those based on electrophoretic methods, those based on chromatographic methods, and those comprising both chromatographic and electrophoretic components. For completeness and perspective, all methods for preconcentration of inorganic and small organic anions published will be reviewed here, and are summarised in Table 1.6.

1.3.1 Electrophoretic methods

Electrophoretic preconcentration methods for CE are generally based on the principle of velocity difference induced focusing (V-DIF). This is where analyte preconcentration is achieved by analytes possessing different velocities in two different zones in the capillary. This is perhaps best illustrated by field amplified stacking, the most common preconcentration method for CE. In this method, the sample has a lower conductance than the electrolyte (at least by a factor of 3). When the voltage is applied, as the resistance of the sample is higher than the electrolyte the field strength over this zone is higher than the rest of the electrolyte. As electrophoretic mobilities are directly proportional to field strength, ions will rapidly migrate out of the sample zone into the electrolyte zone where they effectively stop due to the reduced field strength. In this way, analytes are focused along the boundary between the sample and the electrolyte. Other V-DIF methods include isotachophoretic stacking and sweeping (discussed in section 1.3.3).

1.3.1.1 Stacking

As mentioned above, field amplified stacking is present in all electrophoretic methods when the sample has a lower conductance than the electrolyte and the

Table 1.6: Approaches to the preconcentration of inorganic and small organic anions for CE.

Analytes	Method (factor)	Electrolyte	Limit of detection (ppb)	Column dimensions	Detection	Ref
Bromide, chloide, sulfate, oxalate, chlorite, malonate and fluoride (in 0.9 M boric acid)	Electrokinetic injection (10)	5 mM sodium chromate, 0.01 mM TTAB, pH 8.1	Bromide (0.3) chloride (0.5) sulfate (0.2) nitrate (0.3) oxalate (0.4) chlorite (0.4) malonate (0.4) fluoride (0.7)	700 mm x 75 μm i.d. (850 mm total)	Indirect UV, 254 nm	[73]
Bromide, chloride, sulfate, nitrite and nitrate (in snow)	Electrokinetic injection	6 mM 2-aminopyridine, 3 mM chromate, 0.05 mM CTAB, pH 8.2	NS	300 mm x 50 μm i.d. (350 mm total)	Indirect UV, 254 nm	[74]
Bromide, iodide, chromate, nitrate, thiocyanate, molybdate, tungstate, bromate, clhorate, arsenate and iodate (in water)	Stacking (33-43)	20 mM phosphate, pH 8.0	Bromide (24), iodide (33), chromate (53), nitrate (14), thiocyanate (23), molybdate (40), tungstate (75), bromate (99), clhorate (82), arsenate (260) and iodate (74)	500 mm x 50 μm i.d. (645 mm total) polyethylene glycol coated capillary	Direct UV, 200 nm	[75]
Bromide, chloide, sulfate, oxalate, chlorite, malonate and fluoride (in 0.9 M boric acid)	LVSS (100)	5 mM sodium chromate, 0.01 mM TTAB, pH 8.1	Bromide (0.07) chloride (0.04) sulfate (0.02) nitrate (0.04) oxalate (0.03) chlorite (0.05) malonate (0.05) fluoride (0.89)	700 mm x 75 μm i.d. (850 mm total)	Indirect UV, 254 nm	[73]
Dimethylarsenic acid, monomethylarsenic acid and arsenic(V) (in water)	LVSS with polarity switching at 95% of normal current (10-20)	20 mM disodiumhydrogen phosphate adjusted to pH 6 with phosphoric acid	NS	620 mm x 75 μm i.d. (700 mm total)	Direct UV, 195 nm	[76]

Table 1.6: Approaches to the preconcentration of inorganic and small organic anions for CE. (ctd)

Analytes	Method (factor)	Electrolyte	Limit of detection (ppb)	Column dimensions	Detection	Ref
Dimethylarsenic acid, monomethylarsenic acid and arsenic(V) (in water)	LVSS (30-40)	20 mM disodiumhydrogen phosphate, 0.41 mM TTAB adjusted to pH 6 with phosphoric acid	NS	620 mm x 75 μm i.d. (700 mm total)	Direct UV, 195 nm	[77]
Fumaric and maleic acid (in water)	LVSS (300)	40 mM potassium hydrogen phthalate, 1 mM phosphoric acid, pH 3.27	NS	460 mm x 50 μm i.d. (610 mm total)	Direct UV, 200 nm	[78]
Bromide and nitrate (in 0.8 M boric acid)	LVSS (300)	40 mM potassium hydrogen phthalate, 1 mM phosphoric acid, pH 3.27	NS	460 mm x 50 μm i.d. (610 mm total)	Direct UV, 210 nm	
Bromate, nitrate and bromate (in water)	LVSS (100)	75 mM phosphate, pH 1.9	Bromide (2.22), nitrate (1.83), bromate (6.51)	560 mm x 50 μm i.d. (645 mm total)	Direct UV, 200 nm	[79]
Iodide, nitrate, nitrite and iodate (in sea water)	LVSS (10)	500 mM potassium chloride, pH 4.0	Iodide (177), nitrate (20), nitrite (19), iodate (192)	500 mm x 50 μm i.d. (720 mm total)	Direct UV, 210 nm	[80]
Bromate, nitrate and bromate (in water)	FESI (1000)	75 mM phosphate, pH 1.9	NS	560 mm x 50 μm i.d. (645 mm total)	Direct UV, 200 nm	[79]

Table 1.6: Approaches to the preconcentration of inorganic and small organic anions for CE. (ctd)

Analytes	Method (factor)	Electrolyte	Limit of detection (ppb)	Column dimensions	Detection	Ref
Chloride, sulfate, nitrate, oxalate, fluoride, formate, phosphate, acetate and propionate (in water)	Single column t itp (400)	Leading/CE electrolyte : 10 mM sodium chromate, 0.5 mM OFM anion BT, adjusted to pH 8 with sulfuric acid Terminating : 75 μM octanesulfonate added to sample	Chloride (0.5), sulfate (0.3), nitrate (0.8), oxalate (0.6), fluoride (0.3), formate (0.5) phosphate (0.3), acetate (0.8)and propionate (0.6)	520 mm x 75 μm i.d. (600 mm total)	Indirect UV, 254 nm	[81]
Chloride, sulfate, nitrate, fluoride and phosphate (in water)	Single column t-itp (NS)	Leading/CE electrolyte : 2.25 mM pyromellitic acid, 6.50 mM sodium hydroxide, 0.75 mM hexamethonium hydroxide, 1.6 mM triethanolamine, pH 7.7 Terminating 50 μM octanesulfonate added to sample	Chloride (0.5), sulfate (0.6), nitrate (1.5), fluoride (0.9) and phosphate (2.0)	450 mm x 50 μm i.d. (500 mm total)	Indirect UV, 215 nm	[82]
Nitrite, fluoride and phosphate (in water with a 200-2000 fold excess of chloride or sulfate)	Dual column t-itp (NS)	Leading: 8 mM BALA-Chloride. 3 mM Bis-Tris, 0.2 % MHEC, pH 3.4 Terminating: 4 mM BALA-ASP, pH 4 CE electrolyte: 10 mM BALA-ASP, 0.2% MHEC, pH 3.4	Nitrite (0.2), fluoride (0.3), phosphate (0.6)	Itp: 150 mm x 850 μm i.d. FEP CE: 150 mm x 300 μm i.d. FEP	Conductivity detection	[83]

Table 1.6: Approaches to the preconcentration of inorganic and small organic anions for CE. (ctd)

Analytes	Method (factor)	Electrolyte	Limit of detection (ppb)	Column dimensions	Detection	Ref
Bromide, chloride, sulfate and nitrate (in hydrofluoric acid)	Single column t-itp (NS)	Leading/CE electrolyte: 7.5 mM potassium chromate, 0.2 mM TTAOH, pH 8.5 Terminating: 100-500 mM fluoride in sample	Sulfate (288), chloride (175), nitrate (310)	700 mm x 50 μm i.d. (860 mm total)	Indirect UV, 254 nm	[84]
Chloride, sulfate, nitrate and chlorate (in water)	Single column t-itp (NS)	Leading/CE electrolyte: 5 mM potassium chromate, 0.15 mM TTAOH, pH 8.4 Terminating: 1-400 mM fluoride in sample	NS	650 mm x 75 μm i.d. (800 mm total)	Indirect UV, 254 nm	[85]
Bromide, chloride, sulfate, nitrate, oxalate, chlorate, perchlorate, malonate, formate, phosphate, acetate, propionate and carbonate (in water)	Single column t-itp (NS)	Leading: 0-400 mM hydroxide in sample Terminating/CE electrolyte: 7.5 mM sodium salicylate, 0.1 mM TTAOH, pH 8	NS	650 mm x 75 μm i.d. (800 mm total)	Indirect UV, 232 nm	
Bromide, chloride, sulfate, nitrate, oxalate, chlorate, perchlorate and phosphate	Single column dual t-itp (NS)	Leading 1/CE electrolyte: 7 mM chromic acid, 17 mM Tris, 1 mM DoTAOH, pH 7.9 Terminating 1/Leading 2: 10 mM fluoride in sample terminating 2: 10 mM acetate in sample	NS	700 mm x 75 μm i.d. (860 mm total)	Indirect 274 nm	

Table 1.6: Approaches to the preconcentration of inorganic and small organic anions for CE. (ctd)

Analytes	Method (factor)	Electrolyte	Limit of detection (ppb)	Column dimensions	Detection	Ref
Iron(III) EDTA (various water samples)	Dual column t-itp (NS)	Leading: 10 mM hydrochloric acid, 20 mM Lhistidine, 0.1% HPMC, pH 6. Terminating: 5 mM MES CE electrolyte: 25 mM MES, 10 mM Bis-Tris, pH 6.6	NS	Itp: 160 mm x 800 μm i.d. FEP CE : 900 mm x 300 μm i.d.	Conductivity and direct UV, 254 nm	[86]
Chloride, nitrite, nitrate and sulfate (in water)	Single column t-itp (NS)	Leading/CE electrolyte: 50 mM CHES, 20 mM Lithium hydroxide, 0.03% Triton X, pH 9.2 Terminating: 5 ppm octane sulfonate added to sample	NS	600 mm x 50 μm i.d. (600 mm total)	Conductivity detection	[87]
Bromide, iodide, nitrate, nitrite and iodate (in sea water)	Single column t-itp (2)	Leading: Sample conatining 0.05 M KCl Terminating/CE electrolyte: 20 mM 18-crown-6, 90 mM potassium chloride, 10 mM potassium fluoride (pH 4.0)	NS	400 mm x 50 μm i.d. (480 mm total)	Direct UV, 210 nm	[80]

Table 1.6: Approaches to the preconcentration of inorganic and small organic anions for CE. (ctd)

Analytes	Method (factor)	Electrolyte	Limit of detection (ppb)	Column dimensions	Detection	Ref
Gold cyanide (water and gold leaching solution)	Non-automated off-line SPE (Sep-pak C18 cartridge modified by adsorption of PIC A) – CE	2.5 mM trimellitate, 0.8 mM hexamethonium bromide, pH 9.5	NS	520 mm x 75 μm i.d. (600 mm total)	Indirect UV, 254 nm	[88]
Iron(II) cyanide, cobalt(III) cyanide, iron(III) cyanide, nickel(II) cyanide, palladium(II) cyanide, platinum(II) cyanide, copper(I) cyanide, chromium(III) cyanide and silver(I) cyanide (in water)	Non-automated, off-line SLM (methyltrioctylammonium chloride in dibutyl either with perchlorate as the stripping solution)	15 mM perchlorate, 0.1 mM cyanide	6.0×10^{-9} M for iron(III) cyanide – 1.2×10^{-7} M for palladium(II) cyanide	520 mm x 75 μm i.d. (600 mm total)	Direct UV, 214 nm	[89]
Bromide, nitrite, nitrate and iodide (in water)	Automated on-line SPE (Amberlite IRA-410 anion exchanger) – CE (5)	25 mM sodium chloride, 0.3 mM CTAC	NS	450 mm x 50 μm i.d. (800 mM total)	Direct UV, 200 nm	[90]

Table 1.6: Approaches to the preconcentration of inorganic and small organic anions for CE. (ctd)

Analytes	Method (factor)	Electrolyte	Limit of detection (ppb)	Column dimensions	Detection	Ref
Bromide, nitrite, nitrate and iodide (in water)	Automated off-line SPE (IonPac TAC-LP1 Dionex anion concentrator column) – suppressor – CE (10)	20 mM tetraborate, 0.09 mM CTAB	NS	500 mm x 75 μm i.d. (600 mm total)	Direct UV, 200 nm	[91]
Diphenylamine-4-sulfonate, anthrachinone-2-sulfonate, diphentl-4-sulfonate, 1-amino-5-naphthalenesulfonate, 2-amino-1-naphthalenesulfonate, 1-naphthalenesulfonate, 3-aminobenzenesulfonate, 4-chlorobenzenesulfonate, 4-toluenesulfonate, benzenesulfonate, 4,4'-diamino-2-2'-stilbenzenedisulfonate, 1-naphthol-4-sulfonate, 1,5-naphthalenedisulfonate, 2-naphthol-3,6-disulfonate	Non-automated off line SPE (reversed phase, LiChrolut EN) (2000)	25 mM sodium borate, pH 9.3	NS	500 mm x 75 μm i.d. (600 mm total)	LIF excitation 230 nm, emission 335 or 410 nm	[92]

NS – not stated; LVSS – Large volume sample stacking; FESI – Field enhanced sample injection; t-itp – transient isotachophoresis; BALA - β-alanine, Bis-Tris – 1,3-bis[tris(hydroxymethyl)methylamino]propane; ASP – Aspartic acid; MHEC – methylhydroxyethylcellulose; FEP –Fluorinated ethylene polymer; CHES - 2-(cyclohexylamino)ethanesulfonic acid, Tris – tris(hydroxymethyl)amino methane, DoTAOH – dodecyltrymethylammonium hydroxide CTAC – cetyltrimethylammonium chloride; CTAB – cetyltrimethylammonium bromide; DTAB – dodecyltrimethylammonium bromide; TTAOH – tetradecyltrimethylammonium hydroxide

sample volume occupies less than 5% of the capillary volume. The potential of using this concept to stack large volumes of sample led to the development of large volume sample stacking (LVSS) by Burgi and Chien [71]. In this case, up to 90% of the capillary is filled with sample and a reversed polarity is applied. This results in the EOF being directed back out the injection end of the capillary column. When the current reaches 95% of the normal level, the polarity is returned to its normal configuration and the separation proceeds in the usual manner. While this was a significant development in the improvement of sensitivity, not all instruments possess the ability to perform polarity switching, which limits the general applicability of this method. This was later overcome by reversing the EOF using an EOF modifier added to the electrolyte [72]. When the sample is injected, the modifier dissolves off the wall in the sample zone leaving a negative surface charge which causes the EOF to move towards the column inlet. As the electrolyte is drawn through the capillary, it re-coats the surface with modifier, slowing down the EOF and gradually causing a change in direction, at which stage the separation proceeds normally. While these two approaches provide an excellent means to improve the detection sensitivity, the main limitation is that the sample volume is restricted by the volume of the capillary. Longer capillaries can be used but this prolongs analysis time due to a reduction in field strength and is not a practical alternative.

The use of LVSS with acidic electrolytes for the preconcentration of inorganic anions was first reported by Boden *et al.* [73]. They found that LVSS enabled detection limits for common inorganic anions to be lowered by a factor of 200 over conventional hydronamic injection and a factor of 10 over electrokinetic injection. LVSS was the preferred method as it avoided the discriminatory nature of electrokinetic injection while also providing better reproducibility and lower detection limits. The method was applied to the determination of inorganic anions in boric acid.

A similar approach was undertaken by He and Lee [74] who also used acidic electrolytes for LVSS of inorganic anions. They obtained a 300 fold increase in sensitivity for maleic and fumaric acids and for bromide and nitrate using LVSS. The method was also used to determine bromide and nitrate in boric acid.

The potential of LVSS with and without polarity switching for the preconcentration of arsenic compounds was examined by Albert *et al.* [75,76]. They found that using polarity switching enabled a preconcentration factor of 10-20 to be achieved, while a preconcentration factor of 40 was obtained without the use of polarity switching. No explanation was offered for the better sensitivity obtained without polarity switching.

Quirino and Terabe compared LVSS and field-enhanced sample injection (FESI) for the preconcentration of inorganic anions [79]. FESI is similar to LVSS but instead of filling the capillary with sample, a large water plug is injected into the capillary hydrodynamically and the sample is injected into this using electrokinetic injection. As the water plug migrates out of the capillary in the direction of the inlet, the field across the sample increases and more analyte migrates into the capillary. While FESI provided higher preconcentration factors than LVSS (1000 compared to 100), the system was highly irreproducible, suffering many of the problems inherent with electrokinetic injection, such as non-linear response, irreproducible injection arising from changes in EOF, analyte discrimination based on electrophoretic mobility and susceptibility to changes in sample ionic strength.

Sample stacking for preconcentration of inorganic anions was examined by Soga *et al.* [78]. Using a polyethyleneglycol coated capillary which eliminated EOF, they found that increasing the injection volume resulted in an increase in sensitivity, but the efficiency of the separation decreased. Isotachophoretic preconcentration was also examined, but was found to be more difficult to implement than stacking.

The application of LVSS to the determination of inorganic anions in sea water has been examined by Timerbaev *et al.* [80], who found that a 10 fold increase in sensitivity for nitrate and nitrite could be obtained. While this factor is lower than

other reports of LVSS, the authors noted that this was a substantial development in improving the sensitivity of trace ions in highly saline samples. The detection limits obtained for nitrate and nitrite were 20 ppb in a matrix with a 5 x 10^4 molar excess of chloride.

1.3.1.2 Isotachophoretic preconcentration

The concept of isotachophoretic preconcentration/sample clean up for capillary electrophoresis was first demonstrated by Foret *et al.* [93]. Sample was injected into an isotachophoretic system between a leading (high mobility) and terminating (low mobility) electrolyte with the concentration of anions adjusted by their mobility according to the Kohlrausch regulating function. This method enabled the sensitivity to be improved by a factor of 200 over conventional CE. One potential disadvantage of this method was the need to couple two instruments together, thereby complicating the system.

Isotachophoretic preconcentration was applied to the preconcentration of anions by Bondoux *et al.* [81]. In contrast to the system developed by Foret *et al.* [93] only one instrument was used, however in this case the terminating ion (octanesulfonate) was added to the sample and injection was performed electrokinetically. This enabled a 400-fold increase in sensitivity to be achieved with detection limits below the ppb level being reported for the separation of inorganic anions. The method was applied to the determination of primary and secondary water from nuclear power plants. The electrolyte conditions in this type of system were examined by Wojtusik *et al.* [82] who found that electrolyte pH, anion type and injection voltage were important parameters that needed to be optimised in order to retain the high efficiency of CE. Using their optimised method, sub-ppb levels of inorganic anions were obtained.

Kaniansky *et al.* [83] used a two instrument isotachophoretic – electrophoretic setup to determine trace anions with macro constituents (chloride and sulfate) in water samples. They were able to detect fluoride, phosphate and nitrite in trace levels with

a 2-3 x 10^4 molar excess of chloride and sulfate using the dual-column procedure, illustrating the potential of isotachophoretic preconcentration/clean-up prior to CE for difficult samples.

The potential of isotachophoretic pre-treatment in a single instrument utilising the matrix anions as the leading or terminating ions was examined by Boden *et al.* [84]. The low mobility of fluoride enabled it to act as a terminating ion with chromate being used as the leading/electrolyte ion, allowing the determination of trace ions in hydrofluoric acid without any sample treatment. To extend the method even further, the addition of two terminating ions (fluoride and acetate) to the sample was investigated and found to establish two isotachophoretic preconcentration zones, which extended the mobility range to anions with a mobility lower than the first terminating ion. This was illustrated by determining ions in a HF sample with the addition of acetate as the second terminating ion enabling the analysis of phosphate. An alternative approach of adding the leading ion to the sample (such as hydroxide), was also discussed. A low mobility anion, such as salicylate, was added to the electrolyte and functioned as the terminating ion. This was particularly useful for the analysis of highly alkaline samples.

A single column isotachophoretic – capillary electrophoretic method for the determination of inorganic anions in sea water was examined by Timerbaev *et al.* [80]. By using the chloride in the sample as the leading ion and adding fluoride or phosphate to the electrolyte as the terminating ion, the detection limit could be lowered by a factor of 2. However, better sensitivity for this type of sample could be obtained using LVSS.

1.3.2 Chromatographic methods

Chromatographic methods for preconcentration offer a significant advantage over other preconcentration methods for CE in that the sample volume injected is potentially infinite, being limited only by time and capacity. Solid phase extraction

(SPE) is by far the most popular method, but the use of supported liquid membranes (SLM) has found some applications for sample clean-up and preconcentration.

1.3.2.1 Solid phase extraction

The first application of SPE to CE was by Guzman *et al.* [94] who used a small packed bed placed at the front of the capillary for the preconcentration of methamphetamine prior to electrophoretic separation. Since then, there have been numerous developments with packed beds [95-102], open tubular [103-105], and disks [106] having been examined for SPE [90,107]. While the latter are often preferred due to the high flow rate and low sample elution volume, on-column methods using open tubular or packed beds are becoming increasingly popular due to the ease of automation and implementation. However, the use of packed bed preconcentrator columns suffers from low flow-rates, while OT preconcentrators suffer from having a low sample capacity. Most SPE methods have concentrated on using reversed phase interactions to preconcentrate analytes, but a few reports on SPE for the preconcentration of inorganic and small organic anions by IE interactions have also appeared.

The preconcentration of the gold-cyanide complex prior to CE was reported by Buchberger and Haddad [88]. A reversed phase C18 Sep-Pak cartidge was coated with the ion interaction reagent, PIC A to provide ion-exchange sites onto which the complex could adsorb. A sample volume of 20 mL was passed through the column and eluted in 2 mL of solvent, resulting in a 10 fold increase in sensitivity. Application to a real gold leach sample resulted in a lower than expected recovery due to competition for the IE sites from sample matrix ions, such as chloride and sulfate.

A continuous on-line method for the IE preconcentration of inorganic anions for CE was developed by Arce *et al.* [90], who coupled a flow-injection analysis (FIA) system to a CE. This was accomplished by using a constructed interface which

placed the capillary inlet and electrode into the flow of the FIA system, with injection performed by continuous application of the high voltage. An IE column was placed in the FIA system and elution was performed using a chloride based eluent. Using this method a five fold increase in sensitivity was reported.

An automated off-line method was developed by Novic and Gucek [91] for the preconcentration of inorganic anions. They used an IE column in a FIA system, but in contrast to previous methods, used a carbonate eluent for analyte elution which was suppressed before placing the effluent in a CE vial and using it as the sample for CE separation. Using this method, it was possible to preconcentrate 5 mL down to 0.5 mL giving a 10 fold increase in sensitivity.

The preconcentration of aromatic sulfonic acids was reported by Loos *et al.* [92] who used an off-line method for preconcentration. The procedure was rather lengthy with 200 mL of sample being passed through a C18 column at a flow-rate of 5 mL/min before the resin was washed and dried under nitrogen. The acids were then eluted with 4 mL of methanol-acetone (3:2 v/v), the solvent evaporated and the analytes redissolved in 100 μL of water and injected into the CE instrument. This gave a preconcentration factor of 2000, but this was a labour intensive procedure and would be difficult to automate.

1.3.2.2 Supported liquid membranes

Preconcentration techniques based on SLMs involve an organic liquid phase that is held in the pores of a thin porous support. The aqueous sample flows across one side of the membrane with a small volume of aqueous acceptor phase held in contact with the other side (called the stripping solution). Analytes diffuse through the membrane and preconcentrate on the other side in the stationary stripping solution. This approach has been used for the preconcentration of metallo-cyanide complexes by Kuban *et al.* [89]. Preconcentration was achieved using methyltrioctlyammonium chloride in dibutyl ether as the active component of the liquid membrane. Ion-

pairing interaction of the anions with the cationic amine caused the complex to cross the membrane into an aqueous perchlorate phase which was suitable for direct injection into the CE. This resulted in preconcentration factors between 50 and 600 being achieved for a selection of metal complexes, giving detection limits in the nM range.

1.3.3 Combined electrophoretic and chromatographic methods

The concept of using both electrophoretic and chromatographic methods for preconcentration has only started to receive considerable attention in the last two years. This is predominantly due to the realisation that the combination of the two different techniques can provide exceptionally high preconcentration factors. This has been convincingly shown by Quirino and Terabe [6] who have used the concept of sweeping, which is where a pseudo-phase front passes through the sample focusing all analytes on the front of the pseudo-phase zone, in combination with the electrophoretic preconcentration method of field enhanced sample injection. This provided an improvement in sensitivity of nearly 1,000,000 over conventional injection. While this is an impressive figure, this technique is limited in that the amount of sample that can be preconcentrated is limited by the water plug injected prior to electrokinetic injection.

The use of electrokinetic injection with a heterogenous phase for preconcentration was reported recently by Zhang *et al.* [108]. They used a capillary packed with 3 μm Hypersil ODS material for the preconcentration of basic pharmaceutical compounds with a 17,000 fold increase in sensitivity being obtained. While not as impressive as the preconcentration obtained above, this method has the advantage that a heterogenous phase can be used and the amount injected can potentially be infinite.

Palmer and Landers [109-111] have developed a pseudo-phase stacking method applicable to high ionic strength samples. In this case, a high concentration of a high mobility anion has been added to the sample to cause the micelles to stack on the

electrolyte/sample interface. Analytes migrating through the column are trapped by the micelles on the boundary before being separated by conventional pseudo-phase CEC.

While these methods illustrate the potential to obtain high preconcentration factors, one disadvantage is the use of electrokinetic injection, which is extremely susceptible to changes in sample composition and discriminates analyte injection on the basis of electrophoretic mobility.

1.4 Project aims

From the results in the literature, it is evident that the combination of chromatographic and electrophoretic mechanisms provides significant advantages over conventional electrophoretic approaches. However, there are clearly areas where a fundamental understanding of the principles underlying the combination of these two mechanisms is lacking. This is particularly the case with packed and open tubular columns whereby the fixed capacity of the column dictates that alternative approaches for selectivity control must be sought. Likewise, the variability of using pseudo-phase columns increases the freedom of the system, but there is little understanding of how all the available parameters can be varied to give the desired outcome. Finally, no on-line solid phase extraction methods for the preconcentration of inorganic anions have been reported.

Therefore the general aim of this work has been to examine the potential of IE-CEC using pseudo- and open tubular ion-exchange phases for the improvement of the separation of inorganic and small organic ions. The specific aims of the project were to:

- Examine the extent to which open tubular columns can be used for the separation of inorganic anions by IE-CEC and the extent to which the experimental

parameters can be varied to control the separation selectivity and the separation efficiency.

- Investigate the extent to which the experimental parameters can be varied to influence the separation of inorganic and small organic anions using a polymeric pseudo-phase,
- Develop a theoretical model based on IE and CE theory to describe the migration of anions in IE-CEC using both OT and pseudo-phase columns, and
- Develop a method for the on-line preconcentration of inorganic anions for CE using an open tubular IE column.

1.5 References

1. V. Pretorius, B.J. Hopkins and J.D. Schieke, *J.Chromatogr.*, 99 (1974) 23.
2. J.W. Jorgenson and K.D. Lukacs, *J.Chromatogr.*, 218 (1981) 209.
3. S. Terabe, K. Otsuka and T. Ando, *Anal.Chem.*, 57 (1985) 834.
4. S. Terabe, K. Otsuka, K. Ichikawa, A. Tsuchiya and T. Ando, *Anal.Chem.*, 56 (1984) 111.
5. J.H. Knox, *J.Chromatogr.A*, 680 (1994) 3.
6. J.P. Quirino and S. Terabe, *Anal.Chem.*, 72 (2000) 1023.
7. K.D. Altria, *J.Chromatogr.A*, 892 (2000) 171.
8. J.J. Pesek and M.T. Matyska, *J.Chromatogr.A*, 887 (2000) 31.
9. Q. Tang and M.L. Lee, *TrAC*, 19 (2000) 648.
10. V. Schurig and D. Wistuba, *Electrophoresis*, 20 (1999) 2313.

11. L. Schweitz, L.I. Andersson and S. Nilsson, *J.Chromatogr.A*, 817 (1998) 5.

12. B. Göttlicher and K. Bächmann, *J.Chromatogr.A*, 780 (1997) 63.

13. M.G. Khaledi, *J.Chromatogr.A*, 780 (1997) 3.

14. P.G.H.M. Muijselaar, K. Otsuka and S. Terabe, *J.Chromatogr.A*, 780 (1997) 41.

15. C.P. Palmer, *J.Chromatogr.A*, 780 (1997) 75.

16. P.R. Haddad, *J.Chromatogr.A*, 770 (1997) 281.

17. D. Li, H.H. Knobel and V.T. Remcho, *J.Chromatogr.B*, 695 (1997) 169.

18. S. Kitagawa, A. Tsuji, H. Watanabe, M. Nakashima and T. Tsuda, *J.Microcol.Sep*, 9 (1997) 347.

19. M.L. Ye, H.F. Zou, Z. Liu and J.Y. Ni, *J.Chromatogr.*, 887 (2000) 223.

20. C.W. Klampfl, E.F. Hilder and Haddad P.R., *J.Chromatogr.A*, 888 (2000) 267.

21. E.F. Hilder, M. Macka and P.R. Haddad, *Anal.Commun.*, 36 (1999) 299.

22. E.F. Hilder, C.W. Klampfl and P.R. Haddad, *J.Chromatogr.A*, 890 (2000) 337.

23. F. Svec, E.C. Peters, D. Sykora and M.J. Frechet, *J.Chromatogr.A*, 887 (2000) 3.

24. I. Gusev, X. Huang and C. Horváth, *J.Chromatogr.A*, 855 (2001) 273.

25. N. Ishizuka, H. Minakuchi, K. Nakanishi, N. Soga, K. Hosoya and N. Tanaka, *J.High.Resol.Chromatogr.*, 23 (1998) 67.

26. Q. Tang, B. Xin and M.L. Lee, *J.Chromatogr.A*, 837 (1999) 35.

27. B. He, N. Tait and F.E. Regnier, *Anal.Chem.*, 70 (1998) 3790.

28. W.D. Pfeffer and E.S. Yeung, *J.Chromatogr.*, 557 (1991) 125.

29. T.W. Garner and E.S. Yeung, *J.Chromatogr.*, 640 (1993) 397.

30. J.C. Hsu, W.H. Chen and C.Y. Liu, *Analyst*, 122 (1997) 1393.

31. M.S. Nutku and F.B. Erim, *High Resol.Chromatogr.*, 21 (1998) 505.

32. M.S. Nutku and F.B. Erim, *J.Micro.Sep.*, 11 (1999) 541.

33. F.B. Erim, *Microchmical Journal*, 57 (1997) 283.

34. C.-Y. Liu and W.-H. Chen, *J.Chromatogr.A*, 815 (1998) 251.

35. W.-H. Chen, S.-Y. Lin and C.-Y. Liu, *Anal.Chemica.Acta.*, 410 (2000) 25.

36. C. Finkler, H. Charrel and H. Engelhardt, *J.Chromatogr.A*, 822 (1998) 101.

37. H. Burt, D.M. Lewis and K.N. Tapley, *J.Chromatogr.A*, 739 (1996) 367.

38. M. Chiari, L. Ceriotti, G. Crini and M. Morcellet, *J.Chromatogr.A*, 836 (1999) 81.

39. D.T. Gjerde and L. Yengoyan, *International Patent Application*, (1995) WO 95/10344.

40. W.R. Jones and P. Jandik, *J.Chromatogr.*, 546 (1991) 445.

41. T. Kaneta, S. Tanaka, M. Taga and H. Yoshida, *Anal.Chem.*, 64 (1992) 798.

42. W. Buchberger and P.R. Haddad, *J.Chromatogr.*, 608 (1992) 59.

43. A.H. Harakuwe, P.R. Haddad and W. Buchberger, *J.Chromatogr.A*, 685 (1994) 161.

44. P.R. Haddad, A.H. Harakuwe and W. Buchberger, *J.Chromatogr.A*, 706 (1995) 571.

45. M. Martínez and M. Aguilar, *J.Chromatogr.A*, 676 (1994) 443.

46. N.J. Benz and J.S. Fritz, *J.Chromatogr.A*, 671 (1994) 437.

47. C. Bjergegaard, P. Møller and H. Sørensen, *J.Chromatogr.A*, 717 (1995) 409.

48. F. Guan, H. Wu and W. Liu, *J.Chromatogr.A*, 719 (1996) 427.

49. M.T. Galceran, L. Puignou and M. Diez, *J.Chromatogr.A*, 732 (1996) 167.

50. C. François, Ph. Morin and M. Dreux, *J.High.Resol.Chromatogr.*, 19 (1996) 5.

51. T. Takayanagi, E. Wada and S. Motomizu, *Analyst*, 122 (1997) 1387.

52. T. Takayanagi, H. Tanaka and S. Motomizu, *Anal.Sci.*, 13 (1997) 11.

53. T. Takayanagi and S. Motomizu, *J.Chromatogr.*, 853 (1999) 55.

54. K.K.C. Yeung and C.A. Lucy, *J.Chromatogr.A*, 804 (1998) 319.

55. S. Terabe and T. Isemura, *Anal.Chem.*, 62 (1990) 650.

56. S. Terabe and T. Isemura, *J.Chromatogr.*, 515 (1990) 667.

57. C. Stathakis and R.M. Cassidy, *Anal.Chem.*, 66 (1994) 667.

58. C. Stathakis and R.M. Cassidy, *J.Chromatogr.A*, 699 (1995) 353.

59. O.V. Krokhin, H. Hoshino, O.A. Shpigun and T. Yotsuyanagi, *J.Chromatogr.A*, 776 (1997) 329.

60. O.V. Krokhin, H. Hoshino, O.A. Shpigun and T. Yotsuyanagi, *J.Chromatogr.A*, 772 (1997) 339.

61. O.V. Krokhin, A.V. Adamov, H. Hoshino, O.A. Shpigun and T. Yotsuyanagi, *J.Chromatogr.A*, 850 (1999) 269.

62. O.V. Krokhin, O.V. Kuzina, H. Hoshino, O.A. Shpigun and T. Yotsuyanagi, *J.Chromatogr.A*, 890 (2000) 363.

63. O.V. Krokhin, H. Hoshino, O.A. Shpigun and T. Yotsuyanagi, *J.Chromatogr.A*, 895 (2000) 255.

64. F.B. Erim, *J.Chromatogr.A*, 768 (1997) 161.

65. J. Li, W. Ding and J.S. Fritz, *J.Chromatogr.A*, 879 (2000) 245.

66. J.D. Lamb, B.R. Edwards, R.G. Smith and R. Garrick, *Talanta*, 42 (1995) 109.

67. C.S. Chiou and J.S. Shih, *Analyst*, 121 (1996) 1107.

68. C. Stathakis and R.M. Cassidy, *Can.J.Chem.*, 76 (1998) 194.

69. M. Masár, R. Bodor and D. Kaniansky, *J.Chromatogr.A*, 834 (1999) 179.

70. L. Arce, A. Segura Carretero, A. Ríos, C. Cruces, A. Fernández and M. Valcárcel, *J.Chromatogr.A*, 816 (1998) 243.

71. D.S. Burgi and R.-L. Chien, *Anal.Biochem.*, 202 (1992) 306.

72. D.S. Burgi, *Anal.Chem.*, 65 (1993) 3726.

73. J. Boden, M. Darius and K. Bächmann, *J.Chromatogr.A*, 716 (1995) 311.

74. Y. He and H.K. Lee, *Analytical Chemistry*, 71 (1999) 995.

75. M. Albert, L. Debusschere, C. Demesmay and J.L. Rocca, *J.Chromatogr.A*, 757 (1997) 281.

76. M. Albert, L. Debusschere, C. Demesmay and J.L. Rocca, *J.Chromatogr.A*, 757 (1997) 296.

77. Y. Yang, J. Kang, H. Lu, Q. Ou and F. Liu, *J.Chromatogr.A*, 834 (2000) 387.

78. T. Soga, Y. Inoue and G.A. Ross, *J.Chromatogr.A*, 718 (1995) 421.

79. J.P. Quirino and S. Terabe, *J.Chromatogr.A*, 580 (1999) 339.

80. A.R. Timerbaev, K. Fukushi, T. Miyado, N. Ishio, K. Saitoh and S. Motomizu, *J.Chromatogr.A*, 888 (2000) 309.

81. G. Bondoux, P. Jandik and W.R. Jones, *J.Chromatogr.*, 602 (1992) 79.

82. M.J. Wojtusik and M.P. Harrold, *J.Chromatogr.A*, 671 (1994) 411.

83. D. Kaniansky, I. Zelenský, A. Hybenová and F.I. Onuska, *Anal.Chem.*, 66 (1994) 4258.

84. J. Boden, K. Bächmann, L. Kotz, L. Fabry and S. Pahlke, *J.Chromatogr.A*, 696 (1995) 321.

85. J. Boden and K. Bächmann, *J.Chromatogr.A*, 734 (1996) 319.

86. P. Blatný, F. Kvasnicka and E. Kenndler, *J.Chromatogr.A*, 757 (1997) 297.

87. C. Haber, R.J. VanSaun and W.R. Jones, *Anal.Chem.*, 70 (1998) 2261.

88. W. Buchberger and P.R. Haddad, *J.Chromatogr.A*, 687 (1994) 343.

89. P. Kuban, W. Buchberger and P.R. Haddad, *J.Chromatogr.A*, 770 (1997) 329.

90. L. Arce, P. Kuban, A. Ríos, M. Valcárcel and B. Karlberg, *Anal.Chemica.Acta.*, 390 (1999) 39.

91. M. Novic and M. Gucek, *J.Chromatogr.A*, 868 (2000) 135.

92. R. Loos and R. Niessner, *J.Chromatogr.A*, 822 (1998) 291.

93. F. Foret, V. Sustacek and P. Bocek, *J.Micro.Sep.*, 2 (1990) 229.

94. N.A. Guzman, M.A. Trebilock and J.P. Advis, *J.Liq.Chrom.*, 14 (1991) 997.

95. J.H. Beattie, R. Self and M.P. Richards, *Electrophoresis.*, 16 (1995) 322.

96. M. Dong, R.P. Oda, M.A. Strausbauch, P.J. Wettstein, J.P. Landers and L.J. Miller, *Electrophoresis.*, 18 (1997) 1767.

97. N.A. Guzman, *J.Liq.Chrom.*, 18 (1995) 3751.

98. M. Peterrson, K.-G. Wahlund and S. Nilsson, *J.Chromatogr.A*, 841 (1999) 249.

99. M.E. Roche, M.A. Anderson, R.P. Oda, B.L. Riggs, M.A. Strausbauch, R. Okazaki, P.J. Wettstein and J.P. Landers, *Analytical Biochemistry*, 258 (1998) 87.

100. M.A. Strausbauch, B.J. Madden, P.J. Wettstein and J.P. Landers, *Electrophoresis*, 16 (1995) 541.

101. M.A. Strausbauch, S.J. Xu, J.E. Ferguson, M.E. Nunez, D. Machacek, G.M. Lawson, P.J. Wettstein and J.P. Landers, *J.Chromatogr.A*, 717 (1995) 279.

102. A.J. Tomlinson, L.M. Benson, N.A. Guzman and S. Naylor, *J.Chromatogr.A*, 744 (1996) 3.

103. J. Cai and Z. El Rassi, *J.Chromatogr.*, 608 (1992) 31.

104. J. Cai and Z. El Rassi, *J.Liq.Chrom.*, 15 (1992) 1179.

105. J. Cai and Z. El Rassi, *J.Liq.Chrom.*, 16 (1993) 2007.

106. D.S. Burgi and R.-L. Chien, in J.P. Landers (Editor), *Handbook of Capillary Electrophoresis*, CRC Press, New York, 1997, p. 479.

107. P. Kuban and B. Karlberg, *Anal.Chem.*, 69 (1997) 1169.

108. Y. Zhang, J. Zhu, L. Zhang and W. Zhang, *Anal.Chem.*, 72 (2000) 5744.

109. J. Palmer and J.P. Landers, *Anal.Chem.*, 72 (2000) 1941.

110. N.J. Munro, J. Palmer, A.M. Stalcup and J.P. Landers, *J.Chromatogr.B*, 731 (1999) 369.

111. J. Palmer, N.J. Munro and J.P. Landers, *Anal.Chem.*, 71 (1999) 1679.

Chapter 2

General Experimental

This section describes the instrumentation, chemicals and procedures used throughout this work, unless specified otherwise in a particular chapter.

2.1 Instrumentation

All separations were performed using a Hewlett-Packard HP^{3D} CE system (Agilent Technologies, Waldbronn, Germany), equipped with a diode array detector and connected to a HP^{3D} CE Chemstation (Agilent) for data processing. An external water bath maintained at 30 °C was used in Chapter 6 to provide a more consistent temperature.

Helium or nitrogen was used as an external pressure source. When the instrument was used with external pressure connected, the low pressure was disconnected to avoid damaging the sensor valve on the EMS board [1].

All CE separations were performed using fused silica capillaries (75, 50 and 25 μm i.d. x 360 μm o.d.) obtained from Polymicro Technologies Inc. (Phoenix, AZ, USA).

Detection windows approximately 5 mm in length were burnt using a butane lighter 8.5 cm from the end of the capillary and cleaned with methanol. A standard metallic interface of 50 or 75 μm was used in all cases except when using 25 μm capillaries, in which case a 50 μm non-metallic interface was used to avoid problems when using a negative voltage.

2.2 Reagents

Unless specified otherwise all chemicals were of analytical reagent grade and are listed in Table 2.1 to Table 2.5.

Table 2.1 : Chemicals used as chromatographic phases

Name	Type	Formula	Supplier
AS5A Latex particles	OT	-	Dionex, Sunnyvale, CA, USA.
Poly(dimethyldiallylammonium chloride) PDDAC	PP	(C8H16NCl)n	Aldrich, Milwaukee, WI, USA

OT- Open Tubular; PP – Pseudo-phase

Table 2.2: Chemicals used as buffers

Buffer	pK_a	Formula	Supplier
L-histidine	7.7 (p*I*)	$C_6H_9N_3O_2$	Aldrich
Tris(hydroxymethyl)aminomethane (Tris)	8.05	$C_4H_{11}NO_3$	Aldrich
Diethanolamine (DEA)	9.20	$C_4H_{11}NO_2$	Fluka, Buchs, Switzerland.

Table 2.3: Chemicals used as competing ions

Eluent	Formula	Supplier
1,5-naphthalenedisulfonic acid	$C_{10}H_6(SO_3H)_2$	Aldrich
Acetic acid	CH_3COOH	BDH Chemicals, Kilsyth, Vic, Australia.
Benzoic acid	C_6H_5COOH	BDH Chemicals
Chromium Trioxide	CrO_3	BDH Chemicals
Citric acid	$HOC(CO_2H)(CH_2CO_2H)_2$	BDH Chemicals,
Ethanesulfonic acid, sodium salt	$CH_3CH_2SO_3Na$	Aldrich
Hydrochloric acid	HCl	BDH Chemicals
I-Pentananoic acid	$(CH_3)CCOOH$	BDH Chemicals
Methanesulfonic acid, sodium salt	$HCSO_3Na$	Sigma, St Louis, MO, USA
Perchloric acid	$HClO_4$	Ajax Chemicals, Sydney, NSW, Australia
Phthalic acid	$C_6H_4(COOH)_2$	BDH Chemicals
Sodium acetate	CH_3COONa	Ajax
Sodium bicarbonate	$NaHCO_3$	May and Baker, West Footscray, Vis, Australia.
Sodium carbonate	Na_2CO_3	BDH Chemicals
Sodium chloride	NaCl	Ajax

Table 2.3: Chemicals used as competing ions. (ctd)

Eluent	Formula	Supplier
Sodium chromate	Na_2CrO_4	Ajax Chemicals
Sodium fluoride	NaF	Prolabo, Paris, France.
Sodium formate	HCOONa	Ajax
Sodium sulfate	Na_2SO_4	Aldrich
Sulfuric acid	H_2SO_4	BDH Chemicals

Table 2.4 : Chemicals used as analytes

Analyte	Formula	Supplier
(IR)-(-)-10-camphorsulfonic acid	$C_{10}H_{16}O_4S$	Sigma
1,2-benzenedisulfonic acid, dipotassium salt	$C_6H_4(SO_3Na)_2$	Aldrich
1,3, (6 or 7)-naphthalenetrisulfonic acid	$C_{10}H_5(SO_3Na)_3$	Aldrich
1,5-naphthalene disulfonic acid	$C_{10}H_6(SO_3H)_2$	Aldrich
2-(cyclohexylamino)ethanesulfonic acid (CHES)	$C_6H_{11}NHCH_2CH_2SO_3H$	Aldrich
2,3-dihydroxybenzoic acid	$(HO)_2C_6H_3COOH$	Aldrich
2-morpholinoethane sulfonic acid (MES)	$C_6H_{13}NO_4S.H_2O$	Fluka
2-naphthalenesulfonic acid	$C_{10}H_7SO_3Na$	Aldrich
2-sulfobenzoic acid	$HO_3SC_6H_4COOH$	Aldrich
3-cyclohexylamino-1-propanesulfonic acid (CHAPS)	$C_6H_{11}NH(CH_2)_3SO_3H$	Aldrich
3-morpholinopropane sulfonic acid (MOPS)	$C_7H_{15}NO_4S$	Fluka
4-(2-hydroxyethyl)-1-piperazineethanesulfonic acid (HEPES)	$C_8H_{18}N_2O_4S$	Aldrich
4-aminobenzenesulfonic acid	$NH_2C_6H_4SO_3H$	Unknown
4-hydroxybenzoic acid	HOC_5H_4COOH	Aldrich
5-sulfoisophthalic acid	$NaO_3SC_6H_3$-1,3-$(COOH)_2$	Aldrich
5-sulfosalicylic acid	$(HO)_3SC_6H_3(OH)COOH$	BDH Chemicals
8-amino-2-naphthalenesulfonic acid	$H_2NC_{10}H_6SO_3H$	Aldrich
Adipic acid	$(CH_2CH_2COOH)_2$	Ajax Chemicals

Table 2.4 : Chemicals used as analytes. (ctd)

Analyte	Formula	Supplier
Ammonium molybdate	$(NH_4)_2MoO_4$	Ajax Chemicals
Ascorbic acid	$C_6H_8O_6$	Unknown
Benzenesulfonic acid, sodium salt	$C_6H_5SO_3Na$	Aldrich
Benzoic acid	C_6H_5COOH	Aldrich
Butanesulfonic acid, sodium salt	$CH_3CH_2CH_2CH_2SO_3Na$	Aldrich
Butyric acid	$CH_3CH_2CH_2COOH$	Hopkins and Williams, Essex, England.
Citric acid, trisodium salt	$HOOCCH_2C(OH)(COOH)CH_2COOH$	Aldrich
Dietylenetriamine pentaacetic acid	$[HOOCCH_2)_2NCH_2CH_2]_2NCH_2COOH$	Aldrich
Dipicolinic acid	$NC_5H_3(COOH)_2$	Aldrich
Ethanesulfonic acid, sodium salt	$CH_3CH_2SO_3Na$	Aldrich
Ethylenediamine tetraacetic acid (EDTA)	$[CH_2N(CH_2COOH)CH_2COONa]_2.2H_2O$	Ajax Chemicals
Fumaric acid	HOOCCH=CHCOOH	Unknown
Glutaric acid	$CH_2(CH_2COOH)_2$	Aldrich
Glycolic acid	$HOCH_2COOH$	Sigma
Hexanesulfonic acid, sodium salt	$CH_3CH_2CH_2CH_2CH_2CH_2SO_3Na$	Aldrich
Iminodiacetic acid	$NH_2(COOH)_2$	BDH Chemicals
Isonicotninc acid	C_5NH_4COOH	Aldrich
i-valearic acid	$(CH_3)CCOOH$	BDH Chemicals
Lactic acid	$CH_3CH(OH)COOH$	Sigma
Malonic acid, sodium salt	$CH_2(COONa)_2$	Ajax Chemicals
Methanesulfonic acid, LR	CH_3SO_3	Sigma
n-caproic acid, sodium salt	$C_6H_{11}O_2Na$	Sigma
n-caprylic acid, sodium salt	$C_8H_{15}O_2Na$	Sigma
Nicotinic acid	C_5H_4NCOOH	Sigma
o-aminobenzoic acid	$H_2NC_6H_4COOH$	Unknown
Pentanesulfonic acid, sodium salt	$CH_3CH_2CH_2CH_2CH_2SO_3Na$	Aldrich
Picolinic acid	C_5H_4NCOOH	Sigma

Table 2.4 : Chemicals used as analytes. (ctd)

Analyte	Formula	Supplier
Potassium bromate	$KBrO_3$	Aldrich
Propanesulfonic acid, sodium salt	$CH_3CH_2CH_2SO_3Na.H_2O$	Aldrich
Propionic acid	CH_3CH_2COOH	Aldrich
p-toluene sulfonic acid	$CH_3C_6H_4SO_3H.H_2O$	Aldrich
Salicylic acid	$HOC_6H_4CO_2H$	Aldrich
Sodium acetate	CH_3COONa	Ajax Chemicals
Sodium bromide	NaBr	Sigma
Sodium chlorate	$NaClO_3$	BDH Chemicals
Sodium chloride	NaCl	Ajax Chemicals
Sodium chromate	Na_2CrO_4	Ajax Chemicals
Sodium cyanate	NaOCN	Aldrich
Sodium fluoride	NaF	Aldrich
Sodium formate	CHOONa	Ajax Chemicals
Sodium iodide	NaI	Aldrich
Sodium nitrate	$NaNO_3$	Ajax Chemicals
Sodium nitrite	$NaNO_2$	Ajax Chemicals
Sodium perchlorate	$NaClO_4$	Ajax Chemicals
Sodium sulfate	Na_2SO_4	Aldrich
Sodium thiocyanate	NaSCN	Aldrich
Sodium thiosulfate	$Na_2S_2O_3.5H_2O$	BDH Chemicals
Sorbic acid	$CH_3CH=CHCH=CHCOOH$	Sigma
Succinic acid, sodium salt	$(CH_2COONa)_2.6H_2O$	Aldrich
Sulfamic acid	NH_2SO_3H	Unknown
Tartaric acid, disodium salt	$Na_2C_4H_4O_6.2H_2O$	BDH Chemicals
Thiourea	H_2NCSNH_2	Aldrich

Table 2.5: Other chemicals used in this work

Chemical	Formula	Supplier
Acetonitrile	CH_3CN	BDH Chemicals
Methanol	CH_3OH	BDH Chemicals
Myristyltrimethylammonium bromide (TTAB)	$CH_3(CH_2)_{13}N(CH_3)_3Br$	Aldrich
Cetlytrimethylammonium bromide (CTAB)	$CH_3(CH_2)_{15}NBr(CH_3)_3$	Ajax Chemicals
Sodium hydroxide	NaOH	Ajax Chemicals

2.3 Procedures

2.3.1 Electrolyte and standard preparation

All eluents or electrolytes and analyte standards were prepared with water purified using a Milli-Q (Millipore, Bedford, MA, USA) water system. Eluents were filtered through a 0.45 μm membrane filter of Type HA (Millipore, Bedford, MA, USA) and degassed using vacuum sonication before use.

2.3.2 Sample injection

Injection was performed using pressure in all cases. Typical injection times were 20-50 mbar for 3 s when using 75 μm i.d. capillary columns, 50 mbar for 5 s when using 50 μm i.d. capillary columns, and 50 mbar for 10 s in 25 μm i.d. columns.

2.3.3 Calculations

Thiourea or acetone was used as a flow marker for all separations.

Electrophoretic mobilities were calculated according to the equation:

$$\mu_{eff} = \frac{L_T L_D}{V t_m} \qquad (2\text{–}1)$$

where L_T is the total length of the capillary in metres, L_D is the length to the detector in metres, V is the separation voltage in volts and t_m is the migration time of the analyte in seconds.

Limits of detection (LOD) were determined at a signal to noise ratio of 3:1.

2.4 References

1 Hilder, *E. F. Ion-Exchange Capillary Electrochromatography of Inorganic and Small Organic Anions*. PhD Thesis (2000). University of Tasmania.

Chapter 3

Open-Tubular Ion-Exchange Capillary Electrochromatography of Inorganic Anions

3.1 Introduction

The use of OT columns for CEC provides a simple alternative to the use of packed columns. Their main attraction is the simplicity of the system due to the stationary phase being attached to the inner surface of the capillary. This avoids the need to use frits to hold the packing in the column thus avoiding many of the associated problems and can potentially enable highly efficient separations to be obtained due to the elimination of the eddy diffusion term in the van Deemter equation [1,2]. A further advantage is the low backpressure of the column which allows columns to be flushed easily for rapid column conditioning.

While most OT-CEC applications have involved the separation of neutral analytes by RP mechanisms there are a few reports on the use of IE columns predominantly for the separation of inorganic species [3-6]. In many cases, minimal interaction between the analytes and the IE sites was observed, with only minor (if any) changes in selectivity being obtained. The greatest potential for IE-CEC using OT columns was shown by Gjerde and Yengoyan [7] who used capillaries coated with small cationic particles adsorbed electrostatically to the capillary wall. While they observed large changes in mobility and selectivity for several anions, no methods to vary or control the extent of IE in the separation mechanism were devised.

While the potential to change the selectivity of anions in IE-CEC has been demonstrated, there is no fundamental understanding of how the selectivity can be changed and controlled. This chapter examines the viability of using particle coated OT columns for selectivity manipulation of inorganic anions. Typical IEC

approaches to change the relative contribution of the chromatographic component to the overall mechanism are evaluated. To aid in understanding the IE-CEC system, a theoretical model derived from IE and CE theory is presented to describe the mobility of inorganic anions in IE-CEC. Finally, an experimental study aimed to provide a better understanding of parameters influencing the separation efficiency in the separation of inorganic anions in OT-IE-CEC is also presented.

3.2 Experimental

The general details are given in Chapter 2. Detailed conditions are included in each of the figure captions.

3.2.1 Column preparation

The suspension of cationic latex particles obtained contained a number of additives, such as non-ionic and ionic surfactants and inorganic ions which may influence the adsorption of the particles onto the capillary surface. Therefore clean-up of the suspension before use was performed to remove these potential interferences. The original 11% (w/v) latex suspension (5.0 mL) was circulated for 48 h through a 20 cm length of the dialysis tubing housed in a bath of deionised water to remove any non-ionic impurities. The water was replaced every 2 h for the first 6 h, with 12 h replacements thereafter. The suspension was then diluted to 50.0 mL with deionised water before being passed through a 50 x 1.0 cm diameter mixed bed IE column with the flow-rate kept below 1 mL/min. The first fractions were discarded, and the following effluent then collected. This effluent was free of both non-ionic and ionic impurities, such as surfactants and ions that were used in the synthesis of the latex particles. Coating of the capillary with latex was achieved by slightly modifying the procedure of Kleindienst *et al.* [8]. Differences in the procedure relate to flushing and waiting times (both 20 min). The capillary was then flushed with the

desired electrolyte (930 mbar) for 30 min before initial use and for 10 min when changing electrolytes thereafter.

Scanning Electron Microscopy (SEM) images of inner surfaces of the capillary were obtained using a Hitachi 4500 field emission scanning electron microscope. Pieces of capillary approximately 5 mm in length were fixed onto aluminium stubs with double-sided carbon tape and then plated with gold. The images were taken using the secondary electron signal.

3.2.2 Electrolyte preparation

Electrolytes were prepared by titration of Tris with the corresponding acid of the desired competing ion (HCl, H_2SO_4, $HClO_4$ or Citric acid) to a pH of 8.05. Therefore electrolytes with a concentration of 10 mM of Cl^- will have 20 mM Tris.

3.3 Selectivity manipulation of UV absorbing anions

Regarding the terminology used throughout this discussion, it is important to recognise that although some differences can be argued, from a practical point of view many of the terms in CE and IE can be used interchangeably. For example, when reference is made to a coated capillary, the IE equivalent term is a column. Similarly, electrolyte, electrolyte, mobile phase and eluent are all interchangeable terms.

3.3.1 Influence of AS5A voating on separation of inorganic anions

Fused silica capillaries were coated with AS5A latex particles to give coated OT columns containing IE sites on the capillary wall. Figure 3.1 shows an SEM image of the inside wall of a bare fused silica capillary (a) and an AS5A coated capillary (b). It can be seen that the surface of the coated capillary has small

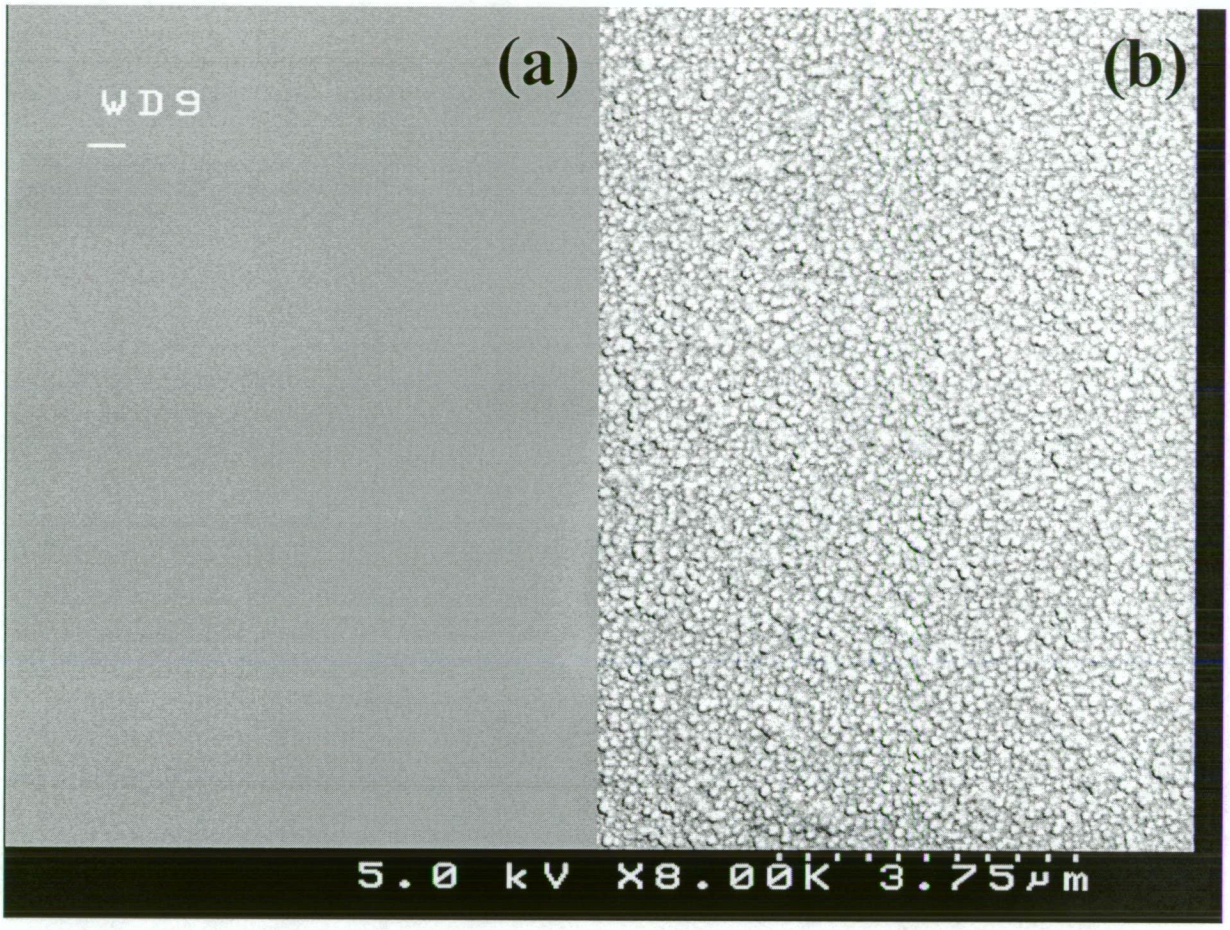

Figure 3.1: SEM images of the inside surface of (a) a bare fused silica capillary and (b) an AS5A coated capillary.

particles of approximately 75 nm which have been adsorbed evenly onto the inner wall of the capillary, thereby providing a suitable stationary phase for IE interactions. The surface of the uncoated capillary is smooth in comparison.

As latex-coated capillaries have been used previously to separate inorganic anions by high temperature OT-IEC [9], it can be anticipated that the adsorbed particles will have two effects on the separation. The first is that the particles will impart a cationic charge onto the surface of the capillary which will result in a reversal of the EOF [7,8], and the subsequent separation will be in the co-EOF mode. Since the particles have quaternary ammonium functionality, the magnitude of the EOF should be independent of changes in pH. To evaluate this, the EOF was measured over the pH range 2-8. Values for μ_{EOF} ranged from -25.39 x 10^{-9} m^2/Vs at a pH of 2.45 to -26.29 x 10^{-9} m^2/Vs at a pH of 8.05, indicating little change in the EOF with pH. The second influence on the separation is due to the bound AS5A particles providing IE sites with which analytes can interact. This interaction with the stationary phase will result in a reduction of the observed mobility of the analyte, with analytes showing a higher IE interaction being retarded more than analytes with a low IE interaction. The IE elution order (and hence the order of IE interaction) for the inorganic analytes studied is $NO_2^- < Br^- < NO_3^- < CrO_4^{2-} < S_2O_3^{2-} < I^- < SCN^-$, while the migration order in CE for the same analytes (from tabulated values of λ [10]) is CrO_4^{2-}, $S_2O_3^{2-} < Br^- < I^- < NO_2^- < NO_3^- < SCN^-$. Therefore a separation in which the IE interactions are dominant should show analytes emerging from the column in the IE elution order, while a separation with small IE interactions will follow the CE order. Any difference from either of these two orders will indicate a separation that has both CE and IE components. Figure 3.2 shows the co-EOF separation of selected inorganic anions in an AS5A coated OT-CEC capillary, compared with that in a bare fused silica capillary in which the EOF has been reversed using 0.5 mM TTAB. Both separations were performed using a 20 mM Tris/10 mM Cl^- electrolyte (pH 8.05). It

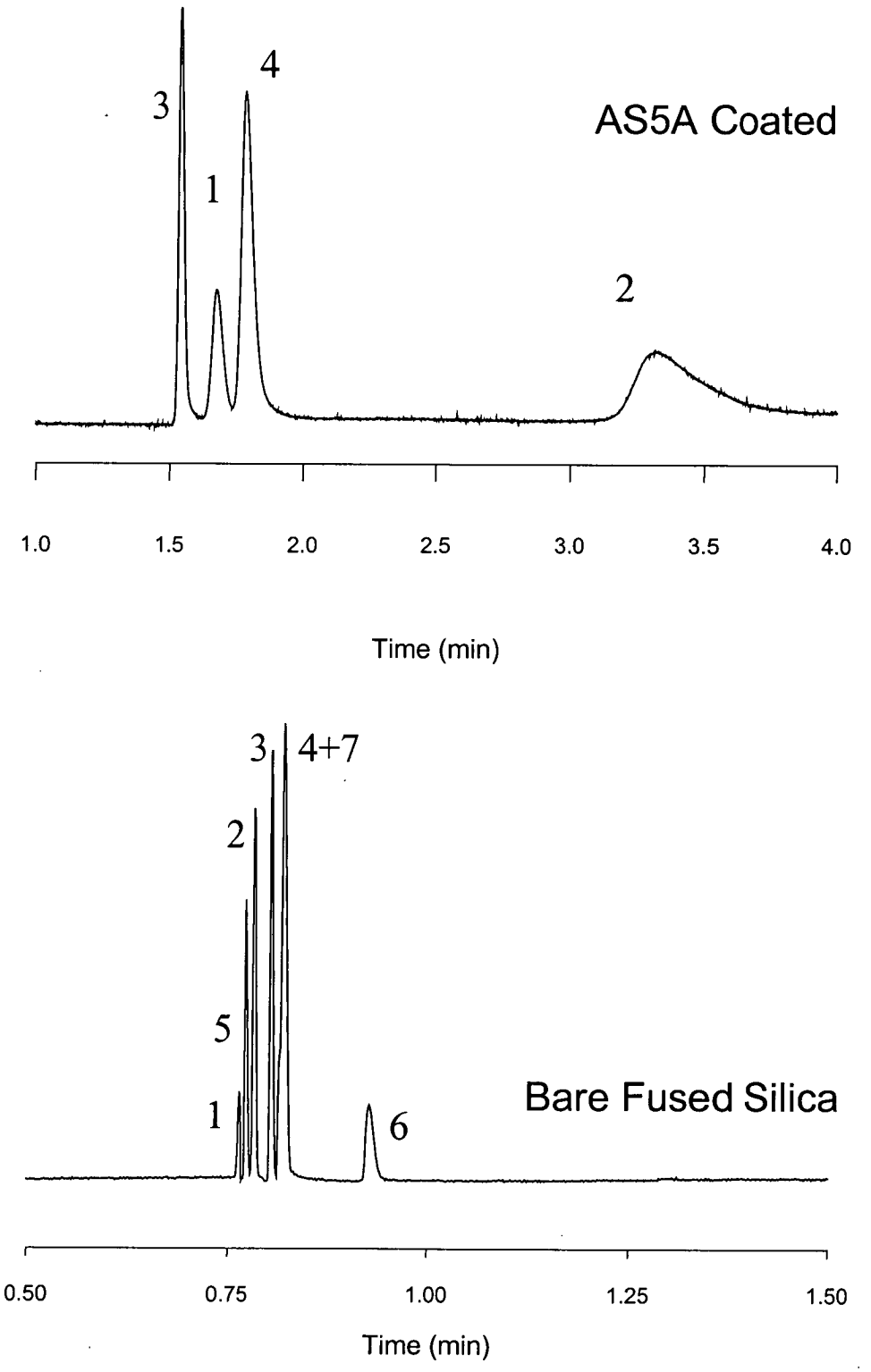

Figure 3.2: Separation of 7 inorganic anions in an AS5A coated capillary (top) and an uncoated bare fused silica capillary (bottom) using 0.5 mM TTAB for EOF reversal. Conditions : 20 mM Tris / 10 mM Cl^- (pH 8.05), 50.0 cm capillary (40.5 cm to detector), -25 kV, direct detection at 214 nm. Injection of 0.5 mM for 4 s at 10 mbar for the AS5A coated capillary and 0.1 mM for 10 s at 10 mbar for the uncoated capillary. Peaks are : 1 = Br^-, 2 = I^-, 3 = NO_2^-, 4 = NO_3^-, 5 = $S_2O_3^{2-}$, 6 = SCN^-, 7 = CrO_4^{2-}.

can be seen that the uncoated capillary provided a separation with relatively small selectivity differences (and hence marginal resolution) between the analytes while the separation in the AS5A coated capillary showed significant selectivity differences between Br^-, NO_2^-, NO_3^- and I^-. This was due to those analytes having a high IE interaction showing marked changes in migration time. For example, I^- (peak 2), migrated well after NO_3^- (peak 4) in the AS5A capillary, while it migrated between Br^- (peak 1) and NO_2^- (peak 3) in the uncoated capillary. Similarly, the position of Br^- (peak 1) has moved to after that of NO_2^- (peak 3) when moving from the untreated to the coated capillary. However, with the introduction of IE interactions, it can also be seen that peak shape deteriorated rapidly as the degree of IE interaction was increased; this is particularly evident in the peak shape for I^- (peak 2). Peaks for SCN^-, $S_2O_3^{2-}$ and CrO_4^{2-}, which theoretically all have a higher degree of IE interaction, were not seen in the AS5A coated capillary under the conditions used, presumably due to a combination of long migration times, broad peaks, and low detector response.

3.3.2 Effect of type and concentration of competing Ion

In IEC, the degree of interaction with the stationary phase can be suppressed by increasing the concentration of the competing ion [11]. In IE-CEC, increasing the concentration of the competing ion should therefore decrease the IE contribution to the separation mechanism, which will result in a higher relative contribution of the electrophoretic mobility to the separation mechanism. In considering the applicable range over which the concentration of the competing ion can be varied, it is noteworthy that high ionic strength buffers are usually avoided in CE because they increase analysis time due to lower voltages that can be applied in order to limit Joule heating. Recently, it has been shown by Ding *et al.* [12] that the addition of 0.5 M NaCl to the running buffer does not significantly decrease the quality of the separation and can even be beneficial in cases of high ionic strength samples, such as

sea water. In that work, Joule heating was observed to influence the electrophoretic mobility of analytes, but no significant reduction of separation efficiency was observed. As a result, buffers up to a concentration of 1000 mM Cl^- were used in the present study in order to evaluate the influence of increasing the concentration of competing ion on the IE influence in the separation mechanism. The influence on the separation selectivity of several different competing ions having differing IE interaction strength, namely chloride, sulfate and perchlorate, was also investigated.

3.3.2.1 Changing the concentration of competing ion

Figure 3.3 shows the separation of 7 inorganic anions in an AS5A coated OT-CEC capillary using varying concentrations of chloride in the electrolyte. Significant IE interactions between the analytes and the stationary phase were obtained with 20 mM Cl^-, with the migration order being $NO_2^- < Br^- < NO_3^- < I^- < SCN^-$. On the other hand, at 1000 mM Cl^- the IE interaction was suppressed completely and the migration order was $Br^- < I^- < NO_2^- < NO_3^- < S_2O_3^{2-} < SCN^- < CrO_4^{2-}$. This order differed from that predicted from values of limiting ionic conductances of the analytes because of the ionic strength of the electrolyte, but agreed with the order obtained using a 100 mM Cl^- electrolyte in an uncoated capillary with the EOF reversed using TTAB. This result indicated that it was necessary to add 1000 mM Cl^- in order to completely suppress the IE interaction in the separation mechanism. It is important to note that with additions of 150 mM Cl^- or more, the separation voltage had to be reduced because the current reached the maximum instrumental limit of 300 μA. This resulted in the voltage being reduced progressively for higher concentration electrolytes leading to the different time scales used for each separation in Figure 3.3. The separation at 100 mM Cl^- was the shortest, due to a combination of the highest applied voltage (-25 kV) and a reduced IE interaction compared to 20 mM Cl^- in the electrolyte. Below 100 mM Cl^-, separation times were

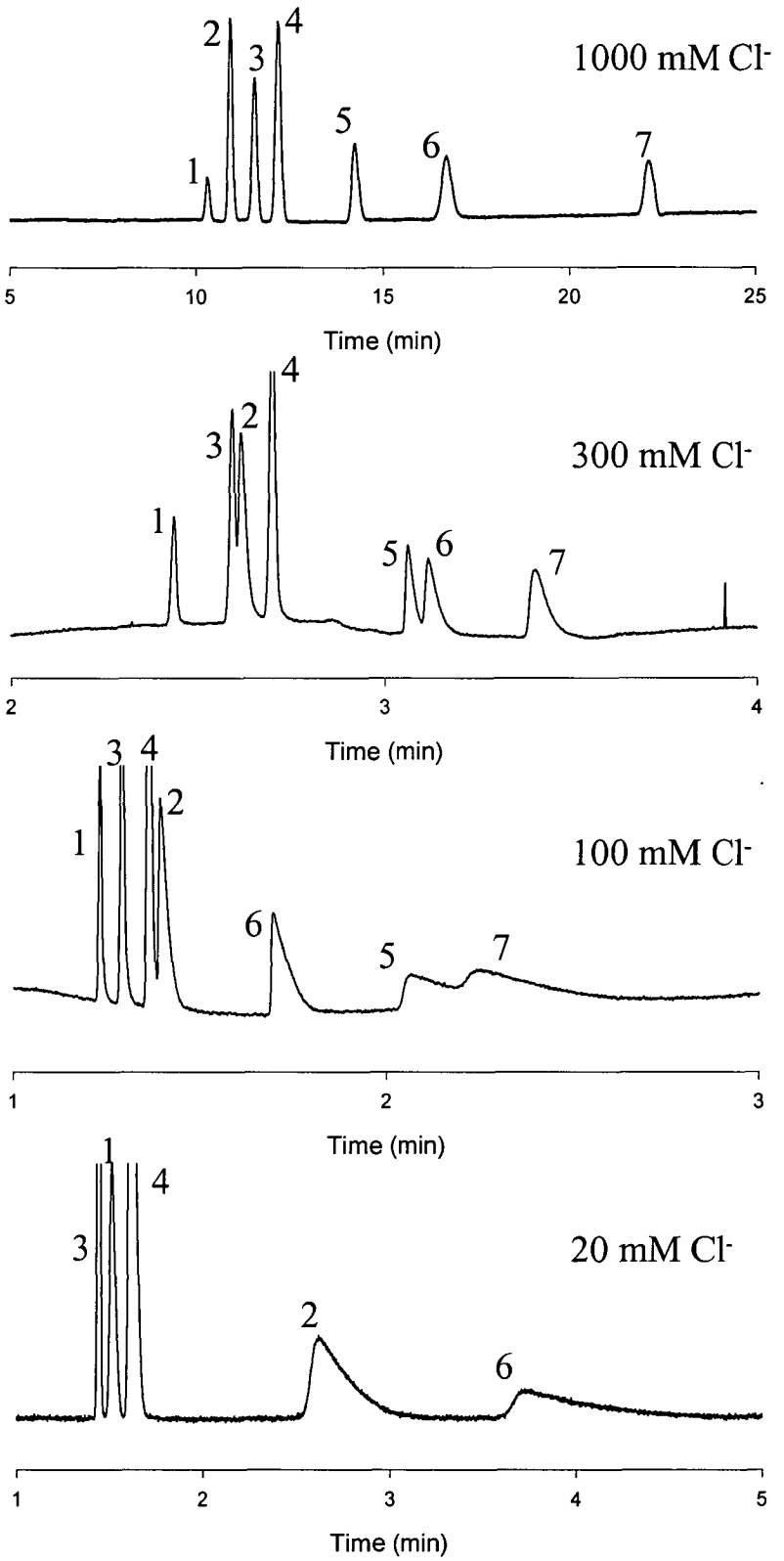

Figure 3.3 : Separation of 7 inorganic anions in an AS5A coated capillary with different concentrations of Cl^- in the electrolyte. Note the different time scales for each separation. Conditions: -25 kV for 20 and 100 mM Cl^-, -14 kV for 300 mM Cl^- and -7 kV for 1000 mM Cl^- (current = 290 μA for 300 and 1000 mM Cl^-). Other conditions as in Figure 3.2. Peaks are : 1 = Br^-, 2 = I^-, 3 = NO_2^-, 4 = NO_3^-, 5 = $S_2O_3^{2-}$, 6 = SCN^-, 7 = CrO_4^{2-}.

longer due to more IE interaction, while above 100 mM Cl^- the reduced voltage led to increased separation times. The use of a stronger competing ion than Cl^- could potentially be much more useful because it would suppress IE interactions at lower concentrations, enabling higher voltages to be used giving shorter analysis times.

3.3.2.2 Different competing ions

To examine the influence of different competing ions on the separation selectivity, perchlorate and sulfate were used in the electrolyte. These anions are known to have high IE selectivity coefficients, are transparent in the UV range, and are suitable for the preparation of electrolytes with only the single anion of interest as the competing ion (i.e. by titration of a suitable acid with Tris). The separation of a mixture of inorganic anions using 15 mM of both competing ions (and chloride) is shown in Figure 3.4. It can be seen that as the strength of the competing ion increased ($Cl^- < SO_4^{2-} < ClO_4^-$) the IE interaction with the stationary phase was reduced, which is particularly evident from the changes in selectivity for Br^- and I^-. Perchlorate is the strongest competing ion and therefore has the greatest potential to provide a wide range of operational conditions over which its concentration can be varied before Joule heating becomes the limiting factor.

Figure 3.5 shows the separation of 7 anions obtained using different concentrations of perchlorate as the competing ion. The IE component of the separation mechanism was suppressed completely with the addition of 100 mM ClO_4^-, compared to 1000 mM Cl^- necessary to achieve the same result (Figure 3.3), and the higher voltage that can be applied resulted in a shorter analysis time (2.5 min for ClO_4^- compared to 25 min for Cl^-). Because the IE selectivity coefficient of ClO_4^- is much stronger than that of Cl^-, a high level of IE interactions could not be obtained unless ClO_4^- was used at <2 mM, leading to these electrolytes having little or no buffering capacity.

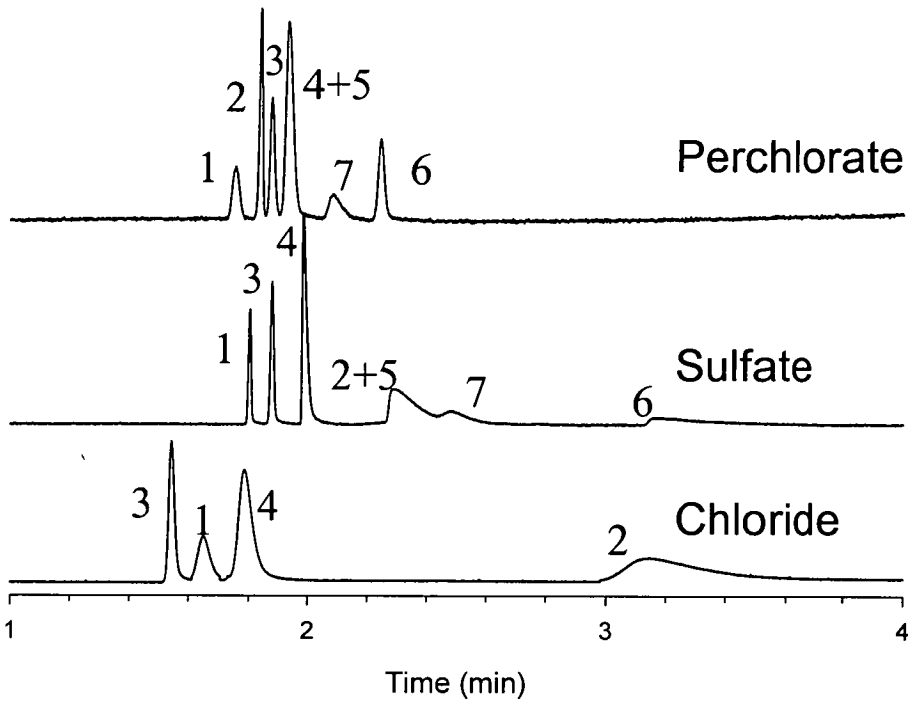

Figure 3.4: Separation of inorganic anions using 15 mM of different competing ions in the electrolyte. Other conditions as in Figure 3.2. Peaks are : 1 = Br^-, 2 = I^-, 3 = NO_2^-, 4 = NO_3^-, 5 = $S_2O_3^{2-}$, 6 = SCN^-, 7 = CrO_4^{2-}.

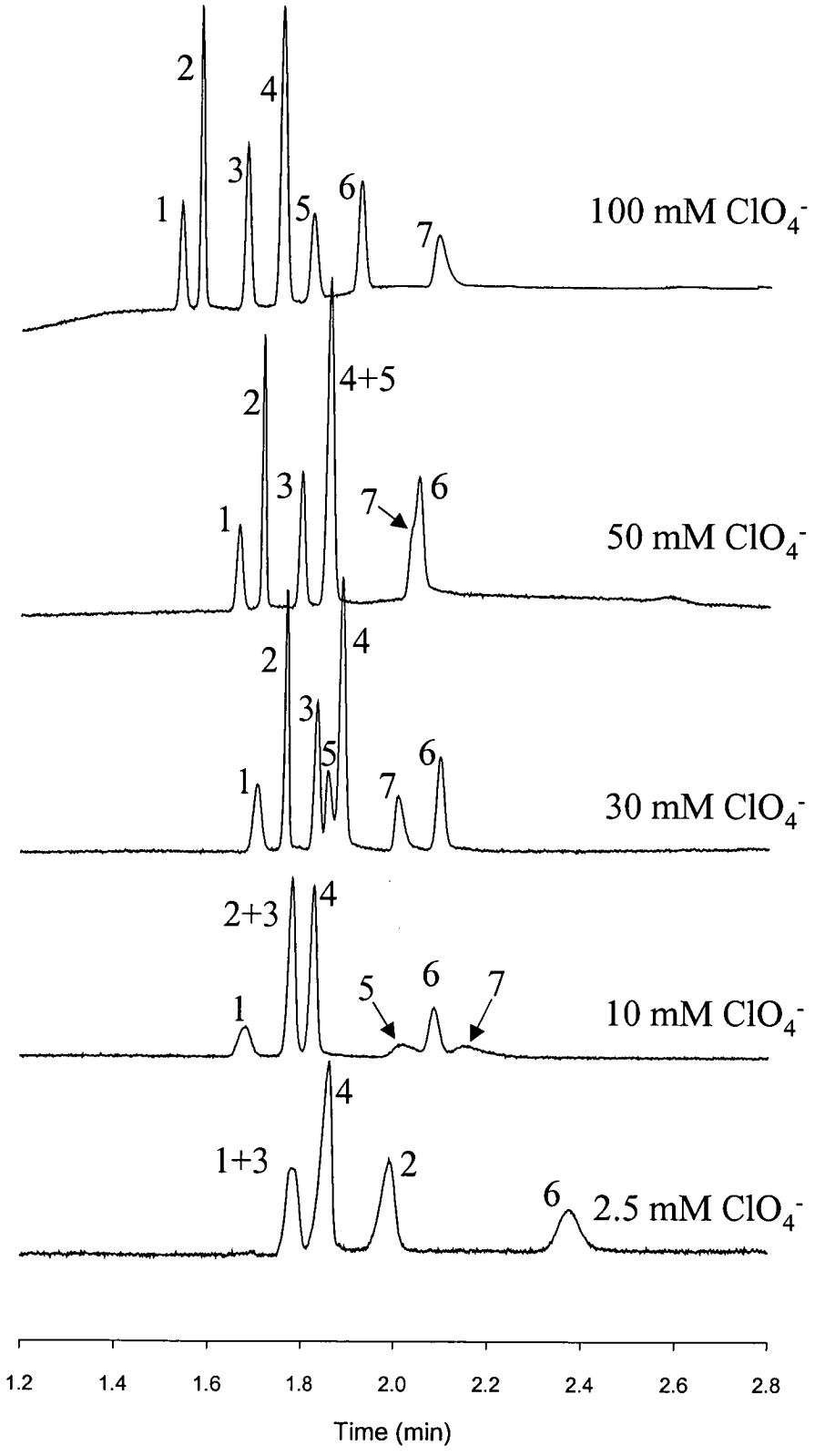

Figure 3.5: Separation of 7 inorganic anions in an AS5A using different concentrations of perchlorate in the electrolyte. All separations at -25 kV, other conditions as in Figure 3.2. Peaks are : 1 = Br^-, 2 = I^-, 3 = NO_2^-, 4 = NO_3^-, 5 = $S_2O_3^{2-}$, 6 = SCN^-, 7 = CrO_4^{2-}.

Several selectivity changes were evident over the range of ClO_4^- concentrations studied, as shown in Figure 3.6. It should be noted that two different trends occurred as the concentration of competing ion was increased. The first was an increase in the observed mobility of the analytes (i.e. the analytes migrated more rapidly) due to a reduction of the IE interaction with the stationary phase. The second was a reduction in the relative electrophoretic mobility (i.e. the analytes migrated more slowly) due to an increase in ionic strength. This second effect was particularly apparent for CrO_4^{2-} and $S_2O_3^{2-}$ for ClO_4^- concentrations >20 mM. Selectivity changes occurred between Br^- and NO_2^-, NO_2^- and I^-, NO_3^- and I^-, $S_2O_3^{2-}$ and NO_3^-, and SCN^- and CrO_4^{2-} over the range of ClO_4^- concentrations studied.

3.3.2.3 *Analytical potential*

To show the potential of controlling the separation via IE interactions a model mixture was prepared requiring the determination of Br^- and NO_2^- in a 100-fold excess of I^-. Figure 3.7 shows the CE and OT-CEC separations in 50 mM Tris-Cl. In the CE separation, the high concentration of I^- resulted in the closely migrating peaks of Br^- and NO_2^- being obscured by the large I^- peak, making analysis impossible. However, the separation was achieved using the AS5A OT-CEC column by exploiting the large IE interaction of I^- and employing an appropriate concentration of competing ion to move the I^- peak to longer retention times. This enabled the I^- peak to be resolved completely from Br^- and NO_2^-.

3.3.3 *Variation of column capacity*

A further method for varying the contribution of IE interactions to the separation mechanism is to change the IE capacity of the column. While the IE capacity can, for example, be increased by increasing the IE capacity of the latex itself, or by adsorbing more onto the capillary wall, reducing the diameter of the capillary should have a similar effect. Decreasing the capillary diameter was found to increase the

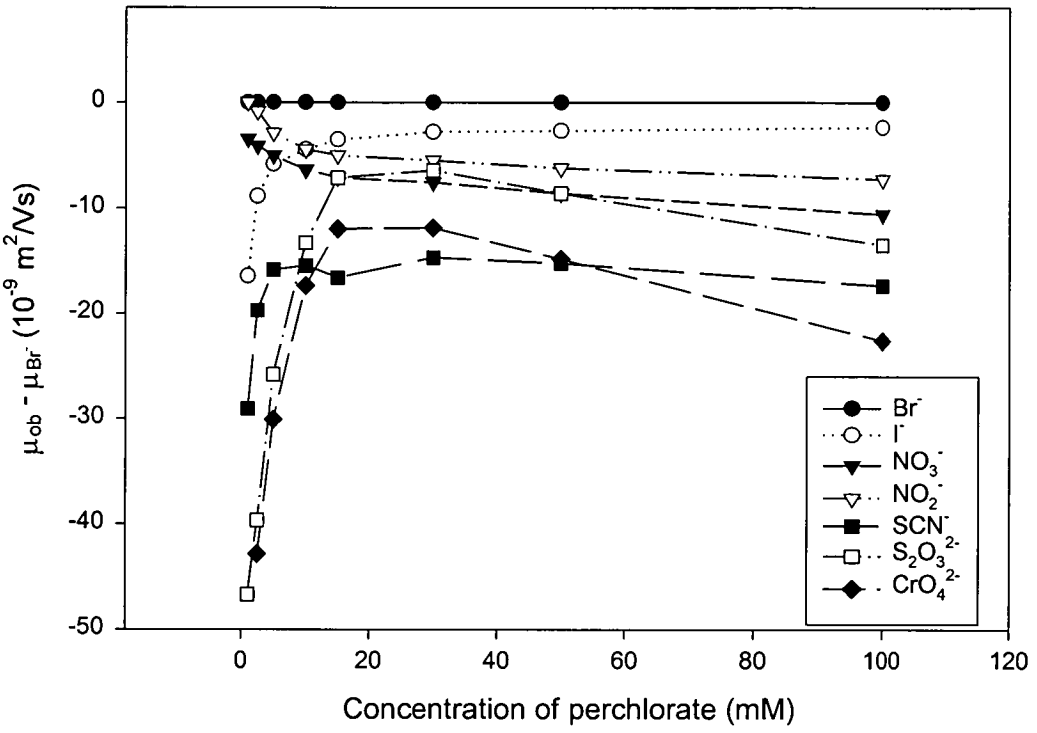

Figure 3.6: Change in observed mobility (with respect to bromide) of inorganic anions with concentration of perchlorate in the electrolyte. Conditions as in Figure 3.5.

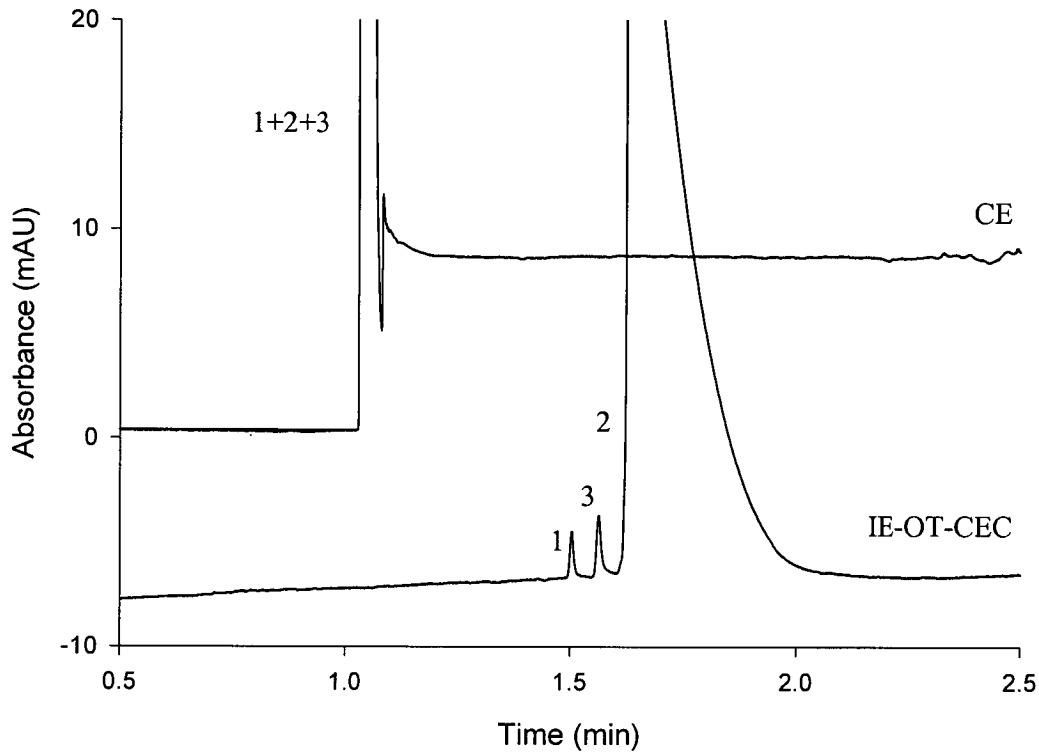

Figure 3.7: Separation of 0.1 mM Br^- and 0.1 mM NO_2^- in 10 mM I^- by CE and OT-CEC using a 100 mM Tris / 50 mM Cl^- (pH 8.05) electrolyte. Peaks are 1=Br^-, 2=I^-, and 3=NO_2^-. Other conditions as in Figure 3.3.

interaction with the stationary phase, i.e. at a given concentration of ClO_4^- more IE interaction was observed in the narrower capillary. This is illustrated in Figure 3.8, which shows that the migration times for strongly interacting analytes such as I^-, SCN^-, $S_2O_3^{2-}$ and CrO_4^{2-} were longest in the narrowest capillary. This is due to changes in the ratio of stationary phase to mobile phase, as seen from Equation (3–1) [11], which relates the retention factor (k'_A) in IEC to, among other parameters, the weight of the stationary phase (w) and the volume of the mobile phase (V_{mp}).

$$\ln k'_A = \frac{1}{y}\ln K_{A,E} + \frac{x}{y}\ln\frac{Q}{y} + \ln\frac{w}{V_{mp}} - \frac{x}{y}\ln\left[E^{y-}\right] \qquad (3\text{–}1)$$

$K_{A,E}$ is the IE selectivity coefficient between the analyte A^{x-} and an eluent competing ion E^{y-}, and Q is the IE capacity of the column. If it is assumed that the weight of latex stationary phase adsorbed onto the surface of the capillary is directly proportional to the surface area available then the following equation relating the amount of stationary phase and volume of mobile phase can be derived:

$$\frac{w}{V_m} = d.\frac{2}{r} \qquad (3\text{–}2)$$

where r is the radius of the capillary and d is a constant relating the surface coverage to the weight of the resin. If it is assumed that the surface coverage in the different diameter capillaries is the same, and that the EOF does not change with capillary diameter, then the change in migration time of the analytes should be directly proportional to the change in the phase ratio of stationary and mobile phases.

Figure 3.9 shows a plot of migration time *versus* 1/r for some of the analytes, and an approximately linear relationship was observed. However, it should be noted that only three different capillary diameters were used to examine this relationship so whilst the experimental results are in agreement with theory, they cannot be regarded as providing unequivocal support.

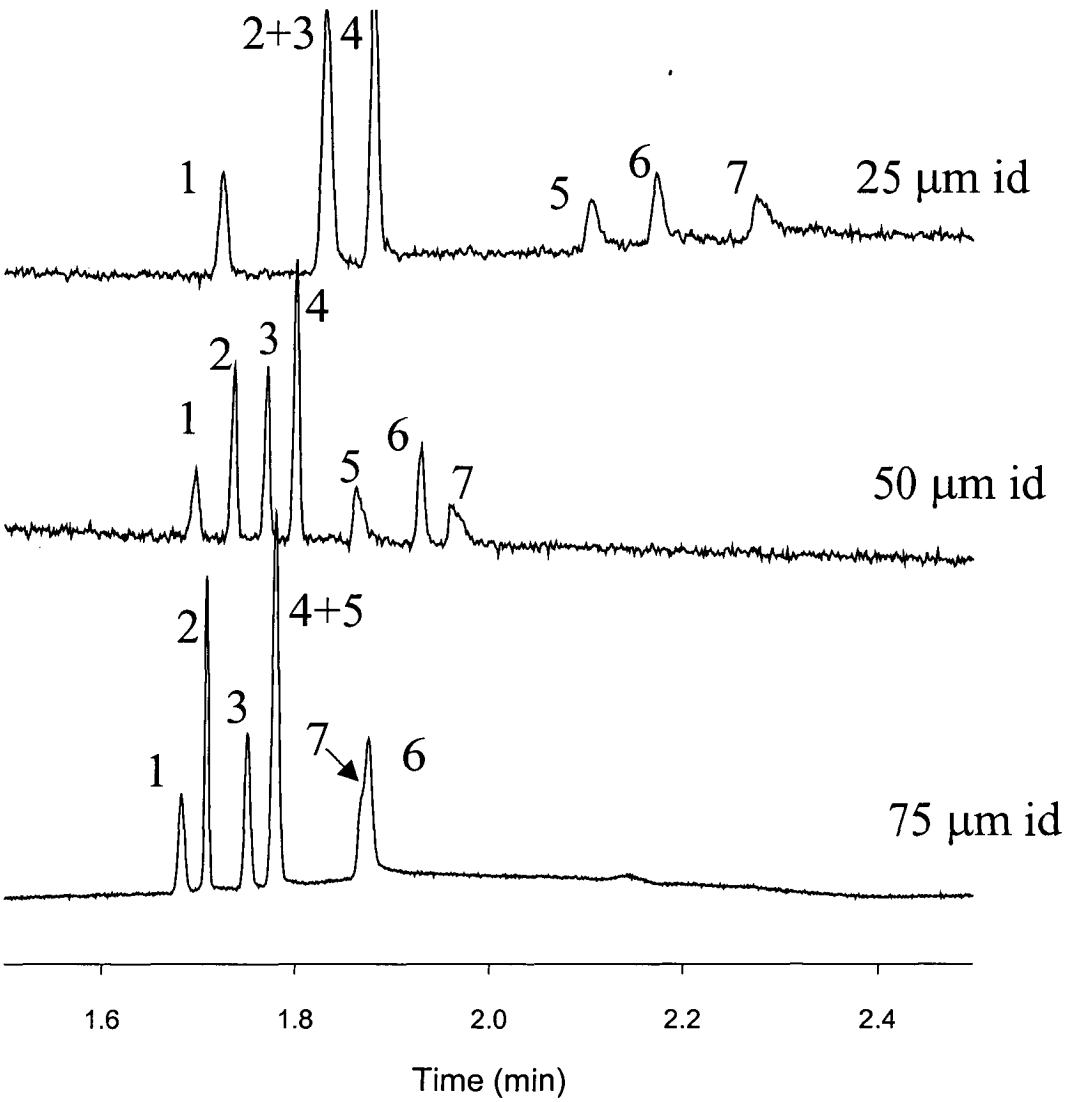

Figure 3.8: Separation of 7 inorganic anions in AS5A coated capillaries of different diameters. Conditions : 100 mM Tris / 50 mM ClO_4^- (pH 8.05). Absorbance scale for 75 (x1), 50 (x2), 25 (x10). Other conditions as in Figure 3.2. Peaks are : 1 = Br^-, 2 = I^-, 3 = NO_2^-, 4 = NO_3^-, 5 = $S_2O_3^{2-}$, 6 = SCN^-, 7 = CrO_4^{2-}.

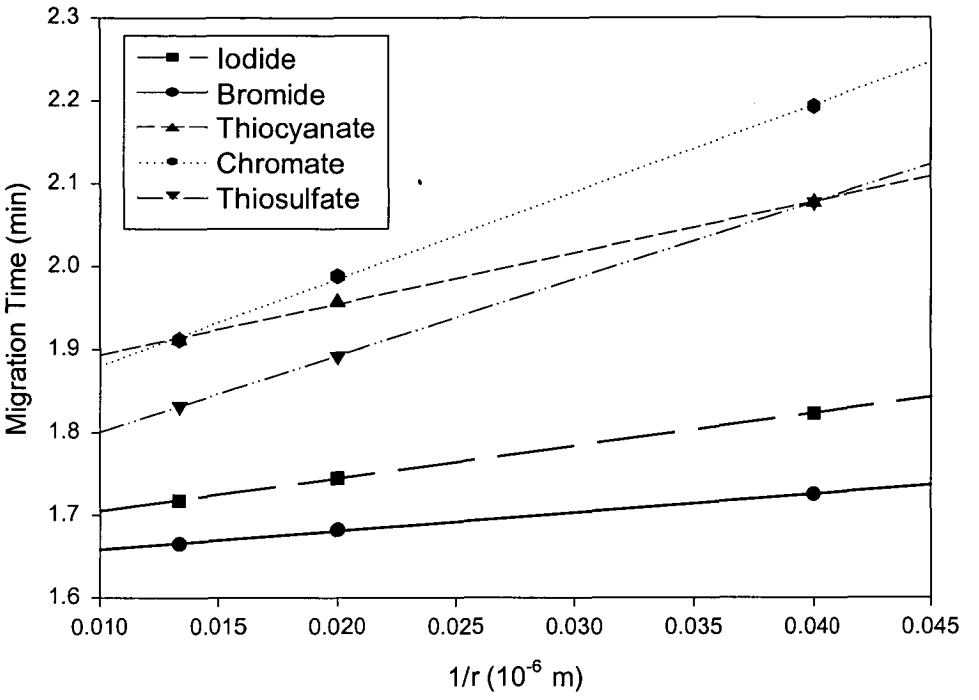

Figure 3.9: Relationship between surface area (1/r) and migration time for analytes in OT-IE-CEC in different diameter capillaries.

There were two practical considerations which arose when using narrow capillaries. First, decreasing the capillary diameter resulted in a lower separation current, so that higher electrolyte concentrations could be used before the applied voltage needed to be reduced due to current limitations. This allowed the use of a greater range of eluent concentrations without the undesirable influence of Joule heating. Second, the use of narrower capillaries made detection (in this case UV/Vis absorption) more problematic due to the reduced path length in the detection cell.

3.3.4 Reproducibility and stability of coated capillaries

Five capillaries were coated to determine the reproducibility of the coating procedure. To determine the column stability, separations of a mixture of thiourea and five inorganic anions (Br^-, NO_2^-, NO_3^-, SCN^- and I^-) using a 10 mM Cl^- electrolyte were made over an extended period. Reproducibility of the EOF was judged to be the most accurate method for determining whether the coatings were similar as any small difference in the surface charge would greatly influence the EOF. The relative standard deviation of the electroosmotic mobility was 3.4%, suggesting that the coating had been applied reproducibly.

The reproducibility of migration times in a single capillary was determined from 20 consecutive injections of thiourea as the EOF marker in 10 mM Cl^-. The %RSD was 0.79%. Long-term stability was determined by calculation of EOF after approximately 400 electrophoretic experiments using the same capillary over a 2 month period, over which period the time for migration of the EOF changed from 3.66 to 4.12 min, showing that the coated capillaries were relatively stable. There was little change in peak shapes and migration times over this period, indicating little or no column degradation. This agrees with the results of Kleindienst *et al.* [8] who observed that similarly coated capillaries could be used for protein analysis for a 2 month period without significant column degradation.

3.4 Selectivity manipulation of UV transparent anions

While the potential of IE-OT-CEC for the selectivity manipulation of UV absorbing anions has been demonstrated, many applications require the determination of non-UV absorbing species. In CE, this is most commonly achieved by using indirect spectrophotometric detection whereby a UV absorbing anion is added to the electrolyte which is displaced by the analytes causing an indirect change in absorbance. The extension of OT-IE-CEC to UV transparent anions will allow more analytes to be analysed.

3.4.1 Requirements for indirect spectrophotometric detection

The use of indirect spectrophotometric detection in CE has been reviewed recently [13] and the major factors influencing optimal performance have been described. First, buffering of the electrolyte is necessary to provide ruggedness and reproducibility [13,14], but this buffering should be provided in a way that does not reduce sensitivity by introducing co-ions that can compete with the probe during analyte displacement or introduce system peaks [15]. Second, matching the mobility of the analytes and the probe, and keeping the probe concentration to a maximum, are necessary in order to minimise electromigrational dispersion [13]. Third, detection sensitivity is maximised by choosing a probe with a high molar absorptivity [14]. In addition to these factors a further constraint is placed on the IE-CEC system by the fact that the probe must also act as an IE competing ion, and throughout the discussion use of the term probe also implies that this species acts as an IE competing ion.

3.4.2 Chromate as an IE-CEC eluent

In CE, chromate is the most commonly used probe for the detection of UV transparent inorganic ions [15]. The migration order of eight common inorganic ions in a chromate electrolyte in CE is $Br^- < Cl^- < SO_4^{2-}$, $SO_3^{2-} < ClO_3^- < F^- < BrO_3^- < IO_3^-$. On the other hand, the elution order of these ions on an AS5A column using a chromate eluent was $F^- < IO_3^- < BrO_3^- < Cl^- < Br^- < ClO_3^- < SO_3^{2-}$, SO_4^{2-}. It is clear that the separation orders by CE and IEC were significantly different, and the introduction of IE interactions into a CE separation should enable the separation selectivity to be changed, similar to that observed for UV transparent ions. Separations performed with a electrolyte containing between 0.5 and 5 mM CrO_4^{2-} showed only slight reductions in electrophoretic mobilities for these ions, indicating that even at low concentrations, the probe was efficiently suppressing any IE interactions. Lower concentrations of chromate could be expected to lead to greater IE interactions, but under these conditions the buffering capacity would be limited, causing poor reproducibility. In addition, electromigration dispersion would become more significant at chromate concentrations of less than 0.5 mM.

3.4.3 Nicotinate and p-toluenesulfonate as IE-CEC eluents

Since chromate was too strong as an IE competing ion, a probe with a weaker IE selectivity coefficient was sought in order to introduce more IE interaction into the IE-CEC system. Nicotinate [16] and *p*-toluenesulfonate [11] have been used in IEC as probes for indirect detection and being singly charged should be weaker eluents than chromate.

Using a similar experimental approach as for chromate, the concentration of nicotinate was varied over the concentration range 1–20 mM. The elution order observed for IE-CEC ($Cl^- < F^- < BrO_3^- < Br^- < ClO_3^- < IO_3^- < SO_4^{2-}$, SO_3^{2-}) using 2 mM nicotinate as the electrolyte closely resembled the usual IEC order ($F^- < IO_3^- < BrO_3^- < Cl^- < Br^- < ClO_3^- < SO_3^{2-}$, SO_4^{2-}), particularly when one examines the relative positions of Br^-, SO_4^{2-} and SO_3^{2-} (moderately strong IE interactions) and F^- (weak IE interaction) (Figure 3.10). The extent of IE interactions can be seen on a qualitative level from the values of effective mobility of the ions, which were reduced significantly when compared to the chromate system (Figure 3.10). For example, the effective mobility of Br^- ranged from –33 x 10^{-9} m^2/Vs to -61 x 10^{-9} m^2/Vs using the nicotinate probe, while it was much higher in the chromate system (–64 x 10^{-9} m^2/Vs to –73.8 x 10^{-9} m^2/Vs). The strongly interacting ions SO_4^{2-} and SO_3^{2-} were not detected in the nicotinate system because they either remained on the column or were eluted very much later in the region of the EOF peak where they were difficult to detect. As in the chromate system, varying the nicotinate concentration over the range available did not result in large changes in selectivity. The higher concentrations of nicotinate did not succeed in significantly reducing the IE interaction of SO_4^{2-} and SO_3^{2-} and at these higher concentrations (20 mM and above) high currents and increased baseline noise were evident. For example, the signal:noise ratio was reduced by approximately one third on increasing the probe concentration from 10 mM to 20 mM nicotinate.

The use of 10 mM *p*-toluenesulfonate as electrolyte in IE-CEC was examined and it was found that this competing ion inhibited significant IE interactions since the observed elution order in IE-CEC (Br^-, $Cl^- < SO_4^{2-}$, $SO_3^{2-} < ClO_3^- < F^- < BrO_3^- < IO_3^-$) was similar to that observed for the chromate system (Figure 3.10). However, the effective mobilities were significantly reduced, for example, the effective mobility of SO_4^{2-} was -56 x 10^{-9} m^2/Vs using the *p*-toluenesulfonate electrolyte

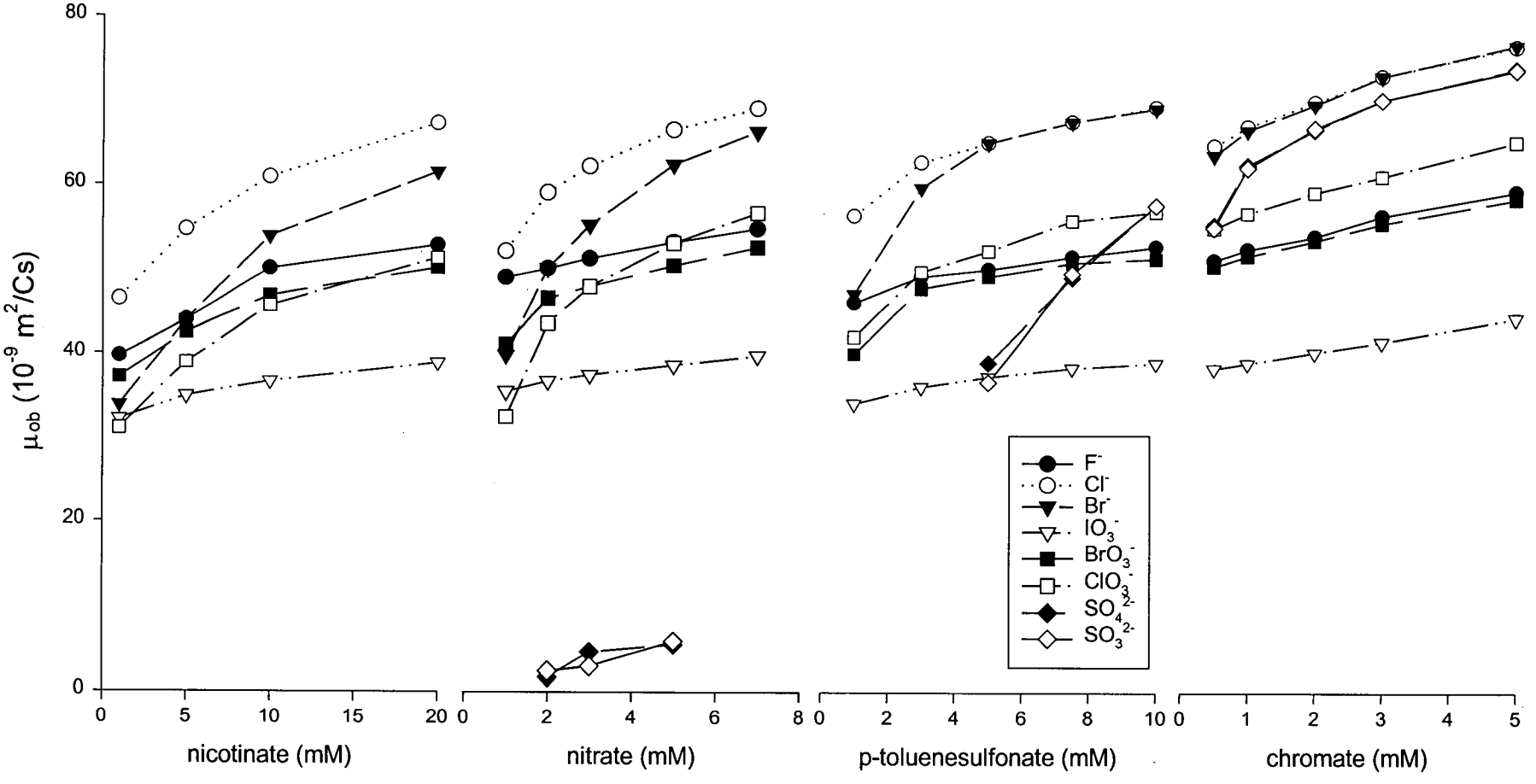

Figure 3.10: Plots of probe concentration *versus* effective mobility for eight inorganic ions and four probes (nicotinate, chromate, *p*-toluenesulfonate, nitrate).

compared to -73.8×10^{-9} m^2/Vs for the CrO_4^{2-} electrolyte. Reducing the concentration of *p*-toluenesulfonate to 7.5 mM resulted in an increase in the IE interactions and an altered elution order with SO_4^{2-} and SO_3^{2-} (μ_{eff} = -49×10^{-9} m^2/Vs) being eluted together after F^- ($\mu_{eff} = -51.5 \times 10^{-9}$ m^2/Vs). Use of a 5 mM probe concentration further increased the interaction of SO_4^{2-} and SO_3^{2-} with the stationary phase ($\mu_{eff} = -39 \times 10^{-9}$ m^2/Vs). At lower concentrations (0.5–5 mM) of the probe, weakly interacting ions such as Br^- and BrO_3^- showed stronger IE effects and this allowed novel separation selectivities to be achieved.

The use of nicotinate and *p*-toluenesulfonate as electrolytes can be summarised as follows. Nicotinate was a weakly competing probe that allowed significant IE interaction, as evident from the typical IEC elution order observed for analyte ions with moderate IE selectivity coefficients. However, varying the concentration of the probe was not a suitable method to manipulate the separation selectivity. On the other hand, *p*-toluenesulfonate was a stronger competing ion than nicotinate and provided separation selectivities intermediate between those of chromate and nicotinate. Varying the concentration of *p*-toluenesulfonate could be used to alter the separation selectivity of the analyte ions, especially the divalent ions SO_4^{2-} and SO_3^{2-}.

While the focus here was to investigate how the selectivity of UV-transparent analyte ions can be manipulated using UV-absorbing probes, it must also be realised that probe selection based on IE strength alone will not necessarily provide the best system. It is well known in CE that for optimal peak shapes it is necessary for the mobility of the analyte to be similar to that of the probe. Mismatching of mobilities is known to lead to distorted peak shapes due to electromigrational dispersion and hence a reduction in the separation efficiency [15]. It is therefore not surprising that when analysing inorganic anions with *p*-toluenesulfonate ($\mu_{ep} = -28.6 \times 10^{-9}$ m^2/Vs) as probe significantly fronted peaks were obtained, as observed in Figure 3.11.

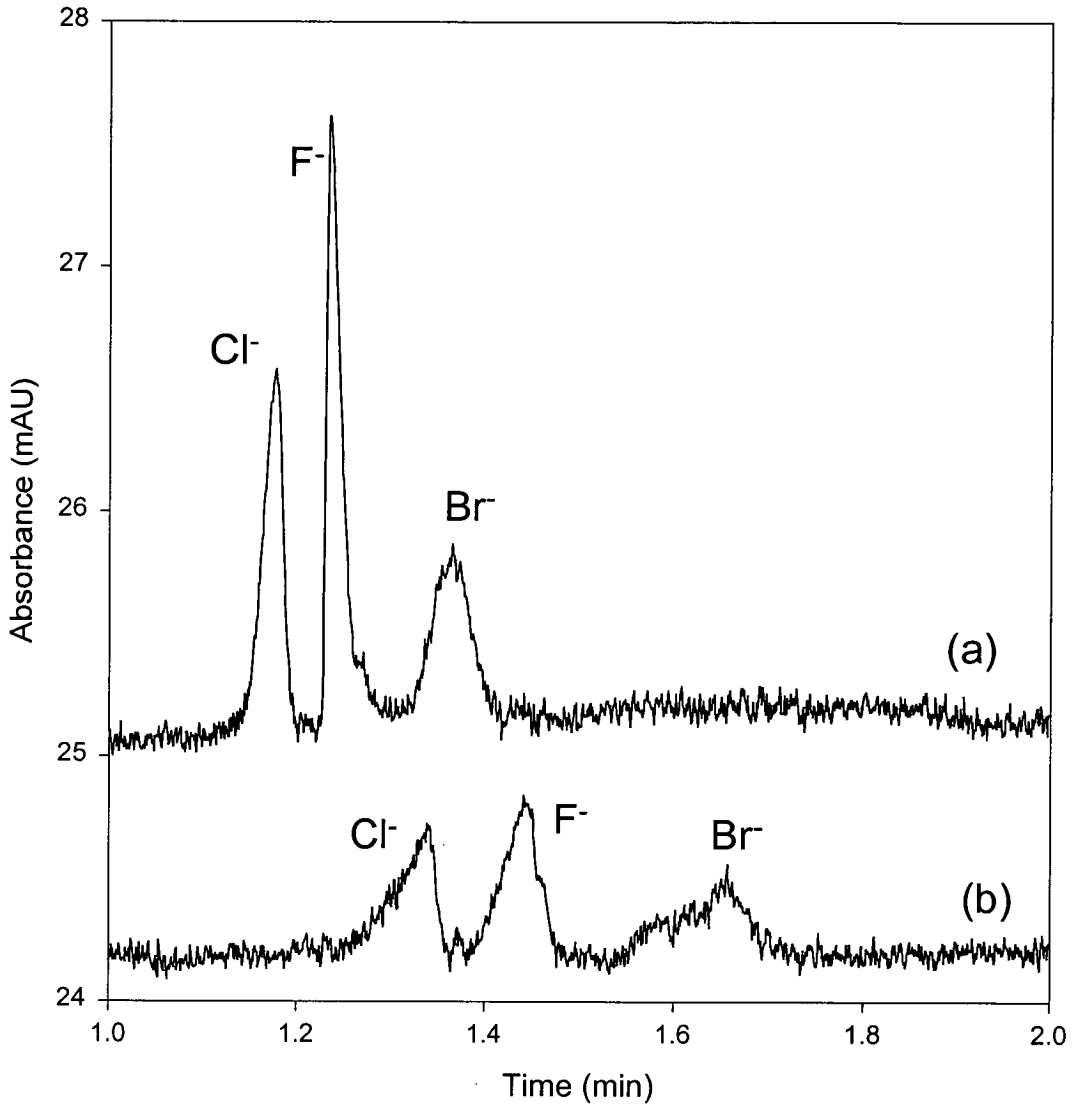

Figure 3.11: Separation of 3 inorganic ions using (a) 1mM nitrate/2 mM diethanolamine (DEA, pH 9.2) and (b) 0.5 mM *p*-toluenesulfonate/1 mM DEA (pH 9.2) as the eluent. Conditions: 50 cm capillary (41.5 cm to detector), -30 kV, indirect detection at 214 nm. Hydrostatic injection of 1.0 mM for 1s.

The ideal probe for this situation is one that will have a similar IE strength to *p*-toluenesulfonate, but a higher mobility.

3.4.4 Probe selection based on chromatographic and electrophoretic properties

The results obtained using the three different probes (chromate, *p*-toluenesulfonate and nicotinate) indicate that UV-absorbing probes can be used effectively as eluents in IE-CEC with indirect spectrophotometric detection, and that the choice of probe (in particular its eluting strength and electrophoretic mobility) is important in obtaining a desired separation. Whilst simple variation of the probe concentration was a suitable method for varying the selectivity of UV absorbing anions, this approach cannot be used here due to the concentration range being limited by practical considerations. Therefore, a range of probes of differing eluting strength and electrophoretic mobilities is required so that the desired separation selectivity can be achieved whilst still maintaining suitable peak shapes.

The eluting power of a number of potential probes was determined by IEC, with each probe being injected onto an AS5A column and eluted using 150 mM Cl^- / 300 mM diethanolamine (DEA), pH 9.2 as eluent, with direct spectrophotometric detection. The retention factors for each of the probes are listed in Table 3.1. Electrophoretic mobilities were measured by CE in a 10 mM chromate/40 mM DEA electrolyte (pH 9.2) and values are also shown in Table 3.1. The three probes studied in detail earlier were eluted in the order nicotinate < *p*-toluenesulfonate < chromate, which corresponded to the observed IE interactions for these probes, while the electrophoretic mobilities are in the order chromate > nicotinate > *p*-toluenesulfonate. It is therefore expected that *p*-toluenesulfonate will give the most

Table 3.1: Retention factors (k') and mobility data for a number of probes.

Probe	k'*	Mobility** 10^{-9} $m^2/(V.s)$
Iodate	0.078	-42.6
Nicotinate	0.164	-33.8
Nitrite	0.124	-75.3
Sorbate	0.357	-31.6
Nitrate	0.599	-73.1
Benzoate	0.599	-29.6
Benzenesulfonate	1.66	-33.0
Molybdate	1.71	-72.8
Phthalate	1.96	-51.6
p-Hydroxybenzoate	2.36	-31.8
p-Toluenesulfonate	2.39	-28.6
Chromate***	3.30	-72.2
Iodide	3.46	-76.2
Salicylate	4.128	-28.5
3,5-Dihydroxybenzoate	4.328	-27.1
Thiocyanate	5.381	-63.0
1,2-Benzenedisulfonate	8.737	-47.6
1,5-Naphthalenedisulfonate***	> 15	-54.4

* The ions were separated on a 4 x 150 mm Ion Pac AS5A, (5 mm) IE column using 150 mM Cl^- /300 mM DEA (pH 9.2) as the eluent, direct detection and a flow rate of 0.5 mL min^{-1}

** The ions were separated on a 50 cm capillary (41.5 cm to detector) using 10 mM chromate/ 40 mM DEA (pH 9.2) and 0.5 mM TTAB as the eluent, indirect detection at 254 nm and an applied voltage of -20 kV.

*** measured counter EOF in DEA – Sulfate (10 mM / 40 mM, pH 9.2)

electrophoretic dispersion with moderate IE eluting power, and chromate will give the least electromigration dispersion and the most IE eluting power. This suggests that the data in Table 3.1 can be used to select a probe of a desired IE strength with an appropriate electrophoretic mobility for the analytes of choice.

To demonstrate this, Table 3.1 shows that there are several probes that are intermediate in IE interactions between *p*-toluenesulfonate and nicotinate. For instance, NO_3^- and MoO_4^{2-} have mobilities close to many of the inorganic anions used in this study and therefore should minimise electromigrational dispersion. To examine this, nitrate was investigated as it was available in the laboratory in high purity and in an acidic form which could be buffered with DEA without introducing system peaks [15].

Figure 3.12 shows the separation of inorganic ions in IE-CEC using 3 mM nitrate as the probe. As expected, the extent of IE interactions lie between those observed for the nicotinate and *p*-toluenesulfonate eluents, with SO_4^{2-} and SO_3^{2-} being eluted after F^- and before the EOF. The effective mobility for SO_4^{2-} in CE is -76.7 x 10^{-9} m^2/Vs, compared to only -5 x 10^{-9} m^2/Vs in the IE-CEC system. The range over which nitrate would function as a suitable probe is shown in Figure 3.10 where it can be seen that high concentrations of probe (6 mM) give a separation order that is similar to that of *p*-toluenesulfonate, while a low concentration (1 mM) gives an order resembling that in nicotinate. Intermediate selectivities are substantially different from those obtained with nicotinate and *p*-toluenesulfonate due to the change in mobilities of moderately interacting analytes such as Br^- and ClO_3^-. These results show that nitrate does indeed offer separation selectivities which are intermediate between those of *p*-toluenesulfonate and nicotinate.

The significance of probe mobility is clearly evident when separations involving Br^-, Cl^- and F^- using 0.5 mM *p*-toluenesulfonate and 1 mM nitrate are compared (Figure 3.11). Both probes at the given concentrations gave similar separation selectivities

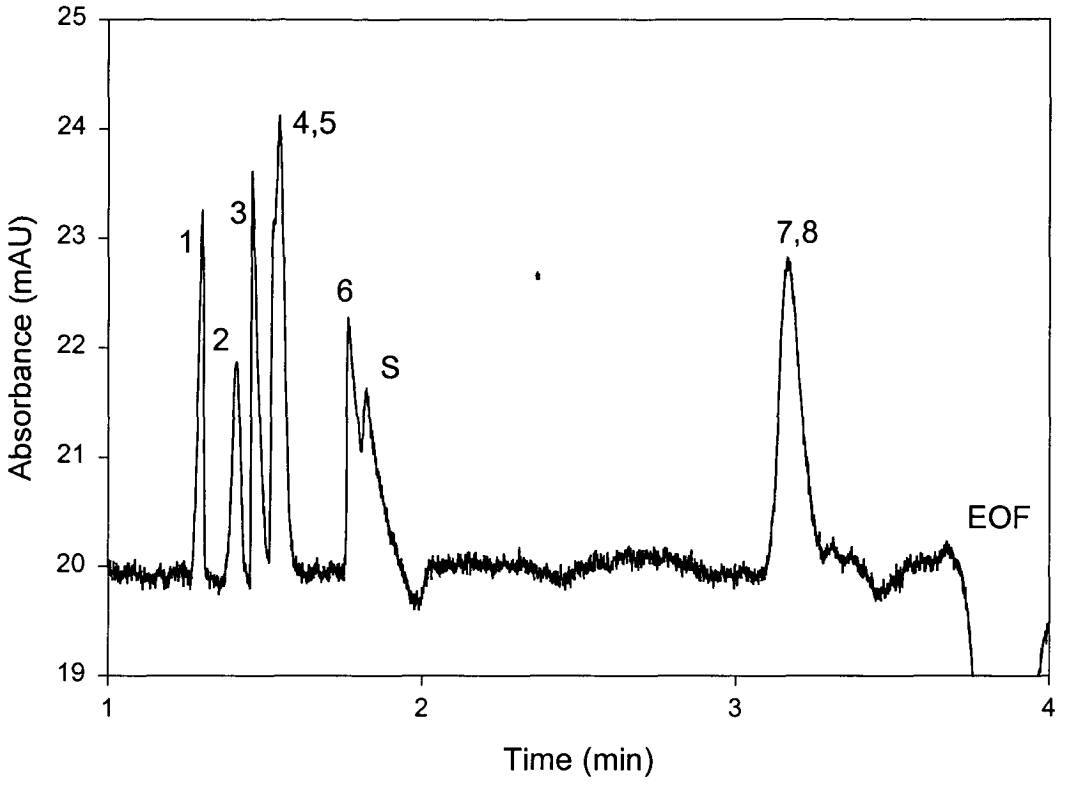

Figure 3.12: Separation of 8 inorganic ions using 3 mM nitrate as the probe. Conditions: 3 mM NO_3^- /6 mM DEA (pH 9.2), 50 cm capillary (41.5 cm to detector), -30 kV, indirect detection at 214 nm. Hydrostatic injection of 1.0 mM for 3 s. Peaks are 1 = Cl^-, 2 = Br^-, 3 = F^-, 4 = BrO_3^-, 5 = ClO_3^-, 6 = IO_3^-, 7 = SO_3^{2-}, 8 = SO_4^{2-} and S = system peak.

for these analytes, but the separation using *p*-toluenesulfonate was poorer. *p*-Toluenesulfonate has a low mobility and this factor, coupled with the low probe concentration used, led to electrophoretically distorted peaks. In contrast, much better peak shapes were obtained with nitrate due to the similar mobilities of the analytes and the probe and the higher probe concentration.

3.5 Modelling the migration

It has been shown in the previous sections that typical IEC approaches to selectivity manipulation (i.e. by changing the type and concentration of a competing ion in the electrolyte), could be used to alter the mobility and hence selectivity of inorganic anions. However, it is clear that to be able to control the separation selectivity in IE-CEC, an understanding of the relative contributions of chromatographic and electrophoretic processes to the overall separation mechanism is required. Therefore a theoretical model was derived from IE and CE theory to describe the mobility of an anion in IE-CEC. It is important to note that in electrochromatographic systems without pressure-assisted flow, the electrophoretic contribution is constant, while the chromatographic component can be varied according to the degree to which the analytes interact with the stationary phase. For this reason, emphasis is placed on determining the influence of the IE component in the separation mechanism and subsequent control of this interaction in order to manipulate the separation selectivity of the system.

3.5.1 Theory

The observed mobility of an analyte in CEC can be regarded as the proportional sum of the effective mobilities in the mobile and stationary phases [17-20]

$$\mu_{ob} = \alpha_{mp}.(\mu_{mp} + \mu_{eof}) + \alpha_{sp}.(\mu_{sp} + \mu_{eof}) \qquad (3\text{–}3)$$

where α_{mp} is the mole fraction in the mobile phase, α_{sp} is the mole fraction in the stationary phase, μ_{ob} is the observed mobility, μ_{mp} is the effective mobility in the mobile phase, μ_{sp} is the effective mobility in the stationary phase, and μ_{eof} is the effective electroosmotic mobility.

For CEC the stationary phase does not move, and equation (3–3) becomes:

$$\mu_{ob} = \alpha_{mp}.(\mu_{mp} + \mu_{eof}) \tag{3–4}$$

The distribution of analyte between the mobile and stationary phases, given by the mole fraction of the analyte in the mobile phase α_{mp}, can be expressed in terms of the retention factor k', according to the following equation, [20,21]

$$\alpha_{mp} = \frac{1}{1+k'} \tag{3–5}$$

where, k' is defined as:

$$k' = D\frac{w}{V_{mp}} \tag{3–6}$$

with D being the distribution coefficient of the analyte between the mobile and stationary phases, w is the weight of the stationary phase, and V_{mp} is the volume of the mobile phase. The observed mobility of an analyte can be obtained by substituting equation (3–5) into equation (3–4) to give

$$\mu_{ob} = \frac{1}{1+k'}.(\mu_{mp} + \mu_{eof}). \tag{3–7}$$

The influence of increasing the concentration of the competing ion in the electrolyte can be obtained from the general equation in IEC which relates the retention factor to a number of parameters including the eluent concentration [11]:

$$k'_A = \left(\frac{w}{V_{mp}}\right).\left(K'_{A,E}\right)^{1/y}.\left(Q/y\right)^{x/y}.[E]^{-x/y} \tag{3–1}$$

where A^{x-} is the analyte, E^{y-} is the competing ion in the eluent, $K_{A,E}$ is the selectivity coefficient between the analyte and competing ions, Q is the IE capacity of the stationary phase, w is the weight of the stationary phase, and V_{mp} is the volume of the mobile phase. If only the concentration of the eluent is changed, then the equation can be simplified to give:

$$\ln k'_A = c - \frac{x}{y}\ln[E] \tag{3–8}$$

where c is defined as:

$$c = \frac{1}{y}\ln K'_{A,E} + \frac{x}{y}\ln\frac{Q}{y} + \ln\frac{w}{V_{mp}} \tag{3–9}$$

Transposing equation (3–8) for k' and substituting into equation (3–7) gives:

$$\mu_{ob} = \frac{1}{1+e^{c-\frac{x}{y}\ln[E]}}.(\mu_{mp} + \mu_{eof}). \tag{3–10}$$

Changes in the concentration of the competing ion in the electrolyte will not only influence the contribution of IE to the migration of analytes but will also alter the effective mobility of the analyte due to changes in ionic strength. The relationship between electrophoretic mobility and ionic strength can be expressed as [12,22,23]:

$$\mu_{mp} = \frac{b}{\sqrt{I}} \tag{3–11}$$

where b is a constant related to the electrophoretic mobility under conditions of zero ionic strength. Substituting into equation (3–10) gives:

$$\mu_{ob} = \frac{1}{1+e^{c-\frac{x}{y}\ln[E]}}.(\frac{b_{ep}}{\sqrt{I}} + \frac{b_{eof}}{\sqrt{I}}) \tag{3–12}$$

The electrolytes used in this work were prepared by titrating the acid form of the competing anion with the base Tris to a pH of 8.05 (=pK_a). The electrolyte will

therefore contain equivalent concentrations of the competing ion E, and the buffer components Tris and $TrisH^+$. The ionic strength can therefore be calculated from the following equation:

$$I = \tfrac{1}{2}\left(y^2.[E] + 2.|y|.[E]\right). \qquad (3\text{–}13)$$

3.5.2 UV absorbing anions

Seven UV absorbing inorganic anions (Br^-, I^-, NO_2^-, NO_3^-, SCN^-, CrO_4^{2-}, $S_2O_3^{2-}$) were selected as test analytes to cover a broad range of different electrophoretic mobilities and IE selectivity coefficients. Four different competing ions (chloride, sulfate, citrate and perchlorate) were selected on the basis of their eluotropic strengths and charge. Competing ion concentrations were generally varied from a low value (in the range 1-10 mM) to a concentration which was sufficiently high to suppress any IE interaction with the capillary wall (100-1000 mM). The exception to this was citrate, which was restricted to ≤50 mM due to high baseline absorbance. Eight different electrolyte conditions were used for all cases, except when using chloride for which 11 electrolyte conditions were used, to give a total of 224 data points for all analytes in all eluents (see Table 3.2). The OT system permitted the model to be tested over a wide range of electrolyte conditions. For example, when chloride was used as the competing ion the maximum concentration used was 1000 mM (which was necessary to ensure that all IE interactions with the stationary phase were suppressed). However, at these high concentrations of competing ion, the EOF was negligible [12] and measurement of EOF was therefore subject to considerable errors. For this reason it was necessary to reformulate equation (3–12) so as to eliminate the μ_{eof} term. This was done by expressing the observed mobility of the analyte relative to that of an internal reference analyte. The analyte selected for this purpose was Br^-.

Table 3.2: Experimental conditions used to validate the model.

	Electrolyte			
	Chloride	Sulfate	Citrate	Perchlorate
Minimum concentration (mM)	10	1	1	1
Maximum concentration (mM)	1000	300	50	100
Number of electrolyte compositions used	11	8	8	8
Concentration when voltage was reduced (mM)	150	50	50	-

The relative observed mobility for analyte A, $\mu_{ob,rel,A}$ can be defined as:

$$\mu_{ob,rel,A} = \mu_{ob,A} - \mu_{ob,Br} \tag{3–14}$$

Substituting expressions for $\mu_{ob,Br}$ and $\mu_{ob,A}$ from equation (3–7) the following expression is obtained:

$$\mu_{ob,rel,A} = \frac{1}{1+k'_A}.\left(\frac{b_{ep,A}}{\sqrt{I}} + \frac{b_{eof}}{\sqrt{I}}\right) - \frac{1}{1+k'_{Br}}.\left(\frac{b_{ep,Br}}{\sqrt{I}} + \frac{b_{eof}}{\sqrt{I}}\right) , \tag{3–15}$$

which can be rearranged to give:

$$\mu_{ob,rel,A} = \frac{1}{1+k'_A}.\left(\frac{b_{ep,A}}{\sqrt{I}}\right) - \frac{1}{1+k'_{Br}}.\left(\frac{b_{ep,Br}}{\sqrt{I}}\right) + b_{eof}\left(\frac{k'_{Br} - k'_A}{1+k'_A + k'_{Br} + k'_A.k'_{Br}}\right). \tag{3–16}$$

Assuming that k'_{Br} and k'_A are small numbers of similar magnitude, then:

$$\frac{k'_{Br} - k'_A}{1+k'_A + k'_{Br} + k'_A.k'_{Br}} \approx 0 \tag{3–17}$$

and after substitution for k'_{Br} and k'_A, the model equation can be obtained:

$$\mu_{ob,rel,A} = \frac{1}{1+e^{c(Br)-\frac{x(Br)}{y}\ln[E]}}.\left(\frac{b_{ep,Br}}{\sqrt{I}}\right) - \frac{1}{1+e^{c(A)-\frac{x(A)}{y}\ln[E]}}.\left(\frac{b_{ep,A}}{\sqrt{I}}\right) \quad (3\text{–}18)$$

This equation has a total of 4 unknowns (*c(Br)*, *c(A)*, $\mu_{ep,Br}$ and $\mu_{ep,A}$) requiring experimental data for two different analytes at three different electrolyte conditions in order to solve the equation by non-linear regression.

Equation (3–18) was applied to relative observed mobility data for each analyte using each competing ion and the parameter values determined by nonlinear regression are listed in Table 3.3. The correlation between experimental and calculated relative observed mobilities for all analytes and competing ions is shown in Figure 3.13. A high degree of correlation ($r^2 = 0.982$) between experimental and calculated relative observed mobilities was obtained. The poorer correlation evident for some data points in Figure 3.13 can be attributed to the fact that the model does not compensate for changes in mobility caused by Joule heating experienced for the more concentrated electrolytes when the current was > 70 μA, nor for any secondary interactions between analytes and the stationary phase, nor does it include interactions of the analytes with the buffering cation, Tris.

The trends in values of *c* and b_{mp} evident in the IE-CEC follow well known trends from IEC. For example, when using chloride as the competing ion, values of *c* (and hence the IE selectivity coefficients) were in the order NO_2^-, NO_3^-, Br^-, I^-, SCN^-, CrO_4^{2-}, and $S_2O_3^{2-}$, which agrees with the elution order of these analytes on an AS5A column [11].

The eluotropic strengths of different competing ions can also be assessed from the values of *c* in Table 3.3. Considering I^- as analyte, the value of *c* is 15.12 when using Cl^- as the competing ion, 5.83 when using SO_4^{2-}, and –0.68 when using citrate, so the IE selectivity coefficients for I^- decreased in the order $Cl^- < SO_4^{2-}$ < citrate when these species were used as competing ions. This sequence is the same as that observed for these species in IEC using a stationary phase with quaternary

Table 3.3: Constants determined from non-linear regression for UV absorbing anions.

Analyte	Parameter	Electrolyte			
		Chloride	Sulfate	Perchlorate	Citrate
Br^-	c	10.31	3.307	-0.493	-0.474
	b_{epl}	132.6	136.9	148.4	150.2
I^-	c	15.12	5.825	-0.680	-0.660
	b_{ep}	151.8	137.7	150.0	151.5
NO_3^-	c	7.35	2.652	-0.200	-0.282
	b_{ep}	141.0	133.5	147.9	149.6
NO_2^-	c	6.43	2.338	-0.178	-0.180
	b_{ep}	147.1	134.1	147.8	149.5
SCN^-	c	15.37	6.836	-0.814	-0.897
	b_{ep}	141.0	135.2	149.62	151.3
CrO_4^{2-}	c	25.18	10.640	-2.215	-2.385
	b_{ep}	161.1	158.1	185.9	188.0
$S_2O_3^{2-}$	c	28.5	12.501	-2.900	-3.064
	b_{ep}	165.6	159.7	185.8	187.8
	r^2	0.983	0.977	0.979	0.980
	Slope	0.978	0.962	0.974	0.970
	Intercept	-0.375	-0.291	-0.229	-0.206
	n	66	51	52	55

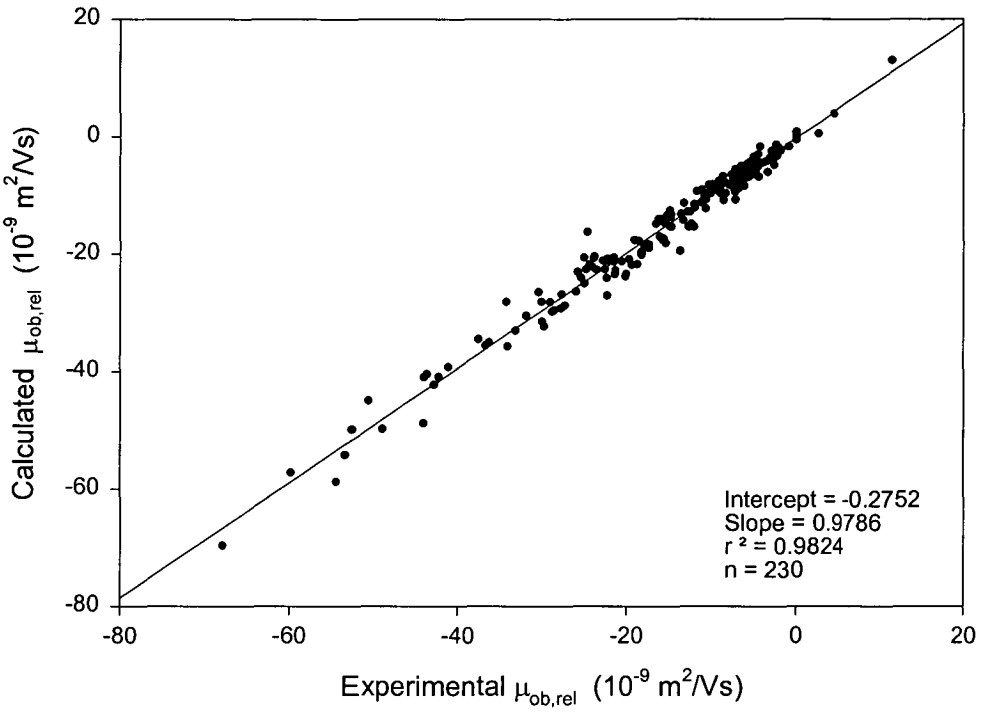

Figure 3.13: Correlation plot for 7 UV absorbing inorganic anions using 4 different competing ions in an AS5A coated capillary.

ammonium functional groups. In addition, the values of c for I^- were very similar when ClO_4^- and citrate were used as competing ions (c = -0.68 and –0.66 respectively), which again is the behaviour expected from IEC. Finally, it is important to note that the model was suitable for competing ions having differing charges (e.g. Cl^-, SO_4^{2-}, $citrate^{3-}$).

Figure 3.14 shows the variation in relative mobilities with increasing chloride concentration in the electrolyte, with experimental data points being represented by the symbols in the figure and the behaviour predicted by equation (3–14) being represented by the lines. The degree to which the relative mobility of a particular analyte changes with concentration of chloride is again correlated with the values of c obtained from the model. The calculated behaviour of relative mobilities fits closely with the experimental data. Figure 3.14 also shows the numerous changes in separation selectivity that could be achieved by selection of the appropriate electrolyte conditions. These changes in separation selectivity can be used to improve the resolution of the separation. This was done by using the model equation to obtain the best separation possible with any of the competing ions using a computerised optimisation method. For this purpose, the normalised resolution product criterion [11], r, was used to select the optimal conditions. This criterion is defined as

$$r = \prod_{i=1}^{n-1} \left(\frac{R_{s(i,i+1)}}{\frac{1}{n-1} \sum_{i=1}^{n-1} R_{s(i,i+1)}} \right) \qquad (3\text{–}19)$$

where $R_{s(i,i+1)}$ is the resolution between adjacent peaks. Values of r fall between 0 and 1, with a value of 1 indicating that the peaks are spread evenly over the available separation space. Calculations of r were performed using Sigma Plot for windows V 3.03. The separation selectivity was optimised by selecting the concentration of eluent that gave the best separation of all analytes. The conditions were then

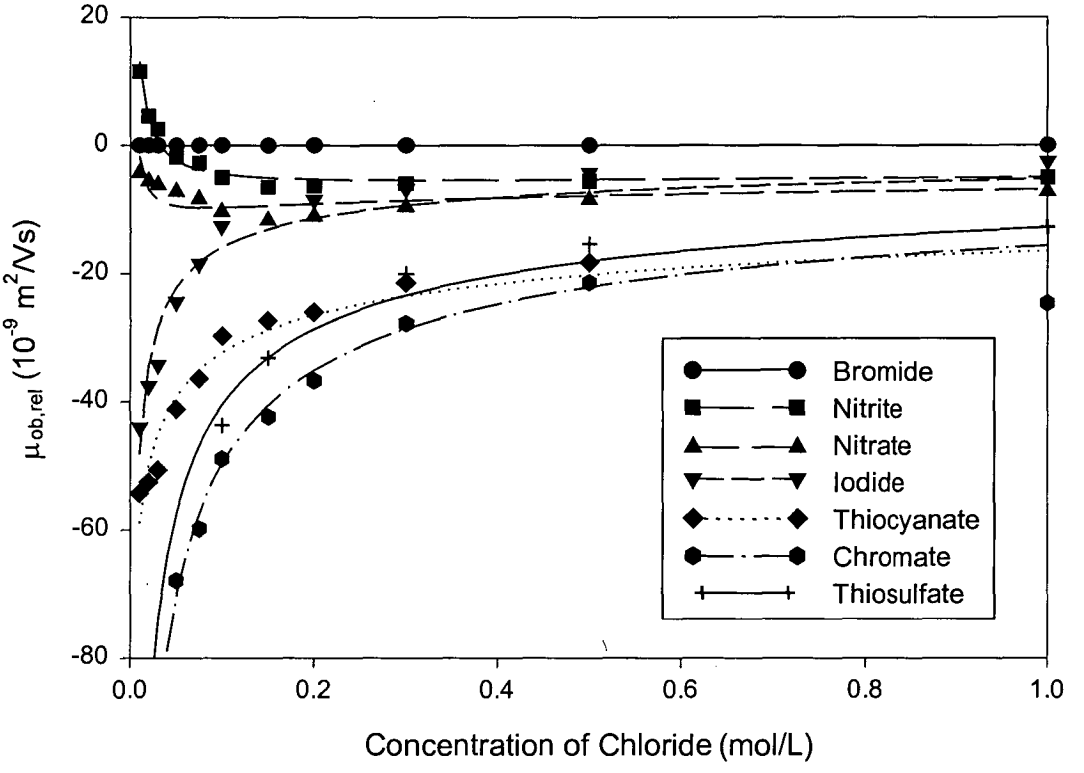

Figure 3.14: Change in relative observed mobility (WRT bromide) with increasing concentration of chloride in an AS5A open tubular column. Lines constructed using parameters determined from non-linear regression. Solid points are experimental values.

Table 3.4: Comparison of experimental and calculated relative mobilities of the test analytes for an open-tubular column using a electrolyte comprising 75 mM Cl^-, 150 mM Tris/$TrisH^+$, pH 8.05. Voltage -25 kV.

Analyte	Migration time (s)	Experimental $\mu_{ob,rel}$	Calculated $\mu_{ob,rel}$
Br^-	68.04	0.00	0.00
I^-	80.82	-18.46	-18.27
NO_2^-	69.66	-2.72	-2.79
NO_3^-	73.20	-8.26	-8.71
SCN^-	98.64	-36.27	-35.07
CrO_4^{2-}	138.66	-59.80	-57.55

restricted to provide the best separation in the shortest analysis time, with a electrolyte containing 75 mM Cl^- selected as the optimum conditions. A separation was performed under these conditions and Table 3.4 lists the observed migration times, observed relative mobilities and predicted relative mobilities for this separation. Again, good agreement between theory and experiment was obtained.

3.5.3 UV transparent anions

Eight UV transparent inorganic anions (F^-, IO_3^-, BrO_3^-, Cl^-, Br^-, ClO_3^-, SO_3^{2-} and SO_4^{2-}) were selected as test analytes to cover a broad range of different electrophoretic mobilities and IE selectivity coefficients. Four different competing ions (nicotinate, nitrate, *p*-toluenesulfonate and chromate) were selected on the basis of their eluotropic strengths. Competing ion concentrations were generally varied from a low value (0.5 to 1 mM) to a concentration where the baseline became excessively noisy (10 to 20 mM). Five different buffer conditions were used for nitrate and *p*-toluenesulfonate, with 4 different buffer conditions used for nicotinate and chromate giving a total of 119 data points for all analytes in all eluents.

Due to the low concentration range of competing ion examined in this case, the influence of ionic strength on EOF was negligible and values for the EOF could be measured in all cases. It was therefore possible to use equation (3–12) to model the

changes in mobility of the ions with the correlation between experimental and calculated observed mobilities illustrated in Figure 3.15. A high degree of correlation (r^2=0.983) between experimental and calculated observed mobilities was obtained.

Values for the constants determined from non-linear regression of equation (3–12) are shown in Table 3.5. Values for the constants for SO_4^{2-} and SO_3^{2-} when using nicotinate as a probe could not be calculated as the analytes were difficult to detect due to migration after the EOF. As for UV absorbing anions, values of c represent the strength of the IE interaction with the stationary phase while values of b_{ep} are related to the electrophoretic mobility of the analytes. Ordering the analytes from lowest to highest values of c (i.e. in order of increasing IE interaction in the IE-CEC system) gives $F^- < BrO_3^- < IO_3^- < Cl^- < ClO_3^- < Br^- < SO_3^{2-}$, SO_4^{2-} (see Table 3.5) which agrees with the order obtained by IEC.

Comparing values of c for different competing ions enables a quantitative comparison of eluotropic strength to be made. For example, values of c for Cl^- decrease from 0.63 to -0.99 to -2.59 on changing the electrolyte anion from nicotinate to *p*-toluenesulfonate to chromate. The value of c for Cl^- when using nitrate was -0.59 indicating that it is much closer in elution strength to *p*-toluenesulfonate than to fluoride.

3.6 Sources of band dispersion

While the introduction of a chromatographic phase on the capillary wall enables the separation selectivity to be varied and controlled, the separation efficiency for many of the analytes was substantially lower than for conventional CE. In order to improve the peak shapes of anions separated by OT-IE-CEC, an understanding of the possible sources of peak tailing in both the CE and IEC separation mechanisms is necessary. An important source for zone broadening in CE is electromigration dispersion resulting from differences in mobility between the co-ion (in this case, the

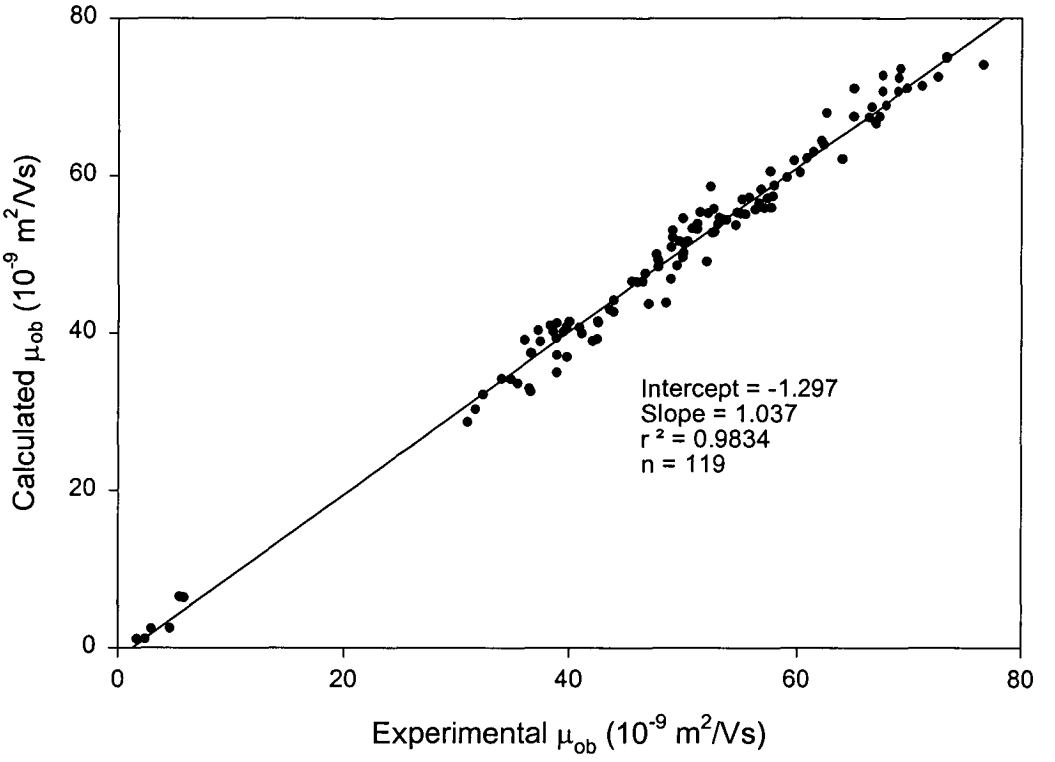

Figure 3.15: Correlation plot for 8 UV transparent inorganic anions using 4 different competing ions in an AS5A coated capillary.

Table 3.5: Constants determined from non-linear regression for UV transparent anions.

Analyte	Parameter	Electrolyte			
		Nicotinate	Nitrate	*p*-Toluenesulfonate	Chromate
F^-	c	0.34	-1.53	-1.48	-3.37
	b_{ep}	-56.5	-57.0	-56.8	-57.0
IO_3^-	c	0.35	-1.36	-1.45	-3.29
	b_{ep}	-41.4	-42.2	-42.3	-42.2
BrO_3^-	c	0.54	-0.93	-1.06	-3.34
	b_{ep}	-55.7	-55.7	-55.8	-57.0
Cl^-	c	0.63	-0.59	-0.99	-2.95
	b_{ep}	-73.8	-76.3	-76.3	-76.3
Br^-	c	1.33	0.11	-0.24	-2.36
	b_{ep}	-74.8	-78.1	-78.1	-78.1
ClO_3^-	c	1.21	0.01	-0.54	-2.65
	b_{ep}	-62.1	-64.6	-61.6	-64.6
SO_3^{2-}	c	-	5.65	3.47	-1.62
	b_{ep}	-	-79.9	-80.1	-80.0
SO_4^{2-}	c	-	5.67	3.59	-1.61
	b_{ep}	-	-80.0	-79.9	-79.9
	r^2	0.990	0.996	0.962	0.988
	Slope	1.04	1.02	1.16	0.995
	Intercept	-1.90	-0.942	-6.36	0.162
	n	18	36	41	24

eluent ion) and the analyte [24]. This results in analytes that have a mobility greater than the co-ion giving fronted peaks, those that have a mobility less than the co-ion giving tailed peaks, and those having a mobility equal to that of the co-ion giving symmetrical peaks. It should be noted that tailed peaks in CE caused by electromigration dispersion appear triangular in shape in contrast to the typical curved tailed peak shape often seen in chromatography. In IEC, inefficiency is characterised generally by the van Deemter equation, which identifies contributions due to inefficiency from three sources: flow inequalities in the column packing, axial diffusion in the mobile phase, and resistance to mass transfer effects in both the stationary and mobile phases [11]. Since the column used in this study was an open tubular column with an adsorbed monolayer of stationary phase [8], only the mass transfer effects in the mobile and stationary phases are likely to have significance [25]. Resistance to mass transfer in the stationary phase may arise from diffusion in the stationary phase and/or slow adsorption/desorption kinetics. In this case, as the support for the latex particles has a similar charge to that of the analytes, diffusion in the stationary phase does not contribute significantly to inefficiency [11]. With regard to the kinetics of adsorption/desorption, it has been shown by Fornstedt *et al.* [26] that when there are two mechanisms contributing to retention, then even if the second mechanism only influences retention to a minor extent, the influence on inefficiency can be quite significant. For the polarisable anions examined in this case, Pohl *et al.* [27-29] have shown that secondary interactions are involved in their separation on agglomerated IE columns and these interactions result in poor peak shapes. To overcome this, the addition of *p*-cyanophenol to the eluent has been used in IEC to block adsorptive sites, leaving only IE interactions to control retention.

To summarise, the main dispersion mechanisms in question are (i) electromigration dispersion and the resistance to mass transfer in both the (ii) mobile and (iii) stationary phase. The corresponding experimental parameters which influence these effects are (i) differences in mobility between the eluent co-ion and the analyte, (ii)

capillary diameter and separation temperature, and (iii) the influence of secondary interactions. These parameters were investigated and are discussed below.

3.6.1 Electromigration dispersion

In section 3.3 and 3.4, it was demonstrated that the apparent mobility of an analyte anion could be reduced significantly due to the presence of IE interactions with the stationary phase, especially when the eluent contains a relatively weak competing ion. Therefore, the migration through the capillary of an analyte with IE interactions (e.g. I^-) will be influenced more by the stationary phase than that for an analyte with weak IE interactions (e.g. Cl^-).

When trying to foresee the effect of chromatographic retention on electromigration dispersion, an assumption that the electrophoretic mobility of the analyte (rather than its effective mobility) governs electromigration dispersion leads to the conclusion that no adverse effect on peak shape should occur as the IE interaction, and hence retention, of analyte ions increases. On the other hand, if it is assumed that the effective mobility of the analyte governs the electromigration dispersion, then greater electromigration dispersion should be observed for I^- than Cl^-, due to the slower migration of Cl^-. Because of the complexity of this phenomenon and a lack of clear evidence from the literature, the significance of electromigration dispersion in OT-CEC was examined experimentally.

In order to investigate the influence of the mobility of the electrolyte competing ion (co-ion) on peak shape, formate was used as the electrolyte competing ion since it has a low absolute value of mobility (-54.6×10^{-9} m^2/Vs) and is a weak IE competing ion. An electrolyte was prepared containing 5 mM of formate and 10 mM Tris (pH 8.05). The electrophoretic mobility of formate is nearly identical to that of BrO_3^-, which also has a low IE interaction. According to the above principles governing electromigration dispersion [24], peaks that migrated before BrO_3^- should be fronted, while those that migrated after BrO_3^- should be tailed. As can be seen

from Figure 3.16, NO_2^- (peak 1) which migrated before BrO_3^- (peak 2) did not exhibit the triangular shape characteristic of fronted peaks in CE, and also clearly showed chromatographic tailing, indicating that some other factors were involved. Figure 3.16 also shows that there was a large difference in peak shape between analytes, with Br^- (peak 3) and NO_3^- (peak 4) giving considerably broad peaks and IO_3^- (peak 5) and BrO_3^- (peak 2) giving quite sharp peaks. BrO_3^- and IO_3^- have low IE selectivity coefficients and as such, their migration was dominated by their electrophoretic mobility. This should result in BrO_3^- having a near symmetrical peak shape, and IO_3^- showing slight electrophoretic tailing. If electromigration dispersion is the major source of peak broadening, then any peak migrating between BrO_3^- and IO_3^- should have a peak shape better than IO_3^- but worse than BrO_3^-. However, the peaks for Br^- and NO_3^-, which due to their IE interaction migrated between BrO_3^- and IO_3^-, were broad and this indicates that it was not the electrophoretic component but the chromatographic component of the separation mechanism which was the source of the poor peak shapes.

3.6.2 Resistance to mass transfer in the mobile phase

There are several approaches in OT-LC which are commonly used to improve the resistance to mass transfer in the mobile phase. The first approach, as proposed by Knox and Gilbert [1] is to reduce the distance that the analyte must diffuse to reach the stationary phase. They have shown that in order to obtain an OT-CEC separation which has a higher efficiency than the corresponding packed column LC separation, it is necessary to use OT columns of 10 μm or less due to the slow diffusivity of analytes in solution. The second approach is to increase the rate at which the analytes diffuse, which can be achieved by increasing the operating temperature. Liu *et al.* [30] reported that an increase in column temperature from 25°C to 200°C resulted in an improvement in efficiency similar to that achieved by decreasing the capillary diameter from 50 μm to 12 μm. Recently Pyo *et al.* [9] have studied the

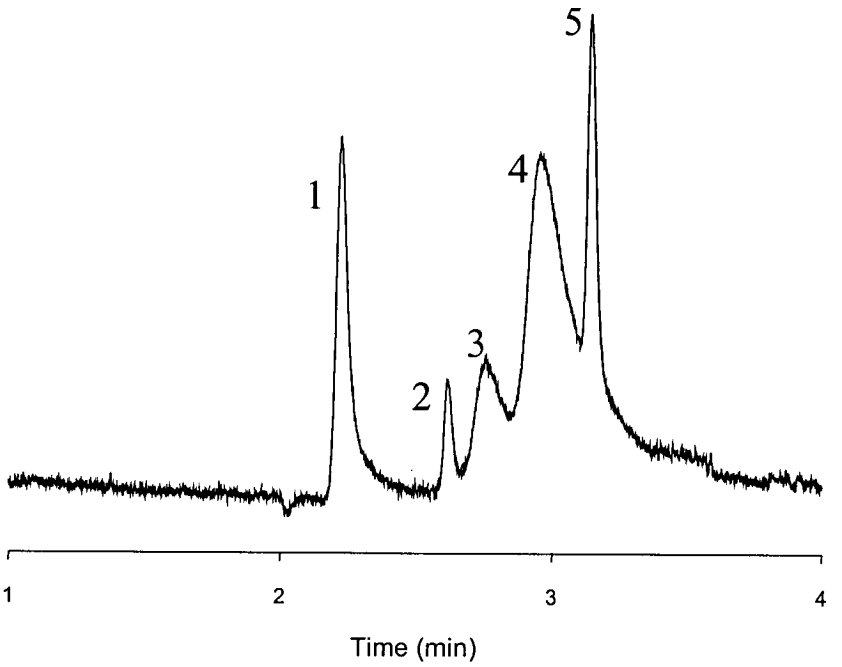

Figure 3.16: Separation of 5 inorganic anions in an AS5A coated capillary using 5 mM formate / 10 mM Tris (pH 8.05) as the electrolyte. Conditions : 50 cm capillary (41.5 cm to detector) x 75 μm i.d., -25 kV, injection of 0.2 mM at 5 mbar for 10 s. Peaks are : 1= NO_2^-, 2= BrO_3^-, 3= Br^-, 4= NO_3^-, 5=IO_3^-.

effect of increased temperature on OT-IEC separations of inorganic anions and found that increasing temperature caused a significant improvement in efficiency.

3.6.2.1 Effect of capillary diameter

To examine the effect of changing capillary diameter on peak shape, experiments were performed in 25, 50 and 75 μm i.d. AS5A coated capillaries using perchlorate as the competing ion. According to Knox and Gilbert [1], reducing the capillary diameter should reduce the contribution to inefficiency from resistance to mass transfer in the mobile phase. However, changing the diameter of the capillary also influences the effective IE capacity of the column (discussed in section 3.3.3), so a direct comparison of peak shapes in the different columns is difficult. In order to gain some insight into the influence of capillary diameter, it is necessary to ensure that analytes interact with the stationary phase to the same extent in the capillaries of different diameters. This requires different concentrations of competing ion to be used in the electrolyte which, in turn, changes other factors which influence peak shape such as Joule heating, the extent of stacking, the speed of the analysis due to viscosity changes in the electrolyte, kinetics of adsorption/desorption, etc. To ensure that analytes had a similar IE interaction in each capillary and to enable some semi-quantitative comparison to be made, the concentration of perchlorate in the electrolyte was adjusted so that $S_2O_3^{2-}$ (peak 8), SCN^- (peak 7) and CrO_4^{2-} (peak 9) migrated in sequence. The injection times were also adjusted to ensure the same volume of sample was injected for each capillary diameter. Figure 3.17 shows the separations in 75 μm (10 mM ClO_4^-), 50 μm (30 mM ClO_4^-) and 25 μm (50 mM ClO_4^-) AS5A coated capillaries. While it is recognised that changing the concentration of competing ion will have some influence on peak shape, it is believed that this will mainly affect the width of the peak and should exert only a minor influence on peak tailing. Comparing the peaks in the different diameter capillaries (Figure 3.17) shows that the peaks for CrO_4^{2-} and $S_2O_3^{2-}$ in the 25 μm i.d.

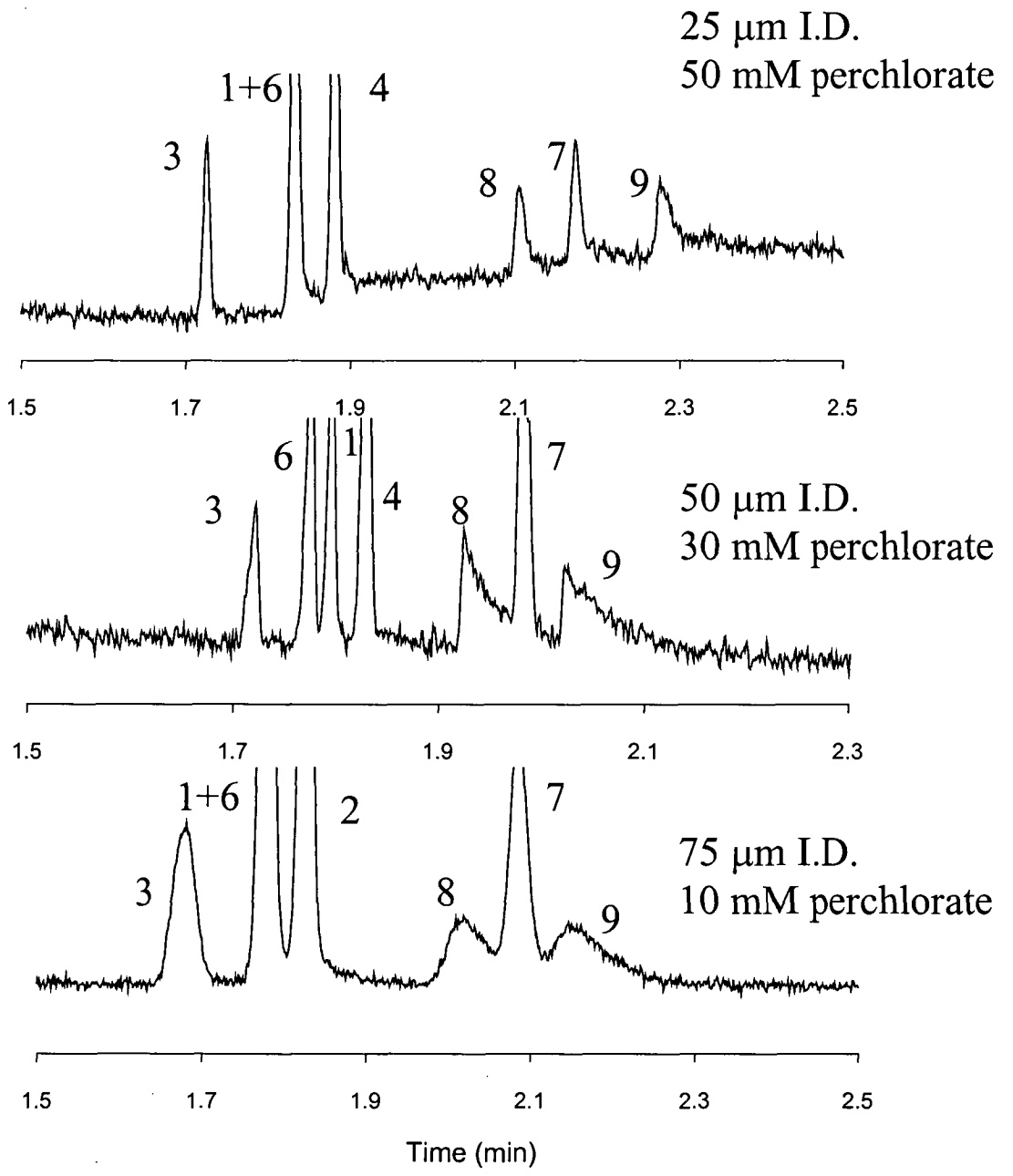

Figure 3.17: Comparison of separations in different diameter capillaries with approximately the same IE interaction obtained by changing the competing ion (perchlorate) concentration. . Peaks are : 1= NO_2^-, 2= BrO_3^-, 3= Br^-, 4= NO_3^-, 5=IO_3^-, 6= I^-, 7 = SCN^-, 8= $S_2O_3^{2-}$, and 9= CrO_4^{2-}. Other conditions as in Figure 3.16.

capillary were much narrower than in the larger diameters and they also showed less chromatographic tailing. This suggested, as expected from theory, that the resistance to mass transfer in the mobile phase contributed significantly to the observed inefficiency. However, it must be noted that using narrow capillaries is not a viable option when using UV absorbance detection because of the significant reduction in detection sensitivity due to the shorter optical path length.

3.6.2.2 Effect of temperature

To examine the influence of changing the temperature on OT-CEC separations, the separation of Br^-, NO_2^-, NO_3^- and I^- in 10 mM Cl^- was investigated at temperatures between 25 and 55°C. It should be noted that these values represent the temperature at which the capillary column was set and does not include any change in temperature from Joule heating. In addition, instrumental limitations allowed only about 70 % of the capillary length to be thermostated and the buffer reservoirs were maintained at room temperature. Figure 3.18 shows that as the temperature was increased, the migration times decreased due to a decrease in viscosity. The separation at 55 °C was complete in nearly half the time required for the same separation at 25 °C, with a subsequent loss in resolution between Br^-, NO_2^- and NO_3^-. Increasing the temperature from 25- 55 °C appeared to have a beneficial effect on separation efficiency with efficiencies for the I^- peak improving from 5 000 to 10 000 plates/m even though an increase in temperature will reducee efficiency through an increase in longitudinal diffusion. Similar results were reported by Jakubetz *et al.* [31] who observed an increase in efficiency (6 600 to 10 000 plates/m) when the temperature was increased from 20 to 60 °C when separating enantiomers of hexobarbital by OT-CEC. Whilst increasing the temperature resulted in higher efficiencies and better peak shapes, it is questionable as to whether the improvement in peak shapes is solely due to an improvement in resistance to mass transfer in the mobile phase or whether there are influences from kinetics, etc.

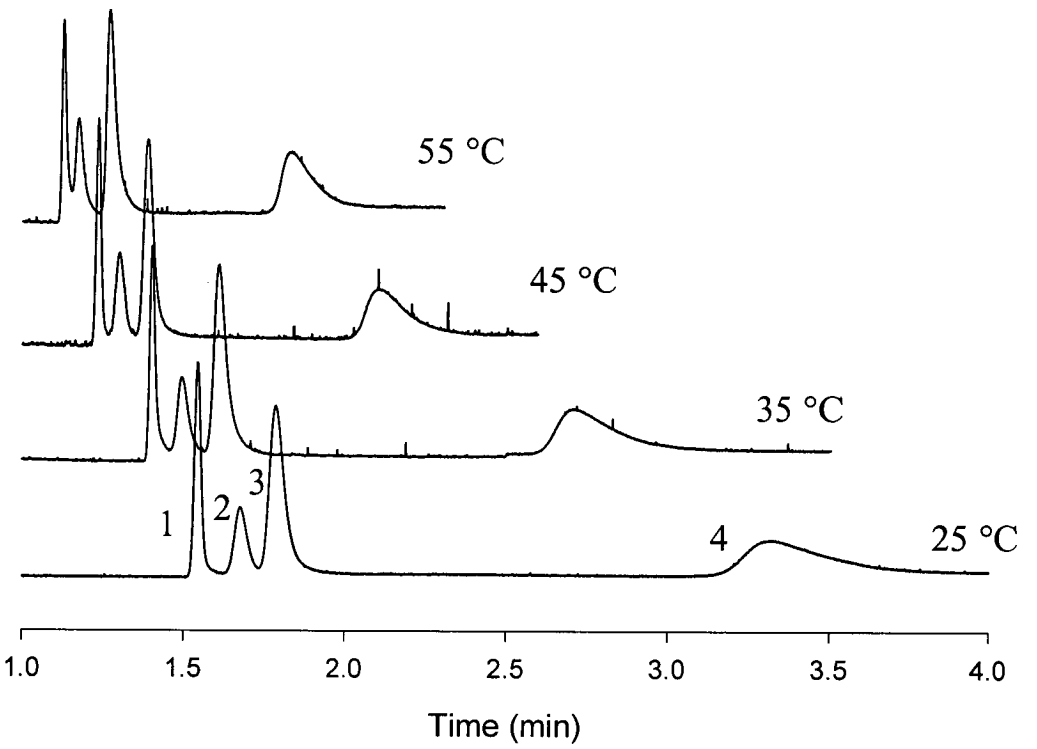

Figure 3.18: Separation of inorganic anions in 75 μm at different temperatures in 10 mM Cl^- / 20 mM Tris (pH 8.05) at different temperatures. Other conditions as in Figure 3.17. Peaks are 1 = NO_2^-, 2 = Br^-, 3 = NO_3^- and 4 = I^-.

In order to make a semi-qualitative judgement, it was necessary to compare peak shapes of the same analyte at different temperatures and at approximately the same retention time. This was accomplished by adjusting the ionic strength of the electrolyte at 25 °C such that the I^- peak migrated at approximately the same time as at 55 °C when using a 10 mM Cl^- electrolyte. Again, it is recognised that increasing the concentration of the electrolyte will have other influences on the separation efficiency, but an indication of the effect on peak shape may be inferred. It can be seen from Figure 3.19 that there was no significant improvement in peak shape for I^- (peak 6) indicating that there was little benefit from using elevated temperatures. This result is in contrast to findings in OT-LC where it has been shown that an increase in temperature did have a significant influence on peak shape [9,30]. In discussing possible reasons for this difference, calculations presented by both Liu *et al.* [30] and Pyo *et al.* [9] can be used to estimate the decrease in capillary diameter which would be equivalent in terms of efficiency gains to benefits achieved by an increase in temperature. If it is assumed that the actual capillary temperature was changed from 25°C to 55°C, this correlates to changing the capillary diameter from 75 μm i.d. to 55 μm i.d. If we now consider that the buffer was not pre-heated before entering the capillary, then a loss in efficiency of as much as 30% may arise from the 'cold point' effect [30]. Recalculating the corresponding capillary diameter to account for this reduced influence of temperature gives the equivalent capillary diameter as 65 μm i.d. Considering that changing the capillary diameter from 75 μm to 50 μm i.d. (Figure 3.17) did not improve peak shape significantly, it is expected that the improvement in using a 65 μm i.d. capillary would be insignificant. It should also be noted that the increase in temperature will also result in broader peaks due to an increase in longitudinal diffusion which may partly offset any improvement in mass transfer, and that the influence of temperature on the kinetics of adsorption and desorption on separation efficiency are not clear.

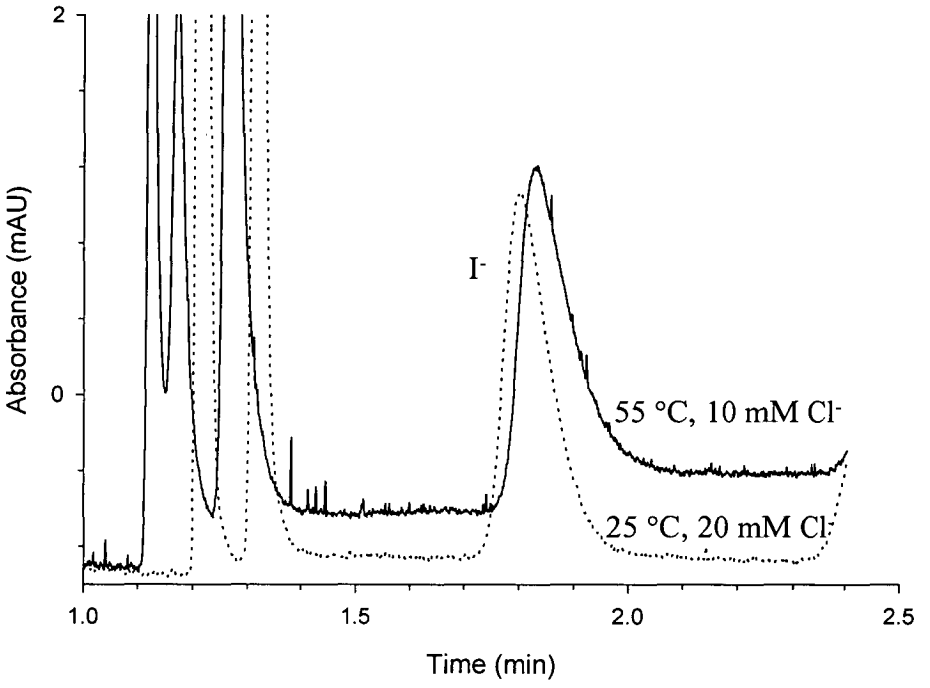

Figure 3.19: Comparison of peak shape for I (peak 6) at 55°C, 10 mM Cl^- and 25°C, 20 mM Cl^- /40 mM Tris (pH 8.05). Other conditions as in Figure 3.17.

3.6.3 Resistance to mass transfer in the stationary phase

The resistance to mass transfer in the stationary phase is made up of contributions from diffusion in the stationary phase and the kinetics of adsorption/desorption. As discussed previously in section 3.6, only the kinetics of adsorption/desorption, which are generally considered not to be a problem in IEC, should have an influence on peak shape. Fornstedt *et al.* [26] have shown that peak tailing is usually caused when the kinetics of a secondary retention mechanism are much slower than those of the primary retention mechanism. Pohl *et al.* [27-29] have shown that secondary interactions are involved in the separation of polarisable anions on agglomerated IE columns and these result in peak shapes typically being poor. To overcome this, the addition of *p*-cyanophenol to the eluent has been used in IEC to block adsorptive sites, leaving only IE interactions to control retention. The addition of *p*-cyanophenol also influences the separation of other ions, such as Br^- and NO_3^- [27] which also interact with the stationary phase via π-π type interactions. Figure 3.20 shows that with increasing additions of *p*-cyanophenol, the migration times of strongly retained analytes, such as I^- and SCN^- were reduced quite significantly, indicating that secondary retention equilibria contributed to the retention of these analytes. To determine the influence of *p*-cyanophenol on peak shapes, similar retention was required in electrolytes with and without *p*-cyanophenol. Again it must be re-iterated that while this will not provide conclusive results, it may provide some insight into probable causes. Figure 3.21 shows the separation of several polarisable inorganic anions, with the retention adjusted by the addition of *p*-cyanophenol so that I^- had approximately the same degree of IE interaction. It can be seen that there was no improvement in peak shape, and in fact the separation without the addition of *p*-cyanophenol appears to be slightly better. This is in contrast to expectations from IEC, and may be explained by the differences in ionic strength used to obtain a similar retention so that a suitable comparison could be made.

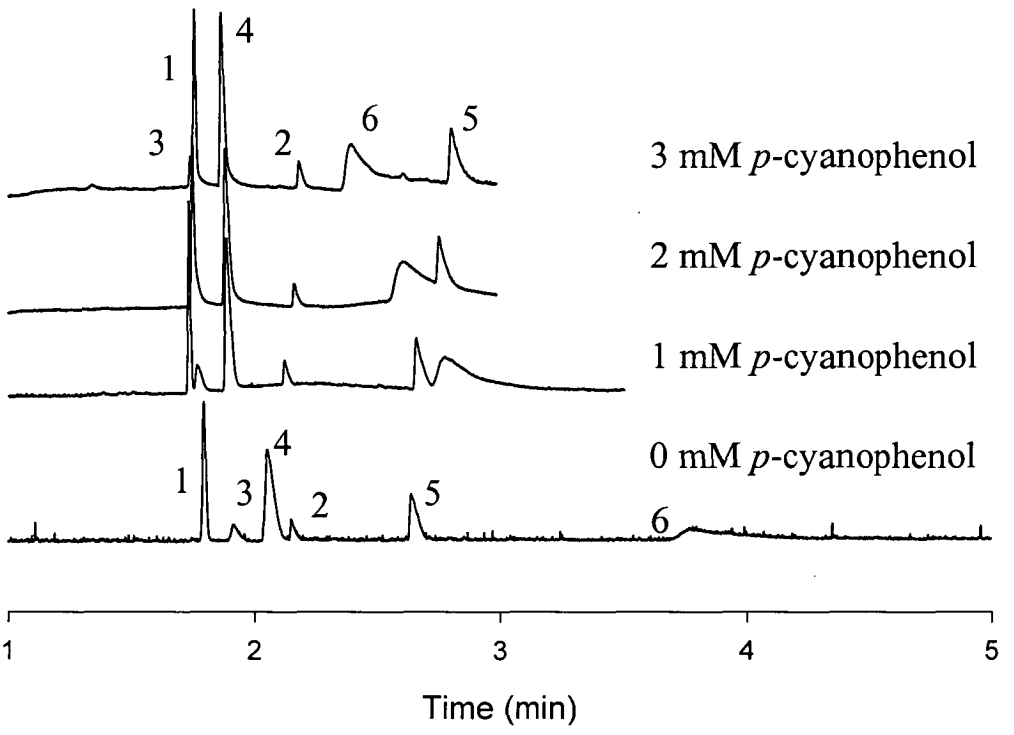

Figure 3.20: Influence of the addition of *p*-cyanophenol to a 10 mM Cl^- / 20 mM Tris (pH 8.05) electrolyte on the separation selectivity of inorganic anions in an AS5A coated capillary. Other conditions as in Figure 3.17. 1= NO_2^-, 2= BrO_3^-, 3= Br^-, 4= NO_3^-, 5=IO_3^- and 6= I^-.

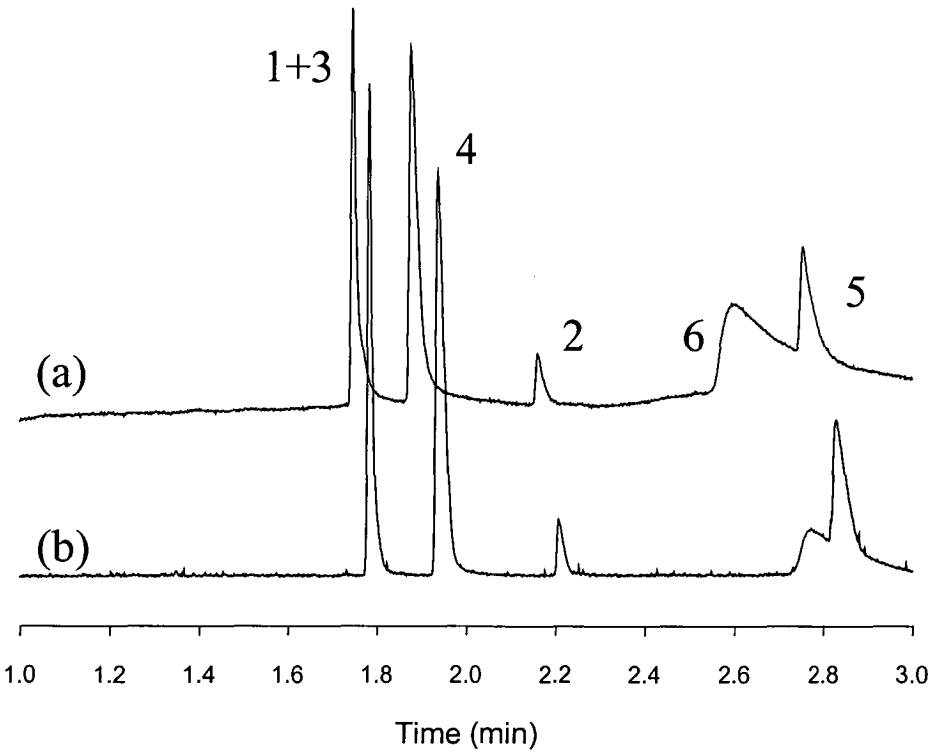

Figure 3.21: Comparison of peak shapes with and without the addition of *p*-cyanophenol to the electrolyte. (a) 2 mM *p*-cyanophenol + 10 mM Cl^-/20 mM Tris, (b) 20 mM Cl^- / 40 mM Tris. Other conditions as in Figure 3.17. 1= NO_2^-, 2= BrO_3^-, 3= Br^-, 4= NO_3^-, 5=$IO_3^-$and 6= I^-.

An alternative method to determine the influence of secondary equilibria effects is to compare the separation of polarisable and non-polarisable analytes that have similar mobilities and similar retention. For this purpose, the peak shapes of I^- and SO_4^{2-} were compared when both analytes had a migration time of around 4 min. Indirect absorbance detection was necessary to detect SO_4^{2-} and Figure 3.22 shows the separation of SO_4^{2-} and other UV-transparent anions using an AS5A coated capillary and NO_3^- as the absorbing competing ion in the electrolyte. Comparing the peak for I^- in 10 mM Cl^- (peak 6, Figure 3.18, 25°C) to that of SO_4^{2-} in 2.5 mM nitrate (peak 5, Figure 3.22), several things are apparent. The first is the SO_4^{2-} peak has a lower migration time, hence a stronger interaction with the stationary phase than I^- (k' = 0.9 and 0.8 respectively). Secondly, even with this stronger interaction the peak shape of SO_4^{2-} is very symmetrical and exhibits none of the tailing observed for I^-. Similarly well shaped peaks were observed under the same conditions for $PO_4^{\cdot}$. This suggests that the poor peak shapes obtained for the polarisable anions are not characteristic of the OT-CEC approach, but are characteristic of the analytes and their interaction with the stationary phase. Suitable stationary phases that are not able to interact with polarisable analytes through π-π interactions should result in superior peak shapes superior to those observed in this work.

A further possibility to explain poor peak shapes is column overloading arising as a result of the small amount of stationary phase present on the column wall. To investigate this, the concentration of an analyte showing considerable IE interaction with the stationary phase (CrO_4^{2-}) was varied over two orders of magnitude (0.01-1.0 mM) and the results are shown in Figure 3.23. It can be seen that when 1 mM CrO_4^{2-} was injected, there is evidence of overloading in the faster migration time of the peak maximum and also the peak is much broader than the other concentrations. However, it can be concluded that under the given injection conditions, 0.1 mM concentrations of the analytes should not cause significant column overloading and this factor is therefore not responsible for the observed peak shapes.

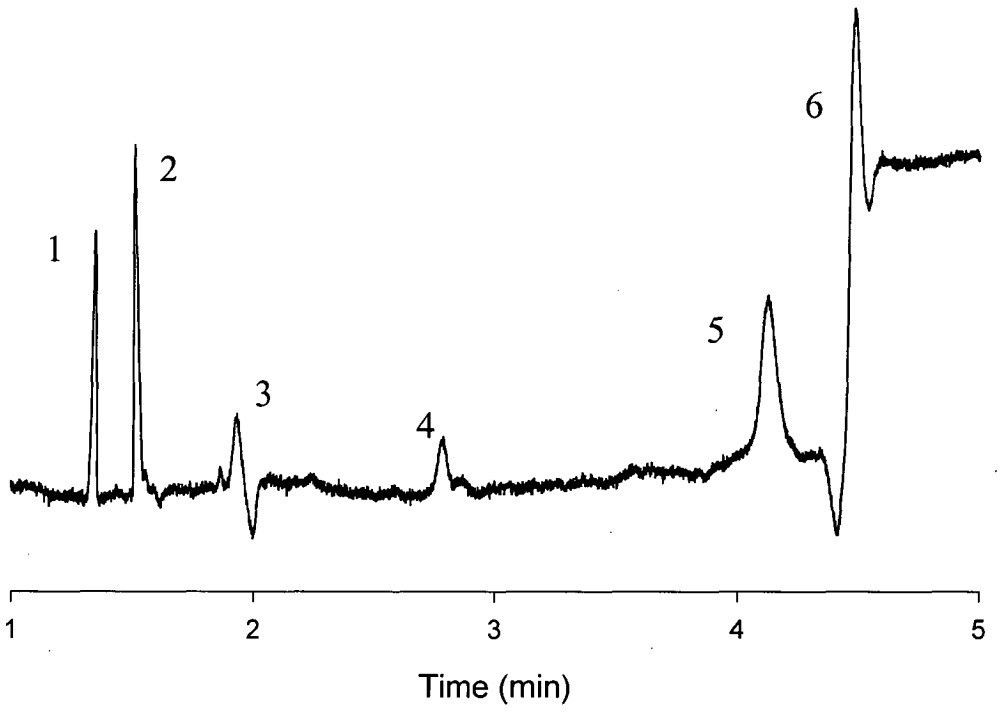

Figure 3.22 Separation of inorganic anions using indirect UV detection in an AS5A coated capillary. Conditions: 2.5 mM nitrate, 5.0 mM DEA (pH 9.0), -25 kV, injection of 1 mM ions for 2 s at 10 mbar. Peaks are : 1=Cl^-, 2=F^-, 3, 4 = system peaks, 5=SO_4^{2-}, 6=EOF.

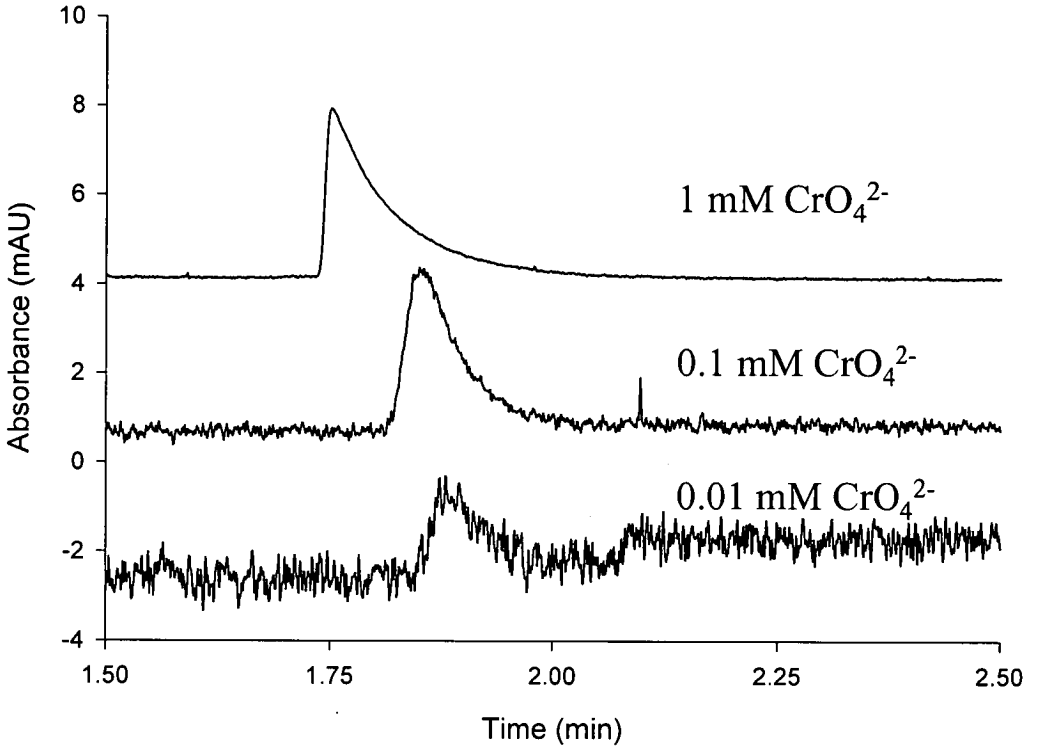

Figure 3.23: Injection of decreasing amounts of chromate in an AS5A coated capillary. Electrolyte: 10 mM ClO_4^-/20 mM Tris (pH 8.05) detection at 254 nm. Scale adjusted for 0.1 mM CrO_4^{2-} (x5) and 0.01 mM CrO_4^{2-} (x5). Other conditions as in Figure 3.18.

3.7 Conclusions

Capillaries coated with cationic latex particles in the nm size range can be used in OT-CEC for introducing IE interactions into a CE separation mechanism. More importantly, the strength of the IE interactions, which govern the contribution of the IE component to the separation mechanism, can be controlled by varying the concentration and type of competing ion and/or by variation of the column capacity by changing the capillary diameter. This enables the separation selectivity to be changed to give an elution order as for CE or IEC, or a combination of both. Selectivity manipulation of UV transparent ions is more difficult than UV absorbing ions due to the competing ion also functioning as the indirect absorbance probe. This limits the concentration range of a particular probe. At low concentrations of probe electromigration dispersion and poor buffering capacity reduce the performance of the system, while at high concentrations, high currents and increased background absorbance are responsible for decreased performance. As a consequence, a probe can be used over a relatively narrow concentration range with the result that most probes provide only a discrete range of separation selectivities. To overcome this, variation of the separation selectivity can be best achieved by varying the nature of the probe, rather than its concentration.

The migration behaviour of inorganic anions in OT-IE-CEC was modelled by an equation derived from IEC and CE theory. The model accounts for the change in effective mobility due to ionic strength effects. Using a range of analyte anions and varying the competing anion in the background electrolyte, good agreement between experimental and calculated mobility data was obtained with correlation coefficients >0.98 for both UV absorbing and UV transparent anions. System constants determined from non-linear regression enabled a quantitative comparison of IE strengths and for UV absorbing ions, these constants were used to optimise the separation of 7 inorganic anions.

Peak shapes in OT-IE-CEC are influenced by both electrophoretic and chromatographic sources. While the electrophoretic component (electromigration dispersion) is not the major contribution to band broadening in many cases, appropriate competing ion mobility is still important. The resistance to mass transfer in the mobile phase can be improved by decreasing the capillary diameter, which results in a significant reduction in peak tailing, especially for polarisable anions. However, this is offset by a reduction in detection sensitivity when using UV absorbance detection. The effect of the separation temperature was inconclusive, possibly because of the small range of temperatures studied and the presence of the 'cold point' effect. The addition of *p*-cyanophenol to the mobile phase partially suppressed secondary interactions with the stationary phase, but no improvement in peak shape was observed possibly due to incomplete suppression of the secondary interactions. Symmetrical peaks for well retained non-polarisable analytes such as sulfate were observed in a 75 μm column illustrating that the inefficient separations for polarisable anions are not characteristic of the OT -CEC approach but rather arise from the nature of the ions themselves.

3.8 References

1 J.H. Knox and M.T. Gilbert, *J.Chromatogr.*, 186 (1979) 405.

2 J.H. Knox and I.H. Grant, *Chromatographia.*, 24 (1987) 135.

3 M.S. Nutku and F.B. Erim, *High Resol.Chromatogr.*, 21 (1998) 505.

1. 4 C. Finkler, H. Charrel and H. Engelhardt, *J.Chromatogr.A*, 822 (1998) 101.

4 H. Burt, D.M. Lewis and K.N. Tapley, *J.Chromatogr.A*, 739 (1996) 367.

5 M. Chiari, L. Ceriotti, G. Crini and M. Morcellet, *J.Chromatogr.A*, 836 (1999) 81.

6 D.T. Gjerde and L. Yengoyan, *International Patent Application*, (1995) WO 95/10344.

7 G. Kleindienst, C.G. Huber, D.T. Gjerde, L. Yengoyan and G.K. Bonn, *Electrophoresis.*, 19 (1998) 262.

8 D. Pyo, P.K. Dasgupta and L. Yengoyan, *Anal.Sci.*, 13 (1997) 185.

9 D.R. Lide, *CRC Handbook of Chemistry and Physics*, CRC Press., London, 1994.

10 P.R. Haddad and P.E. Jackson, *Ion Chromatography. Principles and Applications*, Elsevier, Amsterdam, 1990.

11 W. Ding, M.J. Thornton and J.S. Fritz, *Electrophoresis.*, 19 (1998) 2133.

12 P.A. Doble and P.R. Haddad, *J.Chromatogr.A*, 834 (1999) 189.

13 P.A. Doble, M. Macka and P.R. Haddad, *Electrophoresis.*, 19 (1998) 2257.

14 P.A. Doble, M. Macka, P. Anderson and P.R. Haddad, *Anal.Commun.*, 34 (1997) 351.

15 M. Janecek and K. Slais, *J.Chromatogr.*, 471 (1989) 303.

16 M.G. Khaledi, S.C. Smith and J.K. Strasters, *Anal.Chem.*, 63 (1991) 1820.

17 C. Quang, J.K. Strasters and M.G. Khaledi, *Anal.Chem.*, 66 (1994) 1646.

18 J.K. Strasters and M.G. Khaledi, *Anal.Chem.*, 63 (1991) 2503.

19 S. Terabe, K. Otsuka and T. Ando, *Anal.Chem.*, 57 (1985) 834.

20 S. Terabe, K. Otsuka, K. Ichikawa, A. Tsuchiya and T. Ando, *Anal.Chem.*, 56 (1984) 111.

21 R.F. Cross and J. Cao, *J.Chromatogr.A*, 786 (1997) 171.

22 H.J. Issaq, I.Z. Atamna, G.M. Muschik and G.M. Janini, *Chromatographia.*, 32 (1991) 155.

23 F. Foret, L. Krivánková and P. Bocek, *Capillary Zone Electrophoresis.*, VCH, Weinheim, 1999.

24 J.Å. Jönsson, in J.Å. Jönsson (Editor), *Chromatographic Theory and Basic Principles*, Marcel Decker Inc., New York, 1987,

25 T. Fornstedt, G. Zhong and G. Guiochon, *J.Chromatogr.A*, 741 (1996) 1.

26 R.W. Slingsby and C.A. Pohl, *J.Chromatogr.*, 458 (1988) 241.

27 J.R. Stillian and C.A. Pohl, *J.Chromatogr.*, 499 (1990) 249.

28 C.A. Pohl, J.R. Stillian and P.E. Jackson, *J.Chromatogr.A*, 789 (1997) 29.

29 G. Liu, N.M. Djordjevic and F. Erni, *J.Chromatogr.*, 592 (1999) 329.

30 H. Jakubetz, H. Czesla and V. Schurig, *Journal of Microcolumn Separations*, 9 (1997) 421.

Chapter 4

Pseudo-Phase Ion-Exchange Capillary Electrochromatography of Inorganic and Small Organic Anions

4.1 Introduction

The use of pseudo-phases in CEC is in many ways simpler than using packed and OT columns. In this method, the chromatographic phase is added to the electrolyte to provide a moving phase (hence the term pseudo-stationary phase) with which analytes can interact. In many cases, the pseudo-phase is soluble in the electrolyte so that it is not strictly speaking a separate phase as is the case when using packed and OT columns. Nevertheless, this approach offers significant advantages over packed and OT columns regarding the ease of implementation and flexibility of the system. For example, since the chromatographic phase is a pseudo-phase, it can simply be replaced before each separation by flushing the capillary with electrolyte containing the pseudo-phase, hence forming a new 'column' each time. Furthermore, the type and capacity of the 'column' can be changed simply by changing the type and concentration of pseudo-phase added to the electrolyte.

Water soluble polymers are one of the more popular pseudo-phases due to the high uniformity between molecules and the large number of different polymers available [1-11]. They are particularly useful for the introduction of IE interactions as they are simpler than a surfactant system which has monomers and micelles because there is only 'one' type of polymeric molecule with which the analyte can interact. They have been used extensively for the migration of inorganic and small organic ions in CEC and various methods for controlling both the chromatographic contribution (such as changing the polymer concentration, the electrolyte anion type and its

concentration) have been examined. However, there has been no study on how all of these parameters are interrelated and there has been no attempt to optimise the variation of these parameters to give a desired separation. In Chapter 3, it was shown that the IE contribution to the separation mechanism obtained when using OT columns could be modelled by an equation derived from CE and IEC theory. It was also shown that constants determined from non-linear regression quantified the strength of the competing ions, with numerical values obtained following the trend observed in IEC. However, as the columns used were OT columns, the IE capacity of the column was not a variable parameter.

This chapter describes the use a soluble cationic polymer as a pseudo-stationary phase to introduce IE interactions into a CE separation mechanism. The use of a soluble polymer enables greater flexibility than packed or OT columns due to the fact that both the column capacity, governed by the concentration of polymer, and eluent strength, governed by both the type and concentration of competing ion, can be varied in order to change the IE contribution. A theoretical model is used to describe the migration of analytes in this system and is verified using UV absorbing inorganic and organic anions. This approach is then extended to UV transparent anions, and the potential of the system to resolve a complex mixture of anions is examined.

4.2 Experimental

The general details are given in Chapter 2. Detailed conditions are included in each of the figure captions.

4.2.1 Electrolyte preparation

4.2.1.1 Direct UV detection system

Electrolytes were prepared by titration of 20 mM Tris to a pH of 8.05 with HCl, providing a background concentration of 10 mM Cl^- in each electrolyte. The soluble

polymer, Poly(diallyldimethylammonium chloride) (PDDAC) was added to the electrolyte between the concentration range of 0–1.0% (w/v) as the chloride form. Different competing ions (fluoride, acetate, chloride, sulfate) were added to the electrolyte as the sodium form in the concentration range of 50–150 mM.

4.2.1.2 Indirect UV detection system

Stock solutions of electrolyte containing 500 meq of probe (chromate, phthalate or benzoate) were prepared by titration of Tris to a pH of 7.70 with the acid form of the probe to give a Tris-probe stock. PDDAC was converted to the probe form by following the procedure of Cassidy and Stathakis [3]. Briefly, PDDAC was passed through an IE column previously conditioned with hydroxide. Column effluent was collected in a flask with the appropriate concentration of probe in the acid form giving a stock solution of PDDA-probe.

electrolytes were prepared by mixing appropriate concentrations of Tris-probe and PDDA-probe to give the desired concentration of polymer and probe. All electrolytes were buffered using 10 mM of the ampholytic buffer histidine at a pH of 7.70.

4.3 Theory

For a system comprising a soluble polymer as the pseudo-stationary phase, the observed mobility of an analyte is given by [12,13]:

$$\mu_{ob} = \alpha_{mp}.(\mu_{mp}) + \alpha_{sp}.(\mu_{sp}) \qquad (4\text{–}1)$$

where α_{mp} is the mole fraction of the analyte in the mobile phase, and α_{sp} is the mole fraction of the analyte in the pseudo-stationary phase, μ_{ob} is the observed mobility, μ_{mp} is the electrophoretic mobility of the analyte in the mobile phase and μ_{sp} is the electrophoretic mobility of the analyte in the pseudo-stationary phase. As the analyte

and pseudo-phase have opposite charges (necessary for IE interactions) their mobility is in opposite directions.

The mole fraction of analyte in the mobile and pseudo-stationary phases can be expressed in terms of the retention factor k', according to the following equations, [12,14]

$$\alpha_{mp} = \frac{1}{1+k'}, \tag{4–2}$$

$$\alpha_{sp} = \frac{k'}{1+k'} \tag{4–3}$$

where, k' is defined as [15]

$$k' = D\frac{w}{V_{mp}}, \tag{4–4}$$

with D being the distribution coefficient of the analyte between the mobile and pseudo-stationary phase, w is the weight of the pseudo-stationary phase, and V_{mp} is the volume of the mobile phase.

The observed mobility of an analyte can now be rewritten as:

$$\mu_{ob} = \frac{1}{1+k'}.(\mu_{mp}) + \frac{k'}{1+k'}.(\mu_{sp}). \tag{4–5}$$

An expression for the retention factor of an analyte can be found from IEC in which the retention factor is related to the selectivity coefficient ($K_{A,E}$), the IE capacity of the column (Q), and to the concentration of the competing ion ($[E]$),

$$k'_A = \left(\frac{w}{V_{mp}}\right).\left(K'_{A,E}\right)^{1/y}.\left(Q/y\right)^{x/y}.[E]^{-x/y}. \tag{4–6}$$

Here, x is the charge on the analyte ion and y is the charge on the eluent ion. Substituting equation (4–6) into equation (4–5) gives the following equation:

$$\mu_{ob} = \frac{1}{1+\left(\frac{w}{V_{mp}}\right).\left(K'_{A,E}\right)^{1/y}.\left(Q/_{y}\right)^{x/y}.[E]^{-x/y}}.(\mu_{mp}) + \frac{\left(\frac{w}{V_{mp}}\right).\left(K'_{A,E}\right)^{1/y}.\left(Q/_{y}\right)^{x/y}.[E]^{-x/y}}{1+\left(\frac{w}{V_{mp}}\right).\left(K'_{A,E}\right)^{1/y}.\left(Q/_{y}\right)^{x/y}.[E]^{-x/y}}.(\mu_{sp}) \quad (4\text{–}7)$$

Eqn (4–7) accounts for the influences of increasing the IE capacity of the column and the concentration of the competing ion, as well as changing the type of competing ion (governed by the selectivity coefficient). However, it does not include the influence of increasing the ionic strength on the electrophoretic mobility of both the free zone electrophoretic mobility of the analyte, nor on the mobility of the pseudo-stationary phase.

The electrophoretic mobility changes with ionic strength in an inverse square root relationship [16-18] which can be expressed as

$$\mu_{ep} = \frac{b}{\sqrt{I}} \quad (4\text{–}8)$$

where b is a constant related to the electrophoretic mobility in zero ionic strength. Substituting into equation (4–7) gives the final model equation:

$$\mu_{ob} = \frac{1}{1+\left(\frac{w}{V_{mp}}\right).\left(K'_{A,E}\right)^{1/y}.\left(Q/_{y}\right)^{x/y}.[E]^{-x/y}}.\left(\frac{b_{mp}}{\sqrt{I}}\right) + \frac{\left(\frac{w}{V_{mp}}\right).\left(K'_{A,E}\right)^{1/y}.\left(Q/_{y}\right)^{x/y}.[E]^{-x/y}}{1+\left(\frac{w}{V_{mp}}\right).\left(K'_{A,E}\right)^{1/y}.\left(Q/_{y}\right)^{x/y}.[E]^{-x/y}}.\left(\frac{b_{sp}}{\sqrt{I}}\right) \quad (4\text{–}9)$$

In equation (4–9), w/V_{mp} is defined by the concentration of PDDAC added to the electrolyte (as % (w/v)). Q is likewise defined by the concentration of the polymer, and can be estimated from the number of repeat units of polymer added. The other parameters, x, y, $[E]$ and I are defined by the particular analyte under consideration, and the conditions used. The remaining parameters, $K'_{A,E}$, b_{mp} and b_{sp} are not defined and need to be determined from non-linear regression. It should be noted that when using packed or OT columns for which the mobility of the stationary phase is zero and the column capacity is constant, then equation (4–9) reduces to that already shown to be valid in Chapter 3 (equation 3-12).

Non-linear regression was performed using the solver function in Microsoft Excel 97 for all analytes simultaneously, using minimisation of least squares. This will give 2 constants for each analyte ($K'_{A,E}$ and b_{mp}) and one constant for each electrolyte system (b_{sp}). Constants were determined from 5 experimental points, denoted the "primary set", one in each corner of the experimental area and a centre point to account for any non-linearity.

4.4 UV absorbing anions

4.4.1 Data collection

Observed mobilities were measured for 9 inorganic (Br^-, I^-, NO_2^-, NO_3^-, CrO_4^-, SCN^-, MoO_4^-, IO_3^-, BrO_3^-) and 7 organic (phthalate, benzenedisulfonate, benzenesulfonate, benzoate, *p*-toluenesulfonate, 2-naphthalenesulfonate, 3,5-dihydroxybenzoate) anions which were selected on the basis of their electrophoretic and IE-chromatographic properties. The concentration of polymer was varied between 0 and 1.0% (w/v) in order to change the column capacity. Separations with 0% PDDAC were done in capillaries coated with the cationic polymer which reversed the EOF providing a co-EOF separation of the inorganic anions. Capillaries were coated by rinsing with a 0.2% solution of PDDAC in the electrolyte before rinsing with electrolyte (no polymer) for a further 2 minutes before separation. The concentration of competing ion was varied between 50–150 mM and the type of competing ion used was varied from fluoride to acetate, chloride and sulfate to provide different eluotropic effects, with fluoride being the weakest competing ion, and sulfate being the strongest.

4.4.2 Chloride as competing anion

To determine the validity of the derived model, data were collected using a chloride electrolyte with the concentration of chloride varied in 25 mM increments between

50 and 150 mM, and the concentration of PDDAC varied between 0 and 1.0% (w/v) in 0.2% increments. This provided a two-dimensional experimental space and data for each of the analytes were measured at 30 different buffer conditions. The electrophoretic mobility of PDDAC was measured to be 39.94 x 10^{-9} m^2/Vs and was used in all non-linear regression calculations. The EOF was reversed due to adsorption of PDDAC onto the capillary resulting in the pseudo-phase migrating counter-EOF, in contrast to the analytes migrating co-EOF.

System constants were determined from the application of the model equation using mobility data acquired at five points in the experimental space, namely the four corner points and the centre point. These data points will be referred to as the "primary set". All remaining data points (referred to as the "validation set") were used to provide mobility data to validate the system constants determined above. Excellent agreement was obtained between experimental and predicted values of mobility for the validation set, with an overall correlation of 0.99 for all analytes under all conditions. The maximum relative difference between experimental and observed mobilities was 10% while the average was 1.8%.

Values for the constants determined from non-linear regression using chloride as the competing ion are shown in Table 4.1. In particular, values of $K_{A,E}$ represent the IE selectivity coefficient between analyte A and the competing ion E, indicating the degree to which IE interactions will influence their observed mobility. Ordering the analytes by increasing values of $K'_{A,E}$ results in the following order : IO_3^-/BrO_3^- < benzoate < NO_2^- < NO_3^- < benzenesulfonate < *p*-toluenesulfonate < Br^- < phthalate < 3,5-dihydroxybenzoate < 2-naphthalenesulfonate < SCN^- < I^- < MoO_4^- < CrO_4^- < benzenedisulfonate. This generally agrees with IE elution order of these analytes from a strong-base IE resin [15]. Values of b_{mp} indicate the influence of ionic strength on the electrophoretic mobility of each analyte, while b_{sp} indicates the influence of ionic strength on the electrophoretic mobility of the stationary phase.

Table 4.1: Values of constants in equation (4-9) determined from non-linear regression of analytes in electrolytes of different eluotropic strength. All parameters determined from only 5 experimental points. Analytes are arranged in migration order obtained in a Co-EOF separation performed in a 10 mM Cl-/20 mM Tris (pH 8.05) electrolyte with the EOF reversed using 0.5 mM CTAB.

	Fluoride			Acetate			Chloride			Sulfate		
b_{sp}	2.34			2.57			3.05			3.10		
Analyte	$K_{A,E}$	b_{mp}	r^2	$K_{A,E}$	b_{mp}	r^2	$K_{A,E}$	b_{mp}	r^2	$K_{A,E}$	b_{mp}	r^2
Bromide	0.594	-2.064	0.957	0.495	-2.037	0.958	0.102	-1.469	0.998	0.002	-1.346	0.986
Iodide	2.242	-2.121	0.951	1.862	-2.272	0.954	0.329	-1.638	0.992	0.186	-1.339	0.989
Nitrite	0.241	-1.883	0.973	0.059	-2.354	0.981	0.016	-1.426	0.975	0	-1.272	0.955
Nitrate	0.451	-1.812	0.965	0.393	-2.087	0.968	0.069	-1.482	0.989	0	-1.376	0.985
Chromate	21.43	-0.734	0.973	14.58	-0.872	0.975	0.924	-1.422	0.992	0.062	-1.266	0.956
Thiocyanate	2.531	-1.791	0.956	1.987	-1.553	0.960	0.320	-1.457	0.994	0.279	-1.224	0.987
Molybdate	17.19	-0.880	0.970	12.03	-0.935	0.976	0.762	-1.474	0.995	0.026	-1.215	0.966
Bromate	0.085	-1.402	0.981	0.025	-1.216	0.990	0	-1.271	0.965	0	-1.086	0.950
Benzenedisulfonate	87.35	-0.240	0.988	57.47	-0.994	0.989	1.744	-1.41	0.995	0.535	-1.123	0.970
Phthalate	1.703	-0.915	0.970	1.331	-0.814	0.937	0.161	-1.187	0.966	0	-1.020	0.959
Iodate	0	-1.915	0.986	0	-1.165	0.968	0	-1.142	0.955	0	-0.891	0.909
Benzenesulfonate	0.613	-1.142	0.958	0.506	-1.145	0.979	0.071	-1.008	0.994	0.002	-0.705	0.985
Benzoate	0.168	-0.960	0.985	0.131	-0.969	0.979	0.002	-0.931	0.978	0	-0.640	0.973
p-toluenesulfonate	1.527	-0.729	0.995	0.569	-1.097	0.979	0.077	-0.973	0.993	0.005	-0.654	0.983
2-naphthalenesulfonate	2.847	-0.974	0.955	2.108	-1.151	0.971	0.224	-1.038	0.967	0.905	-0.499	0.979
3,5-dihydroxybenzoate	4.815	-0.879	0.933	2.480	-1.097	0.963	0.219	-1.014	0.965	11.63	-0.484	0.991

The influence of varying both the concentration of NaCl added to the electrolyte and the concentration of polymer is shown in Figure 4.1 for benzenesulfonate and benzoate (Figure 4.1(a)) and Br^- and I^- (Figure 4.1(b)). It can be seen that the mobility of benzenesulfonate was reduced significantly as the concentration of polymer was increased, demonstrating strong interactions with the pseudo-stationary phase. In this case, the interaction was significant enough to induce a selectivity reversal between benzoate, which has little or no IE interaction, and benzenesulfonate, which has considerable IE interaction. Conversely, increasing the concentration of salt decreased the IE interaction and resulted in the normal CE migration order being obtained due to suppression of the interaction of benzenesufonate with the pseudo-phase. It should also be noted that increasing the salt concentration will also reduce the electrophoretic mobility of the analytes as well as influencing the degree of IE interaction. Similarly, it can be seen in Figure 4.1(b) that the resolution between Br^- and I^- increased significantly upon addition of PDDAC to the electrolyte.

It may seem that the best separation of Br^- and I^- can be obtained by maximising the IE interaction with the pseudo-stationary phase, and if only the selectivity is considered, then this is indeed the case. However, with increasing interaction with the pseudo-stationary phase, peak efficiency decreases. This is shown in Figure 4.2 where the concentration of PDDAC has been increased outside the experimental space to demonstrate the influence of having a separation mechanism which is dominated by IE. It can be seen that for analytes like IO_3^- and NO_2^- which have very low values of $K_{A,E}$, the separation efficiency did not decrease substantially, however for benzenesulfonate the efficiency decreased slightly corresponding to its moderate interaction, and for I^- and benzenedisulfonate, the efficiency decreased substantially.

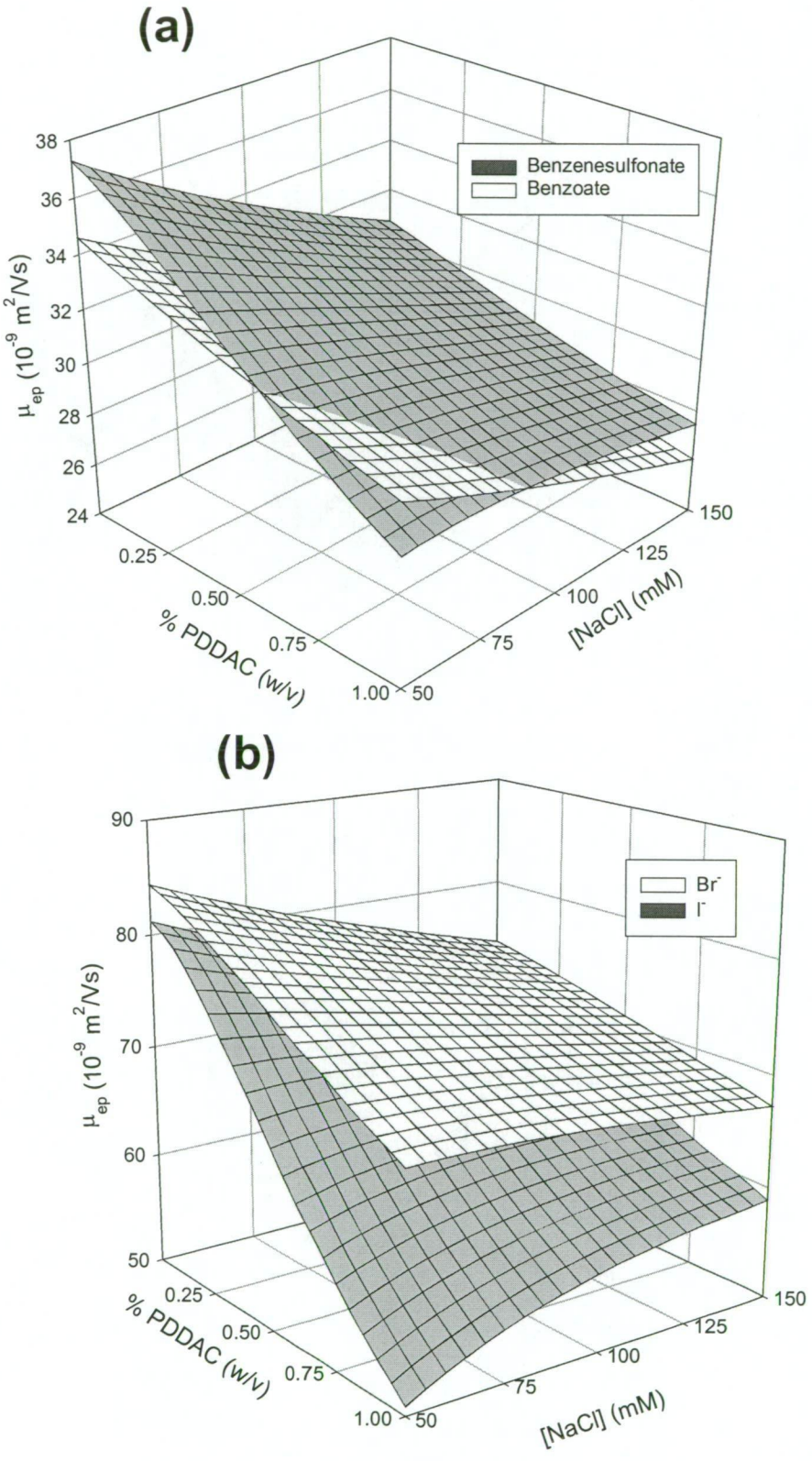

Figure 4.1: Influence of NaCl and PDDAC on the mobilities of (a) benzenesulfonate and benzoate, (b) bromide and iodide. Conditions given in experimental.

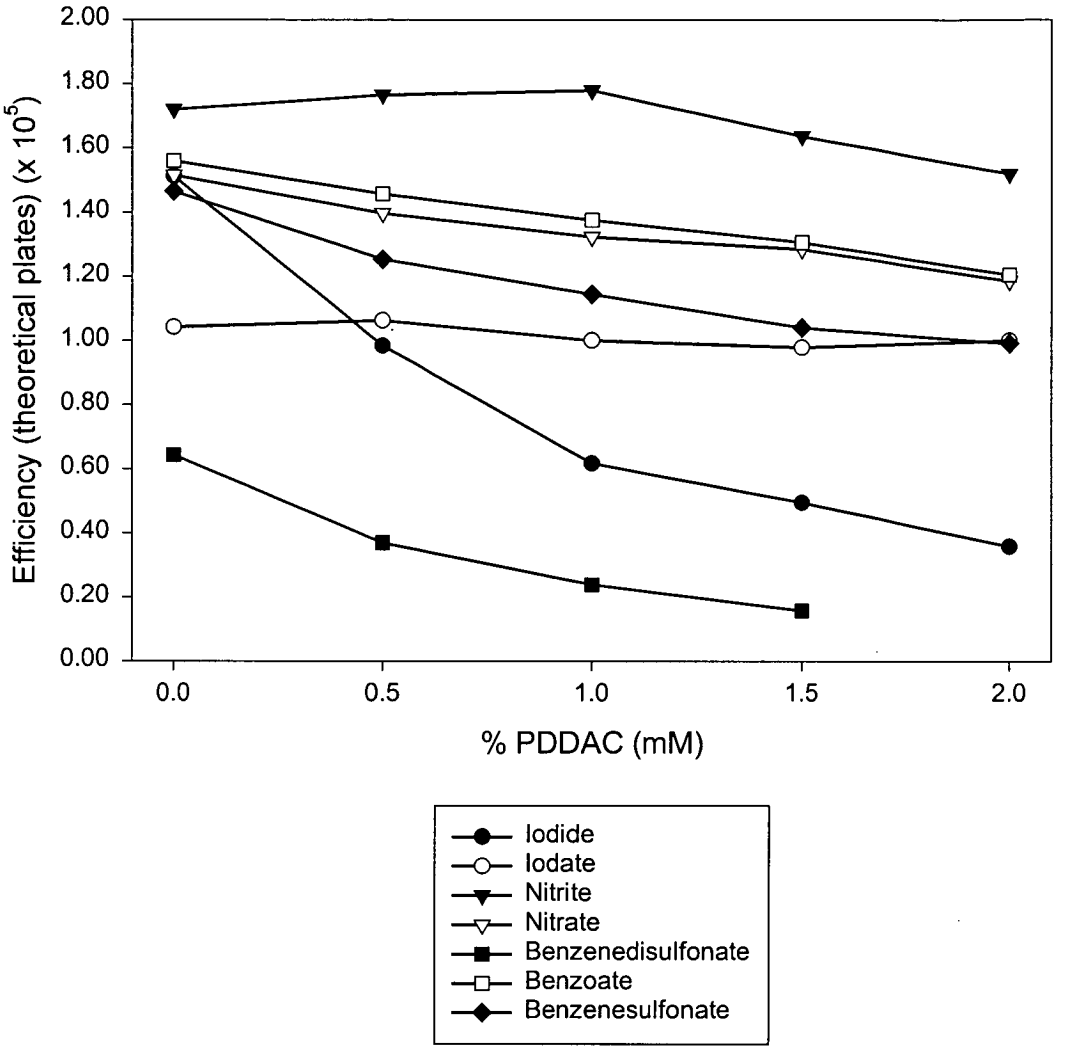

Figure 4.2: Influence of IE interaction with the pseudo-stationary phase on peak efficiency. The concentration of NaCl added to each electrolyte was 100 mM.

4.4.3 Sulfate as competing anion

Agreement between experimental and predicted mobilities using a electrolyte containing chloride as the competing anion demonstrated that the model was applicable for monovalent competing ions. However, sometimes it is desirable to use stronger competing ions than chloride, especially when strongly interacting analytes are to be separated. In IEC, strong competing ions are typically highly polarisable ions, such as perchlorate, or polyvalent ions as these typically interact more strongly with the stationary phase due to their higher charge. In investigating the use of stronger competing ions, it should be noted that the use of perchlorate as a competing ion was not possible in this study as it caused the polymer to precipitate.

It has been shown by Li *et al.* [11], that sulfate could be used effectively as a strong competing ion. For modelling purposes, this provides a rigorous test for the model equation, as it is well known from IEC [15] that the effective charge of divalent ions differs greatly from the theoretical value of –2 due to the influence of ionic strength. To determine the validity of the model when using a divalent competing ion, the model was applied to a primary set of 5 experimental points in the same manner as used for chloride. A further 8 experimental points throughout the experimental space were used as the validation set. Figure 4.3 shows the correlation plot for all 16 analytes in the 13 different buffer conditions. As can be seen, agreement between experimental and calculated mobilities was good, indicating the suitability of the model equation without the inclusion of ionic strength effects on the eluent charge.

Values for the constants determined using a sulfate electrolyte are shown Table 4.1. Arranging the analytes in order of increasing values of $K'_{A,E}$ resulted in a similar order to that obtained using chloride as the competing anion. The order of the weakly interacting analytes could not be determined as all species returned a $K'_{A,E}$ value of zero, indicating that in this electrolyte, there was no measurable interaction of these analytes with the stationary phase.

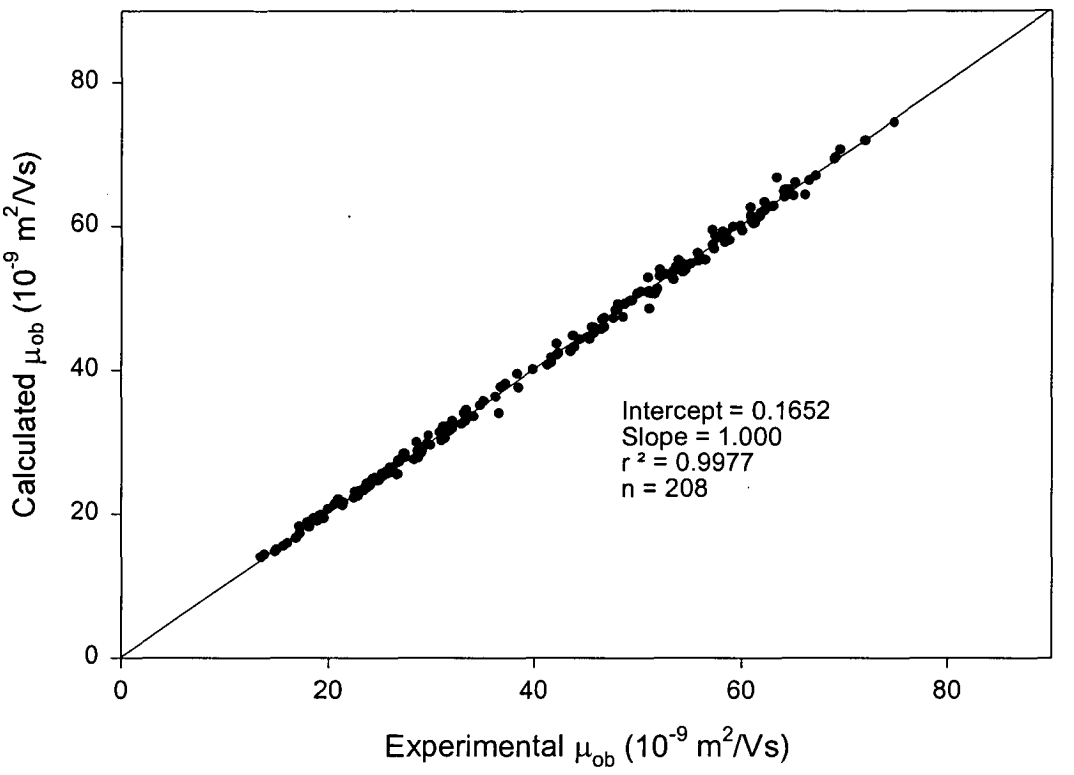

Figure 4.3: Correlation plot for 16 analytes in 13 different buffer conditions using sulfate as the competing anion. Predicted values were obtained from the model equation using constants determined from the primary set of 5 experimental points.

4.4.4 Fluoride and acetate as competing anions

The use of sulfate provided a means to suppress strong IE interactions, but it is also of interest to analyse solutes that have small IE interactions and to see if the separation selectivity could be altered significantly. This entails using a competing ion that is weaker than chloride. Fluoride was selected in order to maximise IE interactions, while acetate was also used as an example of a competing ion having elution strength intermediate between fluoride and chloride. System constants were determined from a primary set of 5 experiments. A further validation data set was deemed to be unnecessary due to the excellent performance of the model obtained using chloride and sulfate as competing anions. Values for system constants using fluoride and acetate determined from non-linear regression are shown in Table 4.1. Once again, trends similar to those obtained for chloride and sulfate were observed.

4.4.5 Quantitative comparison of eluotropic strength

The determination of IE selectivity coefficients of the analytes provides an opportunity to quantitatively evaluate the strength of the IE interactions. From the values of the constants in Table 4.1, several obvious trends can be seen. The first is that the values of the selectivity coefficients generally decreased in the order fluoride, acetate, chloride and sulfate, as illustrated by NO_3^- which has values of $K_{A,E}$ of 0.451, 0.393, 0.069 and 0 for the above competing anions, respectively. This indicated that NO_3^- interacted to a greater extent with the polymer in a fluoride electrolyte than when chloride and sulfate were present, and that acetate was closer in eluting strength to fluoride than chloride. This is not surprising given the elution order of these analytes in IEC, namely F^- < acetate < Cl^- < SO_4^{2-} [15]. The second trend is that different eluents showed different selectivities for different analytes. For example, I^- had a $K_{A,E}$ value of 0.329 in chloride and 0.186 in sulfate, while CrO_4^{2-} had values of 0.924 and 0.062, indicating that I^- had less interaction with the pseudo-stationary phase than CrO_4^{2-} when chloride was used as the eluent, but the reverse

was true when sulfate was used. This is probably due to the influence of secondary interactions with the non-polar section of the polymer backbone. It is also interesting to note that 3,5-dihydroxybenzoate had a much higher value of $K_{A,E}$ in sulfate than fluoride, again suggesting the influence of secondary interactions in the separation mechanism.

Figure 4.4 demonstrates the variation of mobility of I^- using the different competing ions. As can be seen, the observed mobility using sulfate as competing anion was lower than for the other two competing anions, which is due to the increased ionic strength in this electrolyte which results in a relatively unchanged observed mobility as the concentration of polymer was increased. This is due to the complete suppression of the IE interactions due to the strong eluotropic strength of sulfate. Comparing the mobility changes with fluoride and chloride, it can be seen that the mobility changed more rapidly with increasing polymer concentration with fluoride than with chloride. This is not surprising considering that I^- had a higher selectivity coefficient in fluoride than chloride.

4.4.6 Optimisation

The determination of analyte-specific constants enabled the separation to be optimised using a suitable optimisation algorithm. In this process, an initial number of experiments (in this case the primary set of 5 data points) was used to determine the system constants for the model equation and these constants were then used to predict the mobility of the analyte over the experimental space. Determination of the best conditions to achieve a desired outcome (whether it be the separation of all analytes, or the separation of a particular pair of analytes) was then undertaken using a suitable numerical criterion to assess the quality of the separations possible over the entire experimental space. A separation under the predicted optimal conditions was then performed and the experimental mobilities compared with those predicted by

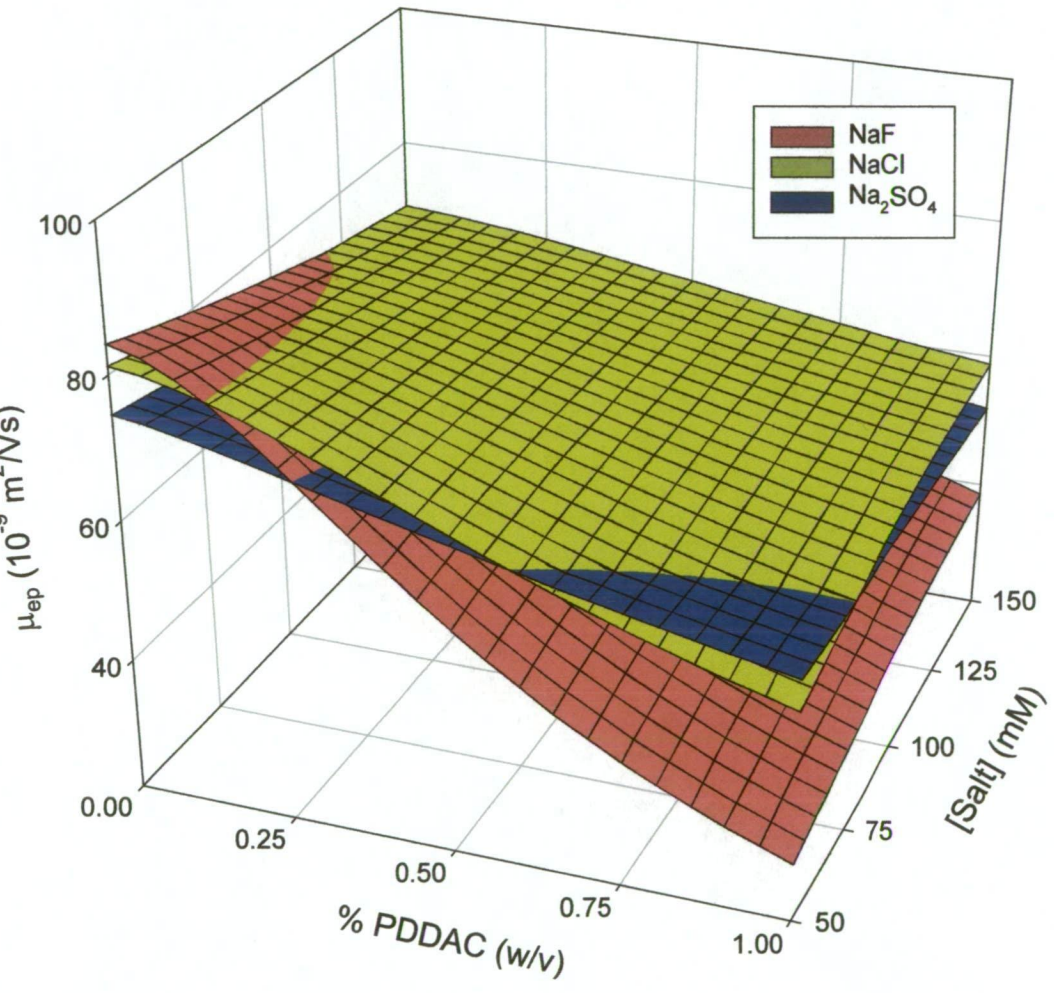

Figure 4.4: Influence of varying the nature of the competing ion on the observed mobility of iodide over the experimental space.

the model. When significant differences occurred, the measured data were added to the primary set and new analyte constants determined. This process was repeated until the agreement between predicted and observed data was within a specified limit, in this case 1%. It should be noted that the following discussion focuses on the optimisation of selectivity and does not cover other criteria such as peak shapes, or detection sensitivity.

4.4.6.1 Optimisation using the normalised resolution product criterion

The normalised resolution product (r) is a resolution criterion that is designed to achieve its highest value when all of the analytes under consideration are evenly separated and is given in equation (3-19).

On the basis of the constants determined for the 4 competing ions above, the normalised resolution criterion was used to determine the best conditions for the overall separation of all the analytes. The normalised resolution product surface obtained for a chloride eluent is shown in Figure 4.5, with the optimum separation conditions (the highest value of r) being at 110 mM NaCl and 0.35% PDDAC. The separation obtained under these conditions is shown in Figure 4.6, which also shows the optimised separations obtained with SO_4^{2-} and F^- competing anions. It should be noted that peaks are numbered in order of decreasing electrophoretic mobility as determined from co-EOF CZE experiments using CTAB as an EOF reversal agent. As can be seen from Figure 4.6, all the separations were very similar, with differences in analysis time resulting from differences in applied voltages and ionic strengths. Changes in separation selectivity can be seen, in particular with regard to benzenedisulfonate and phthalate (peaks 10 and 11 respectively) in which benzenedisulfonate migrated first in both the F^- and Cl^- systems, but migrated after phthalate in the SO_4^{2-} system. Also, the separation between CrO_4^- (peak 5) and SCN^- (peak 6) differed considerably, with these species being only partially separated in the F^- system, but with increasingly larger resolution in the Cl^- and SO_4^{2-} systems.

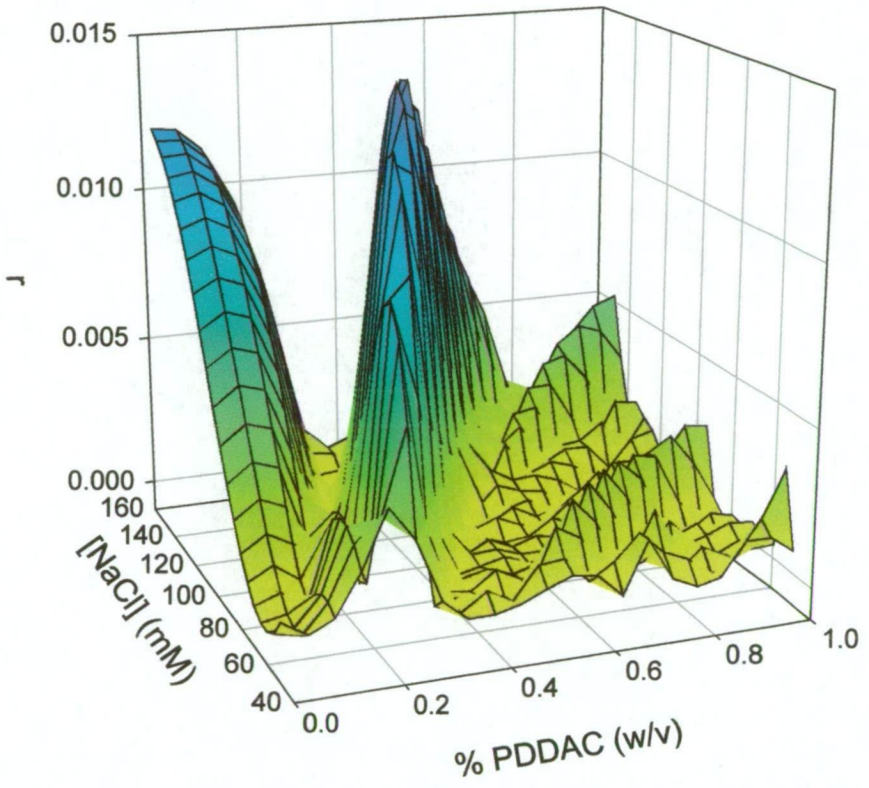

Figure 4.5: Normalised resolution product (r) surface for 16 analytes in a electrolyte containing chloride as the competing ion. Optimum conditions are at 110 mM and 0.35% PDDAC.

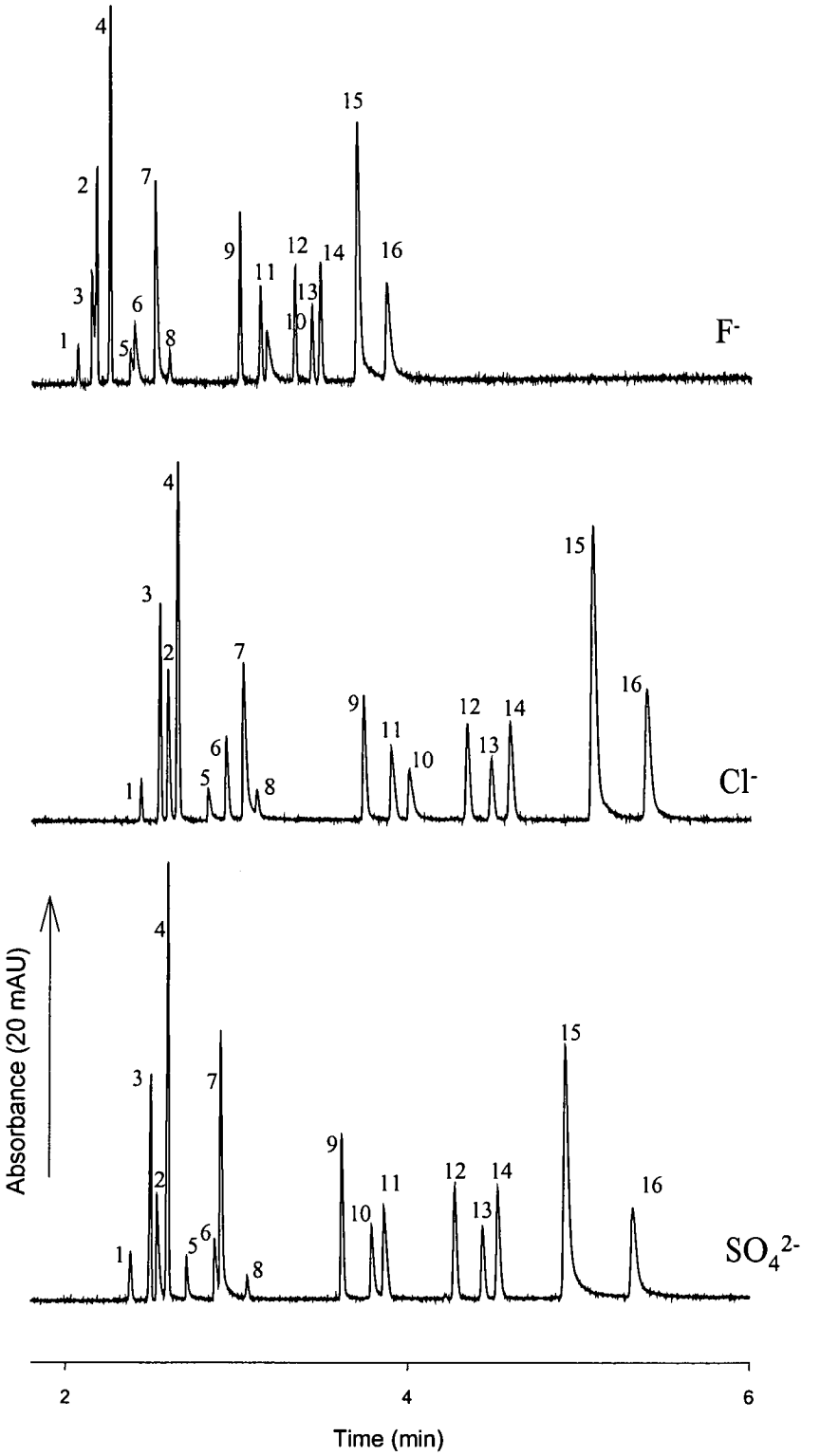

Figure 4.6: Optimised separations determined using the normalised resolution product criterion. Optimum conditions are (i) for chloride: 110 mM NaCl, 0.35% PDDAC, -15.4 kV; (ii) for fluoride: 150 mM NaF, 0.05% PDDAC, -14.3 kV; and (iii) for sulfate: 50 mM SO_4^{2-} and 0.30% PDDAC, -15.5 kV. Peaks are 1 = Br^-, 2 = I^-, 3 = NO_2^-, 4 = NO_3^-, 5 = CrO_4^{2-}, 6 = SCN^-, 7 = MoO_4^{2-}, 8 = BrO_3^-, 9 = phthalate, 10 = 1,2-benzenedisulfonate, 11 = IO3-, 12 = benzenesulfonate, 13 = benzoate, 14 = *p*-toluenesulfonate, 15 = 2-naphthalenesulfonate, 16 = 3,5-dihydroxybenzoate.

4.4.6.2 Optimisation using the minimum resolution criterion

When applied to the test analytes, the normalised resolution product criterion gave optimal conditions which provided a separation having a selectivity that was similar to CE (with some slight differences for the stronger interacting analytes). An alternative approach is to use the minimum resolution criterion, in which the resolution value for the pair of adjacent peaks having the worst separation is calculated as follows:

$$r_{\min} = \min\left(R_{s(i,i+1)}\right). \qquad (4\text{–}10)$$

The conditions leading to the maximum value of $r_{\min}$ are then determined and become the optimal conditions.

The minimum resolution criterion was applied to the experimental space for the F^- competing anion system, which was selected for study because it covered the largest range of IE interactions for the systems studied, shown in Figure 4.7. MoO_4^{2-} was omitted from the test mixture of analytes because of difficulties in separating it from CrO_4^{2-} at high concentrations of polymer. The optimised separation determined using the minimum resolution criterion and NaF as the added salt is shown in Figure 4.8. Again, the peaks are numbered according to their migration order in a co-EOF CE separation system, that is in order of decreasing electrophoretic mobility. It can be seen that the introduction of the IE interactions greatly altered the separation selectivity. In particular, Br^- (peak 1) was eluted after NO_2^- (peak 3), and I^- (peak 2) after IO_3^- (peak 11). Peak broadening was observed for the strongly interacting ions (such as I^-, CrO_4^{2-}, benzenedisulfonate), due to interaction with the adsorbed PDDAC on the capillary wall and 80 mM NaF was insufficiently strong to eliminate this interaction. On the other hand, the peak for Br^-, which also exhibited significant changes in mobility, was still quite sharp suggesting that wall interactions were suppressed under the electrolyte conditions used.

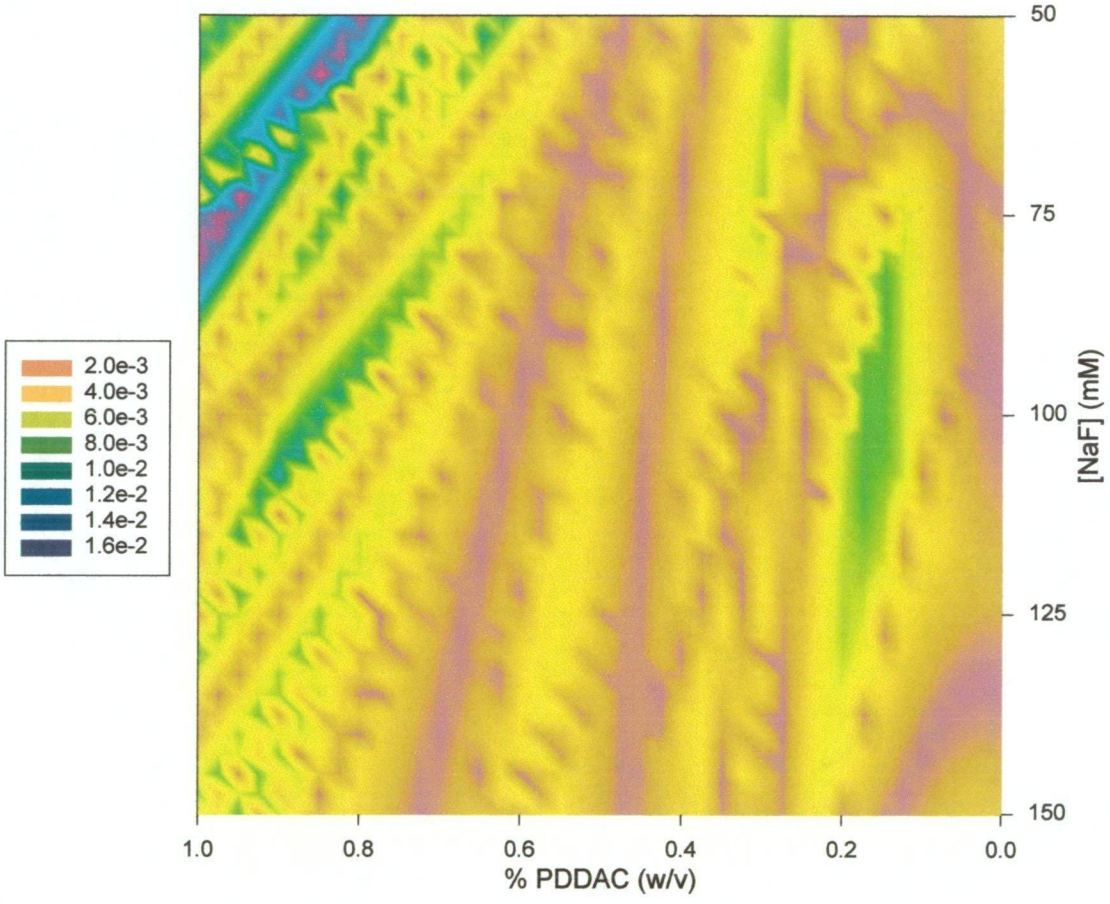

Figure 4.7: Minimum resolution (r_{min}) surface for 16 analytes in a electrolyte containing fluoride as the competing ion. Optimum conditions are at 80 mM NaF and 0.9% PDDAC.

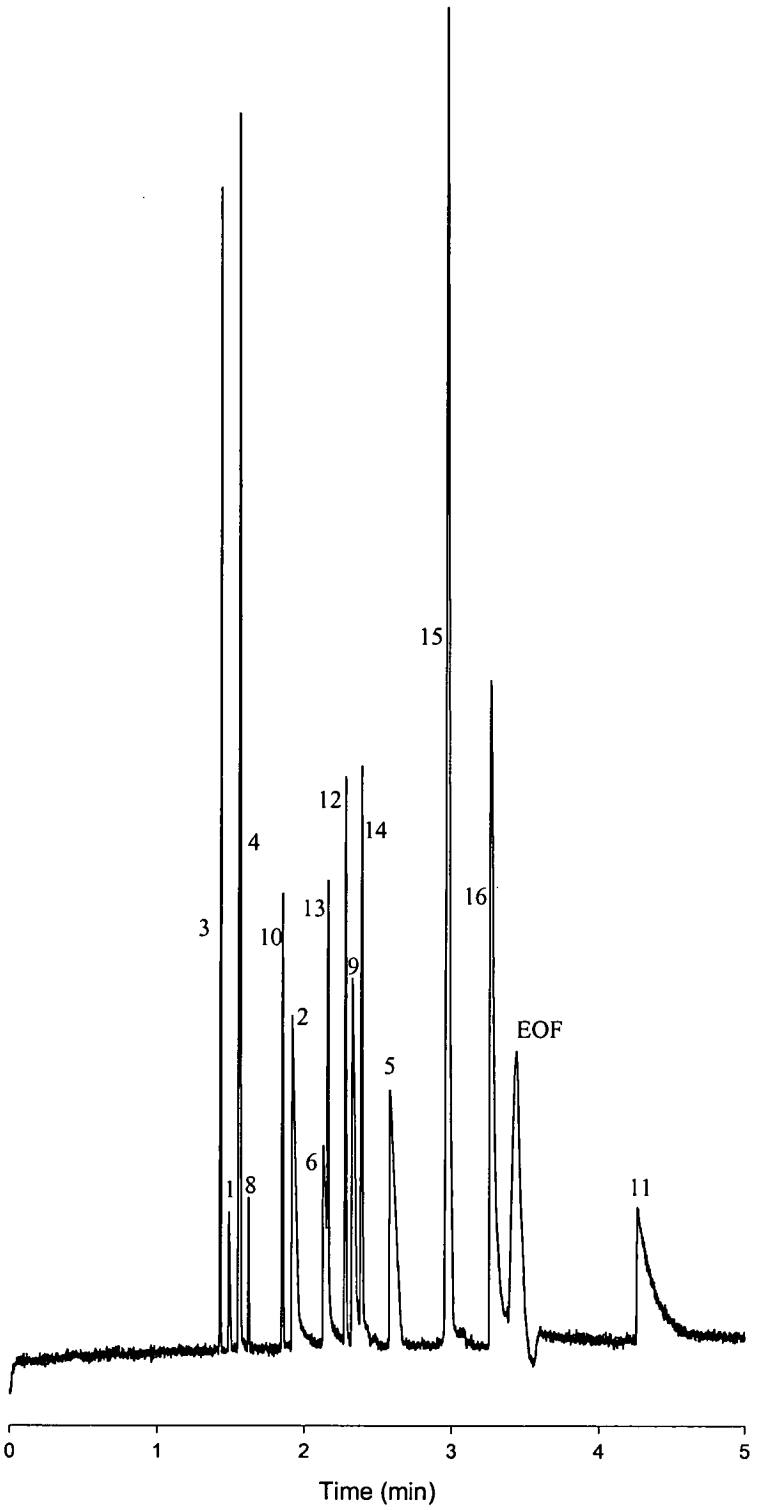

Figure 4.8 Optimised separation determined using the minimum resolution criterion in the NaF experimental system. Conditions are 80 mM NaF, 0.9% PDDAC, -19.8 kV. Experimental minimum resolution is 0.012 between SCN- and benzoate , while the theoretical value for the minimum resolution (also between the same peaks) was calculated to be 0.012 from the primary set of 5 experiments. Other conditions as in Figure 4.6. Peaks are 1 = Br^-, 2 = I^-, 3 = NO_2^-, 4 = NO_3^-, 5 = CrO_4^{2-}, 6 = SCN^-, 7 = MoO_4^{2-}, 8 = BrO_3^-, 9 = phthalate, 10 = 1,2-benzenedisulfonate, 11 = IO3-, 12 = benzenesulfonate, 13 = benzoate, 14 = *p*-toluenesulfonate, 15 = 2-naphthalenesulfonate, 16 = 3,5-dihydroxybenzoate.

4.5 UV transparent anions

4.5.1 Requirements for indirect UV detection in pseudo-phase IE-CEC

Indirect detection in CE has been reviewed recently and the following guidelines for appropriate electrolyte composition have been suggested [19]. First, the electrolyte should be buffered in order to provide sufficient ruggedness and reproducibility. This must be performed without introducing any co-ions that can compete with the probe and cause both a reduction in detection sensitivity and the introduction of a system peak. Second, the electrophoretic mobility of the probe should match that of the analytes, and when a selection of analytes with a range of mobilities are to be analysed the probe concentration should be maximised to minimise electromigration dispersion. Third, the molar absorptivity of the probe should be maximised to give the best possible detection sensitivity.

In chapter 3, the above guidelines for indirect UV detection were employed in OT-IE-CEC. In this case, in addition to the requirements already indicated, the probe must also function as the IE competing ion. It was found that indirect UV detection in IE-CEC was feasible but due to the limited IE capacity of OT columns the separation selectivity could not be varied to any significant extent using a single probe ion. A series of probes with differing IE selectivity coefficients was deemed necessary and using an appropriate selection it was demonstrated that the separation selectivity could be changed from predominantly IEC in nature to predominantly CE. Electromigration dispersion was observed to be significant when low concentrations of probes were employed in order to maximise analyte retention.

Indirect detection in IE-CEC using a pseudo-phase has similar requirements to those encountered when using OT columns, but should offer greater flexibility because of the ability to vary the IE capacity of the column. Unlike the situation encountered using OT columns, low concentrations of competing ion are unlikely to be required

because stronger analyte retention can be obtained by increasing the IE capacity rather than lowering the eluotropic strength of the eluent.

4.5.2 Potential of adding unmodified PDDAC to the electrolyte

Indirect detection in CE is best accomplished by having only one co-ion in the electrolyte, namely the probe itself [19]. However, the polymer selected for use in this study was obtained in the chloride form. Nevertheless it would be desirable if the unmodified polymer could be added to a electrolyte containing a UV-absorbing probe. The introduction of an additional co-anion (in this case, Cl^-) would cause a reduction in detection sensitivity and the occurrence of a system peak. The extent to which both of these detrimental factors occurs is dependent on the relative mobilities of both the probe and the co-ion. The occurrence and position of the system peak are of great consequence since this peak will interfere with the separation of surrounding peaks. The position of the system peak generated when two co-ions are present in the electrolyte is given by [20]:

$$\mu_s = (\mu_{A1} - \mu_{A2})x - \mu_{A1}, \qquad (4\text{–}11)$$

where μ_s is the mobility of the system peak, μ_{A1} is the mobility of the first co-ion (higher mobility), μ_{A2} is the mobility of the second co-ion (lower mobility), and x is the mole fraction of the first co-ion. A mixture of equivalent concentrations of two co-ions will give a system peak having a mobility which is the average of the mobilities of the two co-ions. In IE-CEC the addition of polymer to the electrolyte will influence the observed mobility of the analyte anions and it should be theoretically possible to change the position of the analytes relative to the system peak.

To examine the potential of this approach, a two-probe electrolyte containing CrO_4^{2-} and phthalate was prepared using equivalent concentrations of each probe, giving a system peak with mobility between those of the two probes. These UV absorbing

anions were selected for this investigation instead of Cl^-, the form in which the polymer was obtained, so that analytes migrating before and after the system peak could be visualised [20]. The influence of [$PDDA^+$] on the position of the system peak and the peaks of the analytes was determined by adding $PDDA^+$-CrO_4^{2-} to the electrolyte while keeping the total concentration of $CrO_4^{2-}$and phthalate constant at 2.5 mM each. Figure 4.9 shows that as [$PDDA^+$] was increased, the position of the system peak moved to lower mobilities. With 0.8 % $PDDA^+$ added to the electrolyte, the system peak had the lowest mobility and it can be seen that it no longer interfered with the analysis of F^-, although the system peak then interfered with the analysis of ethanesulfonate. Whilst it might be possible to improve the final separation by varying the relative IE selectivity coefficients of the analytes and probes, the approach of using two co-ions was considered to be unsuitable when trying to separate a large number of analytes.

4.5.3 Indirect detection using a single probe anion

The above investigation suggested that addition of unmodified PDDAC to electrolytes used for indirect was undesirable. It was therefore necessary to change the counter-ion of the polymer to one that could act both as a suitable probe and as an IE competing ion. This was achieved by first converting the polymer to the hydroxide form using the method of Cassidy and Stathakis [3] and then titrating this with the acid form of the probe. It should be noted that the polymer was not stable in the hydroxide form for extended periods and immediate titration of the polymer after elution from the IE column used to convert it to the hydroxide form was necessary in order to prevent decomposition of the polymer.

Conversion of the polymer to the probe form restricts the flexibility of the IE-CEC system demonstrated for UV absorbing anions because the concentration of competing ion and polymer are invariably linked. This therefore restricts the size of the available experimental space because the probe concentration can never be lower

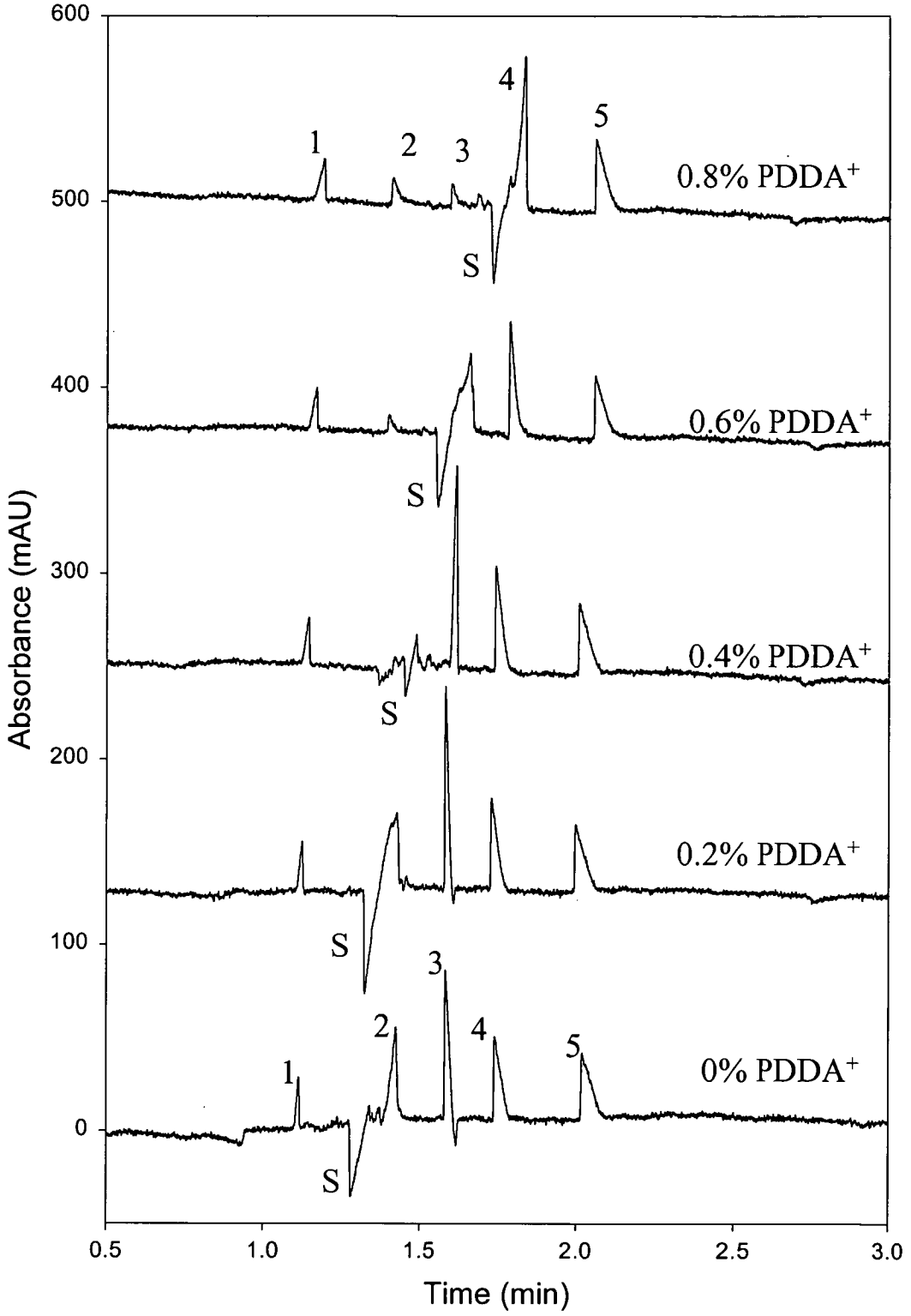

Figure 4.9: Influence of adding $PDDA^+$ on the position of the system peak in the separation of inorganic anions using a multiple probe electrolyte. All electrolytes contain 2.5 mM phthalate and 2.5 mM CrO_4^{2-} prepared from phthalate/Tris (pH 7.70), PDDA-CrO_4^{2-} and Na_2CrO_4 to give the appropriate concentration of $PDDA^+$ and were buffered with the addition of 10 mM histidine. Separation was performed in a 50.0 cm capillary (41.5 cm to det) x 75 μm i.d. with a voltage of –30 kV. Peaks are : 1 = Cl^-, 2 = F^-, 3 = C_1-SO_3^-, 4 = C_2-SO_3^-, 5 = C_5-SO_3^-, S = system peak.

than the concentration required to satisfy electroneutrality with the polymer. A higher concentration of probe can be employed by adding the probe as an alternative form (such as Na^+).

To examine the requirements for indirect UV-detection in pseudo-phase IE-CEC, three different competing ions, CrO_4^{2-}, phthalate and benzoate, were selected on the basis of their relative IE strengths and the experimental space was defined between 0 and 0.64% $PDDA^+$ and 10-40 meq of probe (5 – 20 mM for CrO_4^{2-} and phthalate, and 10-40 mM for benzoate). The influence of the variation of each of these parameters is discussed below in further detail.

4.5.3.1 Variation of polymer concentration

Increasing the concentration of polymer in the electrolyte is equivalent to increasing the column IE capacity in IEC. This will result in a decrease in the observed mobility of the analytes due to a higher degree of interaction with the polymer. Figure 4.10 shows the influence of increasing [$PDDA^+$] on the observed mobilities of 16 analyte anions using phthalate as the competing ion. It can be seen that some analytes were influenced by the addition of $PDDA^+$ more than others, for example the mobility of oxalate was reduced substantially in comparison to acetate. This enabled the separation selectivity to be varied. Data for all 24 analyte anions were obtained but 8 analytes are not included in Figure 4.10 to improve the clarity of the figure.

4.5.3.2 Variation of probe concentration

The influence of increasing the concentration of the competing ion in an IE system is well established and results in a decrease in interaction between the analytes and the stationary phase, causing analytes to be eluted earlier. The same situation occurs in IE-CEC, with interaction between the analytes and the polymer being suppressed at higher concentrations of competing ion, resulting in an increase in observed

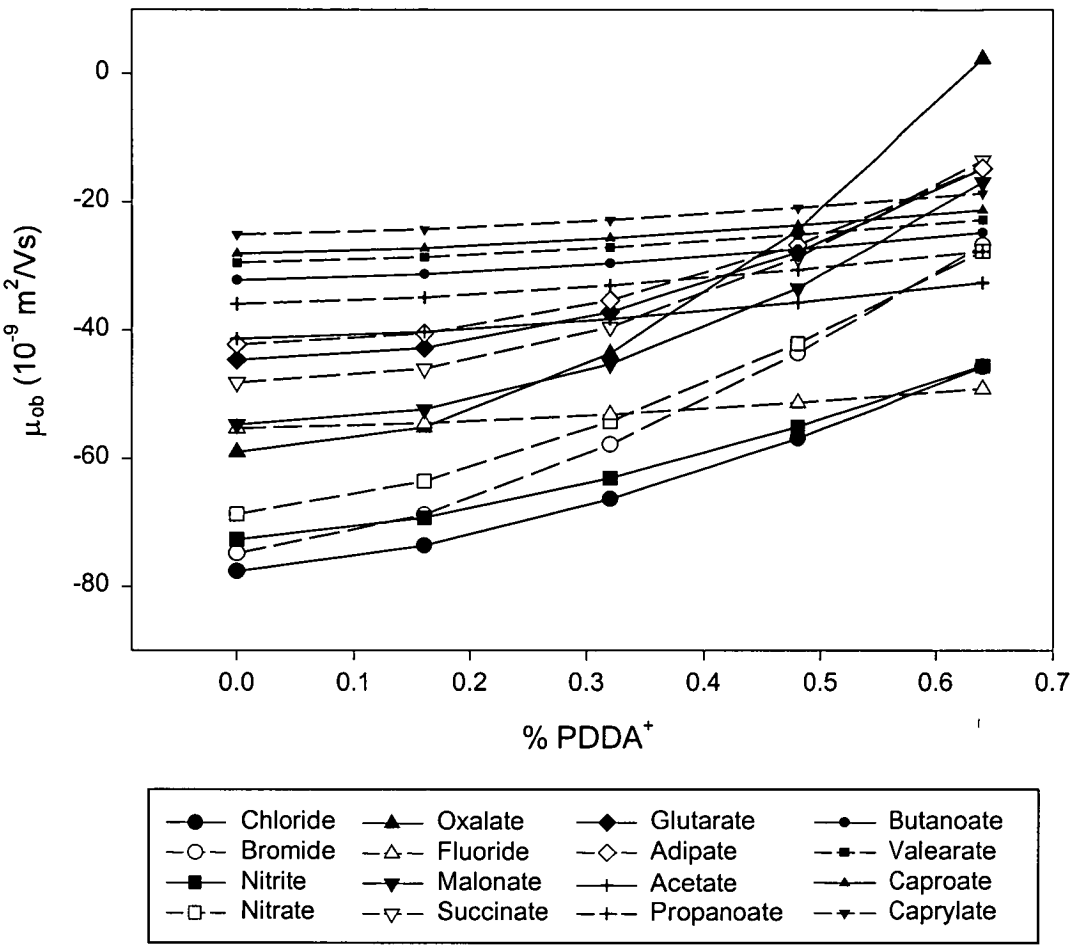

Figure 4.10: Influence of increasing the concentration of $PDDA^+$ on the separation selectivity of selected anions in a phthalate electrolyte. The electrolyte was prepared from phthalate/Tris (pH 7.70) and Phthalate/$PDDA^+$ to give a total concentration of 20 mM phthalate and was buffered with 10 mM histidine. Other conditions as in Figure 4.9

mobilities. Figure 4.11 shows this influence using a constant polymer concentration of 0.40% and 10-20 mM phthalate as the competing ion.

4.5.3.3 Variation of the ion-exchange selectivity coefficient of the probe

The interdependence of the polymer and competing ion concentrations restricts the accessible electrolyte compositions and means that the IE selectivity coefficient of the probe becomes an important parameter. Figure 4.12 shows changes in observed mobility for 16 analyte anions using three different competing anions and equivalent concentrations of polymer. Chromate has the highest IE selectivity coefficient and it can be seen that analytes exhibited the highest observed negative mobilities in this electrolyte indicating a low level of interaction with the polymer. Conversely, analytes exhibited the lowest observed negative mobilities in the benzoate electrolyte, indicating a high degree of interaction with the polymer. Phthalate has an intermediate IE selectivity coefficient, and observed mobilities of the analytes values fell between those for chromate and benzoate. It should be noted that the mobility of ClO_4^- was unchanged when going from the phthalate to benzoate systems because both of these competing ions were ineffective at modifying the interactions of ClO_4^- with the polymer under the conditions used.

The significance of being able to vary the IE selectivity coefficient of the probe becomes important when practical considerations regarding electrolyte composition are made. For example, in a chromate electrolyte with 0.64% $PDDA^+$ added there is only minimal interaction of most of the analytes with the polymer. More interaction can be obtained by increasing the polymer concentration further, however this is not a good option for several reasons: first, as the concentration of polymer increases, the concentration of chromate increases concomitantly and the baseline becomes noisier because of the increased background absorbance. It is also important that the background absorbance remain within the linear range of the detector. Second, the increase in ionic strength of the electrolyte will result in a higher current and

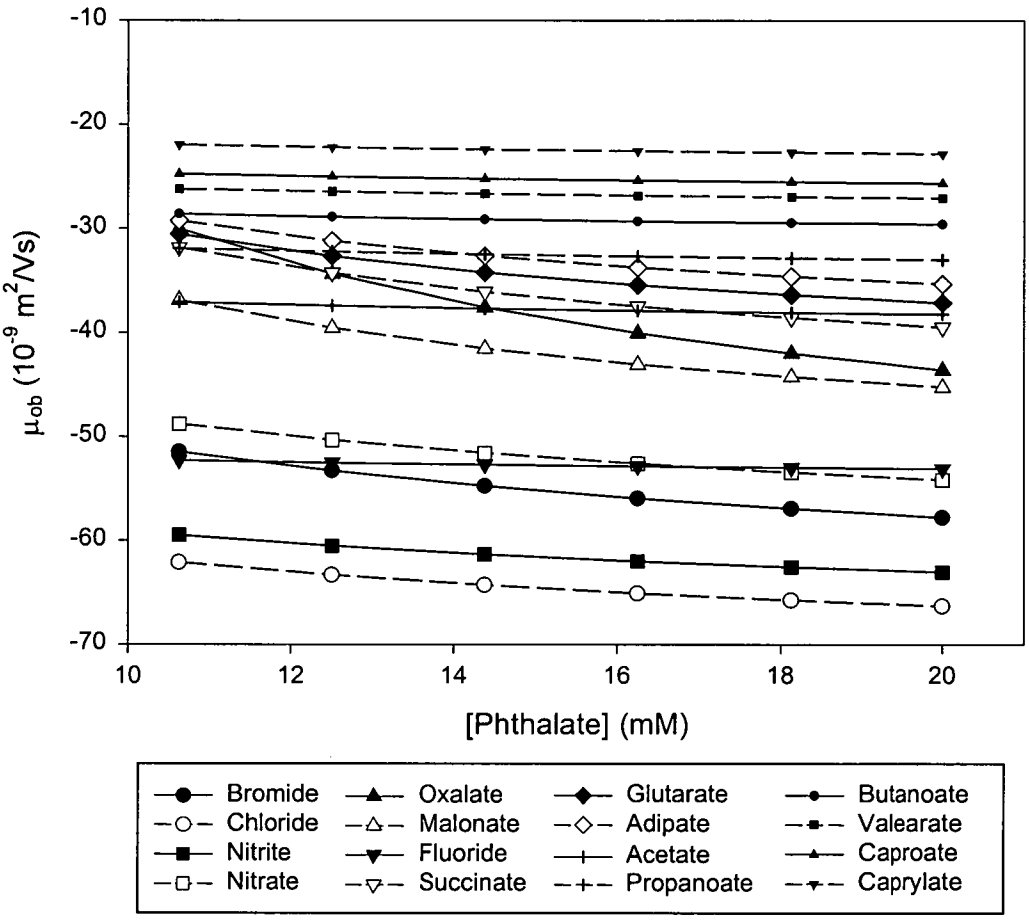

Figure 4.11: Influence of increasing the concentration of phthalate on the separation selectivity of selected anions in a electrolyte containing 0.40 % $PDDA^+$. Other conditions as for Figure 4.10.

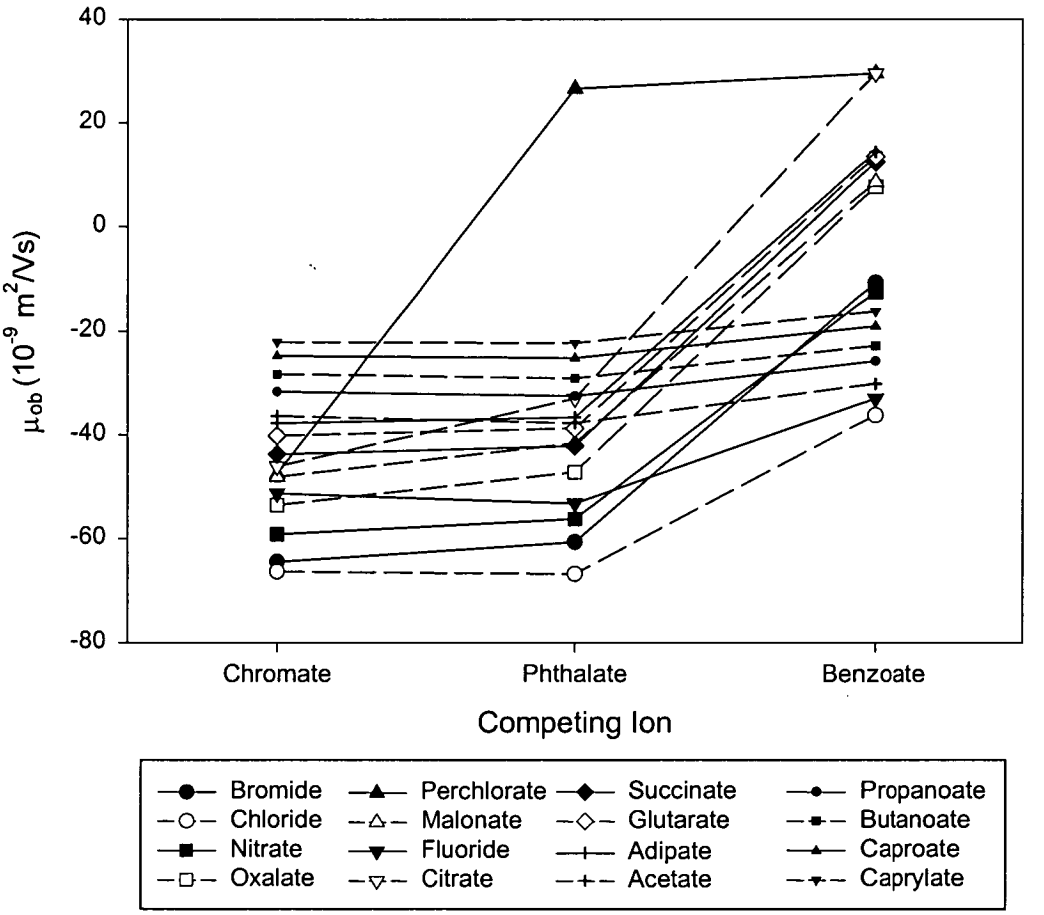

Figure 4.12: Influence of varying the IE strength of the probe on the observed mobilities of selected anions. All electrolytes contain 0.32% $PDDA^+$ and the probe concentration was 20 mM (CrO_4^{2-} and Phthalate) or 40 mM (benzoate). Other conditions as for Figure 4.10.

increased Joule heating, leading to a noisier baseline and a reduction in separation efficiency. Third, the viscosity of the electrolyte increases with increasing polymer concentration until it becomes impractical to add more due to increased analysis and flushing times. Changing the competing ion from CrO_4^{2-} to benzoate would establish a higher degree of interaction between the analytes and the polymer without any of the above problems outlined.

4.5.4 Optimisation of electrolyte conditions

The above discussion indicates that the separation selectivity and hence resolution between analytes, can be adjusted by changing the concentration of polymer, the concentration of competing ion, and/or the type of competing ion. However, when a large number of analytes is to be separated, selecting the appropriate electrolyte conditions can be difficult. It has already been demonstrated that the separation selectivity in pseudo-phase IE-CEC can be optimised from 5 initial experiments using the model equation (4–9) and this approach will be undertaken here.

In order to optimise the electrolyte composition, the constants in equation (4–9) need to be determined. To do this, a data set comprising the observed mobilities of the 24 analyte anions determined at 5 electrolyte compositions (termed the primary data set) was acquired. The primary data set was acquired using 0% $PDDA^+$/10 meq probe, 0% $PDDA^+$/40 meq probe, 0.64% $PDDA^+$/40 meq probe, 0.32% $PDDA^+$/25 meq probe, and 0.16% $PDDA^+$/33 meq of probe. Values for the system constants in equation (4–9) for each analyte are shown in Table 4.2 for three probe ions. A secondary data set containing 5 randomly selected data points over the experimental area showed excellent correlation between the experimental and predicted observed mobilities with correlation coefficients greater than 0.97 being obtained for the three electrolyte systems. It should be noted that values for the selectivity coefficient for perchlorate and citrate could not be obtained in the benzoate electrolyte using the

Table 4.2: Values of constants (for analytes arranged in order of decreasing electrophoretic mobility) in equation (4–9) as determined from non-linear regression

	CrO_4^{2-}		Phthalate		Benzoate	
b_{sp}	3.01		2.98		2.58	
Analyte	$K_{A,E}$	b_{mp}	$K_{A,E}$	b_{mp}	$K_{A,E}$	b_{mp}
Bromide	0.167	-75.1	0.372	-75.5.1	2.27	-72.8
Chloride	0.071	-73.3	0.132	-72.4	1.43	-70.7
Nitrite	0.069	-74.8	0.107	-74.6	1.47	-72.0
Nitrate	0.111	-72.8	0.259	-72.4	2.02	-69.0
Sulfate	2.64	-67.1	3.21	-67.7	18.3	-66.8
Oxalate	3.373	-67.4	7.43	-67.0	19.3	-68.8
Perchlorate	4.17	-64.4	8.64	-67.0	-	-64.3
Chlorate	0.066	-61.1	0.121	-64.2	1.51	-63.9
Malonate	2.07	-56.6	3.03	-54.2	16.7	-52.5
Formate	0.025	-54.5	0.018	-56.3	0.419	-55.8
Fluoride	0.015	-54.5	0.009	-56.3	0.867	-51.6
Bromate	0.035	-54.5	0.031	-55.9	0.817	-53.4
Citrate	2.94	-53.4	14.1	-52.5	-	-55.6
Succinate	1.73	-51.5	1.89	-52.1	14.5	-54.2
Tartrate	2.00	-50.7	2.08	-50.7	18.3	-53.9
Glutarate	1.27	-46.8	1.29	-46.9	13.0	-41.6
Adipate	1.11	-43.9	1.07	-44.1	12.8	-41.6
Iodate	0.011	-39.0	0.004	-39.6	0.318	-35.8
Acetate	0.006	-38.5	0.006	-38.37	0.298	-36.7
Propanoate	0.006	-33.7	0.006	-34.9	0.275	-31.9
Butanoate	0.005	-30.2	0.004	-31.2	0.269	-30.7
Valearate	0.006	-27.8	0.003	-28.5	0.257	-26.3
Caproate	0.005	-26.6	0.003	-27.0	0.272	-25.0
Caprylate	0.004	-23.9	0.003	-24.1	0.278	-22.4
r^2	0.990		0.979		0.986	
Slope	1.02		1.04		1.05	
Intercept	0.864		1.13		1.56	

primary data set due to complete association of this analyte with the polymer, even at the lowest concentrations of polymer employed in this study.

From Table 4.2 it can be seen that the selectivity coefficients were highest when benzoate was used as the competing ion and lowest CrO_4^{2-} was used. Analytes therefore showed significantly more interaction with the polymer in benzoate electrolytes than the phthalate and chromate electrolytes, which was also apparent from Figure 4.12. Several trends are evident from Table 4.2, especially for the weakly interacting carboxylic acids. For example, when considering the mono-carboxylic acids, selectivity coefficients for the benzoate electrolyte decreased as the carbon chain length increased up to C_5 (valerate) and then increased slightly for C_6 and C_8. This trend can be explained in terms of steric hindrance between the analyte and the $PDDA^+$ functional group increasing with analyte size, up to the point where sufficient carbon chain length is reached to cause secondary, hydrophobic interactions with the polymer. A similar reduction in selectivity coefficients is observed for the dicarboxylic acids, oxalate (C_2) through to adipate (C_6). This again is probably due to increased size of the analyte molecule, coupled with the increased distance between the two anionic groups on the analyte.

Optimisation of the separation conditions for the separation of all 24 analyte anions was possible using the determined system constants and a suitable resolution criterion. In this case, the choice of probe was restricted to chromate and phthalate because there was excessive retention of perchlorate and citrate in the benzoate electrolyte. As the goal was to separate all of the anions, the minimum resolution criterion was selected as used previously in section 4.4.6. This criterion takes the value of the resolution between the worst resolved peak pair in the entire separation. The highest criterion value will therefore be when the resolution between the worst pair is at its greatest. Figure 4.13 shows the resolution surface for all 24 ions using a chromate electrolyte. The use of CrO_4^{2-} as the competing ion was found to provide a higher criterion value than phthalate, due largely to higher separation efficiency of

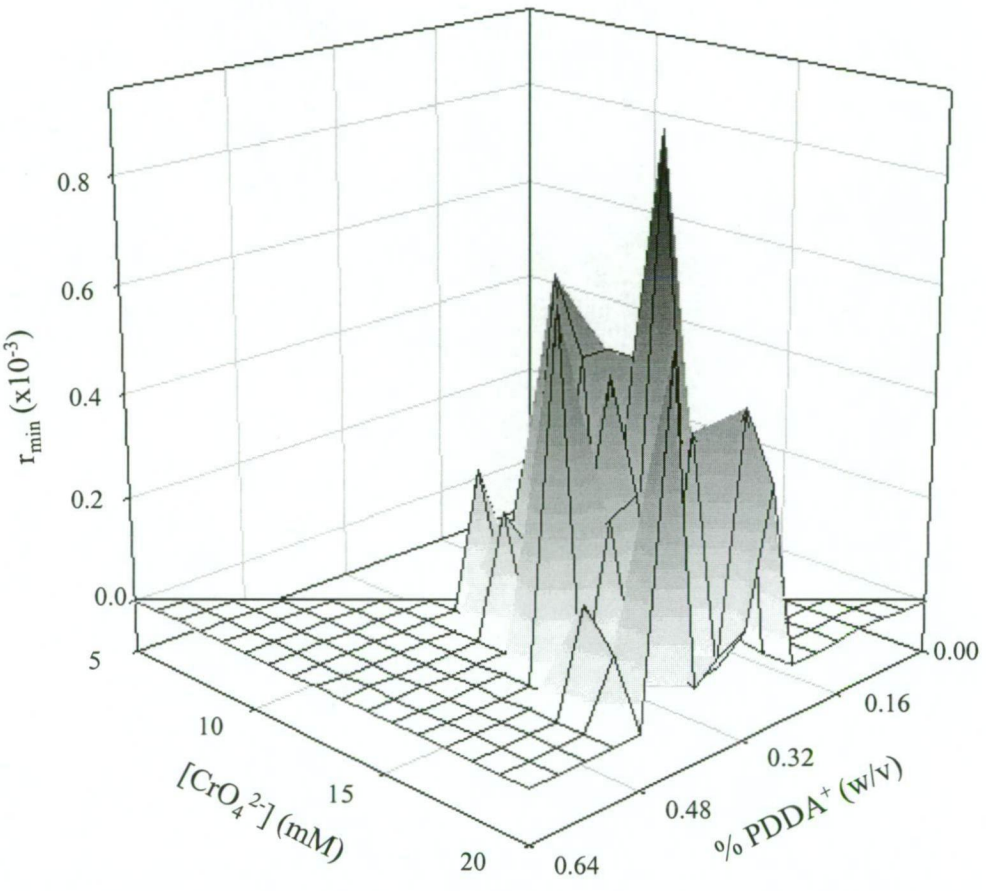

Figure 4.13: Minimum resolution surface response surface for the separation of 24 anions in a CrO_4^{2-}/$PDDA^+$ electrolyte. Optimum separation conditions are at 0.28% $PDDA^+$ and 16.25 mM CrO_4^{2-}. Conditions as in Figure 4.10.

the high mobility inorganic anions as a result of lower electromigration dispersion in this electrolyte. The optimum separation conditions were at 0.28% $PDDA^+$ and 16.25 mM CrO_4^{2-}, and the optimised separation is shown in Figure 4.14. It can be seen that all 24 analytes were well separated and the total analysis time was under 7 min. The analytes are numbered in order of decreasing electrophoretic mobility and the elution sequence in Figure 4.14 indicates that the separation selectivity differed significantly from that obtainable by conventional CE.

4.5.5 Optimisation and separation of components of Bayer Liquor

The determination of anions in Bayer liquor was investigated as a potential application where the advantage of being able to manipulate the separation selectivity would be beneficial. Analytes of interest in Bayer liquor are chloride, oxalate, fluoride, formate, acetate and sulfate. This application is often considered to be problematic by CE due to the high pH of the sample and the high sample ionic strength, both of which result in poor separation efficiencies. A further problem is the potential co-migration of several analytes, particularly fluoride/formate and chloride/oxalate/sulfate. The application of IE-CEC can potentially eliminate this problem by manipulation of the separation selectivity to improve the resolution of important peak pairs. In optimising the electrolyte conditions for this analysis, the concentration of chromate was restricted to > 15 mM as preliminary studies by CE indicated that this provided sufficient ionic strength for analyte stacking to occur for the Bayer liquor sample. The optimum separation conditions identified using the same approach outlined above and again employing the minimum resolution criterion were 20 mM CrO_4^{2-} and 0.55% $PDDA^+$. The separation of synthetic and actual Bayer liquor samples obtained under these conditions are shown in Figure 4.15. It can be seen that peak shapes were well maintained in the standard sample and the resolution between all peak pairs was satisfactory. Application to the real sample gave a similar selectivity to the standard but co-migration of acetate with an

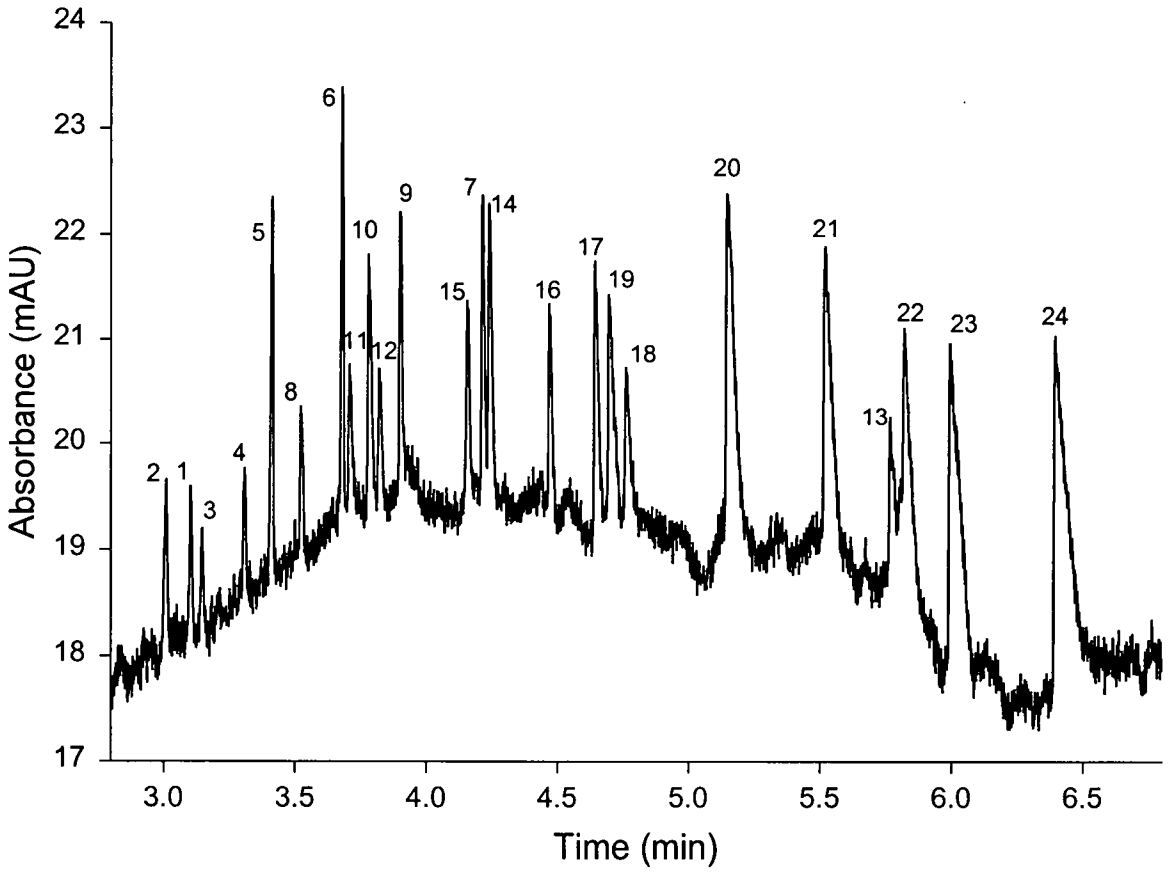

Figure 4.14: Optimised separation of 24 anions by IE-CEC using indirect UV detection with CrO_4^{2-} as the competing ion/probe. Conditions are 0.28% $PDDA^+$ and 16.25 mM CrO_4^{2-} buffered with 10 mM histidine (pH 7.70). Peaks are numbered according to their CZE migration order. Other conditions as Figure 4.10. Peaks are : 1 = Br^-, 2 = Cl^-, 3 = NO_2^-, 4 = NO_3^-, 5 = SO_4^{2-}, 6 = Oxalate, 7 = ClO_4^-, 8 = ClO_3^-, 9 = Malonate, 10 = Formate, 11 = F^-, 12 = BrO_3^-, 13 = Citrate, 14 = Succinate, 15 = Tartrate, 16 = Glutarate, 17 = Adipate, 18 = IO_3^-, 19 = Acetate, 20 = Propanoate, 21 = Butanoate, 22 = isovalerate, 23 = caproate, 24 = caprylate.

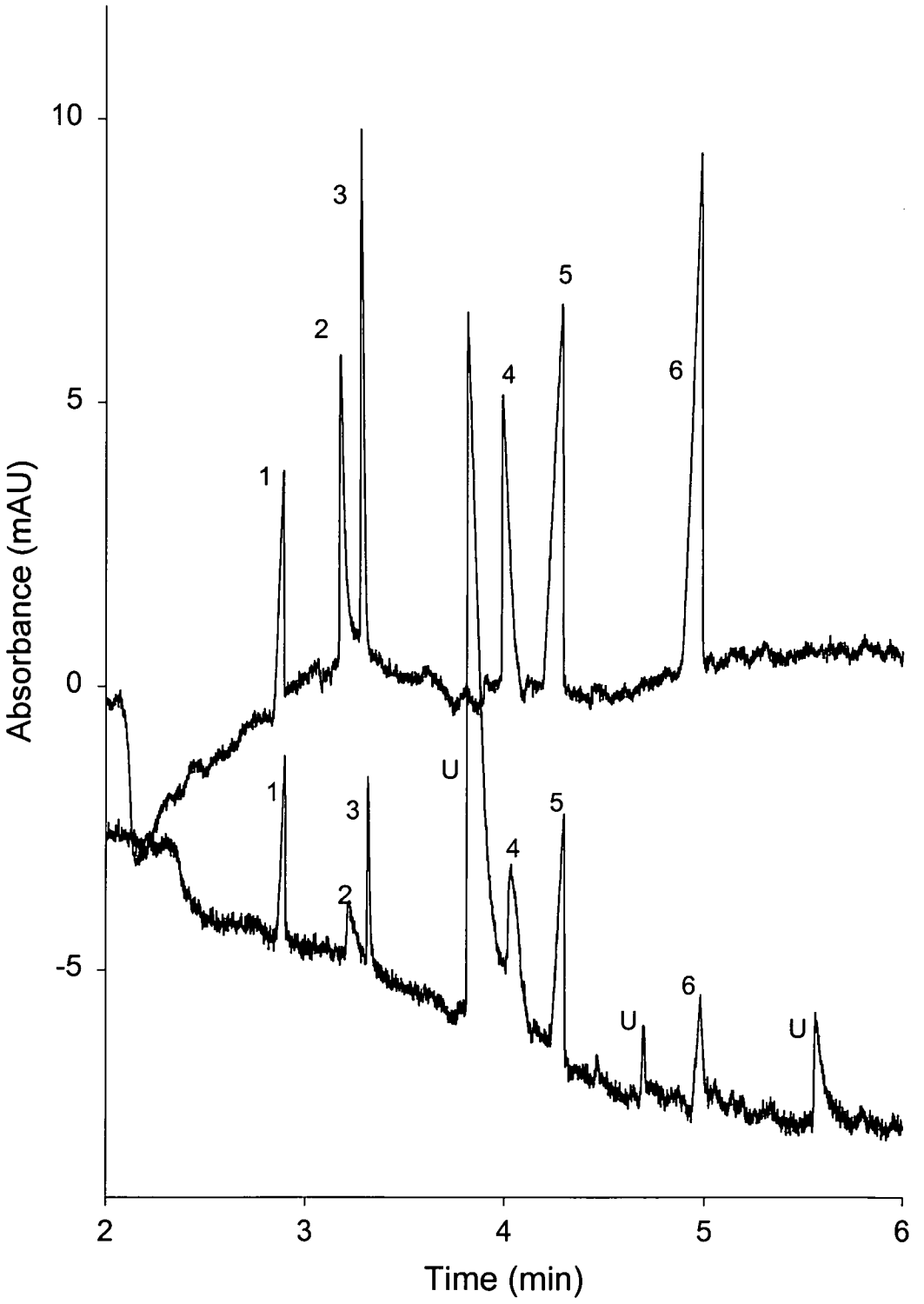

Figure 4.15: Separation of anions found in Bayer liquor. Top trace is a standard solution, while the bottom separation is a real sample. Electrolyte composition contains 0.55% $PDDA^+$ and 20 mM CrO_4^{2-}. Other conditions as in Figure 4.10. Peaks are 1= Cl^-, 2 = F^-, 3 = Formate, 4 = acetate, 5 = sulfate 6 = oxalate, and U = unknown.

unknown peak, possibly CO_3^{2-} occurred. Whilst this example illustrates the potential of IE-CEC to analyse complex samples, a further potential advantage is the possibility for identification of unknown peaks (such as that appearing in the real sample) which is enhanced by the fact that the separation selectivity can be changed substantially by varying the electrolyte conditions and comparison with known standards in different electrolytes would provide substantial supporting evidence for analyte identification.

4.6 Conclusions

The pseudo-phase IE-CEC system described was applicable to the separation of UV absorbing and UV transparent inorganic and organic anions in the same sample. Conditions such as polymer concentration, competing ion type and concentration could be altered either to increase or decrease the IE component of analyte migration. For UV transparent ions, conversion of the polymer to the probe form is required to remove the interference of a system peak created when unmodified polymer is added to the electrolyte. Although this modification restricts the concentration of both polymer and probe that can be employed, the ability to change the IE selectivity coefficient of the probe more than compensates for this limitation. A mathematical model was proposed, which adequately described the complex migration system and successfully predicted optimal conditions for a given separation using as few as five preliminary experiments. This allowed for rapid method development of the separation of a mixture of anions in complex samples and was demonstrated by optimising the separation of 16 UV absorbing and 24 UV transparent anions. Further potential of IE-CEC was demonstrated by separating target anions in Bayer liquor with a separation selectivity differing substantially from that attainable in conventional CE.

4.7 References

1. S. Terabe and T. Isemura, *Anal.Chem.*, 62 (1990) 650.

2. S. Terabe and T. Isemura, *J.Chromatogr.*, 515 (1990) 667.

3. C. Stathakis and R.M. Cassidy, *Anal.Chem.*, 66 (1994) 667.

4. C. Stathakis and R.M. Cassidy, *Can.J.Chem.*, 76 (1998) 194.

5. C. Stathakis and R.M. Cassidy, *J.Chromatogr.A*, 699 (1995) 353.

6. O.V. Krokhin, A.V. Adamov, H. Hoshino, O.A. Shpigun and T. Yotsuyanagi, *J.Chromatogr.A*, 850 (1999) 269.

7. O.V. Krokhin, H. Hoshino, O.A. Shpigun and T. Yotsuyanagi, *J.Chromatogr.A*, 772 (1997) 339.

8. O.V. Krokhin, H. Hoshino, O.A. Shpigun and T. Yotsuyanagi, *J.Chromatogr.A*, 895 (2000) 255.

9. O.V. Krokhin, H. Hoshino, O.A. Shpigun and T. Yotsuyanagi, *J.Chromatogr.A*, 776 (1997) 329.

10. O.V. Krokhin, O.V. Kuzina, H. Hoshino, O.A. Shpigun and T. Yotsuyanagi, *J.Chromatogr.A*, 890 (2000) 363.

11. J. Li, W. Ding and J.S. Fritz, *J.Chromatogr.A*, 879 (2000) 245.

12. S. Terabe, K. Otsuka and T. Ando, *Anal.Chem.*, 57 (1985) 834.

13. C. Quang, J.K. Strasters and M.G. Khaledi, *Anal.Chem.*, 66 (1994) 1646.

14. S. Terabe, K. Otsuka, K. Ichikawa, A. Tsuchiya and T. Ando, *Anal.Chem.*, 56 (1984) 111.

15. P.R. Haddad and P.E. Jackson, *Ion Chromatography. Principles and Applications*, Elsevier, Amsterdam, 1990.

16. R.F. Cross and J. Cao, *J.Chromatogr.A*, 786 (1997) 171.

17. W. Ding, M.J. Thornton and J.S. Fritz, *Electrophoresis.*, 19 (1998) 2133.

18. H.J. Issaq, I.Z. Atamna, G.M. Muschik and G.M. Janini, *Chromatographia.*, 32 (1991) 155.

19. P.A. Doble and P.R. Haddad, *J.Chromatogr.A*, 834 (1999) 189.

20. P.A. Doble and P.R. Haddad, *Anal.Chem.*, 71 (1999) 15.

Chapter 5

On-Capillary Ion-Exchange Preconcentration of Inorganic Anions using Open-Tubular Capillaries for Capillary Electrophoresis

5.1 Introduction

A major problem encountered in capillary electrophoresis (CE) is poor detection limits, particularly when UV absorbance detectors are used with narrow capillaries offering limited optical path lengths. While other methods of detection are available, such as electrochemical (conductivity, potentiometric and amperometric), fluorescence, and more recently mass spectrometry, the UV absorbance detector is still the most widely used [1].

An alternative to using a more sensitive detector is to increase the concentration of the analytes prior to separation. Several preconcentration methods for CE have been developed, the most common being sample stacking (achieved by keeping the ionic strength of the electrolyte at least 3 times higher than that of the sample), isotachophoretic preconcentration, large volume sample stacking and solid-phase extraction (SPE), all of which have been covered in several reviews [2-5]. In all the methods except SPE, the volume of sample injected by pressure is limited to the capillary volume. This limitation can be partly overcome by the use of electrokinetic injection, but this approach generally suffers from poor reproducibility and it discriminates on the basis of analyte mobility. The use of SPE avoids many of these problems while also providing a means with which the sample matrix can be removed.

Solid-phase extraction methods for CE are becoming more popular, particularly with the development of on-column preconcentrators created by packing small sections of capillaries [6]. However, most of the applications are still directed towards using RP packings and neutral analytes [4]. There are only a few reports of the use of IE based SPE for CE and for inorganic anions in particular, there are only two publications [7,8]. Both of these reports involve coupling a FIA system with the CE which complicates the instrumentation and makes automation more difficult.

The use of IE interactions to preconcentrate ionic analytes using an on-column method has not been reported. This chapter presents the use of a single capillary in which a short section has been coated with nanometre-sized cationic latex particles onto which anionic sample analytes are adsorbed. A new method for elution is introduced, namely the use of a transient eluotropic gradient, which is formed from a transient isotachophoretic boundary between two different electrolytes. The concept of using an eluotropic gradient arising from a transient isotachophoretic boundary for analyte elution is discussed and methods for changing the gradient and its influence om analyte elution are examined. A preconcentration method for the CE separation of fast UV absorbing anions based on the optimal conditions was developed and applied to the determination of trace anions in Antarctic ice cores.

5.2 Experimental

The general details are given in Chapter 2. Detailed conditions are included in each of the figure captions.

5.2.1 Electrolyte preparation

Electrolytes containing ClO_4^- were prepared by titration of Tris with $HClO_4$ to a pH of 8.05, while electrolytes containing F^- were prepared from the Na^+ salt.

5.2.2 Capillary coating procedure

Whole capillaries were coated using the procedure described in Chapter 3.

Partially coated capillaries were prepared by flushing with a dilute suspension of particles at 20 mbar for 100 s before being flushed with water at -50 mbar for a further 100 s. This process was repeated 3 times, with the capillary then being flushed with water for 10 min before conditioning with electrolyte. Partially coated particle/polymer columns were prepared by flushing the column with a 1% (w/v) solution of PDDAC after partial coating with the particles.

5.3 Illustration of concept

5.3.1 Principle of the method

Preconcentration using IE interactions to retain analytes is well established in ion chromatography [9] and involves passing a relatively large volume of sample through a small IE column (called the concentrator column) and then removing the adsorbed analytes using an eluent of sufficient eluotropic strength. Applying IE preconcentration techniques to CE is somewhat more challenging due to the small scale of instrumentation and also because column switching techniques are not commonly used. Whilst preconcentration can be performed off-line by adsorbing the analytes onto a suitable stationary phase, desorption of the analytes using a small volume of strong eluent followed by CE analysis is generally not viable because the strong eluent normally has a higher ionic strength than the electrolyte and causes destacking when the voltage is applied.

To overcome this difficulty, the use of an IE stationary phase attached to the capillary wall for preconcentration of the analytes is proposed, coupled with a new electroseparation concept, namely the use of an isotachophoretic gradient as a means of eluting the bound analytes from the stationary phase. In this method, a short section (approximately 8.5 cm) of the capillary was coated with 75 nm diameter

cationic IE particles (functionalised with quaternary ammonium groups) to form a preconcentration section, (Figure 5.1 (a)), with the remainder of the capillary being a conventional fused silica surface. Pressure-assisted injection of several capillary volumes of the sample results in the adsorption of anionic analytes onto the IE stationary phase and preconcentration of the sample (Figure 5.1 (b)). The capillary is then filled from the outlet end with an electrolyte containing an anion with a low IE selectivity coefficient for the stationary phase and also having a low electrophoretic mobility (called the weak electrolyte, WE) (Figure 5.1 (c)). In the next step, the electrolyte vials at each end of the capillary are filled with an electrolyte that contains a competing ion having a high IE selectivity coefficient and a high electrophoretic mobility (the strong electrolyte, SE). On applying the separation voltage some of the more mobile, stronger competing anions from the SE will migrate ahead of the less mobile, weaker competing anions from the WE, establishing a diffuse boundary of increasing eluotropic strength according to isotachophoretic principles (Figure 5.1 (d)). This boundary constitutes a compositional gradient in which the electrolyte changes progressively from WE to SE. Appropriate selection of analyte and electrolyte ions enables the analytes to be focused into an extremely sharp band prior to leaving the IE part of the capillary and then being subsequently separated in the uncoated separation section of the capillary according to normal electrophoretic principles (Figure 5.1 (e)).

The desirable characteristics of an on-capillary sample preconcentration method using a SPE approach are that the analyte ions from a large sample volume should be adsorbed onto the preconcentration stationary phase and then eluted by the gradient as a sharp band for subsequent separation and quantification. In this way, high preconcentration factors and good separation efficiencies can be obtained. In order for the band of analyte ions to become focused on the capillary wall (illustrated in Figure 5.1 (d)), the relative IE strength and mobility of the analyte, WE and SE anions must be selected accordingly. Using the terms K_A, K_{WE} and K_{SE} to denote the

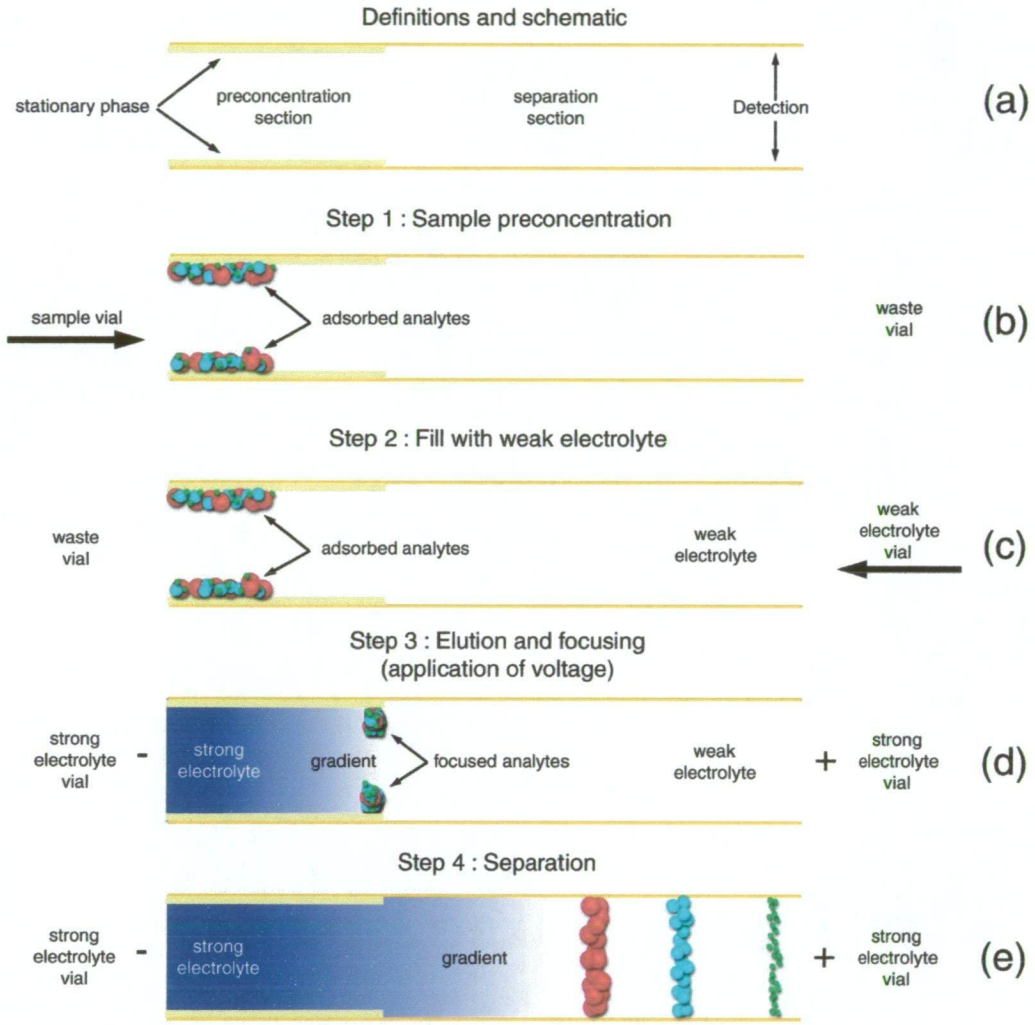

Figure 5.1: Schematic representation of preconcentration and separation procedures. (a) capillary schematic and definitions, (b) injection of the sample and analyte preconcentration, (c) the capillary is filled with weak electrolyte from the outlet end (in order to minimise the possibility of movement of the preconcentrated analytes, (d) application of voltage resulting in the generation of a gradient which focuses and elutes the analytes from the preconcentration section of the capillary, and (e) electrophoretic separation of the focused analytes in the separation section of the capillary.

IE selectivity coefficients for the analyte, weak competing anion, and strong competing anions, respectively, then $K_{WE} < K_A < K_{SE}$ must apply for the preconcentration and desorption processes to function correctly.

The relative mobilities of the analyte and the competing anions in WE and SE also affect preconcentration. There are three possible situations. In the first case ($\mu_A < \mu_{WE} < \mu_{SE}$), the analyte, after being eluted from the stationary phase, will migrate after the end of the isotachophoretic gradient in an electrolyte which contains only the strong IE competing anion. In the second case ($\mu_{WE} < \mu_A < \mu_{SE}$), the desorbed analyte will migrate with the isotachophoretic gradient. In the final case ($\mu_{WE} < \mu_{SE} < \mu_A$), the analyte migrates faster than the strong competing anion in the SE and will move ahead of the isotachophoretic gradient. This is the preferred situation for the proposed method.

The ideal conditions are $K_{WE} < K_A < K_{SE}$ and $\mu_{WE} < \mu_{SE} < \mu_A$. Under these conditions, the analyte will initially be adsorbed onto the particles of stationary phase which coat the capillary wall and will remain adsorbed when the capillary is filled with WE. When the voltage is applied, an isotachophoretic gradient will be established at the diffuse boundary between pure WE and pure SE. The start of this boundary will migrate through the capillary with a mobility equivalent to that of the strong competing anion plus the EOF, while the end of the boundary will migrate with a mobility equivalent to that of the weak competing anion plus the EOF. As the strong competing anion reaches the adsorbed analyte, immediate desorption of the analyte occurs and it then migrates according to its electrophoretic mobility, (which is higher than that of the strong competing anion). The analyte therefore migrates ahead of the gradient front, into a zone of electrolyte containing WE and in which the analyte has a higher interaction with the stationary phase than the competing anion. The analyte will therefore be re-adsorbed onto the wall, only to be again desorbed by the band of strong competing anion which follows. As the gradient boundary moves through the capillary, the band of analyte therefore becomes focused due to its

different migration rates in the two zones and moves with the gradient boundary as illustrated by I^- in Figure 5.2 which shows only the preconcentration part of the capillary containing the adsorbed stationary phase. If the mobility of the analyte is less than that of the SE (illustrated by SCN^-), or the elution strength of the SE is not high enough to completely desorb the analyte (illustrated by CrO_4^{2-}), then analyte focusing will not occur according to the principles outlined above. It should be noted that in Figure 5.2, $\mu_{SE} > \mu_{WE}$ resulting in ions from the SE migrating into the WE zone establishing a compositional gradient in which the electrolyte composition changes from WE to SE in a continuous manner.

An additional factor influencing analyte focusing is the concentration of WE used. This will restrict the concentration of the strong competing anion in the SE as a result of the Kohlrausch regulating function. The capillary will initially be filled with a particular concentration of the weak competing anion, and because of the Kohlrausch regulating function, the concentration of the strong competing anion that migrates into the capillary from the electrolyte vial will be of a similar concentration (assuming both competing ions have similar conductances). For example if 1 mM Cl^- is used in WE, then approximately 1 mM of a stronger competing anion (such as ClO_4^-) will initially migrate into the capillary. While the situation is more complex than this (and is discussed fully in section 5.4), this approach is suitable for illustrative purposes.

5.3.2 Preconcentration of iodide

To demonstrate the elution method, a capillary was completely coated with AS5A particles as described in section 5.2.2. Separations were performed with six inorganic anions to determine the appropriate type and concentration of competing anions that should be used in the WE and SE, keeping in mind the ideal conditions outlined above. Using 10 mM F^- (as WE) and 10 mM ClO_4^- (as SE) a sample comprising 0.1 μM I^-, and 0.5 μM SCN^- and CrO_4^{2-} was preconcentrated (injection at

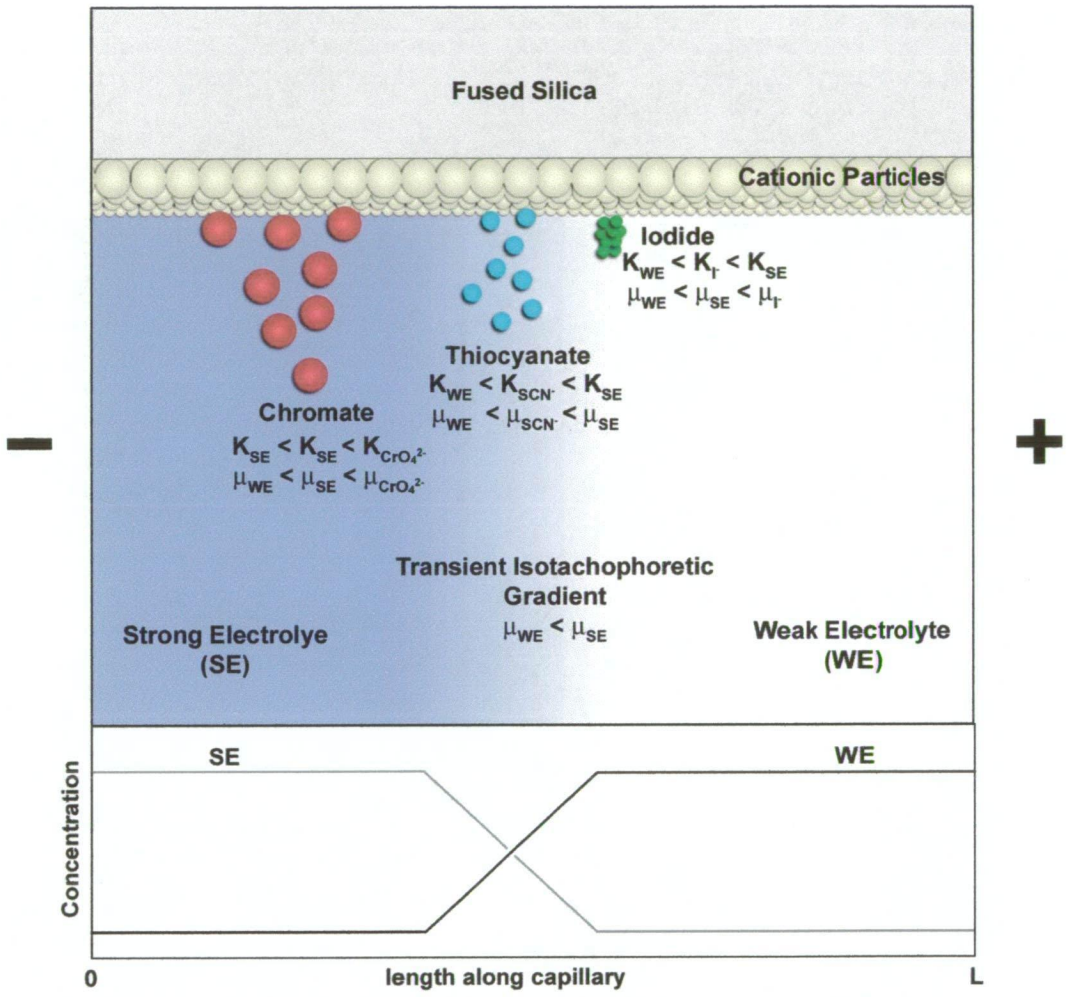

Figure 5.2: Schematic representation of the focusing mechanism using an IE-OT-CEC column and a transient-isotachophoretic gradient, illustrated by I^-. SCN^- is not focused because its electrophoretic mobility is lower than that of the SE, while CrO_4^{2-} is not focused because the eluotropic strength of the SE is too low.

50 mbar for 500 s) and the voltage applied, with the results being shown in Figure 5.3. Iodide was eluted as a very sharp peak at the gradient boundary (in accordance with the mechanism described above), whilst SCN^- and CrO_4^{2-} were eluted somewhat later as broader peaks. SCN^- has a mobility less than that of ClO_4^- and has only weak interactions with the stationary phase in the presence of ClO_4^-. These analytes therefore migrate behind the gradient boundary. The broadening of the CrO_4^{2-} peak evident in Figure 5.3 is the result of residual interactions with the stationary phase which occur during migration of these species along the column by an OT-IE-CEC mechanism due to insufficient elution strength of the SE to prevent interaction with the stationary phase.

Under the injection conditions used, approximately 4350 nL, or two capillary volumes of sample were introduced. This gave an increase in injected sample volume of 174 when compared to a standard injection volume of 25 nL (using 10 mbar for 10 sec). However, where the focusing effect reduced peak width, the effective enhancement of detection sensitivity was much higher. For example, the detection limit for I^- in this system shown in Figure 5.3 was 2.2 nM (using a signal to noise ratio of 3), compared to 5.29 μM for a conventional injection using 10 mbar for 10 s. The detection limit for I^- was therefore reduced by a factor of 2400 as a result of the combined effects of the preconcentration step and the analyte focusing. Detection limits for SCN^- and CrO_4^{2-} were 15 and 116 nM, respectively, which corresponded to a reduction of 353 and 50 compared to conventional injection. The improvements in detection limits for these analytes were less than that for I^- because the peaks were not focussed to the same extent as I^-. In the case of CrO_4^{2-}, it can be noted that the reduction in detection limit (50) was actually less than the factor by which the injection volume was increased (174). The reason for this is that the peak for CrO_4^{2-} was broader in the coated capillary than in an uncoated capillary and this caused some loss of detection sensitivity.

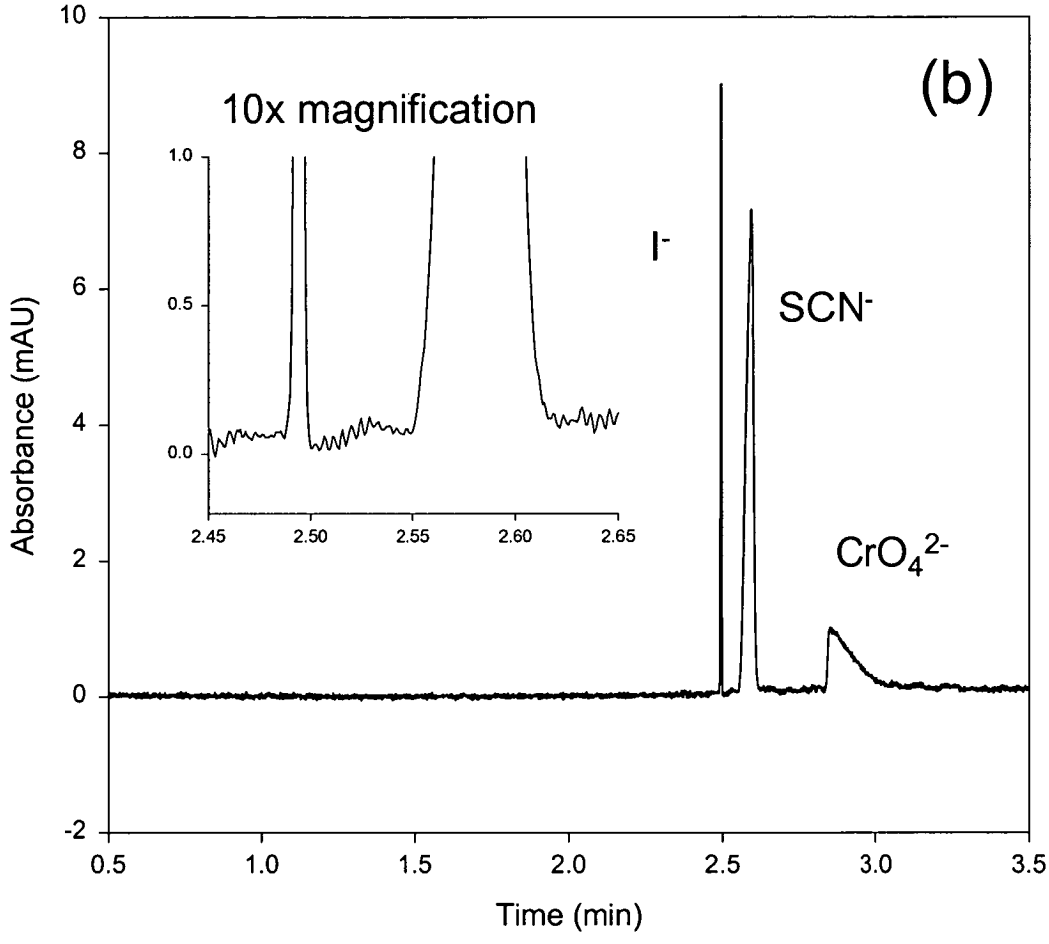

Figure 5.3: Preconcentration and isotachophoretic elution of inorganic anions. Isotachophoretic gradient established using 10 mM F^- and 10 mM ClO_4^-. Sample 0.1 μM I^-, and 0.5 μM SCN^- and CrO_4^{2-} in 10 mM NaF. Injection was at 50 mbar for 500 s. Capillary length was 50.0 cm (41.5 cm to detector) x 75 μm i.d. The applied voltage was -25 kV, with detection at 214 nm.

The performance of the preconcentration step was assessed by calculating recovery values for the loaded analytes. This was done by comparing peak areas obtained for the analytes from a preconcentrated sample (50 mbar and 500 s injection of a 0.5 μM standard solution) and from a direct injection of the same total amount of the analytes (10 mbar and 10 s injection of a 0.5 mM standard solution). Recoveries were calculated to be 97%, 98% and 94% for I^-, SCN^- and CrO_4^{2-} respectively

While this method shows promise for preconcentration and then separation, it should be noted that all analytes which meet the conditions $K_{WE} < K_A < K_{SE}$ and $\mu_{WE} < \mu_{SE} < \mu_A$ will be swept by the gradient front and will migrate together. However, the limitations imposed by the above conditions will restrict these interferences and in the case discussed here, we could not identify any such interferences in the preconcentration and determination of I^- (assuming that the sample has a low ionic strength). The proposed preconcentration method is therefore highly selective for I^-, but due to the slow data acquisition rate of the instrument used in this study (20 Hz) the analytical potential of this method for the determination of I^- could not be examined due to unreliable integration (illustrated in Figure 5.4).

5.3.3 Preconcentration and separation of bromide and nitrate

The preconcentration and focusing of I^- into a sharp peak shows potential as a method to introduce numerous analytes, all compressed in a sharp band, into a separation capillary so they can then be separated. This was examined using Br^- and NO_3^-, which have very similar IE selectivity coefficients on the AS5A stationary phase [9] and mobilities higher than that of ClO_4^-, making them suitable for the peak compression effects observed for I^-. A concentration of 1 mM F^- allowed suitable retention of these analytes in the preconcentration step, while 1 mM ClO_4^- was suitable for their elution from the stationary phase. A 70.0 cm capillary was prepared as described in the section 5.2.2, but only a short section of capillary (~10 cm) at the injection end was coated with stationary phase and the remainder of the capillary was

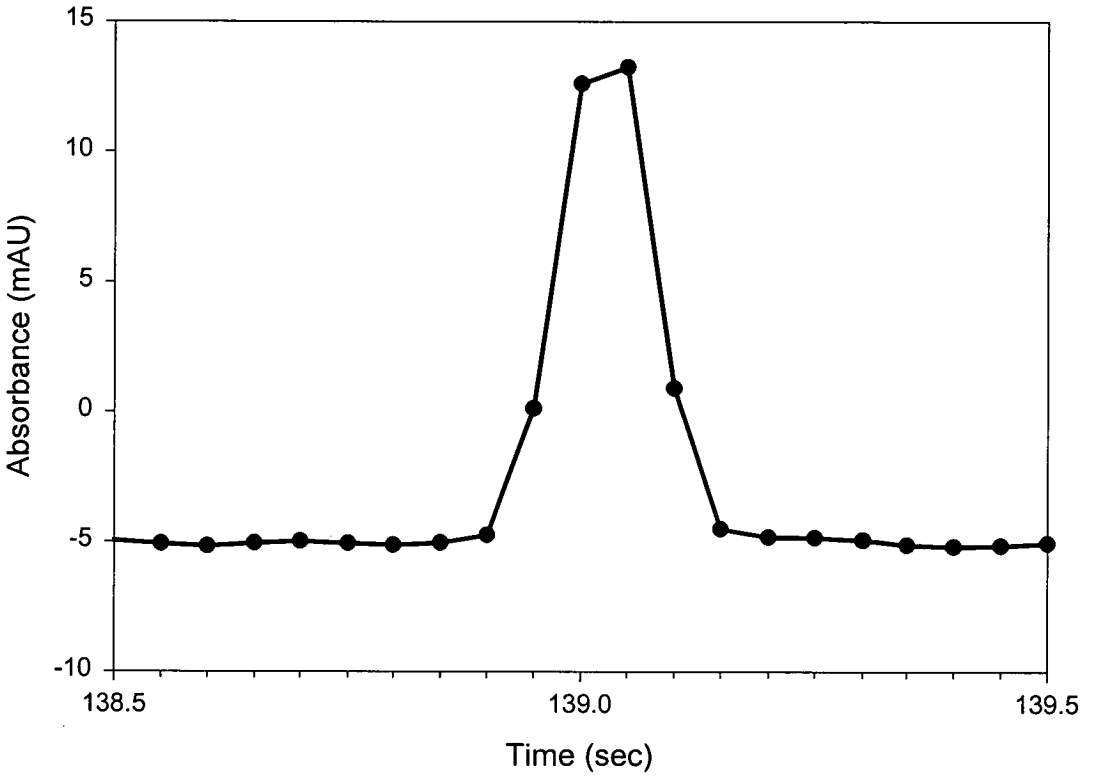

Figure 5.4: Focused peak of I^- illustrating the high efficiency of the focusing mechanism. Data acquisition rate is 20 Hz indicating that the baseline peak width is 8 points, or 0.4 seconds.

bare silica. The resultant capillary effectively acted as two separate capillaries, the first containing the stationary phase where the analytes are concentrated, with the second being a bare fused silica capillary where analytes are separated according to conventional CE principles. Cetyltrimethylammonium chloride (CTAC) was added (0.01 mM) [2] to both WE and SE to ensure that the EOF was in the same direction in both the coated and uncoated parts of the capillary.

Figure 5.5 shows the preconcentration and separation of 1 μM Br^- and NO_3^- after a 50 mbar, 50 s injection. In Figure 5.5(a) the detection window was placed immediately after the coated portion of the capillary so that analytes being eluted from the stationary phase could be monitored. This shows that Br^- and NO_3^- were co-eluted as a single sharp peak, with a peak width of 0.48 s, and that both of these analytes were desorbed by the gradient front. In Figure 5.5 (b) the detection window was in its usual position near the outlet of the capillary and this figure shows that the analytes had been separated after migrating through the uncoated portion of the capillary. Peak widths for the two peaks were 1.03 and 0.84 s giving efficiencies of 138,000 and 236,000 theoretical plates for Br^- and NO_3^-, respectively, with the difference in efficiency exhibited between the two analytes possibly being due to greater electromigration dispersion from the mobility mismatch between F^- and Br^-. Detection limits for Br^- and NO_3^- were 0.86 and 0.32 μM, respectively, corresponding to a reduction in detection limit by factors of 11.7 and 15.6 respectively compared to conventional injection. The longer injection time of 50 mbar for 50 s introduced 311 nL of sample compared to the conventional 25 nL with a 10 mbar 10 s injection, which gave an increase in injection volume of 12.3. Detection limits were reduced by a similar factor indicating that there was no significant loss of efficiency by this elution method from the preconcentration column.

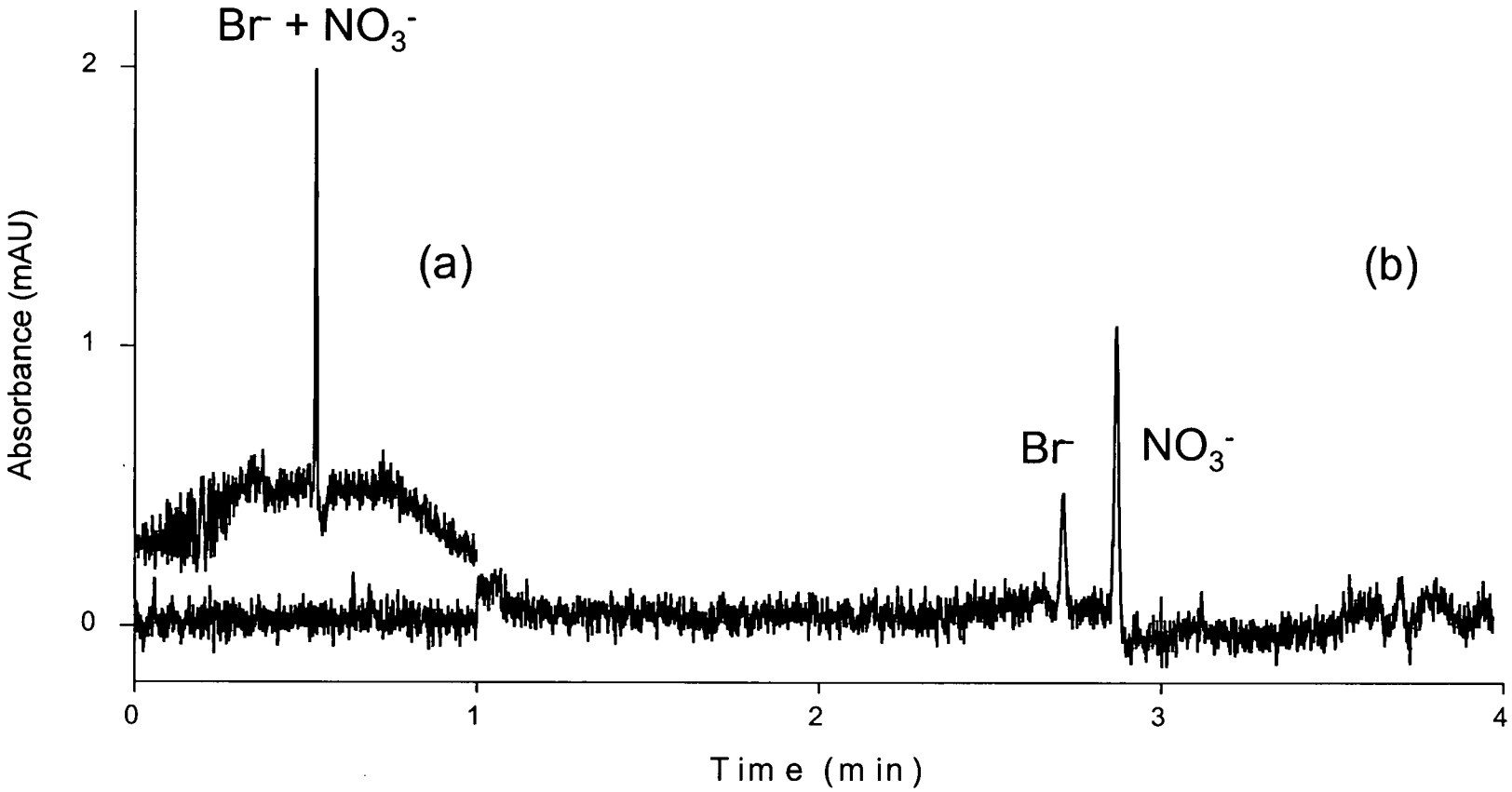

Figure 5.5: (a) Elution of Br^- and NO_3^- from the coated section of the capillary. Isotachophoretic gradient established using 1 mM F^- and 1 mM ClO_4^-. Sample was 1 μM of Br^- and NO_3^- in 1 mM NaF. Injection was at 50 mbar for 50 s. Voltage -25 kV with detection at 195 nm. Capillary was 70.0 cm in length, with the first 10 cm coated with anion-exchange latex. Other conditions as in Figure 5.3. (b) Separation of Br^- and NO_3^- after the preconcentration shown in (a). Conditions as for (a).

5.4 Characterisation of the isotachophoretic gradient

While the potential to use an isotachophoretic boundary as an eluotropic gradient has been demonstrated, the use of perchlorate as a SE anion severely limits the practical application of this technique. These limitations arise mainly from the chromatographic and electrophoretic properties of perchlorate, namely its high mobility (thus SCN^- cannot be focused) and moderate IE strength (thus CrO_4^{2-} cannot be focused). Since each SE anion is unique, changing the SE anion will result in the formation of a different gradient. Because the nature of the gradient is fundamental to analyte focusing, an understanding of how the gradient is generated and its influence on focusing is needed. Once understood, the method can be extended to as wide a range of analytes as possible.

5.4.1 Gradient generation and characterisation

Generation of the elution gradient is accomplished by the use of a transient-isotachophoretic process, and therefore the gradient will differ when different combinations of WE and SE are used. In order to compare different gradients, it is necessary to characterise them using a suitable parameter and the variation in gradient eluotropic strength with electrolyte composition was selected for this purpose.

In illustrating the potential of a transient isotachophoretic gradient to function as an eluotropic gradient, it should be noted that when $\mu_{SE} > \mu_{WE}$, ions from the SE migrating into the WE zone establish a compositional gradient in which the electrolyte composition changes from WE to SE in a continuous manner. Alternatively, when $\mu_{WE} > \mu_{SE}$, a stepwise compositional gradient is created. Assessment of the potential of these two types of gradients for analyte focusing requires consideration of a number of factors. Whilst the use of a stepwise gradient should be ideal for focusing all analytes into a sharp band prior to electrophoretic

separation, the continuous gradient offers the possibility of separation of some analytes during the focusing process. This could be important for analytes having similar mobilities which would be difficult to separate by electrophoretic means if they entered the separation section of the capillary as a single, focused analyte band. In view of the wider possibilities offered by continuous gradients, the discussion in the present work will be confined to the situation where $\mu_{SE} > \mu_{WE}$. A further reason for this decision is that the alternative case ($\mu_{SE} < \mu_{WE}$) has been difficult to implement practically because of a lack of competing anions having appropriate electrophoretic mobilities and IE selectivity coefficients.

5.4.1.1 Eluotropic strength

The eluotropic strength of a particular eluent, and hence the nature of any gradient formed from this eluent, will be a function of the concentration of the eluent competing ion and the affinity of the eluent competing ion with the stationary phase. The eluotropic strength of an eluent E, denoted as S_E, will increase with the charge (y), concentration ([E]) and selectivity coefficient towards a particular univalent analyte, A, ($K_{E,A}$) and can be defined by the following equation [9]:

$$S_E = K_{E,A}[E]^y \qquad (5\text{–}1)$$

Estimates for S_E can therefore be obtained if $K_{E,A}$ and the concentration and charge of SE are known. These parameters are discussed below.

The concentration of SE that migrates into the capillary is given by the Kohlrausch regulating function and is dependent on the electrolyte that fills the capillary when the voltage is first applied [10]. The equilibrium concentration of SE migrating into the capillary is therefore given by:

$$[SE] = \frac{Z_{WE}}{Z_{SE}} \cdot \frac{|\mu_{SE}|}{|\mu_{SE}| + \mu_{cat}} \cdot \frac{|\mu_{WE}| + \mu_{cat}}{|\mu_{WE}|} \cdot [WE] \qquad (5\text{–}2)$$

where Z_{WE} is the charge of the WE anion, Z_{SE} is the charge of the SE anion, and *cat* denotes the counter-cation, assuming this is the same for both WE and SE. It is therefore possible to calculate the [SE] which would result for a particular type of SE competing ion if the composition of WE is known.

Values for $K_{E,A}$ can be obtained by measurement of the IE behaviour of the desired ions on a chromatographic system using the same stationary phase as that employed in the IE-OT-CEC system. The latex particles used to coat the capillary are the same as those used in the latex-agglomerated stationary phase in a Dionex AS5A column. Retention data for potential eluent ions were obtained using a 50 mM carbonate eluent (pH 10.0) for the weakly retained anions, and a 50 mM sodium perchlorate eluent at pH 10.0 (prepared by titration of perchloric acid with sodium hydroxide) for the more strongly retained anions. The selectivity coefficient $K_{E,A}$ for a range of anions to be used as potential eluents (and hence designated as E) can be estimated from these data using a reference analyte and non-linear regression from the following equation [9]:

$$\log \alpha_{E,F} = \frac{1}{1} \log K_{E,F} + \frac{x-1}{1} \log \left(\frac{k'_F . V_m}{w} \right) \qquad (5\text{–}3)$$

where E is the anion, and F is the reference analyte, V_m is the volume of the mobile phase, w is the weight of the stationary phase and x is the eluent anion charge. Values for the selectivity coefficient of E using fluoride as the reference ($K_{E,F}$) can be determined from equation (5–3) and are shown in Table 5.1. These values were calculated using retention factors measured in the carbonate eluent. Since the retention times of some of the more strongly retained analytes could be determined only in the perchlorate eluent, it was necessary to estimate values for their retention factor in the carbonate system. This was done by comparing how the retention factors of selected anions (I^-, 2-sulfobenzoic acid, CrO_4^{2-}, $S_2O_3^{2-}$, citrate, 1,2-benzenedisulfonic acid and sulfosalicylic acid) were related in both the carbonate and

Table 5.1: Electrophoretic mobilities, retention factors (k') and IE selectivity coefficients (relative to fluoride) for selected anions.

Anion	μ_{ep} 10^{-9} m^2/Vs	k' CO_3^{2-}/HCO_3^-	k' ClO_4^-	$K_{E,F}$
Fluoride	-58.12	0.05	-	1.00
Lactate	-37.79	0.06	-	1.00
Acetate	-44.96	0.06	-	1.40
Glycolate	-42.87	0.07	-	1.60
Propionate	-39.82	0.09	-	2.00
n-Butanoate	-35.28	0.11	-	2.40
Iodate	-42.64	0.12	-	2.60
Formate	-60.02	0.13	-	2.80
i-pentanoate	-32.63	0.16	-	3.40
HEPES	-21.52	0.17	-	3.60
Ethanesulfonate	-43.90	0.17	-	3.60
Methanesulfonate	-51.27	0.17	-	3.60
MOPS	-26.24	0.21	-	4.60
MES	-27.99	0.21	-	4.60
HIBA	-33.00	0.21	-	4.60
Propanesulfonate	-39.40	0.25	-	5.40
Sulfamate	-42.17	0.26	-	5.60
Picolinate	-33.00	0.38	-	8.20
Hexanoate	-31.58	0.39	-	8.40
Butanesulfonate	-36.41	0.39	-	8.60
Ascorbate	-26.83	0.45	-	9.80
CHES	-6.98	0.51	-	11.2
octanoate	-27.37	0.52	-	11.4
Camphorsulfonate	-25.08	0.57	-	12.4
Bromate	-61.00	0.69	-	15.0
4-aminophenylacetate	-30.75	0.70	-	15.2
Pentanesulfonate	-33.75	0.72	-	15.6
Nicotinate	-33.79	0.72	-	15.8

Table 5.1: Electrophoretic mobilities, retention factors (k') and IE selectivity coefficients (relative to fluoride) for selected anions. (ctd)

Anion	μ_{ep} 10^{-9} m^2/Vs	k' CO_3^{2-}/HCO_3^-	k' ClO_4^-	$K_{E,F}$
Isonicotinate	-34.37	0.83	-	18.2
Chloride	-76.27	0.84	-	18.4
Sorbate	-31.62	1.02	-	22.2
Nitrite	-75.34	1.27	-	27.6
Hexanesulfonate	-30.82	1.39	-	30.4
Cyanate	-47.86	1.45	-	31.6
Glutarate	-53.09	1.99	-	43.4
Benzoate	-29.57	2.09	-	45.6
Adipate	-50.03	2.14	-	41.9
Succinate	-57.03	2.17	-	42.6
Heptanesulfonate	-25.21	2.68	-	58.4
Malonate	-62.84	2.73	-	53.6
2-aminobenzoate	-28.75	3.13	-	68.2
Bromide	-77.42	3.50	-	76.4
4-aminobenzenesulfonate	-33.12	3.79	-	82.6
Chlorate	-67.33	3.83	-	83.6
Nitrate	-73.11	3.93	-	85.6
Tartrate	-59.44	3.99	-	78.3
Phosphate	-56.74	4.02	-	78.8
Benzenesulfonate	-33.02	4.27	-	93.0
Oxalate	-7.05	5.20	-	102
Octanesulfonate	-13.82	5.44	-	118
Sulfate	-76.79	6.26	-	123
4-toluenesulfonate	-28.62	7.20	-	157
Fumarate	-60.91	8.18	-	160
EDTA	-52.44	13.95	-	246
Phthalate	-51.61	17.86	-	350
Molybdate	-72.83	18.28	0.56	358
Iminodiacetate	-29.90	18.85	-	369

Table 5.1: Electrophoretic mobilities, retention factors (k') and IE selectivity coefficients (relative to fluoride) for selected anions. (ctd)

Anion	μ_{ep} 10^{-9} m^2/Vs	k' CO_3^{2-}/HCO_3^-	k' ClO_4^-	$K_{E,F}$
DTPA	-57.20	27.61	-	487
Salicylate	-28.57	29.94	-	587
Iodide	-75.43	32.64	0.40	711
4-hydroxybenzoate	-31.79	39.47	-	774
Dipicolinate	-51.70	41.44	0.82	812
2-sulfobenzoate	-48.14	43.21	1.17	847
Chromate	-72.23*	43.73	1.25	857
Thiosulfate	-76.86	46.03	1.08	903
Thiocyanate	-62.99	58.19	-	1270
Citrate	-64.69	77.28	1.43	1360
Perchlorate	-63.66	108.0	-	2350
2,3-dihydroxybenzoate	-27.14	157**	1.95	2780
1,2-benzenedisulfonate	-47.62	157.7	1.94	3090
Sulfosalicylate	-27.53	439.2	4.06	7750
5-sulfoisophthalate	-33.77	791**	12.61	14000
1,5-napthalenedisulfonate	-57.38	860**	13.70	16900
Benzenetetracarboxylate	-68.13	6387**	101.8	104000
NapthaleneTrisulfonate	-73.48	7592**	121.0	136000
Indigo carmine	-43.04	13768**	219.5	237000

HEPES = 4-(2-hydroxyethyl)-1-piperazineethane sulfonic acid; MOPS = 3-morpholino propanesulfonic acid; MES= 2-morpholino ethanesulfonic acid; HIBA=2-hydroxyisobutyric acid; CHES = 2-(cyclohexylamino)ethanesulfonic acid; EDTA ethylenediamine tetraaectic acid; DTPA = Diethelenetriamine pentaacetic acid.

* mobility measured in 5 mM sulfate/10 mM DEA electrolyte.

** retention factors in carbonate estimated from scaling the values obtained in perchlorate. Scaling factor determined by the retention factors of anions separated in both eluents.

perchlorate systems and applying the same relationship to retention factors for those anions separated in only the perchlorate system. The effective charge of the eluent ion was calculated at the operating pH of 10.0 using tabulated dissociation constants [11].

The difference in eluotropic strength between SE and WE, denoted S_G (i.e. the eluotropic range of the gradient) can be defined according to the following equation :

$$S_G = S_{SE} - S_{WE} \qquad (5\text{–}4)$$

Combination of equations (5–1), (5–2) and (5–4) shows that S_G for a particular SE/WE combination will be dependent on (i) the concentration of WE, (ii) the mobility of WE, (iii) the mobility of SE, (iv) the mobility of the counter-cation, and (v) the relative charges of WE and SE.

5.4.1.2 Gradient profile

Because the elution gradient is formed from a transient isotachophoretic boundary, its shape can be predicted from isotachophoretic theory. Detailed descriptions and derivations of mathematical equations describing the process have been published by Foret *et al.* [10] and only final equations will be repeated here. It should be noted that for simplification, only electrolytes containing monovalent anions are considered and only for the case when $\mu_{SE} > \mu_{WE}$.

The position of the mixed zone of WE/SE along the column at time t, can be determined from x_{WE} (the position of the pure WE zone, where x is a distance measured from the capillary inlet) and x_{SE} (the position of the pure SE zone), which are given by [10]

$$x_{WE} = \bar{x}_{WE}.t \qquad (5\text{–}5)$$

$$x_{SE} = \bar{x}_{SE}.t \qquad (5\text{–}6)$$

where $\bar{x}_{WE}$ and $\bar{x}_{SE}$ are the linear velocities of the WE and SE zones, respectively, and are given by [10]:

$$\bar{x}_{SE} = \frac{\mu_{SE} I}{SF(\mu_{WE} + |\mu_{cat}|)[WE]_{WE}} \tag{5–7}$$

$$\bar{x}_{WE} = \frac{\mu_{WE}^2}{SF\mu_{SE}(\mu_{WE} + |\mu_{cat}|)[WE]_{WE}} = \frac{\mu_{WE}^2}{\mu_{SE}^2}\bar{x}_{SE} \tag{5–8}$$

where S is the cross sectional area of the capillary, F the Faraday constant, I the cross-sectional current, and $[WE]_{WE}$ is the concentration of WE in the zone containing only WE.

The concentration of SE in the zone $[WE]_{WE}$, given by $x < x_{WE}$, is equal to 0 by definition. The concentration of SE in the zone $[SE]_{SE}$, given by $x_{SE} < x$, is given by Equation (5–2), where SE and WE are both monovalent. The concentration of SE in the mixed zone of WE and SE, denoted by $[SE]_{SE/WE}$, where $x_{WE} < x < x_{SE}$, is given by [10]

$$[SE]_{SE/WE} = [WE]_{WE} \cdot \frac{\mu_{SE}}{\mu_{SE} - \mu_{WE}} \cdot \frac{\mu_{WE} + |\mu_{cat}|}{\mu_{SE} + |\mu_{cat}|} \cdot \left(\frac{1}{F\mu_{WE} Z(x,t)} - 1 \right) \tag{5–9}$$

Where $Z(x,t)$ is defined as:

$$Z(x,t) = \sqrt{\frac{S[WE]_{WE}(\mu_{WE} + |\mu_{cat}|)(x-1)}{F\mu_{SE}\mu_{WE}^2 It}}, \tag{5–10}$$

at any given time t for all $x_{WE} < x < x_{SE}$.

These equations reveal that the position of the gradient will be governed primarily by the relative mobilities of the WE and SE anions. By using defined vales of electrophoretic mobilities of the ions (from Table 5.1), and a value of -30×10^{-9} m^2/VS for the electroosmotic flow (EOF), it is possible to construct a theoretical gradient profile representing how the electrolyte composition changes from WE to SE with time at a defined position along the column. This enables a

direct comparison with experimental gradients if the change in gradient composition at the detection window can be measured.

Different gradients can be compared on the basis of their *slope*, which can be defined as the change in eluotropic strength, S_G divided by the time required for that change, Δt, given by

$$slope = \frac{S_G}{\Delta t} = \frac{S_{SE} - S_{WE}}{t_{SE} - t_{WE}}. \qquad (5\text{–}11)$$

5.4.2 Influence of WE concentration

The concentration of WE will govern the concentration and hence eluotropic strength of SE according to equation (5–2). Figure 5.6 (a) illustrates the theoretical influence of increasing the concentration of a F^- WE on the eluotropic strength of a ClO_4^- SE. It can be seen that as the concentration of WE increases, the eluotropic strength of the ClO_4^- SE increases, while the time over which the gradient is generated should remain unchanged. It should be noted that theoretical gradients were predicted ignoring the influence of ionic strength, which will affect both electrophoretic mobilities and EOF. Figure 5.6 (b) shows the influence of these same F^- WE concentrations on the actual focusing and separations obtained for a series of inorganic anions as analytes using a capillary that had been coated with IE particles along its entire length up to the detection window. It can be seen that at 5 mM F^-, the Br^- and NO_3^- peaks were focused, but I^- and SCN^- were eluted later as broad peaks. As the concentration of WE was increased, the I^- peak moved closer to the focused peak of Br^- and NO_3^-, until above 20 mM it co-migrated with Br^- and NO_3^- due to the increase in eluotropic strength of the resultant ClO_4^- SE evident from Figure 5.6 (a). This same effect is also illustrated by the elution of SCN^- closer to the focused peak when higher concentrations of F^- were used. Increasing the WE concentration did not change the migration time of the SCN^- peak significantly due to the mobility of SCN^- being lower than that of ClO_4^- and hence an inability for a focused peak to be

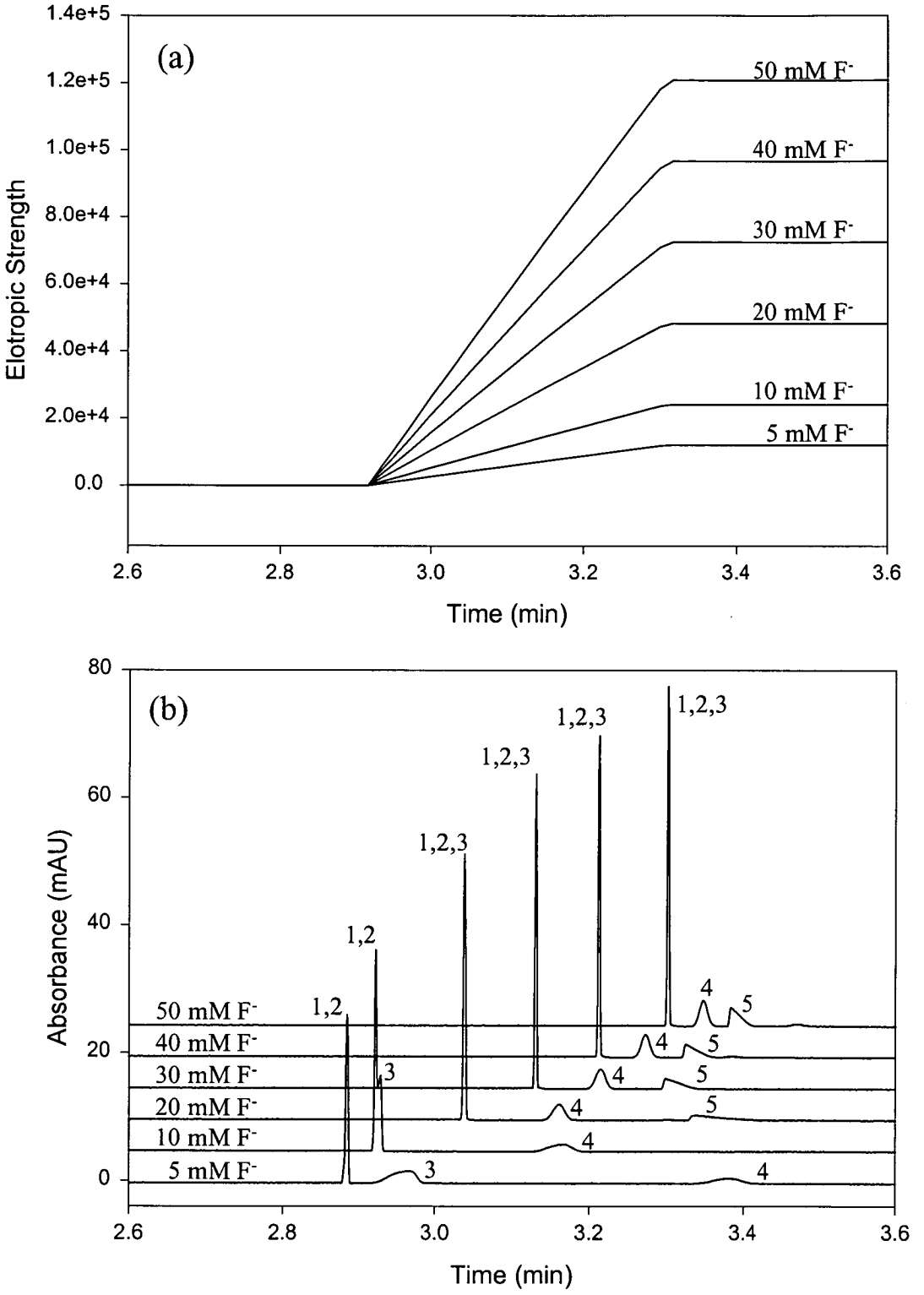

Figure 5.6: (a) Theoretical prediction of the influence of the concentration of the WE competing anion (in this case, F^-) on the eluotropic strength of a ClO_4^- SE entering the capillary. SE: 50 mM ClO_4^-/100 mM Tris, pH 8.05. (b) : Influence of varying the concentration of the WE (NaF) on the preconcentration and elution of inorganic anions. SE: 50 mM ClO_4^-/100 mM Tris, pH 8.05, Voltage = -30 kV, injection was for 4 min of 0.5 μM each anion prepared in WE. Peaks are 1 = Br^-, 2 = NO_3^-, 3 = I^-, 4 = SCN^- and 5 = CrO_4^{2-}.

attained. The peak for CrO_4^{2-} first appeared at 20 mM F^-, and increasing the WE concentration resulted in a decrease in retention. However, even at 50 mM F^-, the concentration of SE entering the capillary was insufficient to completely suppress interaction of CrO_4^{2-} with the stationary phase, leading to a distorted peak. Whilst it would be possible to increase the concentration of F^- so that the resultant concentration of SE would eventually be sufficient to prevent interactions of CrO_4^{2-} with the stationary phase, the concentration of F^- necessary in the WE would cause elution of weakly retained ions (such as Br^- and NO_3^-) when the capillary was first filled with WE prior to application of the voltage (Step 2 shown in Figure 5.1(c)). A further disadvantage is that the increase in ionic strength results in a lower EOF which results in a slower separation, evident in Figure 5.6 (b) as the increasing migration time of the focused peak. An alternative to increasing the concentration of the WE as a means to increase the eluotropic strength of the SE is to use a competing ion in the SE that has a higher selectivity coefficient than ClO_4^-.

Figure 5.7 shows the increase in eluotropic strength which is observed as the concentration of a F^- WE is increased for some of the potential SE anions shown in Table 5.1. It is apparent that the eluotropic strength of a particular SE is strongly dependent on the concentration of F^- in the WE, especially for multivalent eluent ions. This can be seen by comparing adipate and I^-, where the eluotropic strength of adipate increases more rapidly than I^- as the concentration of WE is increased. Thus a SE of higher eluotropic strength will be produced using I^- (rather than adipate) as the SE competing anion if the concentration of F^- in the WE is low, but the reverse is true when high concentrations (>50 mM) of WE are used. In terms of finding a SE competing anion capable of focusing a strongly bound analyte such as CrO_4^{2-}, a high eluotropic strength is required and naphthalenedisulfonate (NDS) is a good candidate. A WE of 10 mM F^- produces a SE containing 4.96 mM NDS, giving an eluotropic strength of 1.7×10^6 (compared to an eluotropic strength of 4.9×10^5 for a SE containing 10.4 mM ClO_4^- which would be formed under identical WE

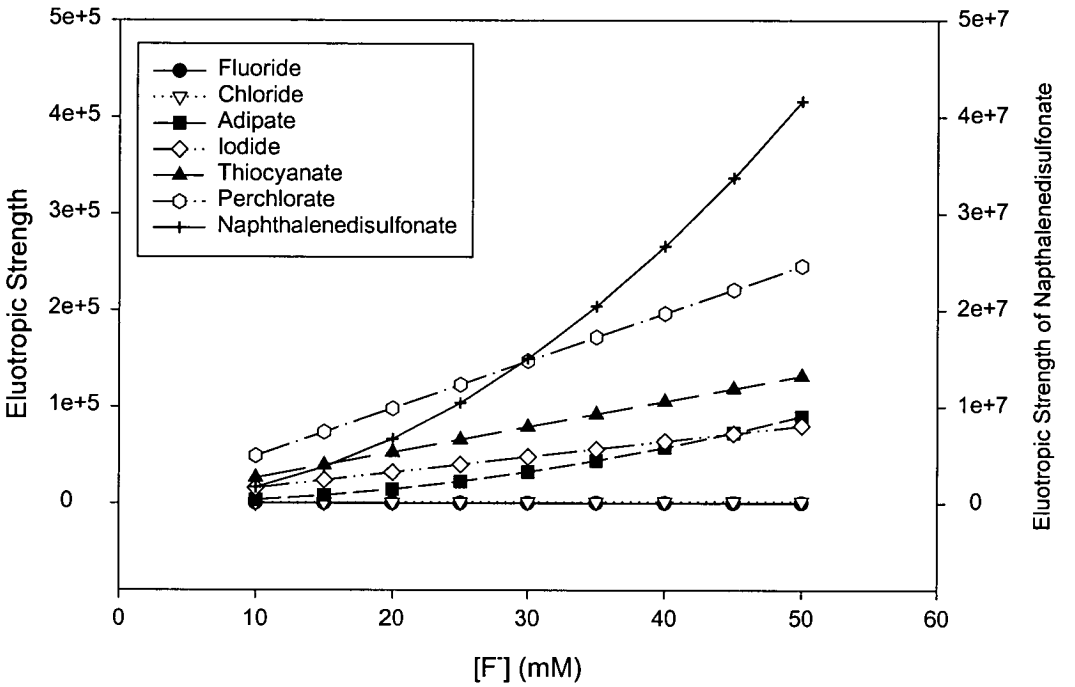

Figure 5.7: Influence of increasing the concentration of WE (NaF) on the eluotropic strength of a SE formed from different competing anions. In all cases, the SE counter-cation was Na^+. Note that naphthalenedisulfonate is displayed on a scale a factor of 100 times higher than the other anions.

conditions) Figure 5.8 shows the use of NDS as SE when using 20 mM NaF as WE and CrO_4^{2-} as analyte. Detection of CrO_4^{2-} was performed at 370 nm while detection at 226 nm enabled the NDS gradient to be visualised. Detection of other inorganic anions at low UV wavelengths was not possible due to the background absorbance of the SE. It can be seen that the peak for CrO_4^{2-} is highly focused, demonstrating that the eluotropic strength of the SE was sufficient to suppress any interaction between CrO_4^{2-} and the stationary phase, and the mobility of NDS is low enough to allow CrO_4^{2-} to be focused.

Selecting the appropriate WE and SE composition for analyte focusing is a complex procedure. The WE must ensure analyte retention, while the SE must immediately desorb the analytes. To achieve this, eluotropic strength should be calculated using both the concentration and IE selectivity coefficient of the competing anion.

5.4.3 Influence of mobility of the counter-cation

Equation (5–2) indicates that the electrophoretic mobility of the counter-cation will influence the concentration of SE entering the capillary. Using equation (5–2) and defining the WE as 10 mM F^- and ClO_4^- as the SE competing anion, the influence of changing the mobility of the counter-cation can be calculated. For the counter-cations Li^+ (μ_{ep} = 38.66), Na^+ (μ_{ep} = 50.08) and K^+ (μ_{ep} = 73.48), the concentration of ClO_4^- produced as the SE varies from 10.36 mM for Li^+ to 10.52 mM for K^+. This suggests that while the counter-cation should theoretically have the highest mobility possible, in practice the increase in SE concentration achieved by changing the nature of the counter-cation is not significant.

5.4.4 Influence of mobility of the WE competing anion

Changing the mobility of the WE competing anion will affect the concentration of SE entering the capillary according to the Kohlrausch regulating function and will also affect the profile of the gradient. To examine the influence of this effect on

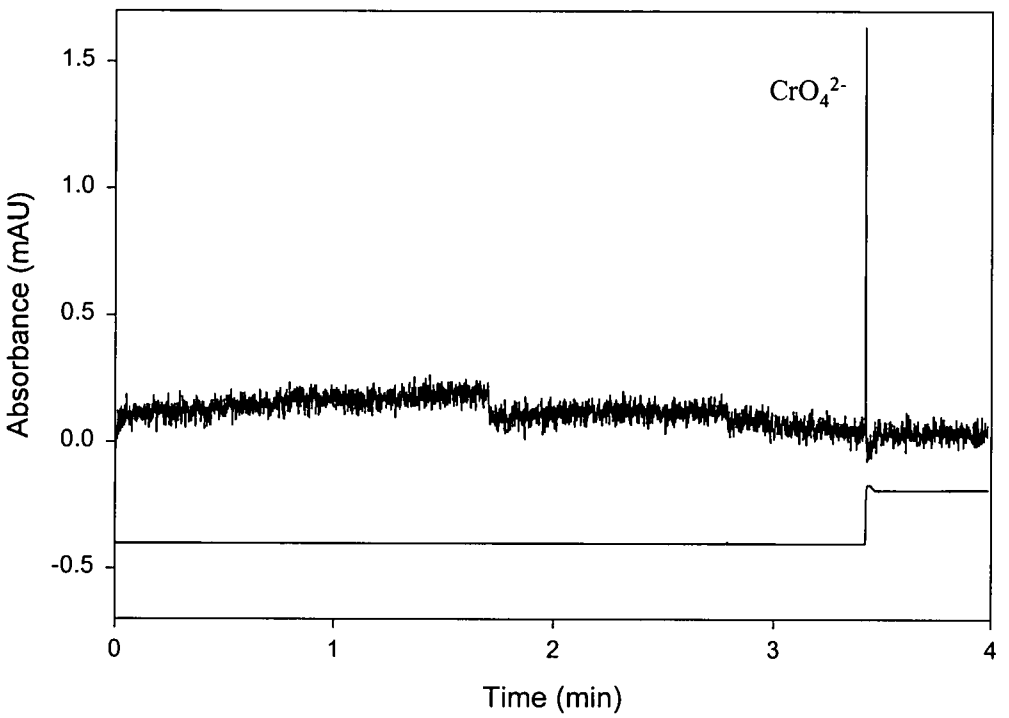

Figure 5.8: Focusing of CrO_4^{2-}. Top trace, detection at 370 nm, bottom trace shows gradient profile by detection at 226 nm. WE : 20 mM NaF, SE : 50 mM NDS/200 mM Tris, pH 8.05, Voltage = -30 kV, injection was for 4 min of a 0.5 μM CrO_4^{2-} solution.

analyte focusing, 4 anions with different electrophoretic mobilities and similar IE selectivity coefficients (Table 5.1) were selected as WE competing anions. The selected anions were *i*-pentanoate (μ_{ep} = -32.63, $K_{E,F}$ = 3.30), ethanesulfonate (μ_{ep} = -43.90, $K_{E,F}$ = 3.59), methanesulfonate (μ_{ep} = -51.27, $K_{E,F}$ = 3.59) and formate (μ_{ep} = -60.02, $K_{E,F}$ = 2.79). Any change in the gradient profile between these anions should be related only to changes in electrophoretic mobility. To enable the gradient profile to be visualised, SCN^- was used as the SE competing anion rather than ClO_4^- since both have similar mobilities and IE selectivity coefficients, but SCN^- is UV-absorbing. Figure 5.9(a) shows the transient gradient profiles predicted from theory for the 4 different WE competing anions and Figure 5.9(b) shows the gradient profiles obtained experimentally.

There is general agreement between Figure 5.9(a) and (b) with regard to the slope of the gradient and the overall increase of SCN^- concentration in the SE as the mobility of the WE competing anion is decreased. Small differences between theory and experiment may be explained by differences in EOF (an average EOF was used in the theoretical case) and as a result of some uncertainty in the mobilities used in the theoretical predictions (due to the fact that there will be some interaction between the anions and the stationary phase, so the mobilities in the present system could differ from those determined from CE experiments). However, there is a major difference between the two figures in that the experimental gradient profiles show an initial stepwise increase in SCN^- concentration (shown by the vertical rise in the plots in Figure 5.9 (b)), followed by the expected gradient profile. This step is due to adsorption of the SE anions on the stationary phase at the front of the gradient due to their high IE selectivity coefficient, so that the gradient becomes compressed until the stationary phase becomes saturated with the SE anions. The influence of this step on analyte focusing can be seen in Figure 5.10 which shows that as the mobility of the WE competing anion decreases, the peak of Br^- and NO_3^- becomes less focused. This is due to a reduction in the size of the step, as seen in Figure 5.9(b). To ensure

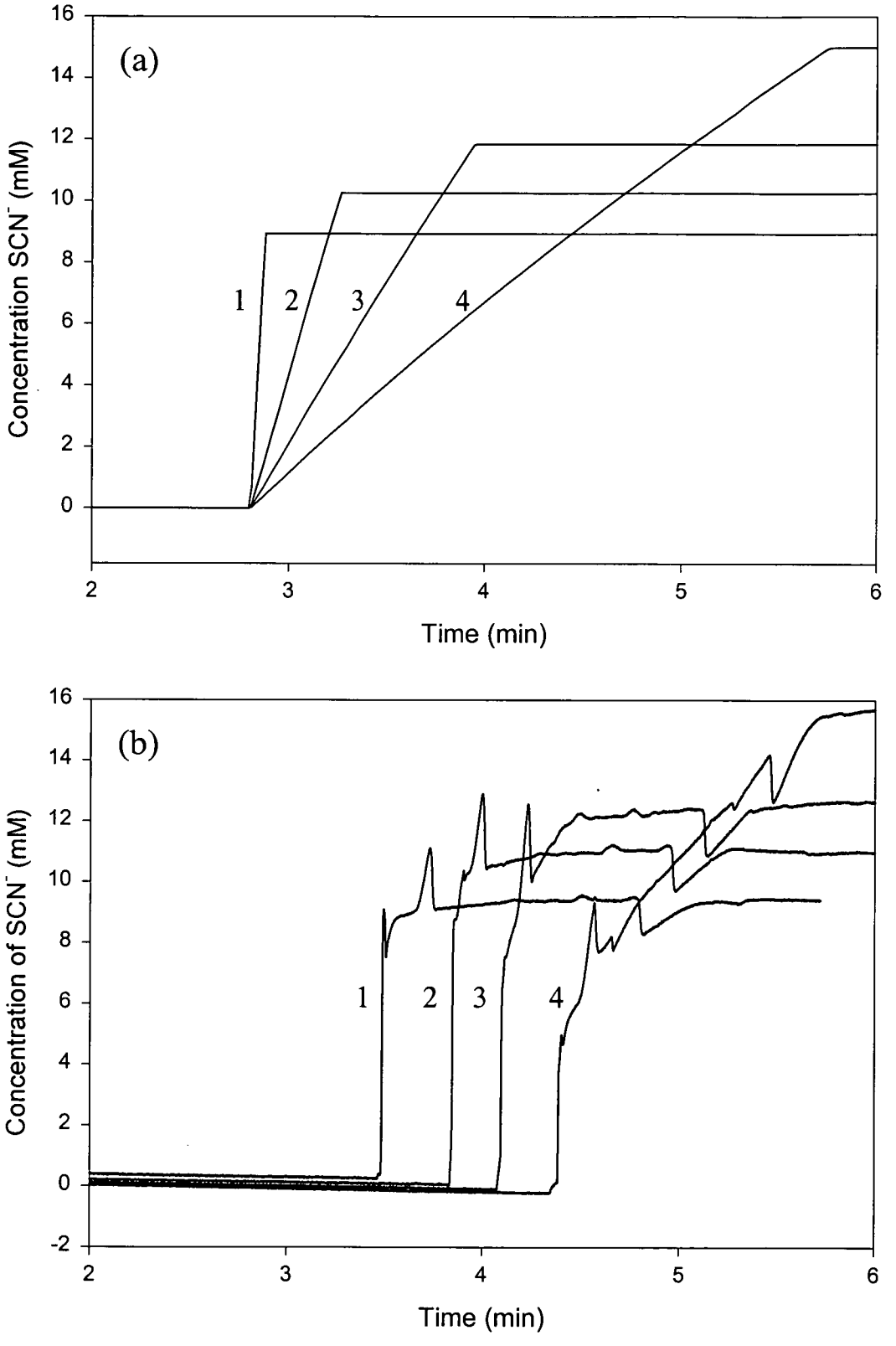

Figure 5.9: Theoretical (a) and experimental (b) gradients showing the influence of varying WE mobility. The WE concentration in all cases was 5 mM and NaSCN was used as the SE at a concentration of 10 mM. WE competing anions are 1 = Formate, 2 = Methanesulfonate, 3 = Ethanesulfonate, 4 = *i*-Pentanoate.

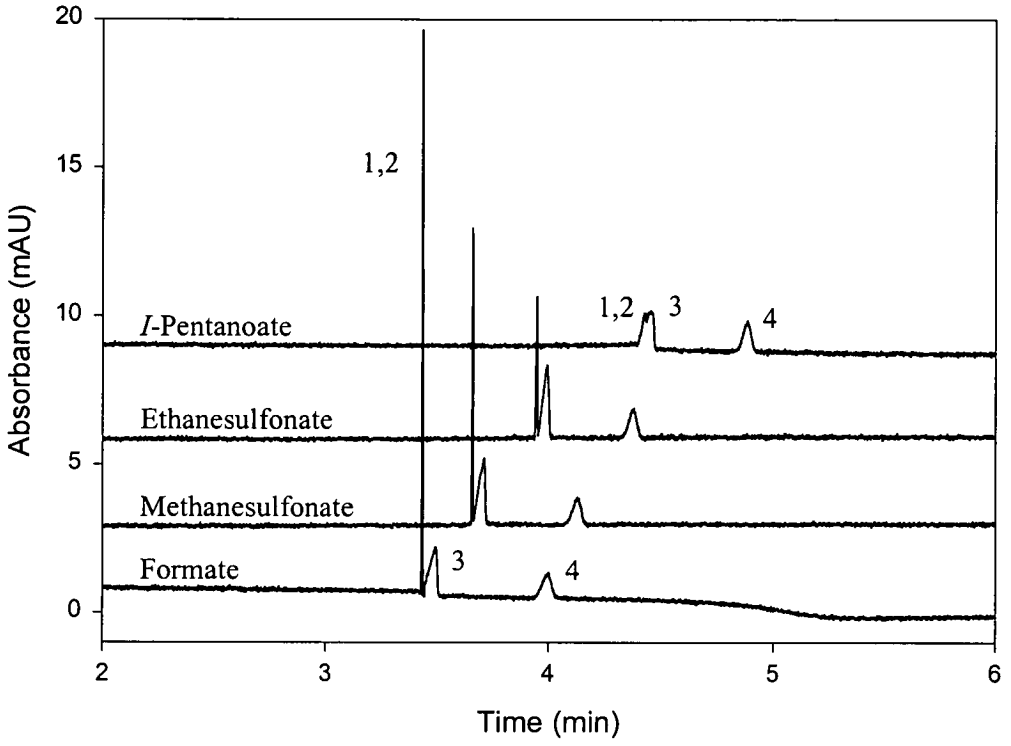

Figure 5.10: Influence of the mobility of the WE competing anion on focusing of selected analytes. All WE concentrations were 5 mM of the sodium salt. SE was 10 mM ClO_4^-/20 mM Tris, pH 8.05. Other conditions as in Figure 5.6. Peaks are 1 = Br^-, 2 = NO_3^-, 3 = I^- and 4 = SCN^-.

that the efficiency of analyte focusing is as high as possible, the above results indicate that the mobility of the WE and SE competing anions need to be as close together as possible to give the maximum gradient slope.

5.4.5 Influence of ion-exchange selectivity coefficient of the SE competing anion

To confirm the origin of the step at the front of the gradient, the IE selectivity coefficient of the SE competing anion was varied by using NO_2^-, I^- and naphthalenetrisulfonate (NTS), all of which are UV-absorbing (allowing the gradient profile to be visualised), have similar electrophoretic mobilities (-75.33, -75.43 and -73.47, respectively, Table 1), but have different IE interactions with the stationary phase ($K_{E,F}$ = 27.6, 712 and 16700, respectively, Table 1). It can be seen in Figure 5.11 that the step is virtually non-existent in the NO_2^- system and is the greatest in the NTS system, suggesting that the front of the gradient is compressed due to retention of the SE competing anion on the stationary phase. It should be noted that the size of this step will be limited by the capacity of the stationary phase and this is apparent when comparing I^- and NTS, which have similar step sizes although NTS has a much higher IE selectivity coefficient. This suggests that both I^- and NTS are adsorbed sufficiently strongly that they both saturate the stationary phase in a short time. It can also be noted that the front of the gradient occurs later for the more strongly interacting SE competing anions and this is due to two reasons. First, the interaction of the SE competing anion with the wall results in this anion having a lower effective mobility than expected, and second, the stronger the interaction between the SE competing anion and the stationary phase on the wall, the lower will be the EOF [12].

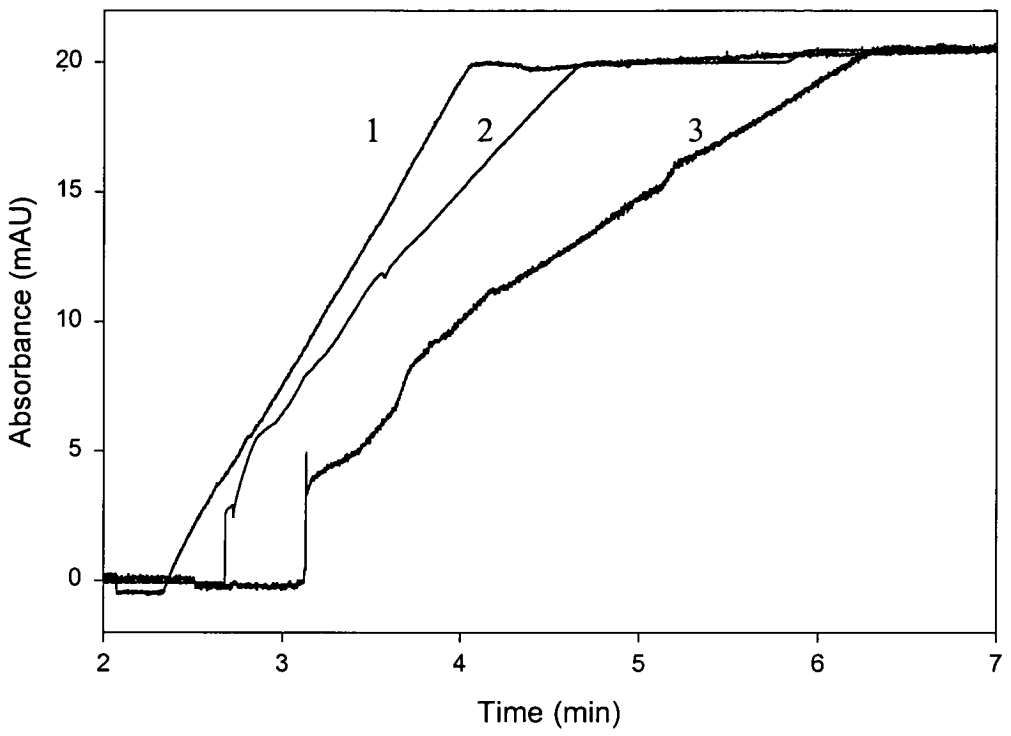

Figure 5.11: Influence of the IE selectivity coefficient of the SE competing anion on gradient profile. WE: 5 mM NaF. SE concentration was 10 mM of the corresponding sodium salt. Absorbance scale has been normalised to enable a relative comparison of the step. SE anions are 1 = NO_2^-, 2 = I^-, and 3 = NTS.

5.5 Method development and application

From the discussion above, the SE and WE should be selected so that: (i) the SE has the highest possible eluotropic strength for a given concentration of WE (ii) the competing anion in the SE has a mobility as low as possible to ensure that the maximum number of analyte anions can be focused, and (iii) the difference in electrophoretic mobility between the WE and SE competing anions is as small as possible. Using these guidelines, F^- was selected as the WE anion due to its low IE selectivity coefficient and NDS was selected as the SE anion due to its high IE selectivity coefficient and moderate electrophoretic mobility. This combination was shown to be suitable for focusing CrO_4^{2-} and therefore has the potential to function as a suitable electrolyte combination for the preconcentration and separation of high mobility inorganic anions. This concept has already been demonstrated using a F^- /ClO_4^- electrolyte system to separate Br^- and NO_3^- (section 5.3.3), but the use of NDS as the SE anion should improve the method by enabling more anions to be preconcentrated and separated. This section examines the use of the F^-/NDS combination for the preconcentration and separation of fast inorganic anions. Factors influencing the performance of the preconcentration (preconditioning, adsorption and elution) and separation (EOF reversal and capillary diameter) components were examined and optimised.

5.5.1 Preconcentration

5.5.1.1 Column pre-conditioning

The first step in the preconcentration procedure was to adsorb the analyte. For this to occur the counter ion at the IE site must be in a form that can be readily displaced by the analyte. The ability of an anion to exchange on to the stationary phase is given by the selectivity coefficient which represents the degree of association of the analyte with the stationary phase when the IE site is in a particular form. In section 5.4, it

was found that out of 77 anions, F^- had the lowest IE selectivity coefficient and should therefore be replaced by most anions. NDS has a high IE selectivity coefficient and will elute most anions and has a moderate electrophoretic mobility, making it suitable to be used as the SE anion. To change the preconcentration section from the NDS to the F^- form prior to sample introduction it was found that it was necessary to first convert the column from NDS to ClO_4^-, which could then be converted to F^-. This was performed by flushing the capillary with one column volume of SE (NDS), followed by ClO_4^- (250 mM) and finally by WE (F^-), before the column was flushed with water and the sample injected. It should be noted that in all cases when changing vials during the preconcentration process, the capillary and electrode tip were rinsed with a water vial, which was replenished using the on-line replenishing system before separation. If water vials were not replenished after each separation, peak heights decreased substantially due to carry-over contamination from previous separations.

5.5.1.2 Analyte adsorption

The second step in the preconcentration procedure was to inject the sample and achieve adsorption of the analytes onto the stationary phase. The time length for injection will have a substantial influence on detector response with longer injection times resulting in a higher response. In practical terms the injection time was limited by the capacity of the stationary phase and after saturation no more analyte could be adsorbed and the response reached a constant level [13,14]. To determine when overloading was achieved, the injection time was increased to a maximum of 15 min. Figure 5.12 shows the variation of peak area (a) and peak efficiency (b) with injection time for I^-, Br^- and NO_3^-. From these figures, it can be seen that an injection of up to 15 min produced a linear increase in peak area, indicating that the column capacity has not been exhausted. However, the efficiency decreased substantially above 10 min injections. This limitation of the focusing mechanism is due to column

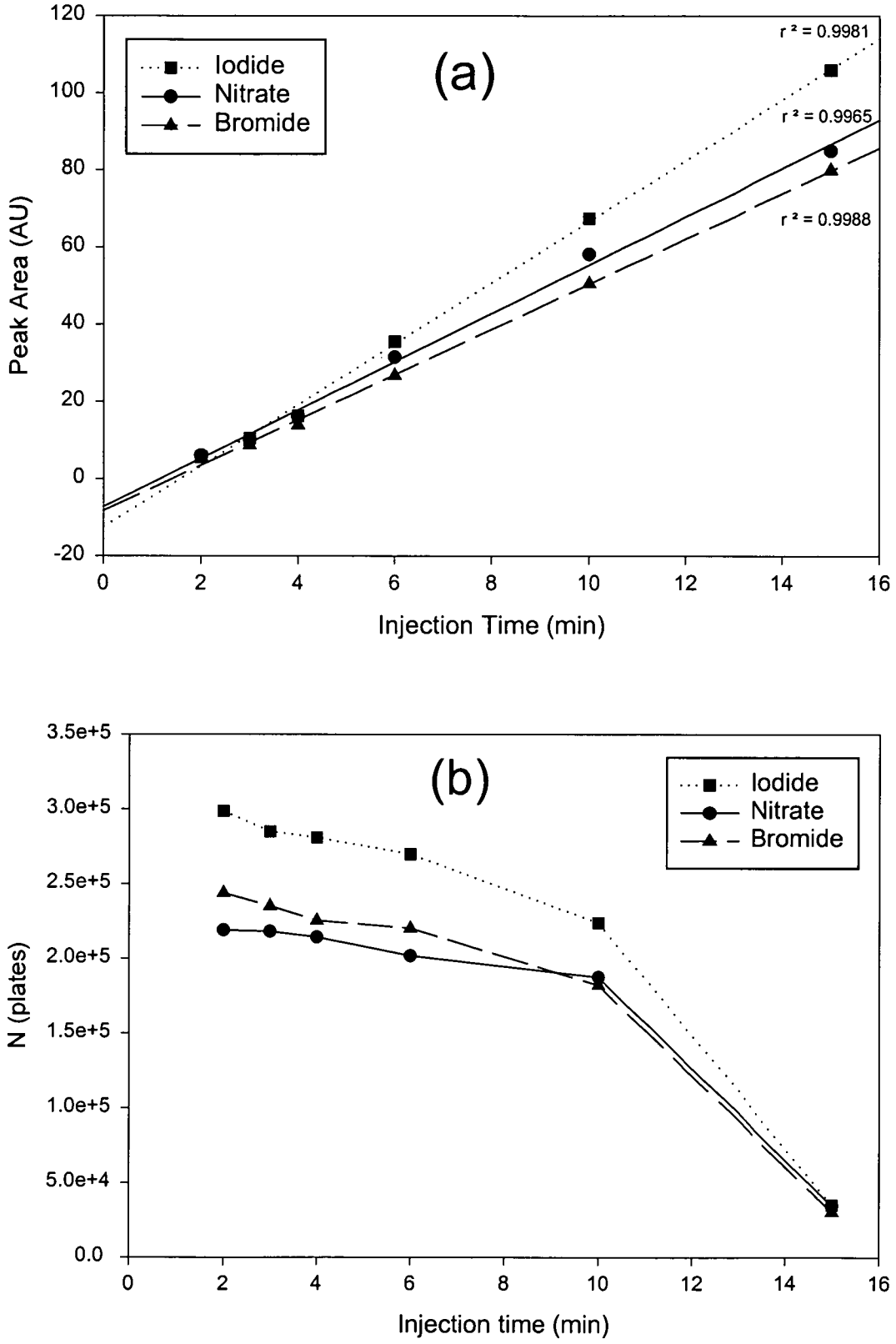

Figure 5.12: Variation of (a) peak area and (b) peak efficiency (theoretical plates) with injection time for I^-, NO_3^- and Br^-. Conditions for Figure 5.16(b).

overload: the localised capacity of the column is exceeded causing the desorbed analyte to migrate ahead of the adsorbed analyte into a zone that has sufficient capacity for it to be retained. This results in the peak height levelling off and the peak width increasing as more analyte was injected.

5.5.1.3 Analyte elution

The final step in the preconcentration procedure was to fill the capillary with the WE so that the transient isotachophoretic boundary could be created and the analytes focused. To ensure that the best possible sensitivity and resolution were obtained, it was important that elution of the analytes from the stationary phase be as efficient as possible.

As the concentration of WE required to maintain CE efficiency in the separation section was relatively high (see section 5.5.2.1) it was not possible to fill the capillary with more than one capillary volume of WE as this resulted in elution of some of the adsorbed analytes from the column. To prevent analyte loss only 95% of the capillary was filled with WE by backflushing the capillary (i.e. filling from the detection end), leaving a water plug (5% of capillary length) in the front of the capillary. Preliminary studies using the backflushing procedure showed a large variation in focusing efficiency and migration time. This was caused by small variations in the size of the water-plug left in the capillary, as a result of slight changes in viscosity of the WE with temperature. After connecting the sample tray to a water bath to reduce the temperature fluctuations, the influence of the size of the remaining water plug on focusing efficiency was examined. This is shown in Figure 5.13 where it can be seen that as the water-plug remaining in the capillary increased in size, the efficiency with which the analytes were focused decreased, the peak heights were reduced and the migration times became longer. A water-plug occupying ~5% of the total capillary volume was found to provide minimal loss of efficiency and peak height and was selected as the optimal value.

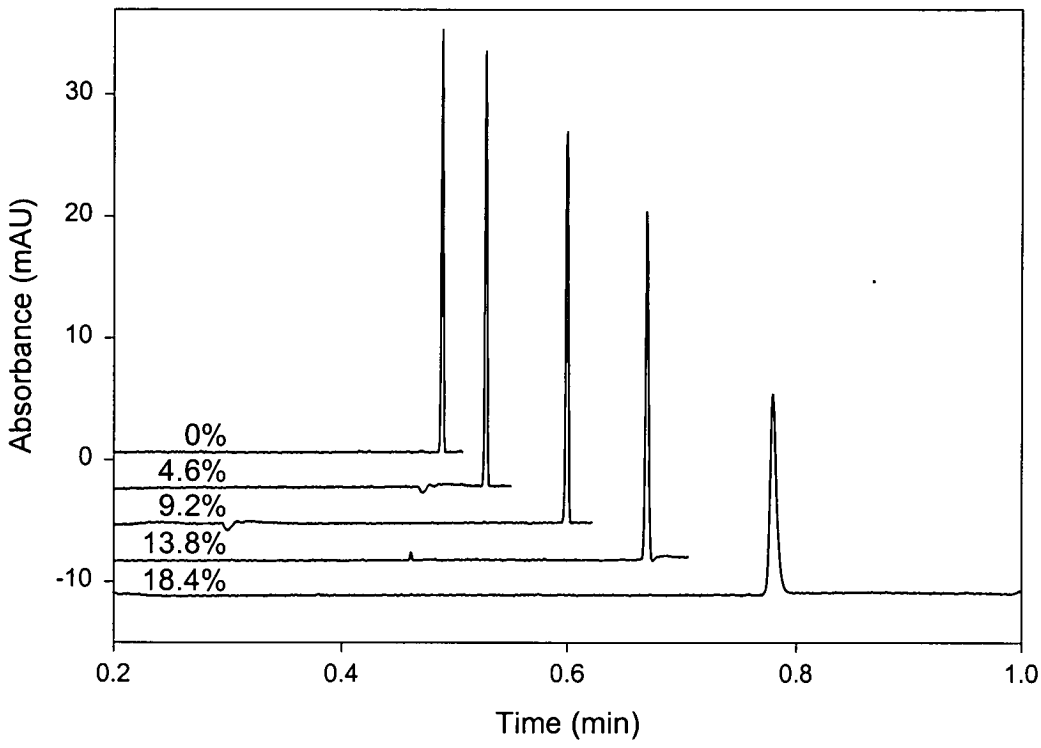

Figure 5.13: Influence of water plug in the front of the capillary on focusing efficiency. The numbers for each separation correspond to the percentage of the capillary volume filled with water before application of the voltage. Conditions : 25 μm i.d. with a length of 34.5 cm (26.0 to detector) fully coated with AS5A latex. Sample was 2 μm I^- in 10 mM NaF and injected for 120 sec @ 2 bar. WE was 10 mM NaF, SE was 10 mM ClO_4^-/TRIS. Voltage –30 kV. Water was injected after injection of the sample @ 2 bar to give the indicated volume.

5.5.2 CE separation

5.5.2.1 EOF reversal

The adsorption of cationic particles onto the capillary wall provided IE sites on which the analyte anions were preconcentrated and also reversed the EOF in this section of the capillary (discussed in chapter 3) [15,16]. To ensure that no efficiency was lost in transferral of the analytes between the two sections, it was important that the EOF in both sections was in the same direction. This was previously accomplished in section 5.3 using a cationic surfactant, cetyltrimethylammonium chloride added to both the WE and SE at low concentrations. However, the addition of any cationic surfactant to solutions containing NDS resulted in precipitation and thus could not be used for EOF reversal with NDS as the SE.

The permanent adsorption of a cationic polymer was investigated as an alternative method for EOF reversal as this has been found to be an easy and reproducible way to reverse the EOF [17]. Flushing capillaries with a dilute solution (0.1% w/v) of the polymer poly(diallyldimethylammonium chloride) (PDDAC) was found to provide a reproducible and reversed EOF. However, the introduction of a cationic polymer introduced IE sites on the capillary wall in the separation section with which the analytes could interact. This resulted in analytes migrating through the separation section by an IE-OT-CEC mechanism, instead of the intended pure CE, which could result in a substantial loss of separation efficiency (discussed in chapter 3). As the analytes were separated in the separation section in a zone of pure WE, the IE interaction with the wall could be potentially suppressed by increasing the concentration of WE. Figure 5.14 shows the variation in efficiency of analytes separated in a PDDAC-coated capillary as the concentration of WE (NaF) was increased from 10 to 100 mM. It can be seen that at lower concentrations of WE, lower efficiencies were obtained due to interaction of the analytes with PDDAC on the capillary wall. A higher concentration of WE ensured that the wall interaction

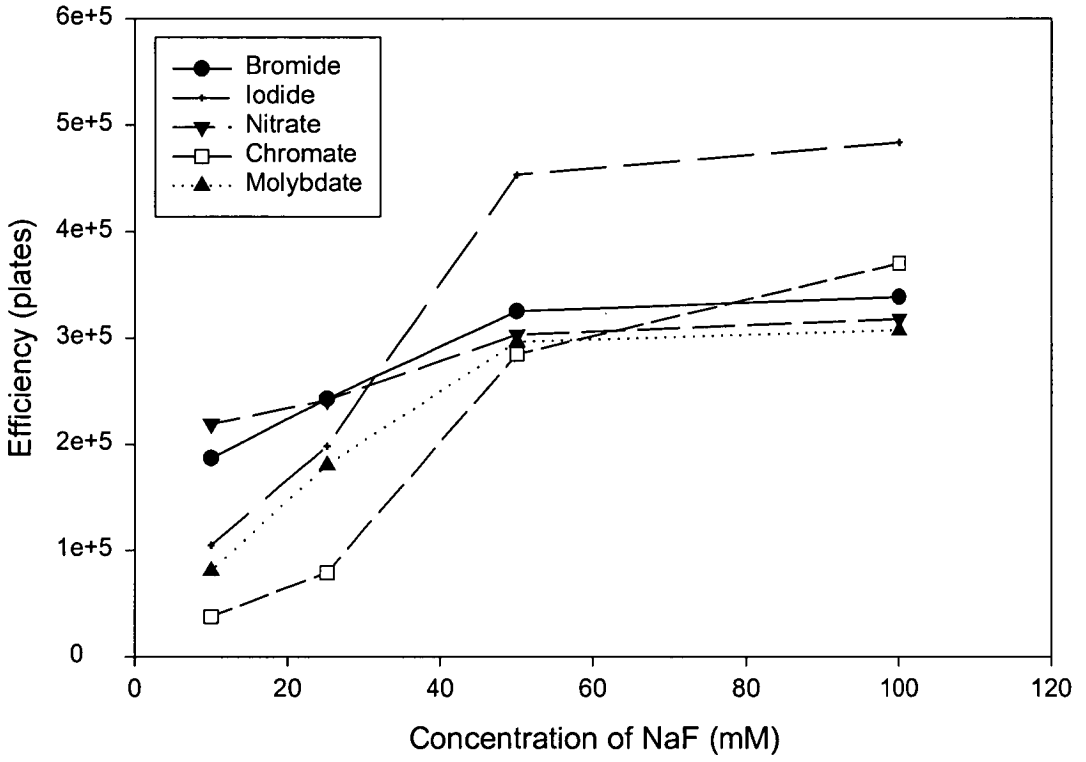

Figure 5.14: Influence of WE concentration on the separation efficiency of inorganic anions separated in a PDDAC coated capillary. Conditions are : 25 μm i.d. capillary with a length of 50.0 cm (41.5 cm to detector), Injection of a mixture 0.5 mM of each anion for 20 seconds @ 50 mbar. Voltage was –30 kV.

was suppressed and a highly efficient separation was obtained. A concentration of 100 mM was found to be sufficient to remove any interaction with adsorbed PDDAC, and this concentration of WE was used for the rest of this study.

5.5.2.2 The role of the capillary diameter

When using photometric detection, the best sensitivity will be obtained in the capillary with the longest pathlength, however this is not the only consideration when deciding the best separation system. Figure 5.15 shows the preconcentration and separation of Br^-, NO_3^- and I^- in 75, 50 and 25 μm i.d. capillaries. While the best sensitivity is obtained with the 75 μm i.d. capillary, the best resolution is obtained in the 25 μm i.d. capillary, where all 3 could be easily baseline separated. This was because there was a substantially lower EOF and therefore longer migration times in the 25 μm i.d. capillary, compared to the 50 and 75 μm i.d. capillaries. This change in EOF was due to the variation of the effective column capacity, which was inversely related to the capillary diameter so that the EOF was highest in the 25 μm i.d capillary. The concentration of WE and SE needed to ensure that the analytes were focused efficiently increased accordingly with lowering the capillary diameter resulting in a reduction in EOF. The concentration of WE ranged from 1 to 100 mM when going from 75 to 25 μm i.d. capillaries, resulting in a substantially lower EOF in the 25 μm i.d capillary. In addition to this effect, it has been shown that a lower EOF will result when the ion has a higher IE interaction with the wall [12]. Therefore, as the apparent column capacity increased, the EOF should decrease because the anions are interacting more with the capillary wall. The combination of these two factors meant that the separation in the 25 μm i.d. had the lowest EOF and provided the best resolution.

A further issue when selecting the best capillary diameter to use is the flushing time for sample injection and filling the capillary with WE. The instrument used in this study could use low pressure (10-50 mbar) or an external pressure (2-12 bar) to flush

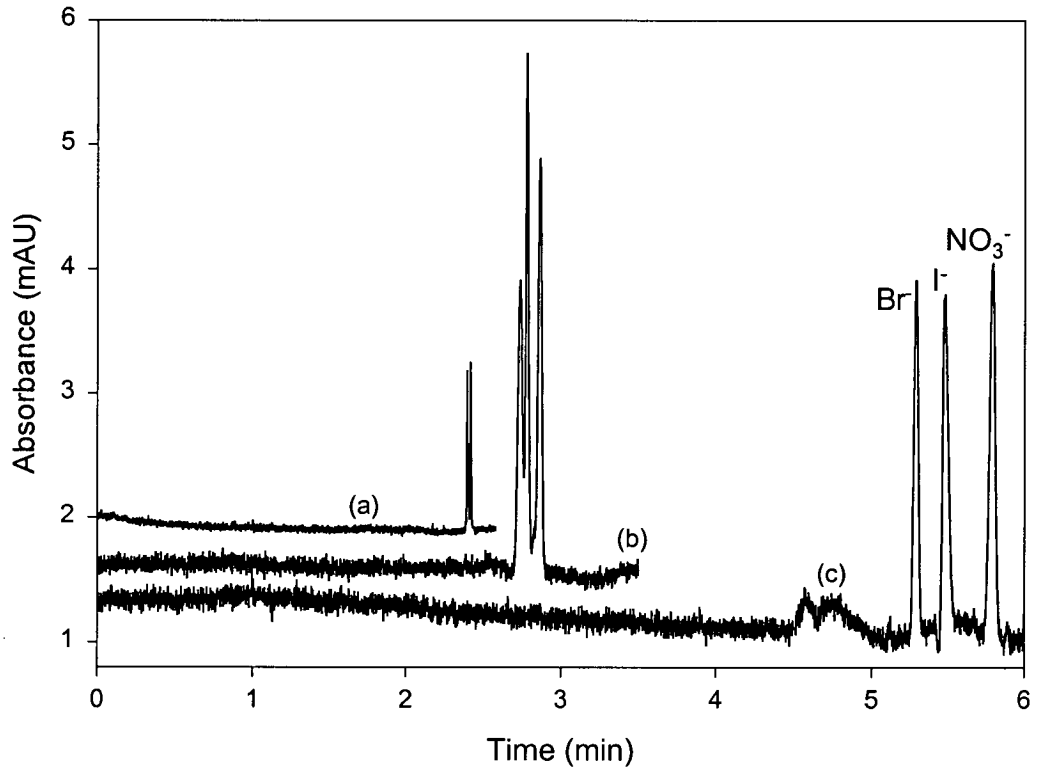

Figure 5.15: Comparison of separations in (a) 75 μm (b) 50 μm and (c) 25 μm i.d. capillaries. All columns were 80.0 cm in length (71.5 cm to detector) and the voltage was –30 kV. Injection was 8 x 10^{-14} moles of each anion (a), 2.5 times more for (b), and was 7.5 times more for (c). Backflushing was for 581 s @ -50 mbar for (a), 1309 s @ -50 mbar for (b) and 90 s @ -3 bar for (c) with the appropriate WE. WE concentrations were 1 mM NaF for (a), 20 mM NaF for (b) and 100 mM NaF for (c).

solutions through the capillary. Using the same length of capillary (80.0 cm), the time to inject one capillary volume of sample using a low pressure of 50 mbar was 581, 1308, and 5237 s for 75, 50 and 25 μm i.d. capillaries, respectively. The flushing times for the same columns using an external pressure of 3 bar (3 bar was the lowest pressure that can be applied to the detection end) were 9.68, 21.8 and 87.2 s. While the backflushing times using low pressure were in the order of 10 min, the time to flush with the lowest external pressure was at most 1.5 minutes for the 25 μm i.d. capillary. Times for the larger capillary diameters using external pressure were very short, and were therefore not as reproducible as the longer times. On the basis of backflushing times, the 25 μm i.d. capillary was the best choice. A shorter 75 μm i.d. capillary could be used to decrease the backflushing time using low pressure, but this advantage was offset by a reduction in peak resolution. Alternatively, a longer capillary could be used to increase the backflushing time using high pressure, but this would result in a longer electrophoretic separation due to a reduction in field strength.

Taking all of these factors into consideration, the best compromise was the use of a 25 μm i.d capillary. While this gave the worst sensitivity, it provided the best separation in a reasonable time. The use of 75 μm i.d. capillaries in which the EOF had been suppressed was a potential alternative to the use of 25 μm i.d. capillaries and these are currently under investigation. It should be noted that the reduction in sensitivity was somewhat offset when keeping the total analysis time to under 30 min because more sample could be injected than with the larger capillary diameters because of the time required for the backflushing step.

5.5.3 Optimum system

Using the optimum conditions discussed above, it was possible to preconcentrate and separate anions which have a moderate IE selectivity coefficient and an electrophoretic mobility higher than -57×10^{-9} m^2/Vs. This is shown in Figure 5.16

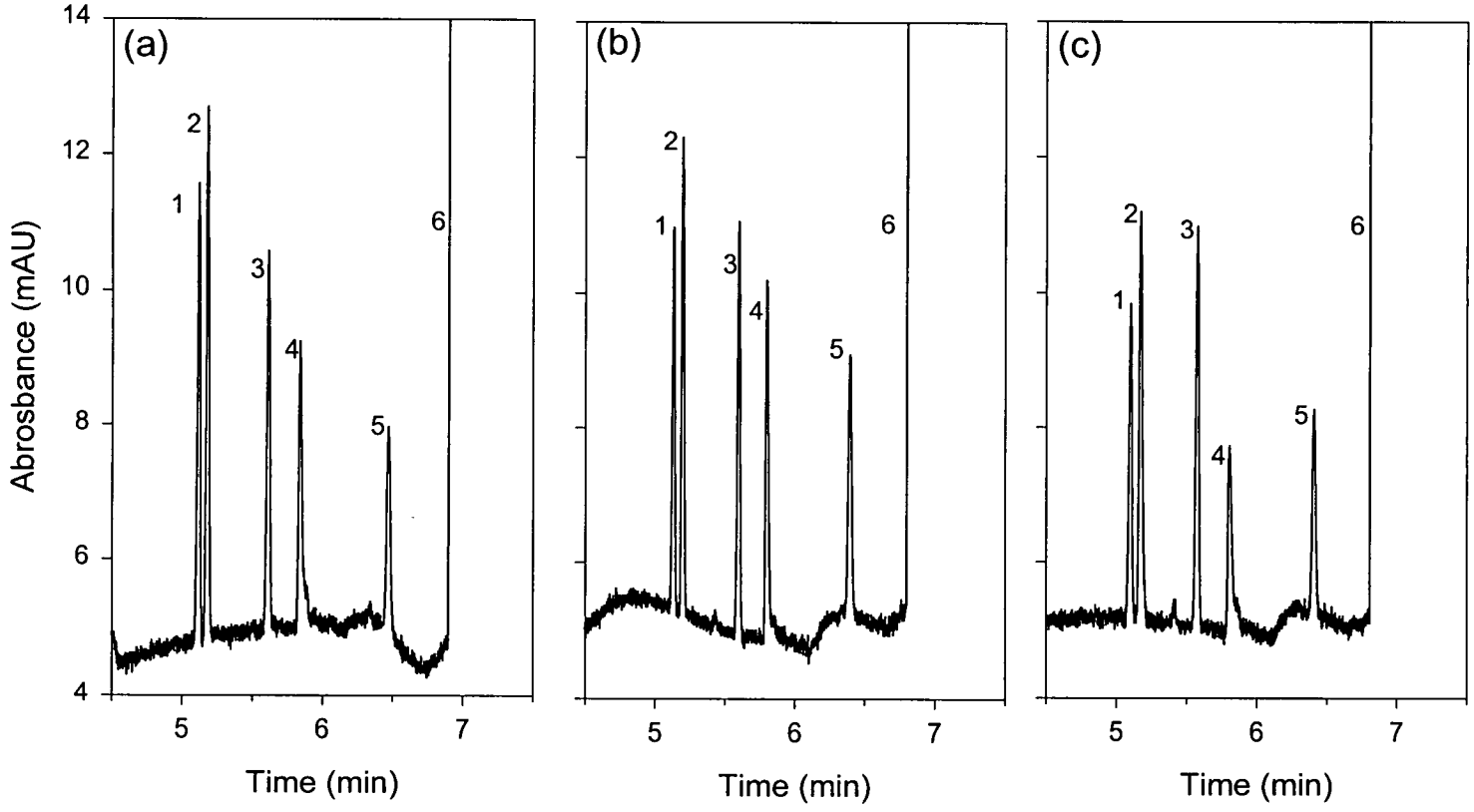

Figure 5.16: Preconcentration and separation of a mixture of inorganic anions. (a) 5 μM Br^-, I^-, NO_3^-, CrO_4^{2-} and 1 μM MoO_4^{2-}, injection for 6 s @ 2 bar. (b) 1:10 dilution of (a) and a 60 s injection @ 2 bar and (c) 1:100 dilution of (a) and a 600 s injection @ 2 bar. Column : 25 mm i.d., 80.0 cm total, 71.5 cm PDDAC / 8.5 cm AS5A @ 29°C. WE : 100 mM NaF; SE : 50 mM NDS/200 mM Tris, pH 8.05. Injection : as indicated above, followed by backflush of WE for 1.40 min @ -3 bar. Voltage : -30 kV.

Table 5.2: Analytical performance of preconcentration and separation method for CE analysis of inorganic anions.

	t_m (%RSD)	Peak Area (%RSD)	Peak Height (%RSD)	N (%RSD)	LOD μM (ppb)
Br^-	5.102 (7.5)	6.6 (5.2)	4.6 (7.9)	338000 (7.6)	0.060 (4.74)
I^-	5.171 (7.4)	9.5 (3.6)	6.0 (8.5)	483000 (8.6)	0.044 (5.58)
NO_3^-	5.577 (7.2)	8.8 (5.4)	5.9 (8.8)	317000 (8.6)	0.047 (2.16)
CrO_4^{2-}	5.806 (7.3)	7.8 (3.2)	3.3 (8.2)	370000 (10.1)	0.100 (11.6)
MoO_4^{2-}	6.408 (7.3)	5.2 (4.1)	3.0 (8.1)	307000 (8.0)	0.018 (2.88)

which shows separations of Br^-, NO_3^-, I^-, CrO_4^{2-} and MoO_4^{2-} under varying conditions of sample concentration and injection time. Figure 5.16 (a) shows the injection of a mixture of anions for 6 s, (b) is the injection of a 1:10 dilution of (a) for 60 s and (c) is the injection of a 1:100 dilution of (a) for 600 s. The amount of sample introduced was 0.04, 0.40 and 4.00 capillary volumes, respectively. It can be seen that peak shapes were well maintained and no significant loss in peak height was obtained, indicating that a 100 fold increase in sensitivity could be obtained using a 10 min injection and a total analysis time of 25 min. Analytical parameters based on the 600 s injection time are shown in Table 5.2, with detection limits in the low ppb range being obtained for most anions. Migration time reproducibity was acceptable with %RSD being typically around 7% for all anions. This was predominantly due to minor variations in temperature causing slight changes in the length of the water plug left at the front of the capillary (see section 5.5.1.3).

To illustrate the potential of this technique to analyse very low concentrations of anions, Figure 5.17 shows a 6000 s (100 min) injection of anions with a concentration between 0.2 and 0.6 ppb. This injection introduced 40 capillary volumes of sample, or approximately 15 μL, giving a total analysis time of 120 min. There was no loss of peak efficiency even with this long injection time, and only a slight loss in adsorbed analytes, with recoveries around 90% being obtained for all

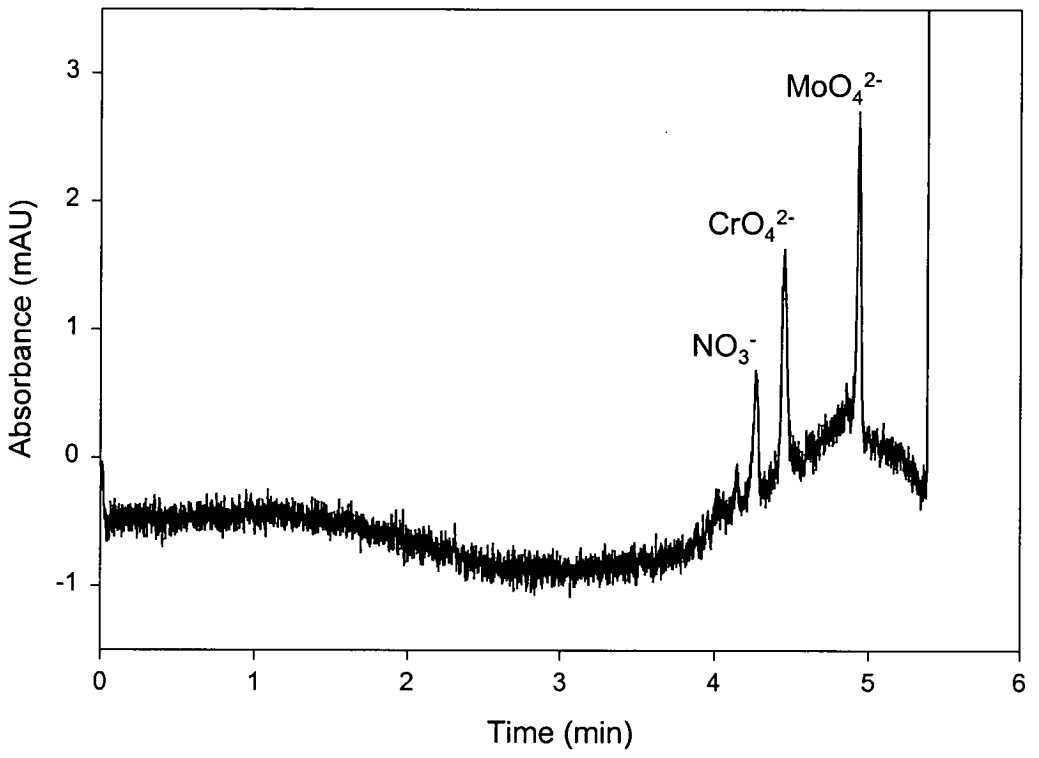

Figure 5.17: Preconcentration and separation of sub ppb levels of inorganic anions. Injection: 100 min @ 2 bar of 5 nM NO_3^-, 10 nM CrO_4^{2-} and 2 nM MoO_4^{2-}. Other conditions as in Figure 5.16.

ions. This gave over a 900 fold increase in sensitivity compared to a conventional injection.

5.5.4 Application : determination of nitrate in Antarctic ice cores

Whilst one of the biggest advantages of CE over other liquid chromatographic methods is the small sample size, many applications require detection limits lower than those which can normally be obtained by CE. One such situation is the analysis of trace ions in Antarctic ice cores in order to provide information related to past climate conditions. The determination of ions in ice cores is limited in the amount of sample that can be provided for chemical analysis, so the development of a method allowing smaller sample volumes would be beneficial since it would allow analysis of small volume samples that cannot be analysed by other methods (such as oxygen isotopes [18]) . Anions including SO_4^{2-}, Cl^-, NO_3^- and $CH_3SO_3^-$ are typically analysed by IEC, with a sample volume of 5 mL and on-line sample preconcentration [19].

The developed CE method is currently only applicable to UV absorbing ions, so of the above analytes, the method is suitable only for the the determination of NO_3^- in ice cores. Nevertheless, this analysis will provide an indication of the potential use for this method. Nitrate is a key ion in polar ice core research and provides information on the variations in atmospheric NO_3^- caused by anthropogenic influences [20], solar activity [21,22,22], post depositional processes [23] and seasonality [24]. Nitrate can also be used for ice core dating [21]. The complexity of the atmospheric NO_3^- cycle and the relative contributions of the various sources and sinks remain poorly understood. The average NO_3^- concentration found in Antarctic ice cores can range between 0.3 μM and 1.2 μM [23]. These levels can be determined using an injection time of 600 s, giving a total analysis time of 25 min.

Separations obtained in the analysis of a real ice core sample from Law Dome, East Antarctica (sample DSS99-102-9) by both IEC and CE are shown in Figure 5.18,

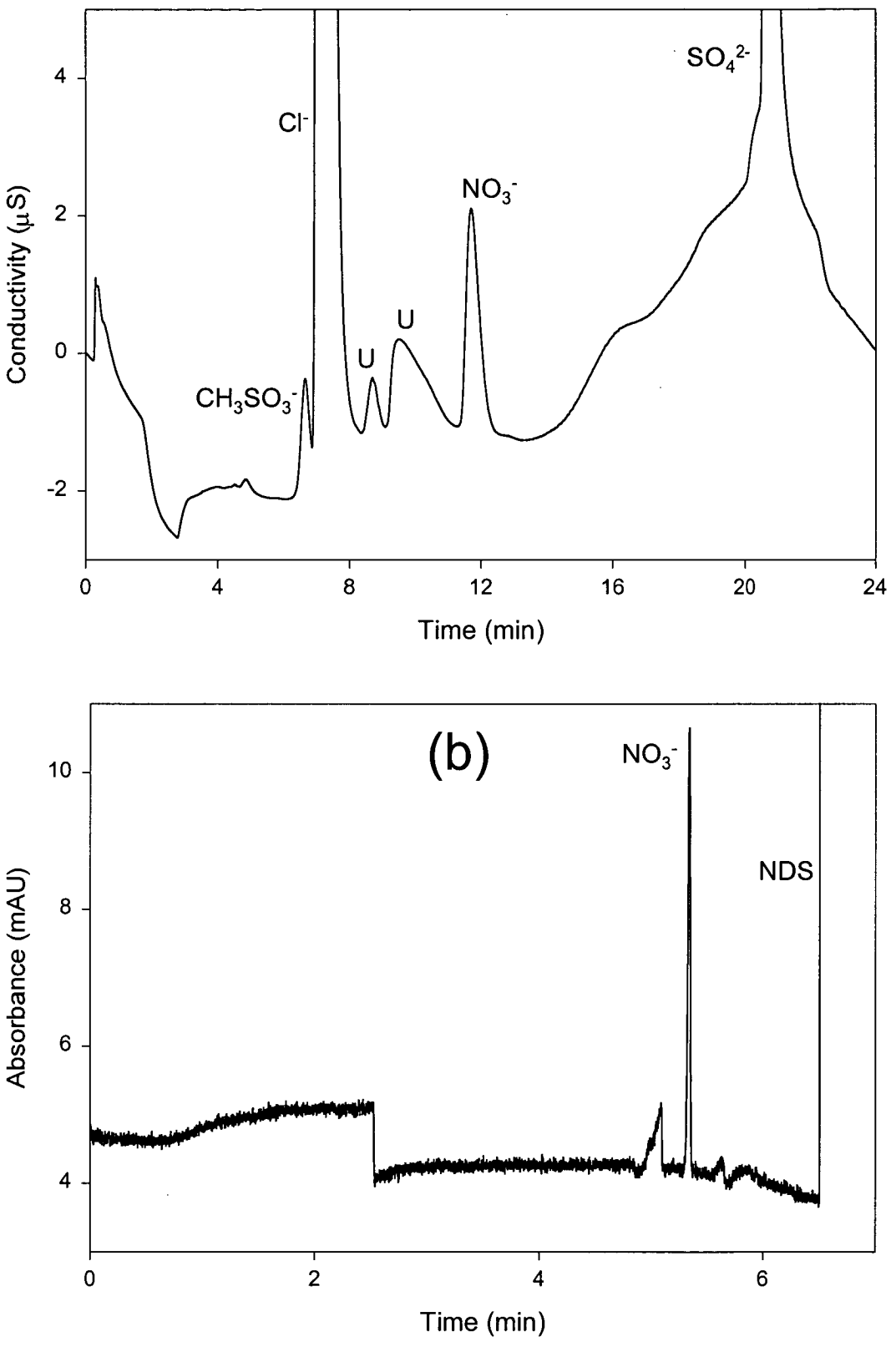

Figure 5.18: Analysis of ice core sample from Law Dome, East Antarctica (sample DSS99-102-9) by (a) IEC method (details in [19]) and (b) CE method (conditions as in Figure 5.16 (c)).

Table 5.3: Comparison of CE and IEC methods for the determination of NO_3^- in Antarctic ice cores.

	CE (using 600 s inj)	IEC
Detection Limit for NO_3^-	0.04 μM	0.005 μM
Sample Volume	< 50 μL	5 mL
Analysis time	25 min	24 min
NO_3^- found in sample	0.304 μM	0.314 μM

with comparative details shown in Table 5.3. There is excellent agreement in the concentration of NO_3^- between CE and IEC for this sample. When comparing the two methods, the CE method offers similar performance to the IEC method with regard to most analytical parameters, and while the IEC method offers a lower detection limit, the CE method allows a smaller sample volume to be used. The volume required for a CE analysis can be less than 50 μL, compared to a practical IEC volume of 5 mL [19], giving a potential 100-fold increase in sample resolution. This increase in resolution is immediately applicable to the dating of the Dome Summit South (DSS) ice core, from Law Dome, by detection of annual layers. In the DSS ice core, the depth (age) limit for seasonal NO_3^- dating using current IEC techniques is about 700 m (1574 years before present (ybp)) due to the required sample volume. Below this depth, thinning of the annual layers due to ice flow reduce the volume available for IEC measurements. Using oxygen isotope ratio analysis, this depth can be increased to 1038 m (4830 ybp) [18], but at depths below this the signal is lost. It is uncertain whether solid ice diffusion of the isotope ratio signal or recrystallisation and movement is responsible. Analysis of thin ice samples for NO_3^- using CE will provide a unique solution as to the cause of signal loss, and potentially increase seasonal dating of the DSS ice core to 1105 m (8100 ybp).

5.6 Conclusions

An on-line SPE method using IE interactions for the preconcentration of inorganic anions for CE has been presented. A novel electroseparation concept, namely the use of an eluotropic gradient formed by a transient isotachophoretic boundary has been introduced to elute anions after preconcentration. This gradient is established by using a weakly eluting low mobility electrolyte ion in the capillary and a more mobile, strongly eluting ion in the electrolyte vials. As the gradient moves through the capillary, analytes which satisfy the conditions $K_{WE} < K_A < K_{SE}$ and $\mu_{WE} < \mu_{SE} < \mu_A$ are focused along the capillary wall into a very sharp band. This peak focusing has been demonstrated for I^- and extended to a mixture of inorganic anions for introduction into a separation capillary.

The gradients were characterised using eluotropic strength and concentration profile. The eluotropic strength of SE is a function of the charge, IE selectivity coefficient and the concentration of the SE competing anion. The concentration is governed by the Kohlrausch Regulating Function and is dependent strongly on the difference in mobility between the WE and SE competing anions. The concentration profile of the isotachophoretic gradient is likewise strongly dependent on the difference in mobility between the WE and SE competing anions, and depends also on the IE selectivity coefficients of these ions. A larger difference in mobility results in a higher final eluotropic strength of SE, but a longer gradient of reduced slope is produced. A high IE selectivity coefficient of the SE competing anion causes compression of the front of the gradient, resulting in a sharp initial change in eluotropic strength. This sharp change is reduced as the gradient slope decreases, resulting in less efficient focusing. The SE and WE should be selected so that: (i) the SE has the highest possible eluotropic strength for a given concentration of WE, (ii) the competing anion in the SE has a mobility as low as possible to ensure that the maximum number of analyte anions can be focused, and (iii) the difference in electrophoretic mobility between the WE and SE competing anions is as small as possible.

Using the guidelines above, a F^-/NDS WE/SE system was developed and optimised for the separation of inorganic anions. Optimisation of the backflushing step and WE concentration were crucial to obtain highly efficient separations. The best separations were obtained in a 25 μm i.d. capillary due to improved resolution due to a reduction in EOF in comparison to 50 and 75 μm i.d. capillaries even though the worst detection sensitivity was obtained. Using an optimised method, a 100 min pressure injection allowing 40 capillary volumes of sample to be injected gave an increase in sensitivity by a factor of 900 without any loss in resolution and separation efficiency, giving sub ppb detection limits for NO_3^-, CrO_4^{2-} and MoO_4^{2-}. A method based on a 10 min injection enabled a 100 fold increase in sensitivity to be achieved for Br^-, NO_3^-, I^-, CrO_4^{2-} and MoO_4^{2-} within a total analysis time of 25 min which is comparable to similar IEC methods. This method was used to determine the concentration of NO_3^- in Antarctic ice cores where the lower sample requirements of CE will allow a 100 fold increase in resolution over the existing IEC methods used for NO_3^- in the Antarctic records.

5.7 Reference List

1. A.R. Timerbaev and W. Buchberger, *J.Chromatogr.A*, 834 (1999) 117.

2. D. Martínez, F. Borrull and M. Callul, *TrAC*, 18 (1999) 282.

3. D.S. Burgi and R.-L. Chien, in J.P. Landers (Editor), *Handbook of Capillary Electrophoresis*, CRC Press, New York, 1997, p. 479.

4. N.A. Guzman, *J.Liq.Chrom.*, 18 (1995) 3751.

5. A.J. Tomlinson, L.M. Benson, N.A. Guzman and S. Naylor, *J.Chromatogr.A*, 744 (1996) 3.

6. M. Peterrson, K.-G. Wahlund and S. Nilsson, *J.Chromatogr.A*, 841 (1999) 249.

7. L. Arce, P. Kuban, A. Ríos, M. Valcárcel and B. Karlberg, *Anal.Chemica.Acta.*, 390 (1999) 39.

8. M. Novic and M. Gucek, *J.Chromatogr.A*, 868 (2000) 135.

9. P.R. Haddad and P.E. Jackson, *Ion Chromatography. Principles and Applications*, Elsevier, Amsterdam, 1990.

10. F. Foret, L. Krivánková and P. Bocek, *Capillary Zone Electrophoresis.*, VCH, Weinheim, 1999.

11. D.R. Lide, *CRC Handbook of Chemistry and Physics*, CRC Press., London, 1994.

12. C.A. Lucy and R.S. Underhill, *Anal.Chem.*, 68 (1996) 300.

13. J. Cai and Z. El Rassi, *J.Liq.Chrom.*, 16 (1993) 2007.

14. J. Cai and Z. El Rassi, *J.Liq.Chrom.*, 15 (1992) 1179.

15. G. Kleindienst, C.G. Huber, D.T. Gjerde, L. Yengoyan and G.K. Bonn, *Electrophoresis.*, 19 (1998) 262.

16. D. Pyo, P.K. Dasgupta and L. Yengoyan, *Anal.Sci.*, 13 (1997) 185.

17. Y. Wang and P.L. Dubin, *Anal.Chem.*, 71 (1999) 3463.

18. N. E. Roberts, *Limit of del18O annual layer detection in the law dome ice cap.* Honours thesis (1999). University of Tasmania.

19. M.A.J. Curran and A.S. Palmer, *J.Chromatogr.A*, submitted (2000)

20. Q. Yang, P.A. Mayewski, S. Whitlow, M. Twickler, M. Morrison, R. Talbot, J. Dibb and E. Linder, *Journal of Geophysical Research*, 100 (1995) 5113.

21. G.A.M. Dreschhoff and E.J. Zeller, *TER-QUA Sypmosium Series, Institute for Tertiary-Quaternary Studies*, 2 (1994) 1-24.

22. A.S. Palmer, T.D. van Ommen, M.A.J. Curran and V. Morgan, *GRL*, submitted (2000)

23. R. Mulvaney, D. Wagenbach and E.W. Wolff, *Journal of Geophysical Research*, 103 No D9 (1998) 11031.

24. M.A.J. Curran, T.D. van Ommen and V. Morgan, *Ann.Glaciol.*, 27 (1998) 385.

Chapter 6

General Conclusions

The following general conclusions can be made regarding the separation of inorganic and small organic anions by ion-exchange capillary electrochromatography (IE-CEC).

Capillaries coated with cationic latex particles in the nm size range can be used to alter the selectivity of inorganic anions in CE by introducing an ion exchange (IE) chromatographic component into the separation mechanism. The strength of the chromatographic interaction can be varied by adapting typical approaches used in ion chromatography (IC), such as varying the concentration and type of competing ion and/or by varying of the column capacity. By selecting appropriate conditions, CE, IE or intermediate selectivities can be achieved which are useful for analysing samples which contain large differences in analyte concentrations.

The manipulation of the selectivity of UV transparent ions is more difficult than UV absorbing ions as the competing ion must also functiong as the indirect absorbance probe. As a consequence, the concentration range of a particular probe is limited by electromigration dispersion and low buffering capacity when low concentrations are used and by high currents and high background absorbance when high concentrations are used. Therefore a probe can only be used over a relatively narrow concentration range with the result that most probes provide only a discrete range of separation selectivities. To overcome this, variation of the separation selectivity can be best achieved by varying the nature of the probe, rather than its concentration.

The migration behaviour of inorganic anions in IE-CEC can be described by a model equation derived from IC and CE theory. The model accounts for the change in observed mobility due to changes in the type and concentration of competing ions in the electrolyte. Using a range of UV-absorbing and UV-transparent anions and

various competing ions, good agreement between experimental and calculated mobilities was obtained ($r^2 > 0.98$). System constants determined from non-linear regression enabled a quantitative comparison of IE strengths and for the UV-absorbing ions, were used to optimise the separation of 7 inorganic anions.

While the use of OT columns results in the ability to change the separation selectivity, the separation efficiency is substantially reduced in comparison to conventional CE. Analysis of both chromatographic and electrophoretic sources of inefficiency reveals that the chromatographic component is the major source of band broadening. While the electrophoretic component is not the major contribution to band broadening, appropriate competing ion mobility is still important in minimising electromigration dispersion. Inefficiency arising from the chromatographic component is dominated by resistance to mass transfer in both the mobile and stationary phases. Resistance to mass transfer in the mobile phase can be improved by reducing the diameter of the capillary, but this improvement is offset by a decrease in optical path length and a reduction in column capacity. Resistance to mass transfer in the stationary phase resulting from the influence of secondary interactions with the stationary phase also affects the separation of polarisable ions. The use of additives to block the secondary sites on the stationary phase proved ineffective with the development of new phases seen as the best prospect for improving efficiency of these ions.

The limited column capacity encountered when using OT columns can be overcome by the use of a polymeric pseudo-phase. This increased the flexibility of the IE-CEC system with conditions since the polymer concentration, competing ion type and competing ion concentration can be varied to increase or decrease the IE component of the separation mechanism. For UV transparent ions, conversion of the polymer to the probe form is required and while this restricts the concentration of both polymer and probe that can be employed, the ability to vary the IE strength of the probe still allows the selectivity to be varied to a greater extent than is possible with a fixed

capacity column. The theoretical model derived to explain migration in OT columns was extended to account for the variation in column capacity when using a pseudo-phase and this was used to successfully predicted optimal conditions for a given separation using as few as five preliminary experiments. This allowed for rapid method development for the separation of anions in complex samples and was demonstrated by optimising the separation of 16 UV absorbing and 24 UV transparent anions. Further potential of IE-CEC was demonstrated by separating target anions in Bayer liquor with a separation selectivity differing substantially from that attainable in conventional CE.

An on-line SPE method using an OT-IE preconcentration column was developed for the separation of inorganic anions by CE. A new electroseparation concept, namely the use of an eluotropic gradient formed by a transient isotachophoretic boundary, has been introduced to elute anions from the preconcentration column. This gradient is established by using a weakly eluting low mobility electrolyte ion (WE) in the capillary and a more mobile strongly eluting ion (SE) in the electrolyte vials. As the gradient moves through the capillary, analytes which satisfy the conditions $K_{WE} < K_A < K_{SE}$ and $\mu_{WE} < \mu_{SE} < \mu_A$ are focused along the capillary wall into a very sharp band, allowing multiple anions to be focused into a sharp band prior to introduction into a separation capillary.

Gradient characterisation was accomplished using the concepts of eluotropic strength and concentration profile. The eluotropic strength of a SE is a function of the charge, IE selectivity coefficient and the concentration of the SE competing anion, the latter of which is governed by the Kohlrausch Regulating. The concentration profile of the eluotropic gradient is strongly dependent on the difference in mobility between the WE and SE competing anions, but also depends on the IE selectivity coefficients of these ions. Ideally, the SE and WE should be selected so that: (i) the SE has the highest possible eluotropic strength for a given concentration of WE, (ii) the competing anion in the SE has a mobility as low as possible to ensure that the

maximum number of analyte anions can be focused, and (iii) the difference in electrophoretic mobility between the WE and SE competing anions is as small as possible.

Using the WE and SE selection guidelines, F^- and NDS were selected as suitable WE and SE anions, respectively. An analytical system using these ions was developed for the preconcentration and separation of high mobility UV absorbing inorganic anions. Optimisation of both the preconcentration and separation components was crucial in order to obtain highly efficient separations. The best separations were obtained in a 25 μm i.d. capillary due to its superior resolution over other capillary diameters. Using an optimised method, a 100 min pressure injection allowing 40 capillary volumes of sample to be injected gave an increase in sensitivity by a factor of 900 without any loss in resolution and separation efficiency. A shorter method based on a 10 min injection enabled a 100 fold increase in sensitivity and was found to be comparable to an IC method for the determination of nitrate. This method was used to determine the concentration of NO_3^- in Antarctic ice cores where the potential of CE will allow a 100 fold increase in resolution for the Antarctic nitrate record.

Finally it should be noted that further research is required in the following areas:

The ability to condition open tubular columns is an advantage over packed columns that has yet to be exploited. This will be particularly beneficial when real samples are used, particularly where the column needs to be conditioned between each sample, a situation that is frequently encountered when analysing many biological samples. This will be particularly important when using mass spectroscopic detection where the use of pseudo-phases is not a viable alternative.

The use of alternative stationary phases is an area of obvious appeal, particularly those phases that show preference for ions with a low IE selectivity such as F^-, BrO_3^- and IO_3^- or those phases that show an intolerance to matrix ions such as Cl^- and OH^-.

The formation of particle-coated capillaries by using the successive multiple ionic layer (SMIL) method is an area that warrants some examination. This is where layers of oppositely charged material are used to alternatively coat the capillary. This approach has been shown to improve column stability with polymeric coated capillaries and should result in more stable and robust particle coated columns.

The use of ultra-high temperature (100 -200 °C) is an area where OT-CEC in larger capillary diameters (50-75 μm i.d.) may yield comparative results to packed columns. High temperatures are frequently used in OTLC to improve efficiency, but so far their use in CE and OT-CEC has been ignored.

One of the advantages a pseudo-phase has over packed and OT columns is the ease with which the 'column' characteristics can be changed. This will be particularly useful as a diagnosis tool whereby the same sample can be analysed using various pseudo-phase conditions to elucidate the composition of the sample.

An area of great potential is the use of a discontinuous pseudo-phase system where analytes encounter different zones of pseudo-phase as they move through the column. This may be useful for simulating a 2-dimensional approach to separations. An extension of this is the use of two pseudo-phases moving in opposite directions, which may provide interesting peak compression effects when positioned either side of an injected sample plug

The extension of the preconcentration approach to larger capillary diameters is an area with immediate potential. This will enable detection limits to be lowered by a similar factor to that already shown for the 25 μm i.d. capillaries and would enable detection in the low ppt range for inorganic anions to be achieved.

The use of alternative forms of detection to enable UV transparent ions to be detected is also an area of immediate potential. This may be done by using either indirect UV detection, or a form of electrochemical detection, such as conductivity detection.

Development of a suitable method would provide a real alternative to IC for the separation of trace ions.

The use of higher capacity preconcentrator columns would be beneficial as it would increase the amount of sample that could be injected before the column was overloaded. This would be particularly beneficial for higher ionic strength samples which on low capacity preconcentrators may elute the analyte ions. This may be accomplished by using packed capillary columns, although it should be expected that the focusing efficiency will not be as efficient due to the multiple flow paths through the packing.